VOLTAMMETRIC SENSORS FOR BIOMOLECULES AND DRUGS

Ph.D. THESIS

by

HIMANSHU CHASTA

DEPARTMENT OF CHECHISTRY
INDIAN INSTITUTE OF TECHNOLOGY ROORKEE
ROORKEE – 247667, INDIA
APRIL, 2015

VOLTAMMETRIC SENSORS FOR BIOMOLECULES AND DRUGS

A THESIS

Submitted in partial fulfilment of the requirements for the award of the degree

of

DOCTOR OF PHILOSOPHY

in

CHEMISTRY

by

HIMANSHU CHASTA

DEPARTMENT OF CHEMISTRY
INDIAN INSTITUTE OF TECHNOLOGY ROORKEE
ROORKEE – 247667, INDIA
APRIL, 2015

INDIAN INSTITUTE OF TECHNOLOGY ROORKEE
ROORKEE

CANDIADATE'S DECLARATION

I hereby certify that the work which is being presented in the thesis entitled, **"VOLTAMMETRIC SENSORS FOR BIOMOLECULES AND DRUGS"** in partial fulfilment of the requirements for the award of the Degree of Doctor of Philosophy and submitted in the Department of Chemistry of the Indian Institute of Technology Roorkee, Roorkee is an authentic record of my own work carried out during a period from July, 2010 to April, 2015 under the supervision of Dr. R.N. Goyal, Professor, Department of Chemistry, Indian Institute of Technology Roorkee, Roorkee.

The matter presented in this thesis has not been submitted by me for the award of any other degree of this or any other institute.

(HIMANSHU CHASTA)

This is to certify that the above statement made by the candidate is correct to the best of my knowledge.

Dated:

(R.N. Goyal)
Supervisor

ABSTRACT

Last few years have seen a great proliferation of research interest by electrochemists at the interface of nanotechnology and electrochemistry. Advancements in electrochemistry make it possible to study and understand the principles as well as different aspects of nanoscience and nanotechnology. Electrochemical determination of variety of biomolecules, medicines, and doping agents in biological samples using electrodes modified with nanocarbon/nanoparticles/polymer film has been performed using various voltammetric techniques. Determination of physiologically important biomolecules always remains an uphill task for researchers as their concentration in biological fluids is normally very low. However, in the case of metabolic disorders and diseases, the concentration of these biological compounds gets abnormally altered. In such cases, detection of their concentration level proves out to be of diagnostic value. Voltammetric sensors have been found to show consistently good results with high sensitivity and selectivity. Quantification of common drugs is important for pharmaceutical industry, and studies on doping agents is needed to keep a check on the doping cases in competitive games. An endeavor has been made in the present investigation to develop simple, selective, and sensitive electroanalytical methods for qualitative and quantitative determination of biologically important molecules and drugs at nanomaterial/polymer film modified electrodes. An outline of the present research with a chapter-wise concise summary of the thesis is given below.

The **first chapter** of the thesis gives a panoramic view on conventional materials, types of nanomaterials, polymeric materials and an introductory background of related materials. The chapter also presents the discussions on the application of nanomaterials and polymer films in various chemical and biosensing applications using electroanalytical techniques. This chapter also briefly adumbrates the methodology used during the investigation.

The **second chapter** of the thesis has been divided into two parts. The first part represents the comparison of basal and edge plane pyrolytic graphite sensors towards the determination of norfloxacin (NF). The compound NF, a member of fluoroquinolones, is the first choice drug for the treatment of diseases caused by *Campylobacter, E. coli, Salmonella, Shigella* and *V. colera*. It is used for the doctoring of gonorrhoea as well as eye and urinary tract infections. The non-target toxicity of antibacterials, including NF, has also been documented in literature. The determination of NF in biological samples and medicine is considered of great importance for human health, food assurance and quality control because of its potential toxicity. When equating with the bare basal plane pyrolytic graphite sensor, the

edge plane pyrolytic graphite sensor gave better response towards the determination of NF, both in the terms of sensitivity and detection limit. The difference in the surface morphology of the two electrodes has been studied. Also, the edge-plane pyrolytic graphite sensor delivered an analytical performance for NF with a sensitivity of 0.9064 μA μM^{-1} and limit of detection of 28.3×10^{-8} M in the concentration range 0.5-50 μM. The method is successfully utilized for the detection of NF in pharmaceuticals formulations and human urine samples.

The second part of the chapter throws light on voltammetric investigation of a well-known sulfonamide drug, sulfamethoxazole (SMZ) at poly-1,5-diaminonaphthalene modified glassy carbon electrode. The oxidation of SMZ occurred in a well-defined peak having peak potential ~850 mV at pH 7.2. The modified electrode showed an excellent catalytic response presenting much higher peak currents than those measured at a bare glassy carbon electrode. The modified sensor was characterized by Field Emission Scanning Electron Microscopy, electrochemical impedance spectroscopy and cyclic voltammetry. Under optimized conditions, SMZ showed linear response in the concentration range of 0.5-150 μM by using square wave voltammetry and the detection limit was found to be 0.05 nM with a sensitivity of 0.085 μA μM^{-1}. In order to assess the pertinency of the proposed sensor, different commercial samples as well as human biological samples containing SMZ have been analyzed.

In **third chapter**, electrochemical and peroxidase-catalyzed oxidation of epinephrine is documented. The hormone epinephrine (adrenaline) is commonly used as the drug of choice as a vasoconstrictor, cardiac stimulator and bronchodilator. It subsists in protonated form at physiological pH. It is synthesized in the human system from L-tyrosine and exuded by the medulla of the adrenal gland along with norepinephrine. Ratiocination of concentration of the monoamine neurotransmitters such as epinephrine is crucial for the canvassing of neurotransmission, for diagnosis of neurological disorders, such as Parkinson's, and for developing medicines to cure the diseases. In view of the importance of epinephrine in the human physiology, an attempt has been made to compare the electrochemical and peroxidase catalyzed oxidation of epinephrine in this chapter. In the electrochemical studies a single well-defined, $4e^-$, $4H^+$, pH-dependent oxidation peak was observed in square wave and cyclic sweep voltammetry at edge plane pyrolytic graphite electrode. The decay of the UV-absorbing intermediate and the first-order rate constants were calculated at different pH. At pH 7.2, the electrooxidation product was characterized using NMR and DEPT studies as leucoadrenochrome. The peroxidase catalyzed oxidation was carried out using horseradish peroxidase and initiated by adding H_2O_2. The identical spectral changes, rate constants for the decay of the UV-absorbing intermediate and product formed during electrochemical and

enzymatic oxidation suggest that the same intermediate species is generated during both the oxidations. It is concluded that the electrochemical pathway and peroxidase-catalyzed oxidation of epinephrine proceed by an identical mechanism.

The **fourth chapter** throws light on simultaneous voltammetric investigation of adenine and adenosine monophosphate at single-walled carbon nanotubes (SWNT) modified edge plane pyrolytic graphite electrode (EPPGE). Under optimized conditions, well-defined oxidation peaks are observed at SWNT modified EPPGE where the peak shifted negatively and the peak current increased remarkably in comparison to bare edge plane pyrolytic graphite electrode. The significant enhancement in current response followed by a decrease in peak potential indicates that SWNT modified EPPGE acts as a promoter to enhance the electrochemical reaction, considerably accelerating the rate of electron transfer. The electrocatalytic activity of SWNT has been assigned due to the metallic impurities present within it. The electrode process is adsorption-controlled and irreversible in nature. The effect of pH revealed that the oxidation of adenine and 5′-AMP at SWNT modified EPPGE involved equal number of electrons and protons. Linear calibration curves are obtained over the concentration range of 5-100 nM for adenine and 10-100 nM for 5′-AMP with sensitivity of 677 and 476 nA nM^{-1} for adenine and 5'-AMP, respectively. The limit of detection for adenine and 5′-AMP was found to be 37×10^{-10} M and 76×10^{-10} M, respectively. The modified electrode exhibited high stability and reproducibility. In order to assess the pertinency of the proposed method, different plasma samples have been analyzed using standard addition method.

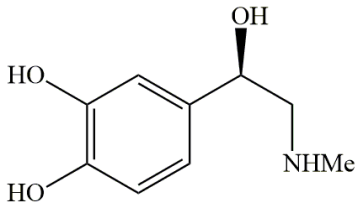

Epinephrine

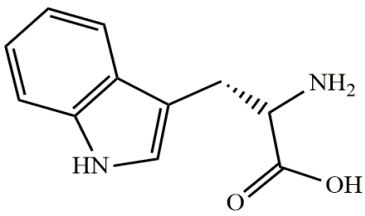

Tryptophan

The **fifth chapter** of the thesis elaborates the effect of surface modification of indium tin oxide (ITO) by the use of multi walled carbon nanotubes (MWNT/ITO) and gold nanoparticles attached carboxylated multi walled carbon nanotubes (AuNP-MWNT/ITO) for the electrochemical oxidation of tryptophan. Tryptophan (2-amino-3-(1H-indol-3-yl)-propionic acid) is an important and essential amino acid for humans and herbivores, and is also a potent precursor of several metabolites such as serotonin, melatonin and niacin. A detailed comparison has been made among the voltammetric response of bare ITO, MWNT/ITO and AuNP-

MWNT/ITO in respects of several essential analytical parameters viz. sensitivity, detection limit, peak current and peak potential of tryptophan. It is observed that the oxidation peak current of tryptophan was found to increase significantly along with a substantial shift in peak potential towards less positive potentials by using AuNP-MWNT/ITO in comparison to bare ITO and MWNT/ITO electrodes. Under optimum conditions linear calibration curve was obtained over tryptophan concentration range 0.5-90.0 μM in phosphate buffer solution of pH 7.2 with detection limit and sensitivity of 0.025 μM and 0.12 μA μM^{-1}, respectively. The oxidation of tryptophan occurred in a pH dependent, $2e^-$ and $2H^+$ process and the electrode reaction followed adsorption controlled pathway. The origin of electrocatalytic properties of nanotubes has been assigned to the embedded metal impurities in CNT samples and edge-plane-like defects which are present at the open ends of nanotubes. The AuNP-MWNT/ITO has also been utilized for the electrochemical determination of tryptophan in human blood plasma and urine samples with reproducible results.

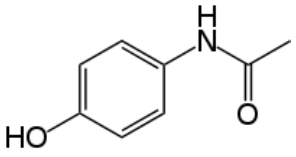

Paracetamol

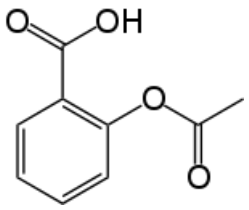

Aspirin

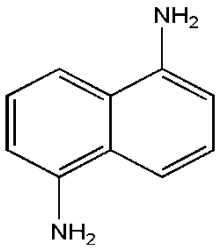

1,5-diaminonapthalene

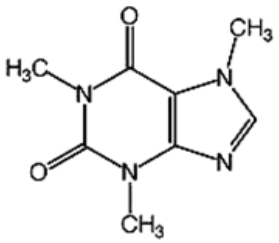

Caffeine

Sixth, the **last chapter** of the thesis is devoted to the simultaneous monitoring of aspirin, paracetamol and caffeine in human urine at poly-1,5-diaminonapthalene modified pyrolytic graphite sensor. Recently, conductive polymers have acquired much attention due to their potential applications to battery electrodes, electrochromic devices, electroluminescent devices, and biological sensors. Of these, aromatic compound possessing two amine groups has been studied for polymer film-coated electrodes in this chapter. Poly-1,5-diaminonapthalene has shown incredible interest due to its fascinating properties. The main advantage of the present method is that poly-1,5-diaminonapthalene layer contributes to its efficiency leading to

the lowering of oxidation peak potential and marked enhancement in the peak current. The electrooxidation of aspirin, paracetamol and caffeine occurred in well-defined peaks at pH 7.2. After optimization of analytical conditions exploiting this sensor, the peak currents for the three compounds were found to increase linearly with increase in their concentration in the range of 0.1-120 nM and detection limits of 0.93×10^{-10}, 0.57×10^{-10} and 0.64×10^{-10} M were observed for aspirin, paracetamol and caffeine respectively. The proposed sensor exhibited good stability and reproducibility towards the determination of aspirin, caffeine and paracetamol in urine samples and tablets. The sensor can also be recommended for detecting doping cases of caffeine at the site of competitive games due to its rapid response and accuracy.

****

ACKNOWLEDGEMENTS

First and foremost, I have big sense of gratitude to the God, the almighty (**Shri Krishna**), who has bestowed grace, mercy and blessing along with courage, wisdom and strength upon me which has indeed allowed me to complete my research successfully. **Srimad Bhagavad Gita** always inspired me. This thesis appears in its current form due to the assistance and guidance of several people. I would therefore like to offer my sincere thanks to all of them.

It gives me a great pleasure to express my unfathomable sense of gratitude to my research supervisor, **Prof. R. N. Goyal**, for the trust, the insightful discussion, offering scientific advices, for his support and encouragement during the entire period of the research, and especially for his extraordinary patience and inspiring guidance during the shaping of the manuscript despite his incredible academic preoccupations. It is precisely because of his sheer motivation, selfless help and above all, unceasing endurance, that I could able to complete my research in time. The thesis would not have been possible without his critical examining and the meticulous insight provided by him on the subject matter which was totally naive for me. As my supervisor, he has constantly verved me to be remain focused on achieving my goal. Throughout my thesis-writing period, his guidance, observations and precious suggestions played a vital role for bringing the present work in the final shape. He has definitely been a great beacon of inspiration and encouragement for me. Further, his extensive discussions about cardinal methods and techniques helped me not only in handling the scientific problems of research but also in exploring the mystery of life. I thank him for the interest he has shown in my academic and personal well-being.

My sincere thanks are due to Prof. Anil Kumar, Head, Department of Chemistry and all other faculty members of the Department of Chemistry for their keen interest in this work. I am also thankful to the members of my SRC committee, Prof. Bina Gupta (Internal member), Department of Chemistry and Prof. R. D. Agarwal (External Member), Department of Chemical Engineering, IIT Roorkee for their invaluable suggestions and encouragement to carry out this work.

I acknowledge my sincerest thanks to the Council of Scientific and Industrial Research (CSIR), New Delhi for providing me with a scholarship to pursue doctoral studies.

I wish to acknowledge Mr. Abdul Haq and Mr. Madan Pal for the technical assistance in the Department. Special thanks to Mr. N. K. Varshney, Draftsman, National Institute of Hydrology, Roorkee for the drawing work. I also acknowledge my heartfelt thanks to The

Head, Institute Instrumentation Centre, for providing me with some instrumental facilities like FE-SEM, ^{1}H NMR during the course of this work. I also wish to thank M/S Pfizer, USA for the gift of pyrolytic graphite pieces.

I feel privileged to offer my sincere thanks and deep sense of gratitude to Sushma Aunty Ji, my supervisor's wife, for her helpful personal advice well along the path of my course. I owe my sincere thanks to every member of her family as I always feel a homely environment there.

I have greatly enjoyed working with Dr. Sanghamitra Chatterjee, Dr Sunita Bishnoi, Dr. Anoop Raj Singh Rana, Dr. Bharati Agrawal, Rakesh, Saurabh, Pankaj, Rosy, Mamta, Neeraj and Purushotham in my Chemistry lab. I have also got a very good support from Dr. Sudhir Kumar Gupta (BABA), Sudhir Yadav, Nishant Gautam. I thank them all for their amicable cooperation and ever needed help throughout to carry out this work and also for being around all the time, be it while partying, playing cricket or discussing academics or doing other crazy things.

When hurdles appeared insurmountable and targets unachievable, the encouragement and camaraderie of friends helped me in keeping things in perspective. I feel greatly obliged to my friends Dr. Hariom Nagar, Dr. Arvind Kumar Bharati, Manoj Kumar Sahani and Himanshu Gupta. I wish to thank all those whose names have not figured alone but helped me explicitly or implicitly throughout my career. I am really indebted to my parents and other family members. Without their support and help over the years towards my education, all this would not have been possible. I have gained great strength from them. Their ultimate patience in the extremely tough conditions gave me continuous inspiration and made my dreams true so they deserve my utmost respect and gratitude. I wish to extend my heartfelt gratitude to my mother, **Mrs. Asha Chasta**, whose eternal love, support, patience and belief in me enabled this thesis to be completed.

I will miss IIT Roorkee very much. I had a really nice experience in IIT Roorkee with the friendly nature of the people. I won't forget IIT Roorkee in my life.

Last but not least, I wish to thank everyone who is involved in helping me, directly or indirectly, throughout my project.

Dated: **(HIMANSHU CHASTA)**

****

LIST OF PUBLICATIONS

[1] R. N. Goyal, S. Chatterjee, A. R. S. Rana, H. Chasta; "Voltammetric sensor using single-walled carbon nanotubes modified edge plane pyrolytic graphite electrode for the simultaneous assay of adenine and adenosine monophosphate". *Sens. Actuators B*, **156** (2011) 198.

[2] R. N. Goyal, S. Bishnoi, H. Chasta, M. A. Aziz, M. Oyama; "Effect of surface modification of indium tin oxide by nanoparticles on the electrochemical determination of tryptophan". *Talanta*, **85** (2011) 2626.

[3] R. N. Goyal, A. R. S. Rana, H. Chasta; "Electrochemical sensor for the sensitive determination of norfloxacin in human urine and pharmaceuticals". *Bioelectrochemistry*, **83** (2012) 46.

[4] R. N. Goyal, A. R. S. Rana, H. Chasta; "Electrochemical and peroxidase-catalyzed oxidation of epinephrine". *Electrochim. Acta*, **59** (2012) 492.

[5] R. N. Goyal, A. R. S. Rana, H. Chasta; "Simultaneous monitoring of aspirin, paracetamol and caffeine in human urine at poly-1,5-diaminonapthalene modified pyrolytic graphite sensor". *J. Electrochem. Soc.*, **160** (2013) G3014.

[6] H. Chasta, R. N. Goyal; "A simple and sensitive poly-1,5-diaminonaphthalene modified sensor for the determination of sulfamethoxazole in biological samples". *Electroanalysis*, **27** (DOI: 10.1002/elan.201400688).

****

LIST OF CONFERENCES/ SCHOOL/SYMPOSIA ATTENDED

[1] Participation in fifth BRNS-AEACI winter school on analytical chemistry organized by Association of Environmental Analytical Chemistry of India (AEACI) from December 03-10, 2012 in Department of Chemistry, IIT Roorkee.

[2] Poster presentation- "Simultaneous sensing of aspirin, paracetamol and caffeine in pharmaceutical formulation and human urine by square wave voltammetry". Rajendra N. Goyal and Himanshu Chasta. ELAC-2013, Fifth ISEAC Triennial International Conference on Advances and Recent Trends in Electrochemistry, organized by Indian Society For Electroanalytical Chemistry (ISEAC) (BARC, Mumbai) at Ramoji Film City, Hyderabad from January 16-18, 2013.

[3] Oral presentation- "Electrochemically synthesized molecularly imprinted sensor based on *o*-aminophenol for the selective determination of norepinephrine in pharmaceutical and biological samples". Rajendra N. Goyal, Himanshu Chasta. 11^{th} ISEAC International Discussion Meet on Electrochemistry and its Applications, organized by ISEAC (BARC, Mumbai) at Radisson Blu, Amritsar from February 20-25, 2014.

****

LIST OF ABBREVIATIONS

CV	Cyclic Voltammetry
SWV	Square Wave Voltammetry
HPLC	High Performance Liquid Chromatography
FE-SEM	Field Emission Scanning Electron Microscopy
ICP-MS	Indirectly Coupled Plasma-Mass Spectroscopy
CNTs	Carbon Nanotubes
SWNT	Single Walled Carbon Nanotubes
MWNT	Multi Walled Carbon Nanotubes
Ag/AgCl	Silver-Silver Chloride electrode
GCE	Glassy Carbon Electrode
PGE	Pyrolytic Graphite Electrode
EPPGE	Edge Plane Pyrolytic Graphite Electrode
BPPGE	Basal Plane Pyrolytic Graphite Electrode
ITO	Indium Tin Oxide
DMF	N,N-dimethylformamide
DNA	Deoxyribose Nucleic Acid
EPI	Epinephrine
PAR	Paracetamol
DHA	Dihydroxyadenine
AuNPs	Gold nanoparticles
AA	Ascorbic Acid
DP	Dopamine
UA	Uric Acid
NF	Norfloxacin
Trp	Tryptophan
ASA	Acetylsalicylic acid
p-DAN	Poly-1,5-diaminonapthalene
CF	Caffeine
SMZ	Sulfamethoxazole
5′-AMP	Adenosine-5′-monophosphate

E_p	Peak Potential
i_p	Peak Current
f	Square Wave Frequency
ν	Scan rate
RSD	Relative Standard Deviation
WADA	World Anti-Doping Agency
NSAIDs	Non-Steroidal Anti-Inflammatory Drugs

****

CONTENTS

****

Chapter 1

INTRODUCTION

1.1 ELECTROCHEMISTRY: AN OVERVIEW

The term electrochemistry is delineated as the study of the chemical changes, which occur at the interface of an electrode (a metal or a semiconductor) and an ionic conductor (the electrolyte). In other words, the term electrochemistry deals with the transfer of electron between the electrode interface and electrolyte. The oxidation or reduction phenomenon in various chemical reactions is conspicuously based on the electrochemistry. A marked mounting ascends in the field of electrochemistry, as it has played a key role in technologically important areas including biomedical research, pollution control, corrosion, energy storage devices, semiconductors and extraction of metals. Electrochemistry is considered as a powerful and invaluable tool for probing the various electrochemical reactions, particularly in living systems. In nature, a number of physiological processes and phenomena are based on electrochemical changes (oxidation/reduction) such as photosynthesis and nerve conductions. There are sufficient evidences showing that electrochemical reactions convincingly resemble biological reactions, such as both reactions are essentially heterogeneous in nature and, specific orientation of the substrate molecules is required for enabling electron transfer at electrode (in electrochemical reactions) or at an active site of enzyme (in biological reactions). Electrochemical reactions occur at the electrode-solution interface similarly in biological reactions, these occur at an enzyme-solution interface. Further, both types of reactions can effectively occur at similar pH as well as at similar physiological temperature. Additionally, Electrochemical as well as biological processes occur adequately in non-aqueous solutions and in the presence of similar concentration of inert electrolyte. Hence, the analogies between electrochemical and biological reactions instigate the ex-situ use of electrochemical techniques for the determination of biomolecules and drugs in biological fluids.

Biomolecules have significant consequences in the transmission of genetic information as well as various important metabolic activities. Any alteration in their concentrations leads to metabolic disorders. Therefore, selective and accurate determination of biologically important molecules always remains a challenging task for researchers due to the fact that these molecules have very low concentration in biological fluids. However, in the case of metabolic disorders and diseases, the concentration of these molecules gets abnormally altered. In such cases, detection of their concentration level is very important from the clinical point of view. Quantification of common drugs in biological fluids and pharmaceutical dosage forms is highly desirable for pharmaceutical industries, biomedical research and healthcare. Molecular diagnosis in clinical

laboratories relies on technologies, which are generally expensive and time consuming and often a reason for delaying medical treatments. Hence, still there is a strong demand to design fast, less expensive and more sensitive techniques for the diagnosis of biologically important molecules and drugs in biofluids.

Electrochemical techniques offer a unique access about the nature of electrons to get mechanistic information of reactions occurring in biological systems. These techniques have a wide range of applications including characterization, fabrication, redox properties of biomolecules or drugs, and understanding of various electrochemical interfaces or electrochemical processes. Voltammetric techniques are powerful and versatile electrochemical techniques that provide cost-effective instrumentation, large linear dynamic range and great sensitivity with accuracy and precision. These techniques have been the center of interest for scientific communities which belong to the rapidly emerging areas of science and technology, mainly nanosciences (nanoelectrochemistry) and life sciences (bioelectrochemistry).

Over the last decade, technological advancements in electrochemistry have contributed significantly to study and understand the principles of nanoscience and nanotechnology. Nanotechnology has numerous fascinating applications in the areas of energy, electronics, environment, and biomedical, particularly in the development of sensing devices. Nanomaterials frequently display unusual physical (structural, electronic, magnetic and optical) and chemical (catalytic) properties and also have large surface-to-volume ratios that make these materials an appealing choice for sensor applications and, it is currently a focal point of nanoscience and nanotechnology. Sensor can be defined as a small device, which is used to measure chemical or molecular target by a chemical interaction or process between the analyte and the sensor and transforms chemical or biochemical information of a quantitative or qualitative type into a meaningful analytical signal. Nanotechnology is currently evolving in discovery of useful new materials to deal with challenging bioanalytical problems, including stability, selectivity and sensitivity. In recent years, electrically conductive polymers have been exploited as an excellent tool to prepare nanofilms or nanocomposites for the detection of biomolecules and drugs in human biological fluids and pharmaceutical formulations. Due to the simple preparation methods and unique catalytic or affinity properties, conducting polymers can be easily utilized to energy storage, electrochemical devices, memory devices, electrocatalysts, especially to design the sensors (electrochemical sensors and biosensors). Conducting polymers as well as nanomaterials based

sensors play a vital role in the improvement of environmental and human health due to the small size, rapid detection, specificity and excellent sensitivity.

Voltammetric sensors have extensively served as a whole or an integral part of environmental monitoring and clinical diagnostics tools and are used to analyze various samples including biological fluids, food samples, cell cultures samples and pharmaceutical samples. For instance, voltammetric electronic tongue (taste sensor), blood gas sensor, glucose sensor, oxygen sensor are well-established voltammetric sensors, which are based on electrochemical principles. Voltammetric, conductivity or capacitance, potentiometric, and amperometric sensors are some important categories of electrochemical sensors. Among these, voltammetric sensors are widely used and are based on the current-potential characteristics of an analyte, resulting from the reduction or oxidation reaction. The signal transduction process is accomplished by measuring the current as a function of varying potential that serves as the driving force for the mass transfer processes of the detecting species. The resulting current is directly proportional to the concentration of the target species and provides the basis for the voltammetric sensors. The construction of voltammetric sensor is very robust that makes it suitable in different aspects of industrial applications. Hence, an endeavor has been made in the present investigations to develop simple, selective electroanalytical methods for qualitative and quantitative analysis of biologically important molecules and drugs using nanomaterial or polymer film modified electrodes. The foremost aim of the present investigation is to assess the utility of the voltammetric techniques using various conventional electrodes and surface modifiers for the determination of biomolecules and pharmaceuticals in human physiological fluids (urine or plasma) with low cost, high speed and sensitivity [1-20].

1.2 WORKING ELECTRODES BASED ON CONVENTIONAL MATERIALS

In electrochemical experiments, the central place is occupied by an electrode due to the fact that the performance of various electrochemical techniques depends on the nature of electrode used, hence it is necessary to select appropriate electrode material for a particular investigation. Vast varieties of materials have been applied as working electrode in different voltammetric techniques over the years. The selection of a working electrode depends on several parameters involving available potential window, electrochemical stability, electron transfer rate, mechanical properties, cost availability, toxicity, redox behavior of the target analyte and background current in the potential region under experimentation. Additionally, adsorption and coatings applied to the

electrode surface in order to enhance the detection of analyte are some other features which need a due consideration while selecting a suitable material to be used as working electrode. An ideal electrode should exhibit following specific characteristics, (1) higher electrical conductivity; (2) low back ground current with stable response; (3) hard and durable (4) good electrochemical inertness (5) rapid kinetics of electron transfer reaction (5) easily shaped and modified (6) low priced (7) morphological and structural stableness over a wide potential range and (8) reproducible physical, electronic and chemical properties. Commonly used conventional working electrodes are based on mercury, semiconductor, noble metals or carbon surfaces.

In voltammetric analysis, platinum, gold, mercury, semiconductor (e. g. indium tin oxide) and carbon surfaces including highly ordered pyrolytic graphite, pyrolytic graphite and glassy carbon are most often employed as a working electrode. Other carbon based working electrodes such as pencil graphite electrode, carbon paste electrode, doped carbon electrode and carbon fiber electrode have also been well documented in literature. In last few decades, electroanalytical chemistry at solid electrodes has become excessively famous with the development of new electrode materials, as many interesting mechanistic and analytical applications have been investigated at their surface, which are not accessible at mercury surface. Thus, choosing an electrode material as a working electrode is very significant for the voltammetric studies of specific molecules.

High hydrogen overvoltage and a highly reproducible, readily renewable and smooth surface of the working electrodes based on mercury are some notable reasons for their popularities and reliabilities in electroanalytical chemistry, despite their serious limitations in anodic range (mercury itself oxidizes) and mechanical inconvenience. Different types of mercury based working electrodes including dropping mercury electrode, amalgam electrodes, hanging mercury drop electrode and mercury film electrode have been reported. Hanging mercury electrodes and mercury film electrodes are used for stripping analysis and cyclic voltammetry, while dropping mercury electrodes are commonly used in polarography and electrocapillary studies. The wide applicability of the dropping mercury electrode is due to the fact that the electrode is self-renewing, so there is no need of cleaning or polishing before each experiment. In addition, every drop of mercury provides uncontaminated and uniform surface for electrochemical experiments. However, application of the mercury based electrodes is severely decreased in the last decade due to toxicity and inconvenience of handling the mercury.

Solid electrodes based on metals such as platinum, gold, nickel, copper, silver and carbon have attracted considerable attention during last few decades due to their extended potential window and favorable electron transfer kinetics. Pure gold or platinum are simply acquired, and the electrodes can be easily prepared and hence, this is one of the reasons for the popularity of these electrodes. Gold electrodes are commonly used for self-assembled mono layers or for stripping analysis of trace metals and are also employed for the determination of carbohydrates. Platinum electrodes are mostly applied in fuel cells due to their catalytic mechanism. Silver is also a good electrode material, which is commonly used for the determination of cyanide or sulfur compounds as well as for the development of chemically modified electrodes. Moreover, cytochrome *c* (protein) possesses the ability of direct electron transfer on silver, hence, silver metal can be directly employed for protein analysis. Copper and nickel substrates are commonly used in the detection of amino acids or carbohydrates due to their stable response. Though, metal based electrodes satisfactorily overcome the limited anodic potential range and toxicity of mercury electrode, but low hydrogen over voltage strictly limits the cathodic potential window. High background current is another drawback associated with these electrodes. Both these disadvantages, along with the toxic effects of mercury electrode, can be circumvented by using carbon electrodes. Carbon electrodes are most widely used in electroanalysis as they incorporates almost all the features of a good electrode material like large potential window, low background current, low cost, chemical inertness and competency of sensing and detection of various physiologically important molecules. Some carbon materials, though, show slightly slower electron transfer rates, but the shortcoming is negligible in comparison to the advantages carbon offers as an electrode material. Carbon electrodes are broadly classified into glassy carbon, pyrolytic graphite, screen printed carbon strips, carbon paste, carbon films, pencil graphite and carbon fiber electrodes [21-23].

Glassy carbon electrodes (GCE) **(Fig. 1.1)** have good mechanical strength and excellent electrical conductivity. In addition, wide potential range, chemically passive, and reproducible performance are some attractive features for their extensive use in the electrochemical investigation of various molecules. Glassy carbon is an amorphous form of carbon and is formed by carbonizing phenolic resins, which are made by reacting phenols with cellulosic aldehydes and ketones. The premodeled polymeric resin body is used for the preparation of glassy carbon using carbonization process at inert atmosphere [24]. In this process, oxygen, nitrogen and hydrogen are completely removed by very slow heating in the temperature range 300-1200 °C. The resultant

glassy carbon has high density and small pore size and exhibits labyrinthine ribbon like cross-linked graphite like sheets. It is a kind of synthetic polymer of carbon that can substitute graphite as an electrode. GCE are used in various electrochemical technologies, including electroanalysis, energy storage devices and electrosynthesis. GCE has also been used in the simultaneous oxidation of natural antioxidants [25], detection of insulin [26], sonoelectrocatalysis of oxygen reduction, hydrogen peroxide formation [27] and electroanalysis of hydrazine [28]. Many electrochemical DNA biosensors and glucose biosensor [29] based on modified GCE have an advantage over other electrodes in electroanalytical studies as their surface can be easily renewed after every run.

Fig. 1.1 Glassy carbon electrode used for electrochemical studies.

Carbon based electrodes have multiplied in their forms and nature in the last few decades. A close observation reflects that there are different types of carbon based working electrodes originated over the last few years, considerably changing the scope and sensitivity of electroanalytical techniques. Carbon electrodes are most extensively used working electrodes in electroanalytical chemistry [30] because of the fact that besides other electrode properties this material also has a wide potential window, surface functional groups for chemical modification and controllable surface activity resulting from pretreatment [31-34]. It is morphologically diverse; existing in a variety of forms suitable for electrochemical applications such as glassy carbon [35-38], carbon fibres [39-42], carbon films, graphite pastes and composites [43-47]. Moreover, carbon materials are economical and easy to use. In the present studies, pyrolytic graphite electrode (PGE) is used as the working electrode hence, its general characteristics are described below.

Pyrolytic graphite is a highly oriented polycrystalline form of carbon, which is widely used as a substrate for electrode modification and high temperature substance due to its thermal and conducting properties. In the temperature range 1900-2500 ºC, the thermal decomposition

(pyrolysis) of carbonaceous gases under reduced pressure is most popular method used for the production of pyrolytic graphite. The pyrolytic graphite thus produced is anisotropic in nature with highly ordered hexagonal carbon rings parallel to the surface of the substrate. Edge and basal plane pyrolytic graphite are fabricated from highly oriented pyrolytic graphite (HOPG). In the construction of edge plane pyrolytic graphite electrode (EPPGE) from HOPG, the perpendicular graphite layers to the disc surface are used, and the exposing edges of the graphite layers contain surface defects, while a basal plane pyrolytic graphite electrode (BPPGE) is prepared by the graphite layers that lie parallel to the surface. The nature of chemical bonding present in graphite is responsible for the different electrochemical properties of the two planes, edge and basal. Different carbon materials have different density of the edge and basal planes. For electrochemistry, the edge plane of pyrolytic graphite layers displays considerably high electrocatalytic activity in comparison to the basal plane. The present studies are mainly based on using EPPGE as the working electrode and the two planes of pyrolytic graphite are represented in **Fig. 1.2**.

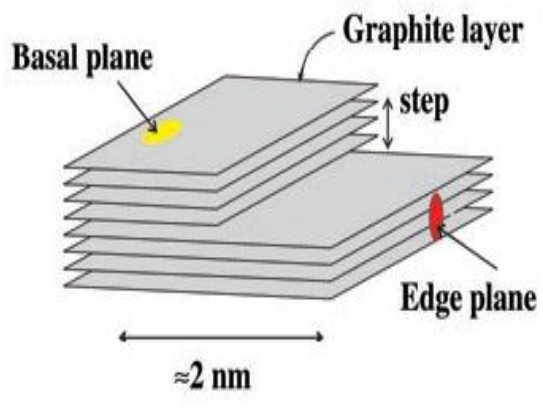

Fig. 1.2 A typical representation of layered structure of pyrolytic graphite.

The applicability of PGE in electrochemical investigations, such as norfloxacin detection [48], direct electron transfer reaction of proteins (e.g. fructose dehydrogenase, hemoglobin, myoglobin and cytochrome c_3**)** [49-51], oxidation of deoxyribonucleic acid [52], direct voltammetric determination of glycoprotein [53], determination of guanine in the presence of guanosine [54], and electroanalytical chemistry of various small biological molecules [55, 56] is attributed to its wide available potential window [57]. It has also been successfully applied as biosensors [58, 59] and electrochemical atomic force microscopic studies of DNA (ssDNA or dsDNA) adsorbed at pyrolytic graphite surface have also been reported in literature [60, 61].

1.3 SURFACE MODIFIERS

The development of various sensors using nanomaterials and electroactive polymers ushered electroanalytical chemistry into its present shape to investigate various electrochemical phenomena occurring in the living systems. In the present investigation, different types of nanomaterials and electroactive polymers are employed for the surface modification. Single wall carbon nanotubes (SWNT), multi wall carbon nanotubes (MWNT), gold (Au) nanoparticles and electroactive polymers play an important role in the fabrication of different electrodes. An overview of these materials exercised in the present dissertation is given in following paragraphs.

Carbon nanotubes (CNTs), one of the allotropes of carbon are hollow cylindrical structures formed by the rolling of graphene sheet with sp^2 and sp^3 bonding. Circular curvature causes quantum confinement and σ-π rehybridization with three σ bonds out of plane and π orbitals delocalized outside the tube, which gives them most interesting properties like high mechanical strength, high thermal and electrical conductivity [62]. The length of the tube can be several hundred times more than its width, which gives CNTs a high aspect ratio. CNTs are mainly classified as SWNT and MWNT. SWNT are constructed of a single sheet of graphite of diameter 0.4-2 nm (**Fig. 1.3(A)**), while MWNT consists of multiple concentric graphite cylinders of increasing diameter of 2-100 nm (**Fig. 1.3(B)**). In terms of electronic properties, SWNT are well-defined system as compared to MWNT. SWNT also have quantum dots and wires at very low temperatures. Several methods are employed for the synthesis of CNTs, which include carbon arc process, chemical vapour deposition and pulse laser deposition technique. CNTs are highly attractive for research due to their remarkable properties like small size, high strength to weight ratio, high transport coefficient etc., which make them appropriate candidate for different applications [63]. Due to their highly desirable properties, CNTs have profound applications such as catalyst support materials for different types of fuel cells [64], nanoelectronics [65], field emission [66], nanofluids [67], chemical as well as physical sensors [68] and hydrogen storage [69]. Recently, attention has been focused on the investigation of the properties and applications of novel nanocomposites made up of one dimensional functionalized CNTs and three dimensional nanocrystalline metals, nanocrystalline metal oxides and polymers. CNTs can serve as an excellent material for the development of biochemical sensors and as a modifier to enhance the electrode kinetics between various electroactive species and the underlying electrode [70].

In recent years, various metal based nanoparticles have been synthesized and these materials provide new dimensions to the electrochemical sensing and other growing field such as

catalysis [71-81]. Among these nanosized materials, gold nanoparticles having sizes from 1.5 to ~100 nm are probably the most extensively investigated systems as a result of their intriguing properties and fascinating applications [82]. Various properties of Au nanoparticles such as excellent chemical stability, biocompatibility, surface plasmon resonance effect and unique catalytic activity have enabled a broad range of applications in areas that include biomedical research [83], electronics [84], information storage [85] and photovoltaic devices [86]. Notable examples include cancer diagnosis [87], molecular ruler [88], DNA sequence detection [89], low-temperature catalysis for the conversion of CO to CO_2 [90] as well as thermal [91] and colorimetric sensing [92]. Not surprisingly, these fascinating applications have fueled research related to the preparation of Au nanoparticles with different sizes, shape, and assorted functionalities [93].

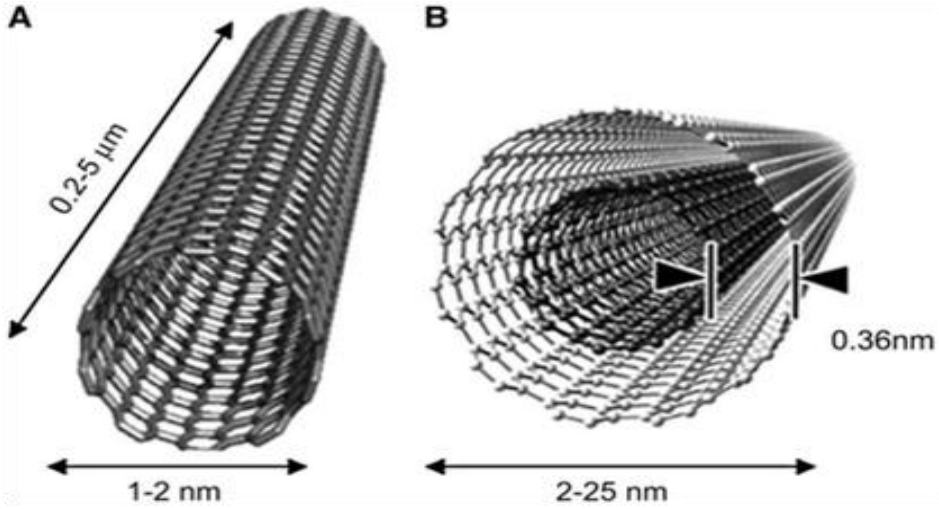

Fig. 1.3 Conceptual diagram of (A) single wall carbon nanotube and (B) multi wall carbon nanotube.

Electroactive polymers have attained remarkable attention from researchers since their discovery in 1977. Since then technological applications including artificial muscles, modification of electronic devices, energy storage and solar cells have bestowed new avenues for scientific communities to investigate and develop new materials based on electroactive polymers. Most frequently used electroactive polymers are shown in **Fig 1.4**. High thermal and chemical stability, mechanical flexibility as well as good electrical conductivity are the most important features, which are attributed to the widespread use of these materials. Also, ease of preparation of polymer films is another important factor. The advantage of electroactive polymers modified electrodes over conventional materials (metal or GCE electrodes) is attributed to the electrocatalytic

ability. Wide multifunctionality leads to the diverse possibilities in applications of electroactive polymers in specialized field such as biosensors, light emitting diodes (LEDs), field effect transistor (FETs), electrochromic displays and smart windows, toxic waste cleanup, supercapacitors, corrosion inhibitors and electromagnetic interference (EMI) shielding etc. [94-104].

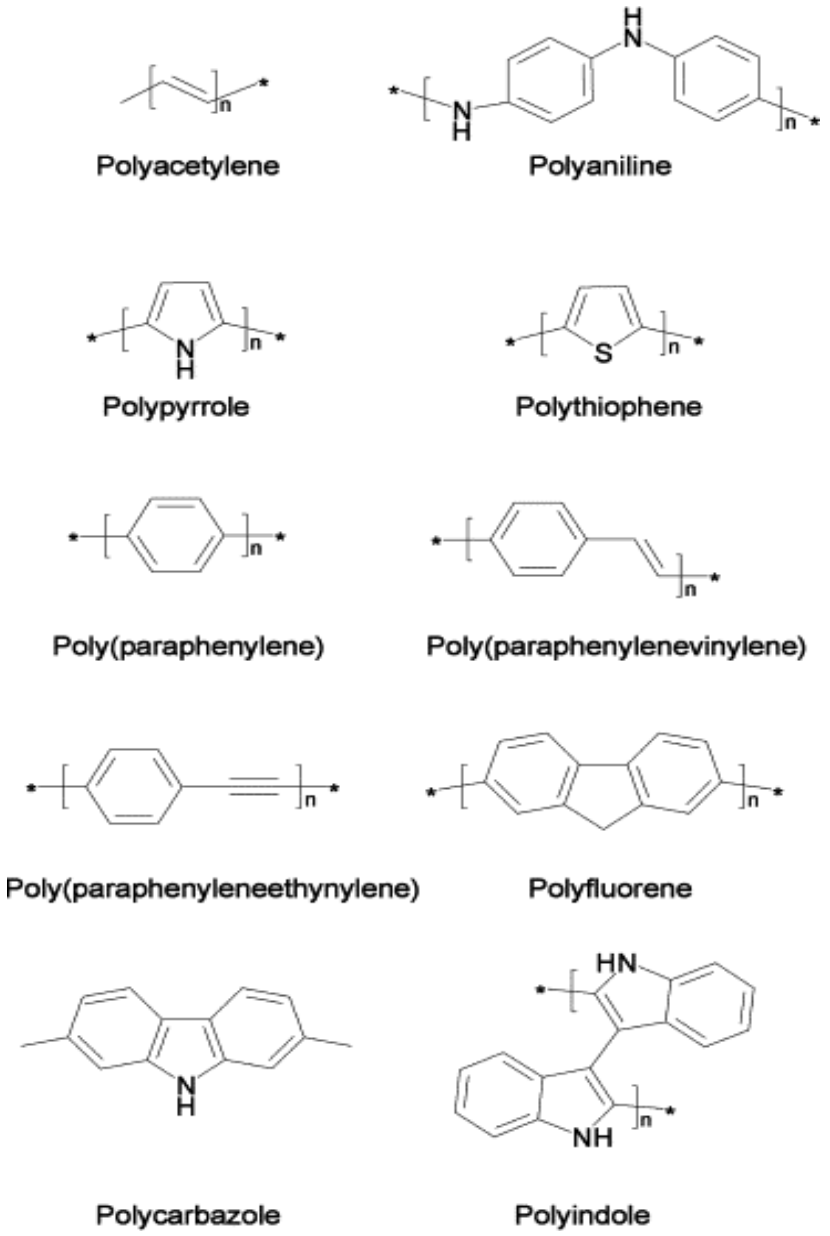

Fig 1.4 Some common electroactive polymers used for the surface modification.

1.4 MODIFIED ELECTRODES

In analytical chemistry, electron transfer mediators used for the modification of electrodes are often responsible for the enhancement of the sensitivity (current) and selectivity of the

electrochemical method. In addition, these mediators improve the electrochemical stability, as well as offer a larger usable potential window and decrease the fouling effect. Electrochemical quantification utilizing mercury-based electrodes, for example, has been used for the detection of thiols and disulfides in complex matrices, including biological fluids [105]. The electrodes based on carbon substrates are preferentially used modified electrodes in electrochemical techniques due to their commercial feasibility, wide potential range, low electrical resistivity and versatility of chemical modification. Various applications of nanomaterials in the field of electronic, optical and mechanical devices and sensors are attributed to their structure-, size- and shape- dependant electronic, optical and magnetic properties, which are different from those of the bulk materials [106, 107]. These nanomaterials significantly contribute to the enhancement of electrocatalytic responses towards the electrochemical reactions of biomolecules such as dopamine [108-116], ascorbic acid [117], adenosine [118], epinephrine [119], norepinephrine [120], uric acid [121], nicotinamide adenine dinucleotide [122], deoxyribose nucleic acid [123, 124] and proteins [125-131]. Above examples extensively demonstrated and regarded as one of their characteristics, resulted from the excellent electrical conductivity, ultra-small size, high surface area, and good biocompatibility of these materials. Among these, Au nanoparticles are the most stable metal nanoparticles and have been exploited as one of the most popular nanomaterials due to their ability to enhance the electrode conductivity by facilitating electron transfer and thus, improve the electrochemical sensitivity and selectivity [132]. The electrochemical and electrocatalytic properties of modified electrodes strongly depend on the novel fabrication procedures and nanomaterials as well as substrate because a slight change in the modification approach can alter the properties of the modified electrode. For instance, the Au nanoparticle-modified indium tin oxide (ITO) electrode prepared by thiol linker molecules, such as (3-mercaptopropyl) trimethoxysilane shows different morphological structure and electrochemical behavior in comparison to the electrode prepared by direct deposition of Au nanoparticles e.g. electrodeposition [133, 134]. Moreover, in the presence of ascorbic acid, it is also found that ITO electrode has good selectivity for the voltammetric determination of neurotransmitters, which is hardly achieved using Au [113, 114], or platinum [135] electrode. Recently, Natan and co-workers have developed Au nanoparticle modified SnO_2 electrode for the direct electron transfer (DET) of redox protein (horse heart cytochrome *c*) to the surface of electrode [125]. Another important work by Pingarron *et al.* and Chen *et al.* using Au nanoparticles immobilized cysteamine modified gold electrode have discussed different strategies for the construction of amperometric

enzymic biosensor [136, 137]. In recent time, Merkoci *et al.* successfully applied Au nanoparticles for the electrochemical sensing of DNA [138]. Furthermore, the authors also discussed some novel strategies using Au nanoparticles, for the detection of DNA. In addition, Au nanoparticles are widely used as an excellent therapeutic agent due the fact that these particles have non-cytotoxicity as well as good biocompatibility, and bear the ability to conjugate with small biomolecules including proteins, enzyme and amino acids. Hence, the development of Au nanoparticles with different morphologies and electrochemical properties provides more novel and sensitive electrochemical sensing strategies, which results in the deeper development of nanobioelectrochemistry.

The usefulness of carbon nanotubes (CNT) is attributed to their extraordinary mechanical and unique electrochemical properties, which have garnered much attention in the past 5 to 10 years. [139]. CNTs present the most common carbon based nanomaterial for the surface modification of electrodes. These have single layer cylinder extending from end to end with excellent uniformity in diameter (down to 7 nm). An ab initio study of water adsorbed on single walled carbon nanotubes shows purely repulsive interaction without any charge transfer, which indicates that intrinsic electronic properties of carbon nanotubes remain unaffected even when they are in direct contact with water. This finding revealed new avenues for the application of carbon nanotubes film modified electrodes as biosensors in aqueous medium. Metal impurities in CNTs samples have been proposed as a potential reason for the high electrocatalytic activity of CNTs. Incorporation of gold nanoparticles in the CNTs has been found to enhance the electrocatalytic properties of the modified electrodes. Recent studies have revealed that CNTs exhibit strong electrocatalytic activity for various compounds, including neurotransmitters [140], NADH [141, 142], hydrogen peroxide [143, 144], ascorbic acid [145], amino acids [146], DNA [147] etc. It is suggested that the ends of CNTs are responsible for their electrocatalytic properties [141].

Since last 20 years, electroactive polymers including polyDAN, polyaniline, polypyrrole, polythiophene and polyindole have been exclusively utilized in sensing applications for biomolecules as signal transducers. The most important example of polymer based sensor is commercially available glucose sensing meters used by diabetic patients. These sensors contain a film of glucose oxidase or glucose dehydrogenase and polymeric mediators. Another significant example is of electronic noses, which are used in quality control and environmental monitoring and use thin film arrays of electroactive polymers [148]. These technologies are now under process in clinical trials for the determination of volatile biomarkers for diseases, especially lung cancer.

Recently, P3MTH films have been applied for the electrochemical oxidation of neurotransmitters in the presence of catechols and ascorbic acid. In the voltammograms, it is observed that the peaks of ascorbic acid, catechol, and *p*-aminophenol are separated from each other, which are contrary to glassy carbon electrodes and thus, these polymeric films offer selectivity to the sensor. Furthermore, electrocatalytic activity of P3MTH films for the detection of dopamine, l-dopa, ascorbic acid and chlorpromazine has also been investigated. The oxidation of these molecules was catalyzed by the electroactive polymer film. These compounds showed a linear voltammetric response for their respective oxidation in the concentration range 10^{-6} to 10^{-5} M. Detection of some biomolecules, such as dopamine, serotonin, uric acid, epinephrine and nitrite in the presence of ascorbic acid are notable examples reported using modified electrodes based on the electroactive polymers incorporating nanoparticles or CNTs. The nanoparticles are responsible for the improved sensitivity of the electrodes, whereas electroactive polymers play an important role in the improvement of peak separation in voltammograms [149-151].

1.5 ELECTROCHEMICAL TECHNIQUES

Electrochemical techniques, in a nutshell, are cost effective and more sensitive and can be used for the rapid and trace analysis of various electrochemically active species. These techniques have tremendous commercial potential in various fields such as pharmaceuticals, biotechnology and energy storage. Electroanalytical techniques are rationally based on the principle of polarography, which was discovered by Czech scientist Jaroslav Heyrovsky in early 1920s. The term “polarography” is generally referred to the technique employing a dropping mercury electrode as a working electrode. In 1959, Heyrovsky was awarded the Nobel Prize in chemistry for his authoritative work on this electroanalytical technique. Later, more advanced techniques were developed using solid electrodes for studying the oxidation/reduction reactions. Among these techniques, voltammetry is the most extensively used due to the following distinct advantages:

1. These techniques have been widely used and have made incredible contributions in the study of electrochemical reactions, electrochemically generated free radicals, enzymatic catalysis, solar energy conversion, environmental monitoring, industrial quality control and for the determination of trace concentration of biological and clinically important compounds because they fulfill the requirements of accuracy and sensitivity.
2. The sensitivity of the voltammetric techniques is proficient and can be enhanced more by the modifications of techniques (fabrication of electrodes using nanomaterials, composite

membrane and polymer films) that significantly increase the selectivity as well as the sensitivity of the method.

3. Analytical properties for the analysis of complex mixtures in different compounds are increased by incorporating these techniques with various separation methods such as flow injection, high performance liquid chromatography and capillary electrophoresis.
4. These techniques can be applied for the analysis of turbid and colored solutions, which are difficult to analyze by other methods. In pharmaceutical analysis, the separation of the excipients is generally not required and this simplifies the procedure of analysis.
5. Only small volumes of samples are required for the analysis of analytes.
6. These techniques (especially voltammetric methods) continue to be a versatile tool for studying redox processes in various media, adsorption processes and electron transfer mechanism on the surfaces of modified electrodes.
7. These procedures have been developed for determining the very low concentration of analytes up to sub-μg/L level.
8. Also, these techniques require low cost of maintenance and environment friendly solvents are used in most of the cases.

These techniques are based on the measurement of current with varying potential due to the oxidation or reduction of chemical spices. The voltammetric experiments are carried out by using a three electrode single compartment electrochemical cell equipped with a working (indicator) electrode, a reference electrode, and usually a counter (auxiliary) electrode **(Fig. 1.5)**. At the suitable applied potential, the reduction or oxidation of an analyte is the main cause for the mass transport of new material to the surface of a working electrode and current is generated. In general, surface of the electrode acts as an interface, across which, the charge transfer takes place and its effects are felt.

At the first glance, various types of voltammetric techniques may appear to be very different but their fundamental principles and applications are derived from the same electrochemical concept. An overview of the electrochemical techniques used in the present investigation is described below.

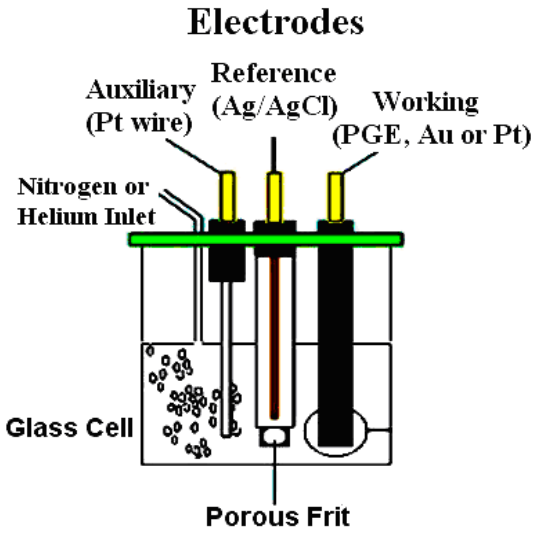

Fig. 1.5 Electrochemical cell setup commonly used in voltammetric experiments.

1.5.1 Linear Sweep Voltammetry (LSV)

LSV is based on the principle of linearly varying potential from an initial value (Initial E) to a final (Final E) value at a constant sweep rate, and the resulting current is measured as a function of applied potential. **Fig. 1.6** represents the potential wave form used in LSV.

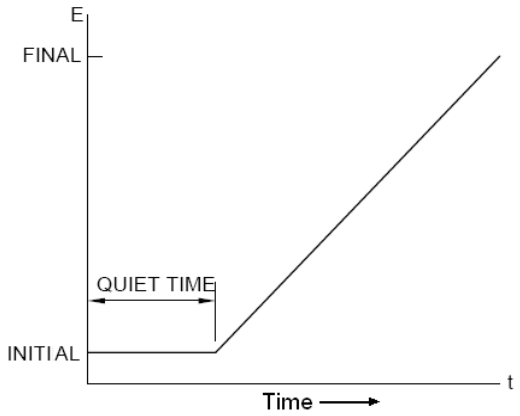

Fig 1.6 Potential wave form used in LSV.

Cyclic voltammetry (CV) is most commonly used variation of LSV. In CV, the scan direction is reversed at the final potential and it is swept again in the opposite direction. Hence, the product of the electrochemical reaction formed in the forward direction of scan can be analyzed in the reverse direction of scan. This characteristic feature is one of the important reasons for the widespread use of CV. The initial potential (Initial E), and High E and Low E (two switching potentials i.e., the potential where the direction of the scan is reversed) are normally required parameters in CV. **Fig. 1.7** depicts the potential wave form for CV. In the simplest I-E curve of

CV, diffusional mass transport is responsible for the asymmetry in the curve. However, there are many other factors that can affect the shape of this curve, which includes rate of heterogeneous transfer kinetics, stability of the oxidized or reduced species and adsorption. In a reversible electrochemical redox process, the rate of heterogeneous electron transfer is rapid (with respect to the timescale of the experiment) and both the oxidized and reduced species are stable (again, on the timescale of the experiment). The mean of the two peak potentials (E_{pa} and E_{pc}) is known as standard redox potential. The separation of the peak potentials is 59/n mV, where n stands for the number of electrons transferred per molecule).

Cyclic voltammetry (CV) has become an extraordinary and broadly applied electroanalytical technique in many areas of chemistry. It is widely used for obtaining information regarding the redox processes, reaction intermediates and products. However, for quantitative determinations, it is rarely used.

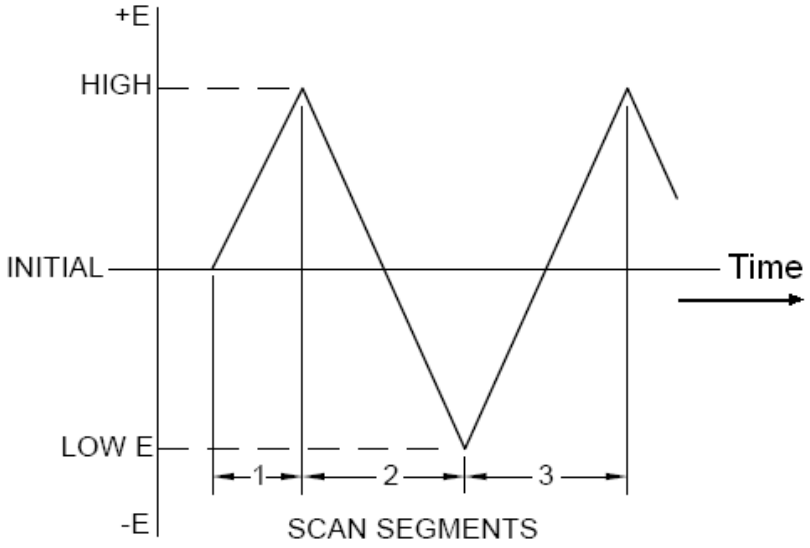

Fig 1.7 Potential wave form used in CV.

The study of the reactions of electrolyzed species is another important application of CV. These species are generated during the forward scan, and their reactivity can be monitored on the reverse and subsequent scans. It is often used as the first technique to characterize a redox system due to its simplicity and speed, and it is a very effective technique for qualitative analysis of kinetics and mechanism of an electrochemical reaction. However, digital simulation is generally required for the quantitative kinetic measurements utilizing CV, since there is no other way to separate the effects of slow electron transfer and chemical reactivity. Existence of charging current

in CV and LSV limits their usefulness as techniques for quantitative analysis in electroanalytical chemistry [152, 153].

In voltammetry, for a reversible reaction, the relation between concentration and peak current is expressed by the Randles-Sevcik (at 25 ºC) equation:

$$\boldsymbol{i_p = (269{,}000)\, n^{3/2} A\, D^{1/2} C\, v^{1/2}} \qquad \textbf{(1.1)}$$

where, i_p = peak current (A)

n = number of electrons transferred per molecule

A = electrode surface area (cm^2)

D = diffusion coefficient (cm^2/s)

C = concentration (mol/cm^3)

ν = scan rate (V/s)

Therefore, for a reversible process, i_p is proportional to the concentration, C, and the square root of the scan rate, $v^{1/2}$. The basis of determination by the voltammetry is the linear i_p vs. C relation.

1.5.2 Square Wave Voltammetry (SWV)

Square Wave Voltammetry (SWV) is interconnected with both A.C. voltammetric techniques and differential pulse techniques. In differential pulse voltammetry (DPV), a symmetric peak (current response) is observed as a result of effective discrimination against background charging currents. The foremost advantage of SWV is its high speed and sensitivity. The potential wave form used in SWV is shown in **Fig. 1.8**.

It depicts a square wave overlapped on a staircase wave form and can also be viewed as a series of pulses alternating in direction (hence, the relation to both DPV and A.C. techniques). At the end of each of the pulses or half-cycles, current is measured. The difference between the forward and reverse currents ($i_{for} - i_{rev}$) is used for the determination of net current (i_{net}), which is centered on the redox potential. The obtained current is directly proportional to the concentration of the electrochemically active molecules and hence, detection limits as low as 10^{-8} M is possible. The greater sensitivity of SWV in comparison to DPV is due to the fact that the difference in current is greater than either the forward or reverse currents for a reversible system. To investigate the reversibility of the electron transfer reaction, the magnitude of the reverse current can be used. The details of square wave voltammetry have been reported by many workers [154-157]. In the

present investigations, a bioanalytical system (BAS CV-50W) controlled *via* a computer is being used for carrying out voltammetric studies (**Fig. 1.9)**.

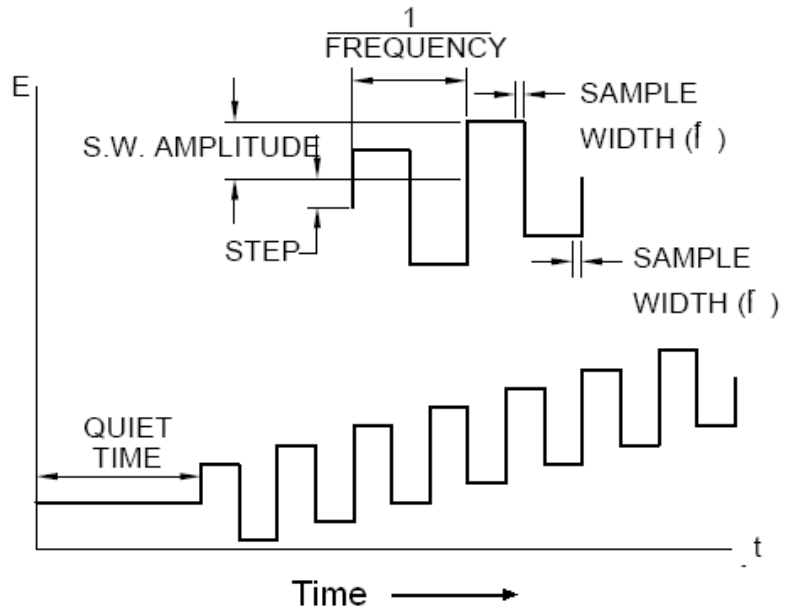

Fig. 1.8 Potential wave form used in SWV.

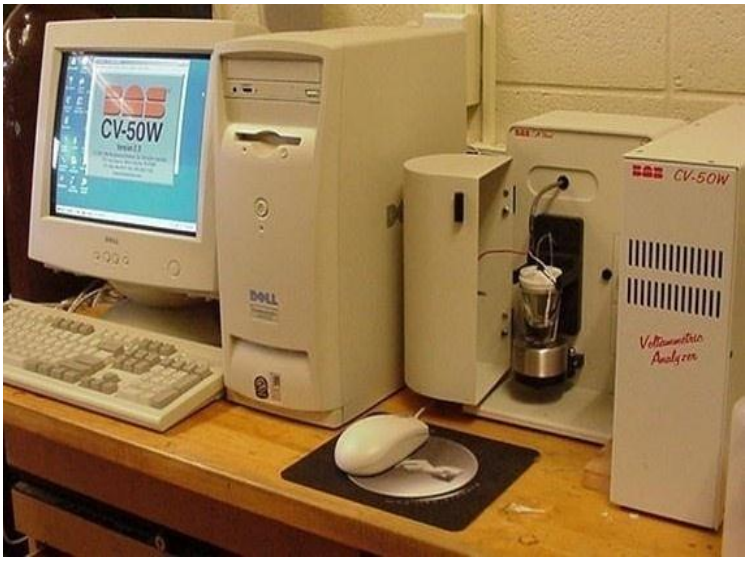

Fig. 1.9 Equipment set up used for electrochemical studies.

1.5.3 Controlled Potential Electrolysis (CPE)

Controlled potential electrolysis is performed at a constant potential and can be utilized to monitor the value of n (number of electrons transferred per molecule) and to prepare sufficient amount of oxidation or reduction products to allow their isolation and characterization [158-162].

The information regarding the number of electrons involved in a process is essential for the elucidation of mechanism of reaction. During this process, a potential is set at a constant value (sufficiently positive to the peak potential) for oxidation to proceed at rapid rate. This value of potential is maintained to oxidize the only species present in the electrolytic solution. The calculation of the total charge (Q) passed during the controlled potential electrolysis is carried out by using Faraday's law:

$$Q = n F N \qquad (1.2)$$

Where, F stands for the Faraday's constant (96500 C mol^{-1}), n is the number of electrons transferred per molecule and N refers the number of moles of the initially present species.

In controlled potential electrolysis, the cell is significantly different from the voltammetric experiments (in which electrolysis of a very small amount of electroactive analyte is carried out). Working electrode with large surface area (for example a pyrolytic graphite plate) and an auxiliary electrode with a large surface area (for example, platinum gauze) enhance the rate of electrolysis. Additionally, the rate of the mass transfer to the working electrode is increased by stirring of electrolytic solution.

The principles and other applications of controlled potential electrolysis are summarized by Lingane [163], Meites [164] and Bard and Santhanam [165]. Specific reviews cover the application of coulometry to clinical analysis [166], analysis of drugs [167] and general industrial analysis [168]. CPE has also been used for the oxidation of amino acids [169], study on bovine erythrocytes [170], elucidation of organic electroreduction mechanism [171] and determination of dyes [172]. The technique also finds its application in electrochemical gas sensor [173, 174] and methods adopted for the separation of actinide ions at the interface [175] of two immiscible electrolyte solutions.

1.6 ANALYTES OF INTEREST

Biomolecules are crucial organic molecules, which are found in all living systems. The functioning of normal life of a living system highly depends on the activity of these molecules. A small change in their concentration causes the alteration in their metabolic and biological activity that reflects as mental and physical disorders. Pharmaceutical drugs produce a biological signal or response as a result of their interaction with macromolecular targets. The resultant biological signals are used for diagnosis, prevention and treatment of diseases. The overdose of these drugs may cause several abnormalities and side effects because of their potential toxicity. Therefore, the

determination of biomolecules and drugs in biological samples and medicines is considered of great importance for human health, food assurance and quality control.

Antibiotics, also known as antibacterials, are the chemical substances, which are entirety or partially produced by chemical pathway or microorganisms. They are responsible for inhibition or destruction of microorganisms by intervening in their metabolic processes. Hence, they are most frequently prescribed medicines for the treatment of infections. In recent time, a number of antibiotics are available in the market and are used according to their course of action against an infection caused by microorganisms. Among them, fluoroquinolones (FQs) have emerged as one of the most extensively used synthetic antibiotics due to their broad-spectrum antibacterial activity and good oral absorption as well. Moreover, they are extensively used as both human and veterinary medications. These FQs selectively inhibit the replication of bacterial DNA by interfering with enzyme DNA gyrase or topoisomerase, which is necessary for the replication of DNA (**Fig. 1.10**). Generally, a unit of FQs consist of 4-oxo-1,4-dihydroquinoline, a piperazinyl group and a fluorine atom. **Norfloxacin** (NF) is an important member of FQs and is most frequently used for the treatment of gonorrhoea as well as eye and urinary tract infections. Overdose of NF may cause several side effects including nausea, diarrhea, dizziness, stomach cramp and headache. Recently, toxicity of FQs in human has been reported. Another important broad spectrum antibacterial drug is **sulfamethoxazole** (SMZ), which belongs to sulfa drugs or sulfonamides. Sulfonamides inhibit the enzyme dihydropteroate synthetase (converts PABA to dihydrophorate) by competitive antagonism of p-aminobenzoic acid (PABA) due to their analogy with PABA. The conversion of PABA to dihydrophorate by dihydropteroate synthetase is a key step for the synthesis of folic acid. Sulfonamides are commonly prescribed in combination with trimethoprim (TMP), which competitively inhibits the enzyme dihydrofolate reductase and blocks the folic acid metabolism. Hence, both the drugs synergistically prevent the synthesis of folic acid, which is necessary for the DNA synthesis. A schematic representation of the combined action of SMZ and TMP is shown in **Fig 1.11**. Sulfonamides are used for veterinary care as well as the treatment of human infections such as meningitis, acute otitis media, Whipple's disease, chronic bronchitis and rheumatic fever. They can accumulate in the food products such as eggs, milk, meat, honey and fish and cause several side effects including hypersensitivity reaction, gastro-intestinal distribution and hematological disorders. In addition, antibiotics in the environment may lead the development of antibacterial resistance in microorganisms. In the light of their positive as well as negative effects on the human health and environment, novel techniques for the

determination of antibiotics are needed to be developed. Hence, an attempt has been made in the present work to develop voltammetric sensors for the sensitive determination of NF and SMZ in human urine and pharmaceuticals [48, 176-178].

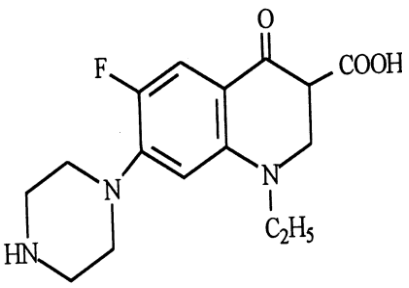

Norfloxacin

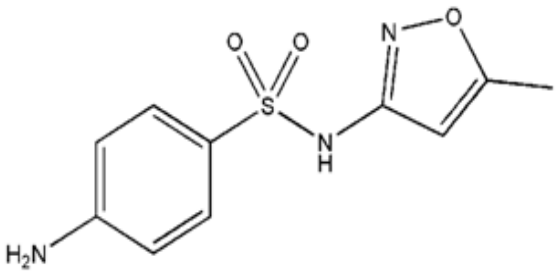

Sulfamethoxazole

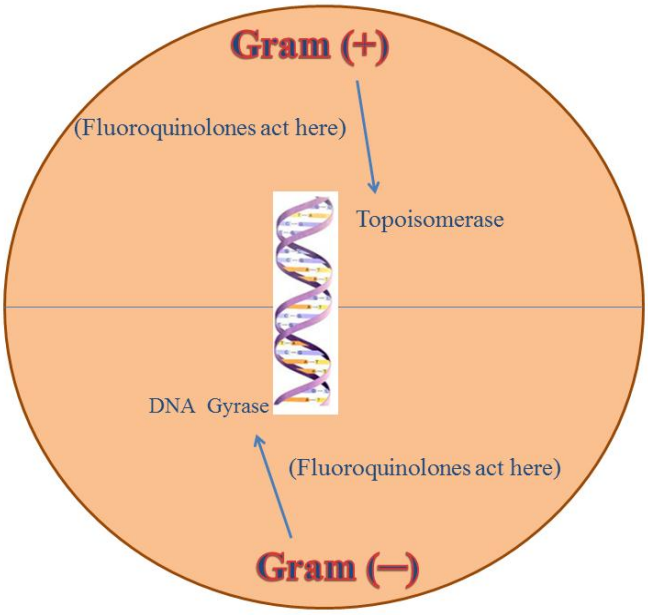

Fig 1.10 Mode of action of fluoroquinolones

Catecholamines are a class of biogenic amines that act as neurotransmitters. The catecholamines such as epinephrine, norepinephrine, and dopamine are all educed from L-tyrosine and contain a catechol (3, 4-dihydroxyphenyl) nucleus and an amine group. Aberrations in catecholamine concentrations have been implicated in the etiology of depression and related disorders. The hormone **epinephrine** (EPI, adrenaline) is commonly used as the drug of choice as a vasoconstrictor, cardiac stimulator and bronchodilator. In the condition of psychological stress,

EPI is exuded by the medulla of the adrenal gland along with norepinephrine. The important steps involved in the biosynthesis of EPI are shown in **Scheme 1.1**. Catecholamine levels are also used for the diagnosis and management of pheochromocytoma, a neuroendocrine tumor of the adrenal medulla. This tumor is signalized by elevated catecholamine levels in plasma, typically epinephrine and norepinephrine. EPI is a potent doping agent which has been banned by World Anti-Doping Agency (WADA). EPI plays a crucial role in the treatment of neurological disorders such as Parkinson's disease and Alzheimer's disease. In view of the importance of EPI in the human physiology and pharmacological process, an attempt has been made to compare the electrochemical and peroxidase catalyzed oxidation in this study [179-182].

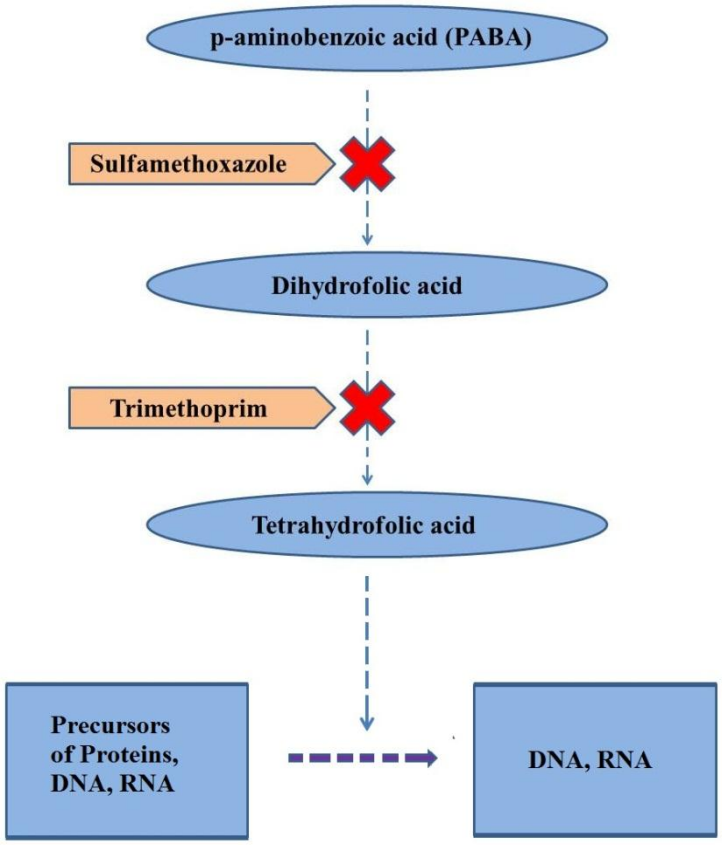

Fig. 1.11 A schematic representation of mechanistic pathway of Sulfonamides.

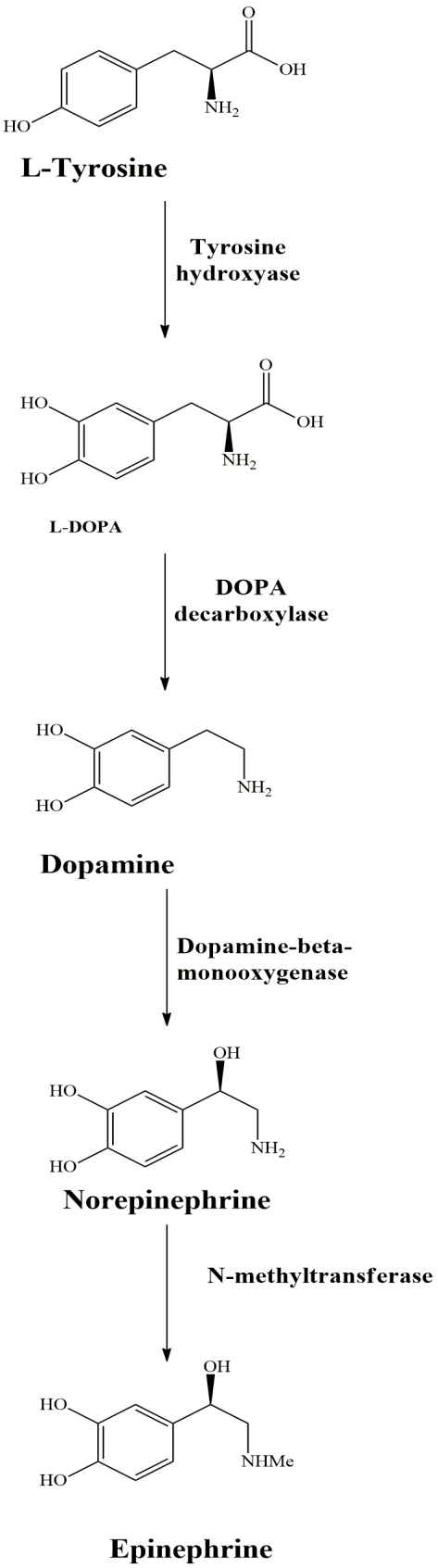

Scheme 1.1 Important steps involved in the biosynthesis of epinephrine.

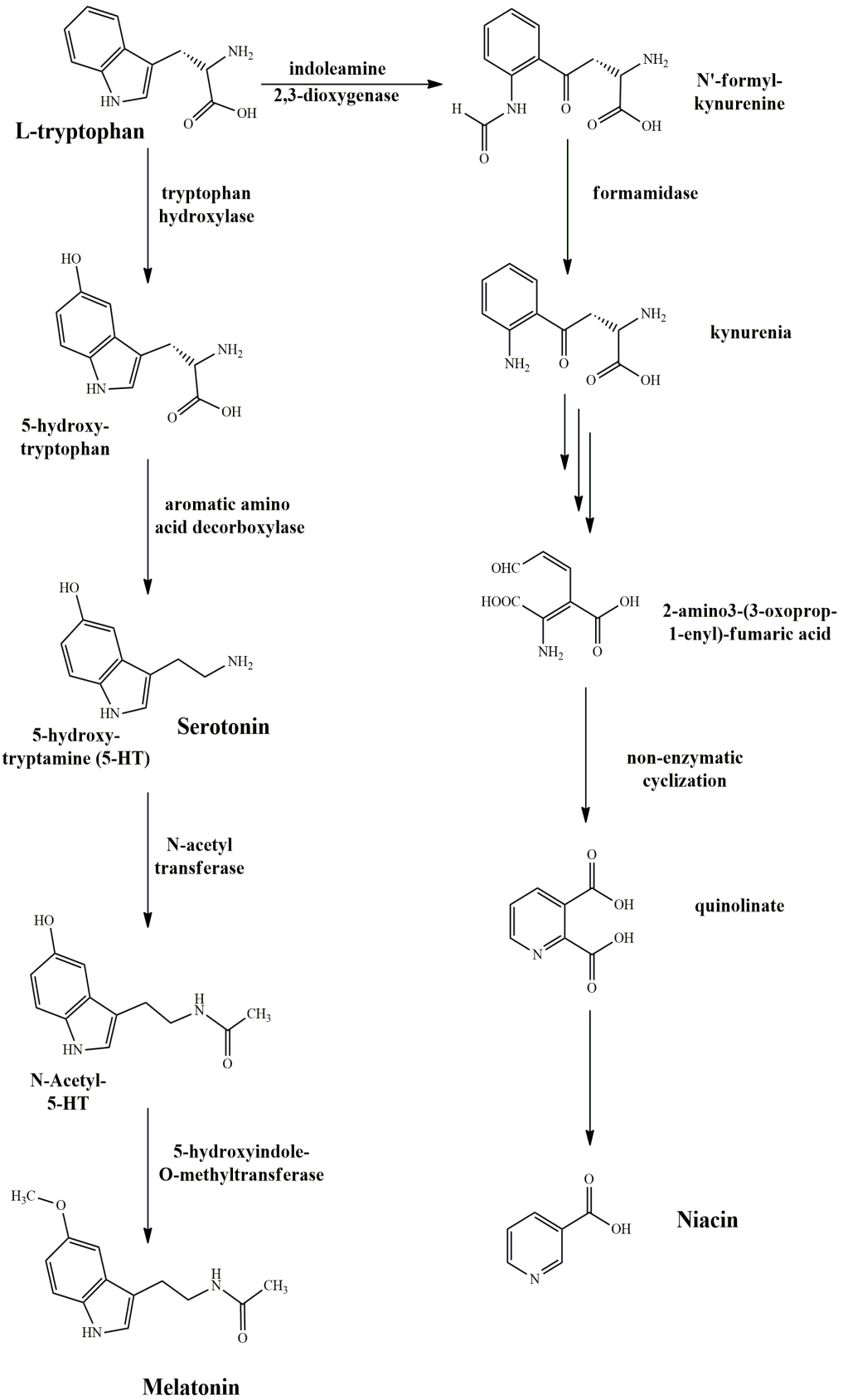

Scheme 1.2 Metabolism of tryptophan in biological systems.

Purine and pyrimidine nucleosides are integral part of nucleotides as well as deoxyribonucleic acid (DNA). Hence, they are considered as fundamental molecules in all biological system. They also exert metabolic and physiological effects in human system. The quantitative determination of these nucleosides is increasingly significant in the field of biomedical research and clinical diagnosis as small alteration in the level of these nucleosides in biological fluids indicate the presence of various diseases and genetic disorders. The increasing concentration of **adenine** nucleoside in biological fluids can be attributed to the damage of DNA. Adenosine and **adenosine-5′-monophosphate** (5′-AMP) have been found to quantitatively metabolize to end product (uric acid) within 15 to 30 min. after administration. The study of the formation of adenine nucleosides also helps to understand the consequence of DNA interactions with pharmaceuticals. Adenine combines with the sugar ribose to form adenosine, which in turn can be bonded with, from one to three phosphoric acid units, yielding the three nucleotides adenosine monophosphate (5′-AMP), adenosine diphosphate (5′-ADP) and adenosine triphosphate (5′-ATP) respectively. The most common isomer of adenosine monophosphate is 5′-AMP and is a component of several important coenzymes and in addition, plays a crucial role in the incorporation of amino acids into proteins. Thus, the simultaneous determination of adenine and 5′-AMP is the subject of considerable interest as these compounds occur simultaneously in body fluids [183, 184]. Thus, keeping in consideration the efficacy of these biomolecules in pharmaceutical industries and their application for biotechnology, a need was felt to develop a fast and sensitive method for the detection of these compounds.

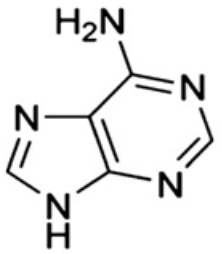

Adenine

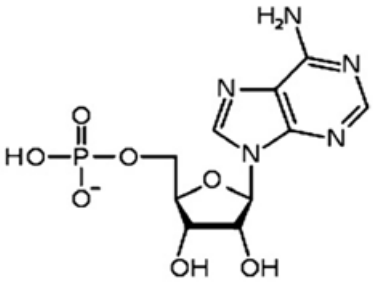

Adenosine monophosphate

Amino acids contain a basic amino group (−NH_2), an acidic carboxyl group (−COOH), and an organic R group (or side chain), that is unique to each amino acid. The polymerization of amino acids results in a specific protein. Each protein has a specific sequence of amino acids held together by peptide bonds. Hence, amino acids are denoted as building blocks of all vegetable and

animal protein. They also play important role as intermediates in metabolic reactions. Amino acids are categorized as essential and non-essential amino acids. A non-essential amino acid is defined as an amino acid that is synthesized in the body, whereas an essential amino, also known as indispensable is the one we must get through the food we eat because our body cannot make them. Hence, the intake of essential amino acids is necessary as a part of the food products and pharmaceutical preparations. Essential amino acids are associated with several functions in our body, such as muscle protein anabolism, protein synthesis, cell signaling, and regulation of hormone secretion. Among these essential amino acids, **tryptophan** (Trp) has an important place as a potent precursor of several metabolites including serotonin, melatonin and niacin as shown in **Scheme 1.2**. Clinically, it is used for the treatment of depression, schizophrenia and hypertension. Trp also influences the hair pigmentation. The concentration of amino acids present in the biological fluids is very low and their altered level causes metabolic disorders, therefore, the rapid and consistent quantitative determination of these amino acids in human body fluids and food products is highly desirable from the point of view of biochemical research and clinical purposes [185-188]. In view of this an attempt has been made in this dissertation to develop a sensitive sensor for the determination of Trp.

The most commonly used drugs for relieving the pain are analgesic drugs, also known as pain killer. Analgesics eliminate pain without affecting the brain (consciousness) are commonly known as non-steroidal anti-inflammatory drugs (NSAID). **Paracetamol** (PAR) and **aspirin** (ASP) are the most familiar example of NSAID and they relief from the pain by inhibiting the synthesis of prostaglandins. In addition, these drugs also exhibit antipyretic effect and PAR is also used to reduce fever and thus also acts as antipyretic drug. ASP in small quantity is used to prevent the heart stroke due to its anti-blood clotting property. **Caffeine** is a stimulant drug and is also used as analgesic adjuvant in combination with some other analgesic drugs (commonly PAR and ASP). It is most widely used stimulant drug that can be considered as a doping agent as its high doses produce ergogenic effects. Despite their several benefits, many disadvantages are also associated with their use, as their overdose cause several abnormalities, such as liver failure, sepsis, hypotension, arrhythmia and tachycardia. The multidrug formulations have been found to be more effective in relieving mild to moderate pain from certain muscle problems. They work by decreasing pain and inflammation, which helps muscle to relax. The combination of PAR, ASP and caffeine is used to treat pain caused by tension headaches, muscle aches, menstrual cramps, arthritis, toothaches, nasal congenstion and many more. The combination was one of the top-

selling over the counter medicine brands in the United States till late 2005 [189]. The caffeine has been found to increase the analgesic effect of ASP or PAR. However, these drugs may cause stomach and intestinal bleeding if taken more than recommended by a doctor. In few cases ASP may even cause a severe skin reaction. Hence, an attempt has been made in the present work for the simultaneous monitoring of the trace quantities in human body fluids and pharmaceutical preparations using voltammetric sensor and it is believed that the development of these voltammetric sensors will provide new insights to the biomedical research and quality control [190, 191].

1.7 SUBJECT MATTER OF THE THESIS

Determination of biological compounds of physiological importance always remains a challenging task for researchers as their concentration in biological fluids is normally very low. However, in the case of metabolic disorders and diseases, the concentration of these biomolecules gets abnormally altered. In such cases, detection of their concentration level proves out to be of diagnostic importance. Voltammetric sensors have been found to show consistently good results with high sensitivity and selectivity in such cases. Quantification of common drugs is important for pharmaceutical industry, and studies on the doping agents are needed to keep a check on the doping cases in sports. An attempt has been made in the present dissertation to develop simple, selective and sensitive sensors for the qualitative and quantitative analysis of biologically important compounds and drugs at nanomaterial/polymer film modified electrodes.

The results of the investigation have been organized in the dissertation as follows:

Chapter 1 Introduction.

Chapter 2 Voltammetric sensors for the determination of norfloxacin and sulfamethoxazole.

Chapter 3 Electrochemical and peroxidase-catalyzed oxidation of epinephrine.

Chapter 4 Application of modified pyrolytic graphite electrode as a sensor in the simultaneous assay of adenine and adenosine monophosphate.

Chapter 5 Effect of surface modification of indium tin oxide by nanoparticles on the electrochemical determination of tryptophan.

Chapter 6 Simultaneous monitoring of aspirin, paracetamol and caffeine in human urine at poly-1,5-diaminonapthalene modified pyrolytic graphite sensor.

1.8 REFERENCES

[1] V. S. Bagotsky; "Fundamentals of electrochemistry". Second Ed., John Wiley and Sons, New Jersey (2005).

[2] J. M. Saveant; "Elements of molecular and biomolecular electrochemistry: An electrochemical approach to electron transfer chemistry (Baker Lecture Series)". Wiley-Blackwell, New Jersey (2006).

[3] K. Rajeshwar, J. G. Ibanez; "Environmental electrochemistry: Fundamentals and applications in pollution sensors and abatement". Academic Press Inc., California (1997).

[4] O. M. Bockris, B. E. Conway, R. E. White; "Modern aspects of electrochemistry no. 34". Springer, New York (2001).

[5] G. Dryhurst; "Electrochemistry of Biological Molecules". Academic Press Inc., New York (1977).

[6] T. Ikeda, K. Kano; "An electrochemical approach to the studies of biological redox reactions and their applications to biosensors, bioreactors, and biofuel cells". *J. Biosci. Bioeng.*, **92** (2001) 9.

[7] B. J. Privett, J. H. Shin, M. H. Schoenfisch; "Electrochemical sensors". *Anal. Chem.*, **80** (2008) 4499.

[8] S. Wang, Y. Kang, L. Wang, H. Zhang, Y. Wang, Y. Wang; "Organic/inorganic hybrid sensors: A review". *Sens. Actuators B*, **182** (2013) 467.

[9] Z. G. Liu, X. J. Huang; "Voltammetric determination of inorganic arsenic". *Trends Anal. Chem.*, **60** (2014) 25.

[10] S. K. Yadav, P. Chandra, R. N. Goyal, Y. B. Shim; "A review on determination of steroids in biological samples exploiting nanobio-electroanalytical methods". *Anal. Chim. Acta*, **762** (2013) 14.

[11] F. Winquist, R. Bjorklund, C. K. Rulcker, I. Lundstrom, K. Ostergren, T. Skoglund; "An electronic tongue in the dairy industry". *Sens. Actuators B*, **111** (2005) 299.

[12] A. Hayat, G. Catanante, J. L. Marty; "Current trends in nanomaterial-based amperometric biosensors". *Sensors*, **14** (2014) 23439.

[13] A. Kamal, K. Kumar, V. Kumar, R. K. Mahajan; "Electrochemical and chromogenic sensors based on ferrocene appended chalcone for selective quantification of copper (II)". *Electrochim. Acta*, **145** (2014) 307.

[14] J. N. Babu, V. Bhalla, M. Kumar, R. K. Mahajan, R. K. Puri; "A chloride selective sensor based on a calix[4]arene possessing a urea moiety". *Tetrahedron Lett.*, **49** (2008) 2772.

[15] P. S. Ramanjaneyulua, P. Singh, Y. S. Sayi, H. M. Chawla, K. L. Ramakumar; "Ion selective electrode for cesium based on 5-(4-nitrophenylazo)25,27-bis(2-propyloxy)26,28-dihydroxycalix[4]arene". *J. Hazard. Mater.*, **175** (2010) 1031.

[16] V. Arora, H. M. Chawla, S. P. Singh; "Calixarenes as sensor materials for recognition and separation of metal ions". *ARKIVOC*, **2** (2007) 172.

[17] V. Suryanti, M. Bhadbhade, H. M. Chawla, E. Howe, P. Thordarson, D. S. Black, N. Kumar; "Novel colorimetric anion sensors based on N-acetylglyoxylic amides containing nitrophenyl signalling units". *Spectrochim. Acta Mol. Biomol.*, **121** (2014) 662.

[18] S. A. Ozkan, B. Uslu, H. Y. A. Enei; "Analysis of pharmaceuticals and biological fluids using modern electroanalytical techniques". *Crit. Rev. Anal. Chem.*, **33** (2003) 155.

[19] S. Jain, N. K. Jain, K. S. Pitre; "Electrochemical analysis of sparfloxacin in pharmaceutical formulation and biochemical screening of its Co(II) complex". *J. Pharm. Biomed. Anal.*, **29** (2002) 795.

[20] I. Siddiqui, K. S. Pitre; "Voltammetric determination of vitamins in a pharmaceutical formulation". *J. Pharm. Biomed. Anal.*, **26** (2001) 1009.

[21] B. Uslu, S. A. Ozkan; "Solid electrodes in electroanalytical chemistry: Present applications and prospects for high throughput screening of drug compounds". *Com. Chem. High T. Scr.*, **10** (2007) 495.

[22] B. Uslu, S. A. Ozkan "Electroanalytical application of carbon based electrodes to the pharmaceuticals". *Anal. Lett.*, **40** (2007) 817.

[23] M. A. Augelli, R. A. A. Munoz, E. M. Richter, A. G. Junior, L. Angnes; "Chronopotentiometric stripping analysis using gold electrodes, an efficient technique for mercury quantification in natural waters". *Electroanalysis*, **17** (2005) 755.

[24] J. C. Bokros; "Carbon biomedical devices". *Carbon*, **15** (1977) 353.

[25] A. J. Blasco, I. Barrigas, M. C. Gonzalez, A. Escarpa; "Fast and simultaneous detection of prominent natural antioxidants using analytical microsystems for capillary electrophoresis with a glassy carbon electrode: a new gateway to food environments". *Electrophoresis*, **26** (2005) 4664.

[26] Y. Wang, J. Li; "A carbon nanotubes assisted strategy for insulin detection and insulin proteolysis assay". *Anal. Chim. Acta*, **650** (2009) 49.

[27] B. Sljukic, C. E. Banks, S. Mentus, R. G. Compton; "Modification of carbon electrodes for oxygen reduction and hydrogen peroxide formation: The search for stable and efficient sonoelectrocatalysts". *Phys. Chem. Chem. Phys.*, **6** (2004) 992.

[28] K. I. Ozoemena; "Anodic oxidation and amperometric sensing of hydrazine at a glassy carbon electrode modified with cobalt (II) phthalocyanine-cobalt (II) tetraphenylporphyrin supramolecular complex". *Sensors*, **6** (2006) 874.

[29] Y. N. Zhu, T. Z. Peng, J. P. Li; "A glucose biosensor based on the enzyme electrode with carbon nanotube/platinum nanoparticle". *Chinese J. Analyt. Chem.*, **32** (2004) 1299.

[30] M. A. T. Gilmartin, J. P. Hart; "Sensing with chemically and biologically modified carbon electrodes: A review". *Analyst*, **120** (1995)1029.

[31] E. Sosa, G. Carreno, C. Ponce-de-Leon, M. T. Oropeza, M. Morales, I. Gonzalez, N. Batina; "Lead deposition onto fractured vitreous carbon: Influence of electrochemical pretreated electrode". *Appl. Surf. Sci.*, **153** (2000) 245.

[32] P. K. Brahman, R. A. Dar, S. Tiwari, K. S. Pitre; "Voltammetric determination of anticancer drug flutamide in surfactant media at polymer film modified carbon paste electrode". *Colloids Surf. A*, **396** (2012) 8.

[33] Y. Sallez, P. Bianco, E. Lojou; "Electrochemical behavior of *c*-type cytochromes at clay-modified carbon electrodes: A model for the interaction between proteins and soils". *J. Electroanal. Chem.*, **493** (2000) 37.

[34] M. Niculescu, T. Ruzgas, C. Nistor, I. Frebort, M. Sebela, P. Pec, E. Csoregi, "Electrooxidation mechanism of biogenic amines at amine oxidase modified graphite electrode". *Anal. Chem.*, **72** (2000) 5988.

[35] Z. Wang, D. Liu, S. Dong; "Study on adsorption and oxidation of calf thymus DNA at glassy carbon electrode". *Electroanalysis*, **12** (2000) 1419.

[36] Q. Fulian, R. G. Compton; "Laser activated voltammetry: Application to the determination of phenol in aqueous solution at a glassy carbon electrode". *Analyst*, **125** (2000) 531.

[37] M. H. Pournaghi-Azar, R. Ojani; "Electrochemistry and electrocatalytic activity of polypyrrole/ferrocyanide films on a glassy carbon electrode". *J. Solid State Electrochem.*, **4** (2000) 75.

[38] A. J. Downard, A. D. Roddick; "Protein adsorption at glassy carbon electrodes: The effect of covalently bound surface groups". *Electroanalysis*, **7** (1995) 376.

[39] R. S. Kelly, D. J. Weiss, S. H. Chong, T. Kuwana; "Charge-selective electrochemistry at high-surface-area carbon fibers". *Anal. Chem.*, **71** (1999) 413.

[40] W. C. Yang, A. M. Yu, Y. Q. Dai, H.Y. Chen; "Determination of hydrazine compounds by capillary electrophoresis with a poly (Glutamic Acid) modified microdisk carbon fiber electrode". *Anal. Lett.*, **33** (2000) 3343.

[41] B. D. Bath, D. J. Michael, B. J. Trafton, J. D. Joseph, P. L. Runnels, R. M. Wightman; "Subsecond adsorption and desorption of dopamine at carbon-fiber microelectrodes". *Anal. Chem.*, **72** (2000) 5994.

[42] E. Csoregi, L. Gorton, G. Marko-Varga; "Carbon fibers as electrode materials for the construction of peroxidase-modified amperometric biosensors". *Anal. Chim. Acta*, **273** (1993) 59.

[43] K. Kinoshita; "Carbon: Electrochemical and physicochemical properties". Wiley-Interscience, New York (1988).

[44] I. Gustavsson, K. Lundstrom; "A pyrolytic carbon film electrode for voltammetry-III: Application to anodic-stripping voltammetry". *Talanta*, **30** (1983) 959.

[45] R. N. Adams; "Carbon paste electrodes". *Anal. Chem.*, **30** (1958) 1576.

[46] F. Cespedes, F. Valero, E. Martinez-Fabregas, S. Alegret; "Fermentation monitoring using a glucose biosensor based on an electrocatalytically bulk-modified epoxy-graphite biocomposite integrated in a flow system". *Analyst*, **120** (1995) 2255.

[47] M. Pedrero, P. Mateo, C. Parrado, J. M. Pingarron; "Metallized graphite ethylene/propylene/diene tetra polymer composte electrodes as electrocatalytic amperometric detectors in flowing systems". *Quim. Anal.*, **19** (2000) 171.

[48] R. N. Goyal, A. R. S. Rana, H. Chasta; "Electrochemical sensor for the sensitive determination of norfloxacin in human urine and pharmaceuticals". *Bioelectrochemistry*, **83** (2012) 46.

[49] E. V. Ivanova, E. Magner; "Direct electron transfer of haemoglobin and myoglobin in methanol and ethanol at didodecyldimethylammonium bromide modified pyrolytic graphite electrodes". *Electrochem. Commun.*, 7 (2005) 323.

[50] M. Tominaga, C. Shirakihara, I. Taniguchi; "Direct heterogeneous electron transfer reactions and molecular orientation of fructose dehydrogenase adsorbed onto pyrolytic graphite electrodes". *J. Electroanal. Chem.*, **610** (2007) 1.

[51] J. Haladjian, K. Draqui, P. Bianco; "Electron transfer reaction of cytochrome c_3 at pyrolytic graphite electrodes". *Electrochim. Acta*, **36** (1991) 1423.

[52] L. L. Wu, J. Z. Zhou, J. Luo; "Oxidation and adsorption of deoxyribonucleic acid at highly ordered pyrolytic graphite electrode". *Electrochim. Acta*, **45** (2000) 2923.

[53] M. Trefulka, E. Palecek; "Direct chemical modification and voltammetric detection of glycans in glycoproteins". *Electrochem. Commun.*, **48** (2014) 52.

[54] G. Dryhurst; "Adsorption of guanine and guanosine at the pyrolytic graphite electrode: Implications for the determination of guanine in the presence of guanosine". *Anal. Chim. Acta*, **57** (1971) 137.

[55] S. Zhu, W. Qu, H. Chen; "Electroanalytical chemistry of small biological molecules: Molecular orientation and surface interaction of guanine, adenine and hypoxanthine on rough pyrolytic graphite electrode". *Huaxue Xuebao*, **51** (1993) 594.

[56] M. Hadi, A. Rouhollahi; "Simultaneous electrochemical sensing of ascorbic acid, dopamine and uric acid at anodized nanocrystalline graphite-like pyrolytic carbon film electrode". *Anal. Chim. Acta*, **721** (2012) 55.

[57] F. Wantz, C. E. Banks, R. G. Compton; "Edge plane pyrolytic graphite electrodes for stripping voltammetry: a comparison with other carbon based electrodes". *Electroanalysis*, **17** (2005) 655.

[58] A. Salimi, R. G. Compton, R. Hallaj; "Glucose biosensor prepared by glucose oxidase encapsulated sol-gel and carbon-nanotube-modified basal plane pyrolytic graphite electrode". *Anal. Biochem.*, **333** (2004) 49.

[59] L. Shang, X. Liu, C. Fan, G. Li; "A nitric oxide biosensor based on horseradish peroxidase/kieselguhr co-modified pyrolytic graphite electrode". *Anal. Chim.*, **94** (2004) 457.

[60] A. M. O. Brett, A. M. Chiorcea; "Atomic force microscopy of DNA immobilized onto a highly oriented pyrolytic graphite electrode surface". *Langmuir*, **19** (2003) 3830.

[61] J. Adamcik *et al*.; "Observation of single-stranded DNA on mica and highly oriented pyrolytic graphite by atomic force microscopy". *FEBS Lett.*, **580** (2006) 5671.

[62] M. Meyyappan; "Carbon nanotubes: Science and applications". CRC Press, Boca Raton, Florida (2004).

[63] P. M. Ajayan, O. Zhou; "Applications of carbon nanotube". In M.S. Dresselhaus, G. Dresselhaus, Ph. Avouris (Eds.), Carbon nanotubes, Springer, Berlin (2001).

[64] Z. Liu, X. Lin, J. Y. Lee, W. Zhang, M. Han, L. M. Gan; "Preparation and characterization of platinum based electrocatalysts on multiwalled carbon nanotubes for proton exchange membrane fuel cells". *Langmuir*, **18** (2002) 4054.

[65] P. Sharma, P. Ahuja; "Recent advances in carbon nanotube-based electronics". *M.R.S. Bulletin.,* **43** (2008) 2517.

[66] A. Buldum, J. P. Lu; "Electron field emission properties of closed carbon nanotubes". *Phys. Rev. Lett.,* **91** (2003) 236801.

[67] S. U. S. Choi, Z. G. Zhang, W. Yu, F. E. Lockwood, E. A. Grulke; "Anomalous thermal conductivity enhancement in nano-tube suspensions". *Appl. Phys. Lett.*, **79** (2001) 2252.

[68] M. Fuji, X. Zhang, H. Q. Xie, H. Ago, K. Takahashi, T. Ikuta, H. Abe, T. Shimizu; "Measuring the thermal conductivity of a single carbon nanotube". *Phys. Rev.,* **95** (2005) 065502.

[69] M. S. Dresselhaus, K. A. Williams, P. C. Eklund; "Hydrogen absorption in carbon materials". *M. R. S. Bull.,* **2** (1999) 45.

[70] Y. Zhang, Y. Cai, S. Su; "Determination of dopamine in the presence of ascorbic acid by poly(styrene sulfonic acid) sodium salt/single-wall carbon nanotube film modified glassy carbon electrode". *Anal. Biochem.*, **350** (2006) 285.

[71] S. K. Guin, H. S. Sharma, S. K. Aggarwal; "Electrosynthesis of lead nanoparticles on template free gold surface by potentiostatic triple pulse technique". *Electrochem. Acta*, **55** (2010) 1245.

[72] S. K. Guin, R. Phatak, J. S. Pillai, A. Sarkar, S. K. Aggarwal; "A mechanistic study on the effect of surface protecting agent on electrochristallization of silver nanoparticles". *RSC Adv.*, **4** (2014) 59927.

[73] S. K. Guin, S. K. Aggarwal; "Prospective use of the potentiostatic triple pulse strategy for the template-free electrosynthesis of metal nanoparticles". *RSC Adv.*, **4** (2014) 55349.

[74] Y. R. Kim, R. K. Mahajan, J. S. Kim, H. Kim; "Highly sensitive gold nanoparticle-based colorimetric sensing of mercury(II) through simple ligand exchange reaction in aqueous media". *ACS Appl. Mater. Interfaces,* **2** (2010) 292.

[75] A. Changotra, R. Gupta, S. Paul; "Selective oxidation of benzyl alcohol over hydroxyapatite-supported Au-Pd nanoparticles". *J. Appl. Chem.,* **3** (2014) 653.

[76] M. Gupta, S. Paul, R. Gupta; "SiO_2-Cu_2O: An efficient and recyclable heterogeneous catalyst for N-benzylation of primary and secondary amines". *Chinese J. Catal.*, **35** (2014) 444.

[77] A. Changotra, R. Gupta, S. Paul; "Reduction of carbon–carbon double bond in α,β-unsaturated ketones over bimetallic Pd and Au nanoparticles immobilized on amine-functionalized magnetite nanoparticles: A novel and highly active bimetallic catalyst". *Der. Pharam. Chemica.*, **6** (2014) 385.

[78] Y. Nakayama, M. Oyama; "Electrocatalytic oxidation of water observed on a nanogold/palladium electrode". *Chem. Commun.*, **49** (2013) 5228.

[79] M. Oyama, A. A. umar, M. M. Salleh, B. Y. Majlis; "Chemical synthesis of metal nanoparticles in aqueous solutions with the presence of some additives". *Sains Malays.*, **40** (2011) 1345.

[80] M. Panunzio, E. Tamanini, Y. S. Denis, F. M. Sabbatini; R. D. Fabio Z. Xia; "Palladium-catalyzed heteroatomic coupling mediated by microwave irradiation". *Synth. Commun.*, **37** (2007) 4239.

[81] P .R. Martins, L. M. C. Ferreira, K. Araki, L. Angnes; "Influence of cobalt content on nanostructured alpha-phase-nickel hydroxide modified electrodes for electrocatalytic oxidation of isoniazid". *Sens. Actuators B*, **192** (2014) 601.

[82] M. C. Daniel, D. Astruc; "Gold nanoparticles: assembly, supramolecular chemistry, quantum-size-related properties, and applications toward biology, catalysis, and nanotechnology". *Chem. Rev.*, **104** (2004) 293.

[83] P. Livisatos; "The use of nanocrystals in biological detection". *Nat. Biotechnol.*, **22** (2004) 47.

[84] T. Dadosh, Y. Gordin, R. Krahne, I. Khivrich, D. Mahalu, V. Frydman, J. Sperling, A. Yacoby, I. Bar-Joseph; "Measurement of the conductance of single conjugated molecules". *Nature*, **436** (2005) 677.

[85] R. J. Tseng, J. X. Huang, J. Ouyang, R. B. Kaner, Y. Yang; "Polyaniline nanofiber/gold nanoparticle nonvolatile memory". *Nano Lett.*, **5** (2005) 1077.

[86] T. Hasobe, H. Imahori, P. V. Kamat, T. K. Ahn, S. K. Kim, D. Kim, A. Fujimoto, T. Hirakawa, S. Fukuzumi; "Photovoltaic cells using composite nanoclusters of porphyrins and fullerenes with gold nanoparticles". *J. Am. Chem. Soc.*, **127** (2005) 1216.

[87] I. H. El-Sayed, X. H. Huang, M. A. El-Sayed; "Surface plasmon resonance scattering and absorption of anti-EGFR antibody conjugated gold nanoparticles in cancer diagnostics: Applications in oral cancer". *Nano Lett.,* **5** (2005) 829.

[88] C. Sonnichsen, B. M. Reinhard, J. Liphardt, A. P. Alivisatos; "A molecular ruler based on plasmon coupling of single gold and silver nanoparticles". *Nat. Biotechnol.,* **23** (2005) 741.

[89] S. J. Park, T. A. Taton, C. A. Mirkin; "Array-based electrical detection of DNA with nanoparticle probes". *Science*, **295** (2002) 1503.

[90] L. M. Molina, M. D. Rasmussen, B. Hammer; "Adsorption of O_2 and oxidation of CO at Au nanoparticles supported by TiO_2". *J. Chem. Phys.,* **120** (2004) 7673.

[91] M. Q. Zhu, L. Q. Wang, G. J. Exarhos, A. D. Q. Li; "Thermosensitive gold nanoparticles". *J. Am. Chem. Soc.,* **126** (2004) 2656.

[92] R. Elghanian, J. J. Storhoff, R. C. Mucic, R. L. Letsinger, C. A. Mirkin; "Selective colorimetric detection of polynucleotides based on the distance-dependent optical properties of gold nanoparticles". *Science*, **277** (1997) 1078.

[93] Y. Yin, C. Erdonmez, S. Aloni, A. P. Alivisatos; "Faceting of nanocrystals during chemical transformation: from solid silver spheres to hollow gold octahedral". *J. Am. Chem. Soc.,* **128** (2006) 12671.

[94] K. Arshak, V. Velusamy, O. Korostynska, K. O. Stasiak, C. Adley; "Conducting polymers and their applications to biosensors: Emphasizing on foodborne pathogen detection". *IEEE Sens. J.,* **9** (2009) 1942.

[95] B. Guoa, L. Glavas, A. C. Albertsson; "Biodegradable and electrically conducting polymers for biomedical applications". *Prog. Polym. Sci.,* **38** (2013) 1263.

[96] U. Riaz, C. Nwaoha, S. M. Ashraf; "Recent advances in corrosion protective composite coatings based on conducting polymers and natural resource derived polymers". *Prog. Org. Coat.,* **77** (2014) 743.

[97] R. Holzea, Y. P. Wu; "Intrinsically conducting polymers in electrochemical energy technology: Trends and progress". *Electrochim. Acta,* **122** (2014) 93.

[98] R. Ramya, R. Sivasubramanian, M. V. Sangaranarayanan; "Conducting polymers-based electrochemical supercapacitors-Progress and prospects". *Electrochim. Acta,* **101** (2013) 109.

[99] X. Li, Y. Wang, X. Yang, J. Chen, H. Fu, T. Cheng; "Conducting polymers in environmental analysis". *Trends Anal. Chem.,* **39** (2012) 163.

[100] S. Shin, J. Kim, Y. H. Kim, S. Kim; "Enhanced performance of organic light-emitting diodes by using hybrid anodes composed of graphene and conducting polymer". *Curr. Appl. Phys.*, **13** (2013) S144.

[101] K. Hayashid, Y. Matsuok; "Electromagnetic interference shielding properties of polymer-grafted carbon nanotube composites with high electrical resistance". *Carbon*, **85** (2015) 363.

[102] T. Y. Lee, Y. B. Shim; "Direct DNA hybridization detection based on the oligonucleotide-functionalized conductive polymer". *Anal. Chem.*, **73** (2001) 5629.

[103] A. A. Abdelwahab, Y. B. Shim; "Nonenzymatic H_2O_2 sensing based on silver nanoparticles capped polyterthiophene/MWCNT nanocomposite". *Sens. Actuators B*, **201** (2014) 51.

[104] D. M. Kig, H. B. Noh; "Applications of conductive polymers to electrochemical sensors and energy conversion electrodes". *J. Electrochem. Sci. Technol.*, **4** (2013) 125.

[105] H. M. A. Killa, D. L. Rabenstein; "Determination of selenols, diselenides, and selenenyl sulfides by reversed-phase liquid chromatography with electrochemical detection". *Anal. Chem.*, **60** (1988) 2283.

[106] C. R. Martin, D. T. Mitchell; "Nanomaterials in analytical chemistry". *Anal. Chem.*, **70** (1998) 322.

[107] A. N. Shipway, E. Katz, I. Willner; "Nanoparticle arrays on surfaces for electronic, optical and sensoric applications". *Chem. Phys. Chem.*, **1** (2000) 18.

[108] M. Lahav, A. N. Shipway, I. Willner; "Au-nanoparticle–bis-bipyridinium cyclophane superstructures: Assembly, characterization and sensoric application". *J. Chem. Soc., Perkin Trans. 2*, (1999) 1925.

[109] R. S. Chen, W. H. Huang, H. Tong, Z. L. Wang, J. K. Cheng; "Carbon fiber nanoelectrodes modified by single-walled carbon nanotubes". *Anal. Chem.*, **75** (2003) 6341.

[110] H. Luo, Z. Shi, N. Li, Z. Gu, Q. Zhuang; "Investigation of the electrochemical and electrocatalytic behavior of single-wall carbon nanotube film on a glassy carbon electrode". *Anal. Chem.*, **73 (**2001) 915.

[111] F. Valentini, A. Amine, S. Orlanducci, M. L. Terranova, G. Palleschi; "Carbon nanotube purification: preparation and characterization of carbon nanotube paste electrodes". *Anal. Chem.*, **75** (2003) 5413.

[112] M. D. Rubianes, G. A. Rivas; "Carbon nanotubes paste electrode". *Electrochem. Commun.*, **5** (2003) 689.

[113] C. R. Raj, T. Okajima, T. Ohsaka; "Gold nanoparticle arrays for the voltammetric sensing of dopamine". *J. Electroanal. Chem.*, **543 (**2003) 127.

[114] J. Wang, M. Li, Z. Shi, N. Li, Z. Gu; "Investigation of the electrocatalytic behavior of single-wall carbon nanotube films on a Au electrode". *Microchem. J.*, **73** (2002) 325.

[115] P. J. Britto, K. S. V. Santhanam, P. M. Ajayan; "Carbon nanotube electrode for oxidation of dopamine". *Bioelectrochem. Bioenerg.*, **41** (1996) 121.

[116] K. Wu, J. Fei, S. Hu; "Simultaneous determination of dopamine and serotonin on a glassy carbon electrode coated with a film of carbon nanotubes". *Anal. Biochem.*, **318** (2003) 100.

[117] J. S. Ye, Y. Wen, W. D. Zhang, L. M. Gan, G. Q. Xu, F. S. Sheu; "Selective voltammetric detection of uric acid in the presence of ascorbic acid at well-aligned carbon nanotube electrode". *Electroanalysis*, **15** (2003) 1693.

[118] A. Brajter-Toth, K. A. El-Nour, E. T. Cavalheiro, R. Bravo; "Nanostructured carbon fiber disk electrodes for sensitive determinations of adenosine and uric acid". *Anal. Chem.*, **72** (2000) 1576.

[119] F. C. Moraes, D. L. C. Golinelli, L. H. Mascaro, S. A. S. Machado; "Determination of epinephrine in urine using multi-walled carbon nanotube modified with cobalt phthalocyanine in a paraffin composite electrode". *Sens. Actuators B*, **148** (2010) 492.

[120] J. Wang, M. Li, Z. Shi, N. Li, Z. Gu; "Electrocatalytic oxidation of norepinephrine at a glassy carbon electrode modified with single-wall carbon nanotubes". *Electroanalysis*, **14 (**2002) 225.

[121] Y. Sun, J. Fei, K. Wu, S. Hu; "Simultaneous electrochemical determination of xanthine and uric acid at a nanoparticle film electrode". *Anal. Bioanal. Chem.*, **375** (2003) 544.

[122] S. Tian, J. Liu, T. Zhu, W. Knoll; "Polyaniline doped with modified gold nanoparticles and its electrochemical properties in neutral aqueous solution". *Chem. Commun.*, **7** (2003) 2738.

[123] J. Wang; "Nanoparticle-based electrochemical DNA detection". *Anal. Chim. Acta*, **500** (2003) 247.

[124] J. Li, H. T. Ng, A. Cassell, W. Fan, H. Chen, Q. Ye, J. Koehne, J. Han, M. Meyyappan; "Carbon nanotube nanoelectrode array for ultrasenstive DNA detection". *Nano Lett.*, **3** (2003) 597.

[125] K. R. Brown, A. P. Fox, M. J. Natan; "Morphology-dependent electrochemistry of cytochrome *c* at Au colloid-modified SnO_2 electrodes". *J. Am. Chem. Soc.*, **118** (1996) 1154.

[126] J. J. Davis, R. J. Coles, H. A. O. Hill; "Protein electrochemistry at carbon nanotube electrodes". *J. Electroanal. Chem.*, **440** (1997) 279.

[127] J. Wang, M. Li, Z. Shi, N. Li, Z. Gu; "Direct electrochemistry of cytochrome *c* at a glassy carbon electrode modified with single-wall carbon nanotubes". *Anal. Chem.*, **74** (2002)1993.

[128] P. Ugo, N. Pepe, L. M. Moretto, M. Battagliarin; "Direct voltammetry of cytochrome *c* at trace concentrations with nanoelectrode ensembles". *J. Electroanal.Chem.*, **560** (2003) 51.

[129] I. H. Min, L. Choi, K. S. Ahn, B. K. Kim, B. Y. Lee, K. S. Kim, H. N. Choi, W. Y. Lee; "Electrochemical determination of carbohydrate-binding proteins using carbohydrate-stabilized gold nanoparticles and silver enhancement". *Biosens. Bioelectron.*, **26** (2010) 1326.

[130] X. Han, W. Cheng, Z. Zhang, S. Dong, E. Wang; "Direct electron transfer between hemoglobin and a glassy carbon electrode facilitated by lipid-protected gold nanoparticles". *Biochim. Biophys. Acta*, **1556** (2002) 273.

[131] G. C. Zhao, L. Zhang, X. W. Wei, Z. S. Yang; "Myoglobin on multi-walled carbon nanotubes modified electrode: direct electrochemistry and electrocatalysis". *Electrochem. Commun.*, **5** (2003) 825.

[132] S. Guo, E. Wang; "Synthesis and electrochemical applications of gold nanoparticles". *Anal. Chim. Acta*, **598** (2007) 181.

[133] W. Cheng, S. Dong, E. Wang; "Gold nanoparticles as fine tuners of electrochemical properties of the electrode/solution interface". *Langmuir*, **18** (2002) 9947.

[134] M. S. El-Deab, T. Ohsaka; "An extraordinary electrocatalytic reduction of oxygen on gold nanoparticles-electrodeposited gold electrodes". *Electrochem. Commun.*, **4** (2002) 288.

[135] A. Ciszewski, G. Milczarek; "Polyeugenol-modified platinum electrode for selective detection of dopamine in the presence of ascorbic acid". *Anal. Chem.*, **71** (1999) 1055.

[136] H. Gu, A. Yu, H. Chen; "Direct electron transfer and characterization of hemoglobin immobilized on a Au colloid–cysteamine-modified gold electrode". *J. Electroanal. Chem.*, **516** (2001) 119.

[137] M. L. Mena, P. Yanez-Sedeno, J. M. Pingarron; "A comparison of different strategies for the construction of amperometric enzyme biosensors using gold nanoparticle-modified electrodes". *Anal. Biochem.,* **336** (2005) 20.

[138] M. T. Castaneda, S. Alegret, A. Merkoci; "Electrochemical sensing of DNA using gold nanoparticles". *Electroanalysis*, **19** (2007) 743.

[139] M. Valcarcel, C. Bartolome, S. S. Cardenas, C. B. Suarez; "Present and future applications of carbon nanotubes to analytical science". *Anal. Bioanal. Chem.,* **382** (2005) 1783.

[140] B. J. Sanghavi, O. S. Wolfbeis, T. Hirsch, N. S. Swami; "Nanomaterial based electrochemical sensing of neurological drugs and neurotransmitters". *Microchim. Acta*, **182** (2015) 1.

[141] M. Musameh, J. Wang, A. Merkoci, Y. Lin; "Low-potential stable NADH detection at carbon-nanotube-modified glassy carbon electrodes". *Electrochem. Commun.,* **4** (2002) 743.

[142] R. R. Moore, C. E. Banks, R. G. Compton; "Basal plane pyrolytic graphite modified electrodes: comparison of carbon nanotubes and graphite powder as electrocatalysts". *Anal. Chem.,* **76** (2004) 2677.

[143] J. Wang, M. Musameh; "Carbon nanotube/teflon composite electrochemical sensors and biosensors". *Anal. Chem.,* **75** (2003) 2075.

[144] S. Hrapovic, Y. Liu, K. B. Male, J. H. T. Luong; "Electrochemical biosensing platforms using platinum nanoparticles and carbon nanotubes". *Anal. Chem.,* **76** (2004) 1083.

[145] Z. H. Wang, J. Liu, Q. L. Liang, T. M. Wang, G. Luo; "Carbon nanotube-modified electrodes for the simultaneous determination of dopamine and ascorbic acid". *Analyst,* **127** (2002) 653.

[146] J. X. Wang, M. X. Li, Z. J. Shi, N. Q. Li, Z. N. Gu; "Electrochemistry of DNA at single-wall carbon nanotubes". *Electroanalysis,* **16** (2004) 140.

[147] M. L. Pedano, G. A. Rivas; "Adsorption and electrooxidation of nucleic acids at carbon nanotubes paste electrodes". *Electrochem. Commun.,* **6** (2004) 10.

[148] A. M. Horgan, J. D. Moore, J. E. Noble, G. J. Worsley "Polymer- and colloid-mediated bioassays, sensors and diagnostics". *Trends Biotechnol.,* **28** (2010) 485.

[149] U. Lange, N. V. Roznyatovskaya, V. M. Mirsky; "Conducting polymers in chemical sensors and arrays". *Anal. Chim. Acta,* **614** (2008) 1.

[150] M. Ates; "A review study of (bio) sensor systems based on conducting polymers". *Mater. Sci. Eng. C*, **33** (2013) 1853.

[151] F. Branzoi, V. Branzoi, A. Musina; "Coatings based on conducting polymers and functionalized carbon nanotubes obtained by electropolymerization". *Prog. Org. Coat.*, **76** (2013) 632.

[152] R. S. Nicholson, I. Shain; "Theory of stationary electrode polarography: Single scan and cyclic methods applied to reversible, irreversible and kinetic systems". *Anal. Chem.*, **36** (1964) 706.

[153] R. H. Wopschall, I. Shain; "Adsorption effects in stationary electrode polarography with a chemical reaction following charge transfer". *Anal. Chem.*, **39** (1967) 1535.

[154] L. Ramaley, M. S. Krause; "Theory of square wave voltammetry". *Anal. Chem.*, **41** (1969) 1362.

[155] R. A. Osteryoung, J. Osteryoung; "Pulse voltammetric methods of analysis". *Phil. Trans. R. Lond. A*, **302** (1981) 315.

[156] J. Osteryoung, J. J. O Dea; "In Electroanalytical chemistry". Marcel Dekker, New York (1986).

[157] A. Chen, B. Shah; "Electrochemical sensing and biosensing based on square wave voltammetry". *Anal. Methods*, **5** (2013) 2158.

[158] P. T. Kissinger, W. R. Heineman (Eds.); "Laboratory techniques in electroanalytical chemistry". Marcel Dekker, New York (1984).

[159] J. E. Harrar, I. shain; "Electrode potential gradients and cell design in controlled potential electrolysis experiments". *Anal. Chem.*, **38** (1966) 1148.

[160] J. Janata, H. B. Mark Jr; "In Electroanalytical chemistry". Marcel Dekker, New York (1969).

[161] J. E. Harrar; "In Electroanalytical chemistry". Marcel Dekker, New York **(**1975).

[162] P. Delahay; "New instrumental methods in electrochemistry". Interscience, New York (1954).

[163] J. J. Lingane; "Electroanalytical chemistry". Inter science Publishers, New York (1958).

[164] L. M. Meites, A. Weissberger, B. W. Rossiter (Eds.); "In physical methods of chemistry". Wiley-Interscience, New York (1971).

[165] A. J. Bard, K. S. V. Santhanam; "Electroanalytical chemistry". Marcel Dekker, New York (1970).

[166] W. C. Purdy; "Application of coulometric titration to clinical and toxicological analysis". *Fresenius J. Anal. Chem.,* **243** (1968) 17.

[167] G. Patriarche; "Use of electroanalytical methods in biochemistry, pharmacy and toxicology". *Sci. Pharm. Proc.,* **2** (1966) 67.

[168] W. Buechler, P. Gisske, J. Meier; "Coulometric titration in industrial analysis". *Frenesius J. Anal. Chem.,* **239 (**1968) 289.

[169] J. A. Cox, T. Gray; "Controlled-potential electrolysis of bulk solutions at a modified electrode: Application to oxidations of cysteine, cystine, methionine, and thiocyanate". *Anal. Chem.,* **62** (1990) 2742.

[170] Z. L. Wang, Q. H. Luo, W. Qian, M. C. Shen; "A study on bovine erythrocyte superoxide dismutase by controlled potential electrolysis and Raman spectra". *Bioelectrochemistry,* **64** (2004) 33**.**

[171] P. Zuman, J. Ludvik; "The use of controlled potential electrolysis with a dropping mercury electrode in elucidation of organic electroreduction mechanisms". *Electroanalysis,* **12** (2000) 879.

[172] M. E. Osugi, P. A. Carneiro, M. V. B. Zanoni; "Determination of the phthalocyanine textile dye, reactive turquoise blue, by electrochemical techniques". *J. Braz. Chem. Soc.,* **14** (2003) 660.

[173] A. R. V. Benvenho, R. W. C. Li, J. Gruber; "Polymeric electronic gas sensor for determining alcohol content in automotive fuels". *Sens. Actuators B,* **136** (2009) 173.

[174] M. Mori; "Controlled potential electrolysis type NO and NO_2 sensors in estimating NO_x removal of photocatalysis". *Kenkyusho Hokoku,* **14** (2000) 76.

[175] Y. Kitatsuji, H. Aoyagi, T. Kimura, Z. Yoshida, H. Kudo, S. Kihara; "New method for the separation of interface between aqueous and organic solutions". *J. Nuclear Sci. Technol.,* **3** (2002) 259.

[176] A. D. G. Pinacho, F. S. Baeza, M. I. Pividori, M. P. Marco; "Electrochemical detection of fluoroquinolone antibiotics in milk using a magneto immunosensor". *Sensors,* **14** (2014) 15965.

[177] M. R. Payan, M. A. B. Lopez, R. F. Torres, J. A. O. Gonzalez, M. C. Mochon; "Hollow fiber-based liquid phase microextraction (HF-LPME) as a new approach for the HPLC determination of fluoroquinolones in biological and environmental matrices". *J. Pharm. Biomed. Anal.,* **55** (2011) 332.

[178] M. Panunzio, A. Malabarba, P. Vicennati; "Synthesis and antibacterial activity of new antibiotics arising from cephalosporin-monobactam coupling". *ARKIVOC,* **13** 2004 36.

[179] Y. Guo, J. Yang, X. Wu, H. Mao; "Study on the co-luminescence effect of Tb-Gd-epinephrine system and its application to the sensitive determination of epinephrine at nanomol level". *Talanta,* **73** (2007) 227.

[180] E. L. Bravo, R. W. Gifford; "Pheochromocytoma: State-of-the-art and future prospects". *N. Engl. J. Med.*, **311** (1984) 1298.

[181] R. N. Goyal, A. R. S. Rana, H. Chasta; "Electrochemical and peroxidase-catalyzed oxidation of epinephrine". *Electrochim. Acta*, **59** (2012) 492.

[182] F. S. Felix, M. Yamashita, L. Angnes; "Epinephrine quantification in pharmaceutical formulations utilizing plant tissue biosensors". *Biosens. Bioelectron.,* **21** (2006) 2283.

[183] Q. Xua, X. Liu, H. B. Li, L. Yin, X. Hu; "Electrochemical determination of purine and pyrimidine DNA bases based on the recognition properties of azocalix[4]arene". *Biosens. Bioelectron.*, **42** (2013) 355.

[184] R. N. Goyal, S. Chatterjee, A. R. S. Rana, H. Chasta; "Voltammetric sensor using single-walled carbon nanotubes modified edge plane pyrolytic graphite electrode for the simultaneous assay of adenine and adenosine monophosphate". *Sens. Actuators B,* **156** (2011) 198.

[185] E. Volpi, H. Kobayashi, M. S. Moore, B. Mittendorfer, R. R. Wolfe; "Essential amino acids are primarily responsible for the amino acid stimulation of muscle protein anabolism in healthy elderly adults". *Am. J. Clin. Nutr.,* **78** (2003) 250.

[186] G. Wu; "Amino acids: Metabolism, functions, and nutrition". *Amino Acids*, **37** (2009) 1.

[187] R. N. Goyal, S. Bishnoi, H. Chasta, M. A. Aziz, M. Oyama; "Effect of surface modification of indium tin oxide by nanoparticles on the electrochemical determination of tryptophan". *Talanta,* **85** (2011) 2626.

[188] A. Roda, C. Cerre, A. C. Manetta, G. Cainelli, A. U. Ronchi, M. Panunzio; "Synthesis and physicochemical, biological, and pharmacological properties of new bile acids amidated with cyclic amino acids". *J. Med. Chem.,* **39** (1996) 2270.

[189] Novartis swallows Excedrin, Daily Mail, April 15, 2005.

[190] B. Muralidharan, G. Gopu, C. Vedhi, P. Manisankar; "Determination of analgesics in pharmaceutical formulations and urine samples using nano polypyrrole modified glassy carbon electrode". *J. Appl. Electrochem.,* **39** (2009) 1177.

[191] K. T. Rotko, I. Beczkowska; "Nafion covered lead film electrode for the voltammetric determination of caffeine in beverage samples and pharmaceutical formulations". *Food Chem.*, **172** (2015) 24.

****

Chapter 2

DETERMINATION OF NORFLOXACIN AND SULFAMETHOXAZOLE

2.1 INTRODUCTION

Antibiotics can be divided into two classes based on their mechanism of action:

- Bacteriostatic antibiotics
- Bactericidal antibiotics

The first type of antibiotics kill bacteria by inhibiting the cell wall synthesis, whereas, the second type slow the growth and reproduction of bacteria by interfering with DNA replication or other aspects of bacterial cellular metabolism. However, there is not a very well defined difference between the two types of antibiotics as high concentration of some bacteriostatic antibiotics may also act as bactericidal. Similarly low concentration of some bactericidal may act as bacteriostatic. In general, both the types of antibiotics are able to effectively treat a bacterial infection.

Bactericidal antibiotics include variety of compounds such as, β-lactam antibiotics, daptomycin, fluoroquinolones, nitrofurantoin, cotrimoxazole (sulfamethoxazole/trimethoprim), telithromycin and many more. All these compounds have been found to inhibit the growth of micro-organisms and are widely used by the physicians for treatment of infections. This chapter has been devoted to the studies involving determination of two important bacteriostatic antibiotic, norfloxacin and sulfamethoxazole. The results of these studies are divided into two parts, part (A) deals with the determination of norfloxacin and part (B) deals with the determination of sulfamethoxazole.

(A) DETERMINATION OF NORFLOXACIN

Norfloxacin (NF) is a member of fluoroquinolones and is chemically named as 1-ethyl-6-fluoro-1, 4-dihydro-4-oxo-7- (piperazin-1-yl) quinoline-3-carboxylic acid. It is the first choice drug for the treatment of diseases caused by *Campylobacter, E. coli, Salmonella, Shigella and V. colera*. It is used for the doctoring of gonorrhoea as well as eye and urinary tract infections [1-4]. Outcome of the antibiotic NF on hyperdynamic circulation, vascular contractility, and extrahepatic vascular protein kinase-G activity in cirrhotic rats has been manifested [5]. NF has a broad spectrum with antibacterial activity against both Gram-positive and Gram-negative aerobic pathogens. The fluorine atom at the 6^{th} position provides increased potency against Gram-negative organisms and the piperazine moiety at the 7^{th} position is responsible for the antipseudomonal activity of NF [6]. It is well known that antibacterials in the environment may elevate the development of antibacterial resistance in organisms [7]. The non-target toxicity of antibacterials, including NF, has also been documented in literature [8]. NF is a fluoroquinolone antibacterial agent that is

extensively used in both human and veterinary medicine. In recent years, NF has been ranked as the second most prescribed fluoroquinolone antibacterial just next to levofloxacin in China. It is the first fluoroquinolone which was synthesized by converting nalidixic acid into a quinolone structure, adding a fluorine atom and a piperazine ring [9]. The determination of NF in biological samples and medicine is considered of great importance for human health, food assurance and quality control because of its potential toxicity. A series of analytical methods have been reported for the determination of NF by spectrophotometry [10], fluorometry [11], electrochemical analysis [12] and high performance liquid chromatography (HPLC) [13-19]. Although, HPLC has been widely applied because of its high sensitivity and selectivity and the ability to minimize interferences, it is time consuming, solvent-usage intensive and expensive (requires expensive devices and maintenance) which limited its use in quality control laboratories for analysis of NF in pharmaceutical dosage forms and human body fluids. Several of the spectrophotometric procedures published, show disadvantages such as heating or extraction step, narrow range of linear response and also need special reagents. Electrochemical detection of analyte is a very elegant method in analytical chemistry. Very few studies involving electrochemical determination of NF have been reported [20, 21]. Therefore, novel techniques for the determination of NF are still needed to be developed. Electrochemical methods have been found as a highly-sensitive, convenient and effective tool for the analysis of important biomolecules including drugs in pharmaceutical formulations and human body fluids owing to their simplicity, low cost and relatively short analysis time as compared to the other routine analytical techniques. Thus, the aim of this study is to develop a simple and rapid method for the analysis of NF in blood samples and also to quantitate the compound in marketed formulations. The square wave voltammetry (SWV) is a pulse technique that offers the advantage of great speed and sensitivity.

The pyrolytic graphite material comprises both edge plane and basal plane graphite, with the basal/edge ratio and graphite monocrystal size depending on the quality of the pyrolytic graphite used [22]. For a large variety of redox couples, electron-transfer rate constants at basal-plane graphite have been found to be over 10^3 times slower than for edge-plane graphite [22]. Compton et al. [23] and Goyal et al. [24] recently reported the analytical use of a carbon electrode populating largely of edge plane-active sites for electroanalytical detection of thiols and steroids respectively. The better analytical performance of edge plane pyrolytic graphite with faster electrode kinetics in comparison to basal plane and other carbon electrodes has been previously reported in literature [25, 26]. The edge plane has been found to give low background currents and

improved electrocatalytic signals as compared to that obtained at basal plane pyrolytic graphite. Edge plane pyrolytic graphite is constructed from HOPG where the graphite layers are perpendicular to the disc surface and are separated with an interlayer spacing of 0.335. Hence, in the present method, edge plane pyrolytic graphite has been used as a sensor to attain a very low detection limit, high sensitivity, and decreased over potentials coupled with increased current values for NF by using SWV.

2.2 MATERIAL AND METHODS

2.2.1 Chemicals

NF **(I)** was acquired from Ishita Drugs & Industries Ltd., Dehradun, (U.K.) India. It was employed without further purification. The NF containing tablets marketed by different pharmaceutical companies were purchased from the local market of Roorkee. Different commercial samples in combination or in pure form containing NF like Norflox-TZ, Norflox-400 (Okasa Pvt. Ltd., Distt.-Nainital, (U.K.), India) and Powerflox (Coronet labs Pvt. Ltd., Distt.-Haridwar, (U.K.), India) were canvassed. Phosphate buffer solutions of ionic strength 1 M were prepared according to the method of Christian and Purdy [27]. Double distilled water was used throughout the investigation. All other reagents and solvents used were of analytical grade.

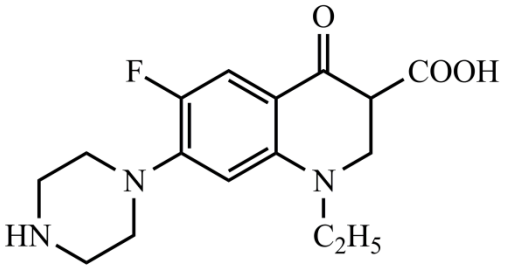

(I)

2.2.2 Apparatus

The voltammetric experiments were accomplished using a three electrode single compartment cell equipped with edge plane pyrolytic graphite sensor (EPPGS) or basal plane pyrolytic graphite sensor (BPPGS) as the working electrode, platinum wire as the counter electrode and an Ag/AgCl (3 M NaCl) reference electrode (BAS Model MF-2052 RB-5B). The edge and basal plane pyrolytic graphite pieces were obtained from Pfizer Inc., New York, USA. Experiments were carried out using a BAS CV-50W voltammetric analyzer (Bioanalytical

Systems, West Lafayette, USA). All the potentials quoted are versus Ag/AgCl electrode at an ambient temperature of 25±2 °C. Cyclic voltammograms were recorded in the sweep range 10-1000 mVs^{-1} with initial sweep to positive potentials. The solutions were deaerated by bubbling nitrogen for 12-15 min before recording the cyclic voltammograms.

2.2.3 Procedure

NF is insoluble in water, hence, the stock solution of NF (1 mM) is prepared by dissolving the required amount of the compound in minimum amount of concentrated hydrochloric acid (~100 µl) and then diluting it with double distilled water upto mark. The solution was ultrasonicated for 30 min. The required amount of the stock solution was added to 2 mL of phosphate buffer solution (μ = 1.0 M, pH 7.2) and the total volume was made to 4.0 mL with double distilled water. The electrode surface was cleaned after each run by abrading it on an emery paper (No. P400). Instrumental conditions for square wave voltammetry were: Initial E: 200 mV, Final E: 1200 mV, Square wave amplitude (E_{sw}): 25 mV, Potential Step (E): 4 mV, Square wave frequency (*f*): 15 Hz. Human urine samples from the patients undergoing pharmacological treatment with NF were obtained from the hospital of Indian Institute of Technology, Roorkee. Urine samples were used after ten times dilution with buffer to reduce the matrix complexity.

2.2.4 Preparation of electrode

A Pyrex glass tube of appropriate length and diameter (10 mm×0.6 mm) was cleaned thoroughly and dried. Thin glass rod was used to apply epoxy resin (Araldite (Ciba)) inside the one end of Pyrex glass tube. An edge plane pyrolytic graphite piece (1×1×3 mm^3) was then slided carefully from the open end of the tube with the help of wire till it gets covered with epoxy resin to avoid any air pocketing between the tube and the graphite piece. The sensor was then dried for 24 h at room temperature, after which the glass tube end was rubbed on an emery paper till the graphite piece was exposed. The surface was then washed with distilled water several times in order to remove fine carbon particles, adhered to the surface of pyrolytic graphite electrode. A sufficient amount of mercury was then placed into the glass tube and a platinum wire of appropriate length was inserted to make proper contact of electrode to the outer circuit. The electrode surface was cleaned after each run by rubbing it on an emery paper followed by washing with a jet of distilled water and touching with soft tissue paper. As the electrode surface area change each time due to the cleaning process, hence, voltammetric measurements are performed in triplicate and an average value of the current is reported.

2.3 RESULTS AND DISCUSSIONS

2.3.1 Determination of surface area

The effective surface area of EPPGS and BPPGS was calculated. For this purpose, cyclic voltammograms for 1 mM $K_3Fe(CN)_6$ using 0.1 M KCl as the supporting electrolyte were recorded at different scan rates. A well-defined redox couple was observed at both the electrodes due to the presence of Fe^{+3}/Fe^{+2}. For a reversible process, the following equation (1) applies:

$$i_p = 0.4463\,(F^3/RT)^{1/2}\,An^{3/2}D_R^{1/2}C_\circ v^{1/2} \qquad (1)$$

where F is Faraday's constant (96485 C/mol), R is the universal gas constant (8.314 J/mol K), A is the electrode surface area (cm^2), i_p refers to the peak current (Ampere), n = 1 for $K_3Fe(CN)_6$, T is the absolute temperature (298 K), $D_R = 7.6 \times 10^{-6}$ cm^2 s^{-1}, v is the scan rate (Vs^{-1}) and C_o is the concentration of $K_3Fe(CN)_6$ in $molL^{-1}$. The slope of i_p versus $v^{1/2}$ plot was then used to calculate the surface area of EPPGS and BPPGS and found as 0.085 cm^2 and 0.084 cm^2 respectively. Thus, it was found that the effective working area of both the sensors is essentially similar.

2.3.2 Voltammetric behavior of NF

2.3.2.1 Cyclic voltammetry

The cyclic voltammograms recorded for 20 μM NF using EPPGS and BPPGS in 1 M phosphate buffer solution of pH 7.2 is illustrated in **Fig. 2.1**. A well-defined single oxidation peak at ~950 mV was obtained at EPPGS which shifted to more positive potentials (~1075 mV) with a marked decrease in peak current at the BPPGS. These results clearly reveal that edge plane sites enhance the kinetics of the electrochemical oxidation of NF. The absence of reduction peak in the reverse scan clearly indicated that the oxidation of NF at this particular voltammetric sensor is irreversible in nature. To ascertain the nature of the electrode reaction, sweep rate studies were performed in the range 10-1000 mVs^{-1}. The peak current was found to increase with increasing sweep rates and the plot of $i_p/v^{1/2}$ versus log v clearly indicated that the electrode process is adsorption controlled [28, 29]. As SWV is considered to be a more sensitive technique in comparison to cyclic voltammetry, hence it is used for the further studies of NF.

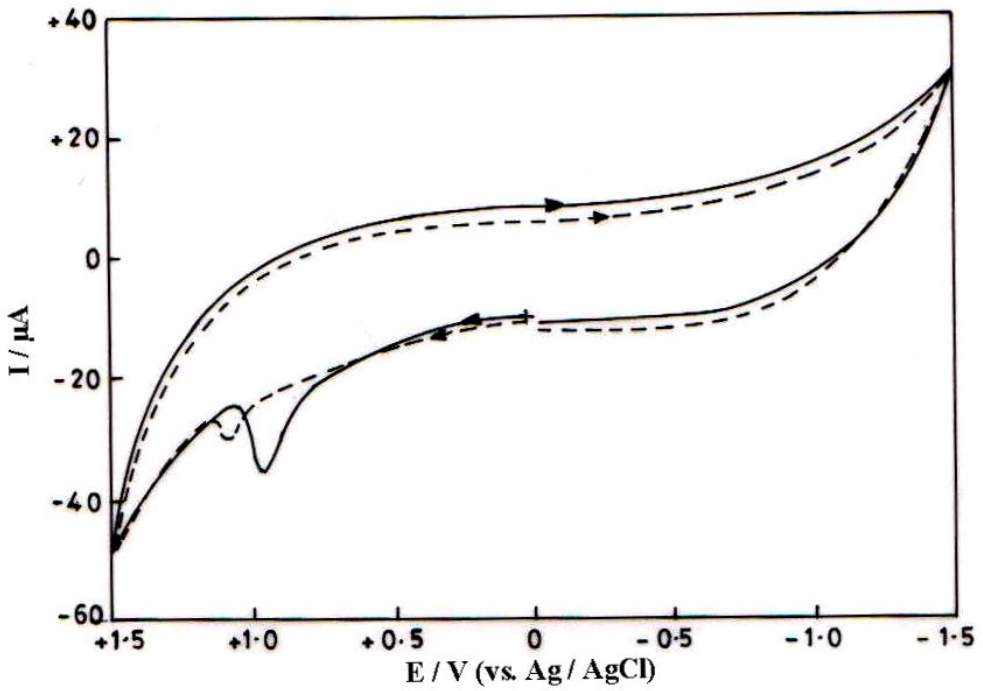

Fig. 2.1 Typical cyclic voltammograms observed for 20 µM NF in phosphate buffer solution of pH 7.2 at EPPGS (——) and BPPGS (− − −) at 20 mVs^{-1}.

2.3.2.2 Square wave voltammetry

Initially, square wave voltammograms were recorded for 20 µM NF at pH 7.2 at the EPPGS and BPPGS. Both the sensors had almost the same effective surface area exposed to the solution. **Fig. 2.2** represents a comparison of square wave voltammograms observed for the drug at different sensors. In the case of BPPGS, a small peak is observed at ~944 mV which shifts to ~821 mV at EPPGS, indicating thereby that the exposed edge plane sites in EPPGS contribute in making it a better substrate for sensing NF than BPPGS. The increase in peak current confirms that the adsorption is much stronger on EPPGS than BPPGS. Thus, the increase in current response along with the lowering of peak potential is a clear evidence of the electrocatalytic activity of edge plane sites of EPPGS towards the oxidation of NF. The different behavior of the NF oxidation on the edge and basal orientations reflects the difference in the surface electrocatalytic properties. A strong interaction between the reactant and the electrode surface is required to facilitate the electron transfer and to provide the adsorption sites for the intermediates.

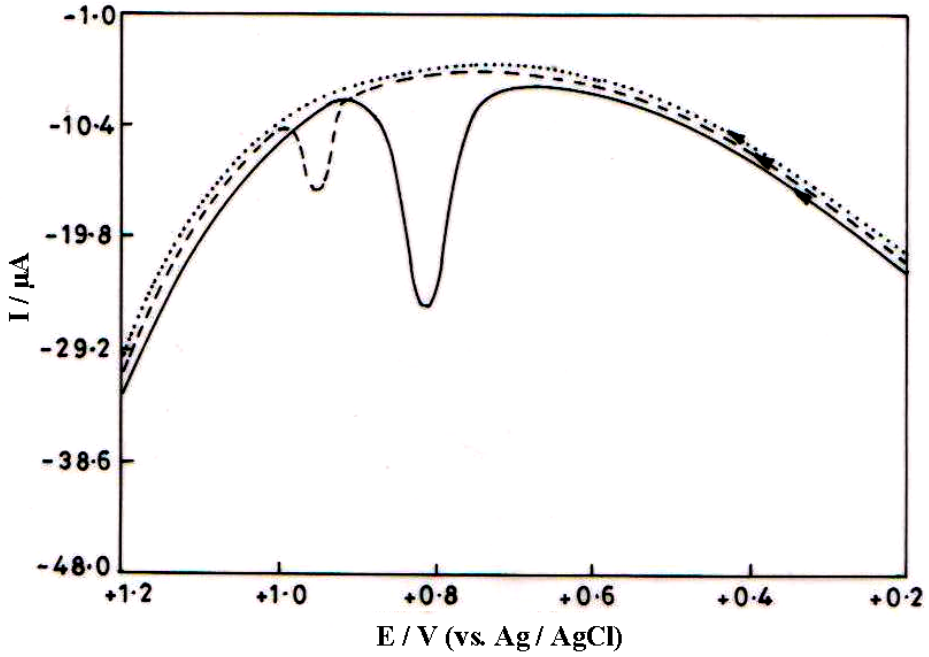

Fig. 2.2 Comparison of square wave voltammograms of 20 µM NF (pH 7.2) at (a) EPPGS (—), (b) BPPGS (– – –), and (c) background phosphate buffer solutions at pH 7.2 at EPPGS (…...).

2.3.3 Influence of pH and square wave frequency

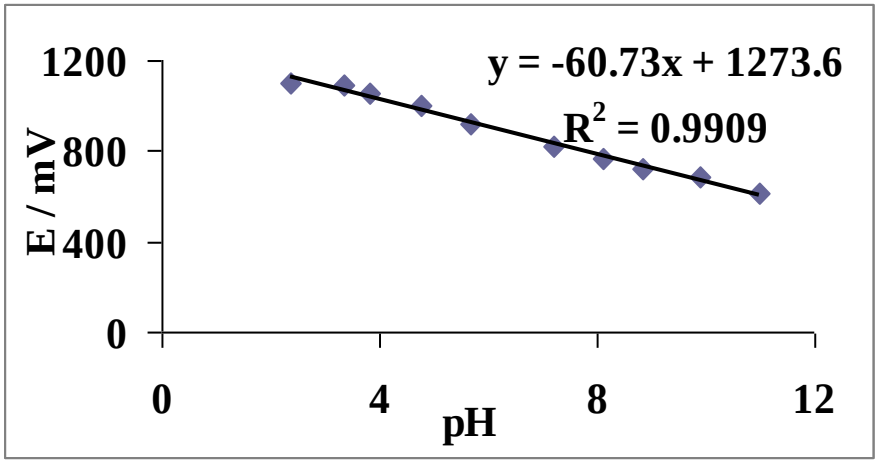

Fig. 2.3 Observed dependence of peak potential on pH for 20 µM NF at EPPGS.

The electrochemical behavior of NF at different pH values and square wave frequencies was studied at EPPGS. The voltammetric oxidation of 20 µM NF was studied in the range 2.4-11.0 in phosphate buffer solution. The pH of the solution strongly affects the peak potential (E_p) of NF,

with the E_p shifting linearly towards less positive potential values with increase in pH as shown in **Fig. 2.3**. The relationship between E_p and pH is represented by the following equation (2):

$$E_p\ (pH) / mV = 1273.6 - b\ pH \qquad (2)$$

Where slope b = dE_p / dpH = (60±2) mV/pH, having correlation coefficient 0.991. The slope of 60.73 mV/pH indicates that the number of protons and electrons involved in the oxidation is equal.

The effect of square wave frequency on peak potential was examined in the range 5-200 Hz at pH 7.2 at EPPGS. The plot of E_p versus log *f* was linear and the peak potential of NF was found to shift towards more positive potentials with increase in square wave frequency. The variation of E_p with log *f* can be expressed by the equation (3):

$$E_p / mV = 138.99 \log f / Hz + 656.63 \qquad (3)$$

with a correlation coefficient of 0.9916.

The peak current (i_p) of NF was found to increase linearly with the increase in square wave frequency in the range 5-200 Hz at pH 7.2 as presented in **Fig. 2.4** and the relation between i_p and *f* can be expressed by the equation (4):

$$i_p\ (f) / \mu A = b\ f + 4.9967 \qquad (4)$$

Where slope b = di_p/df = 0.4556±0.0044 Hz having a correlation coefficient 0.9892. These observations are in agreement with the properties of an adsorption controlled irreversible electrochemical process [30-32]. The results obtained also supported the inferences obtained from cyclic voltammetry studies.

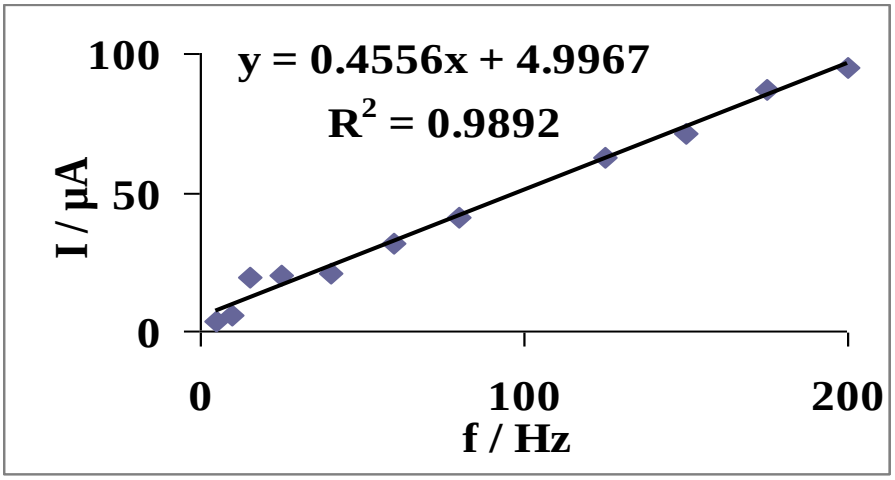

Fig. 2.4 Plot of anodic peak currents as a function of square wave frequency for 20 µM NF at pH 7.2 at EPPGS.

2.3.4 Concentration study

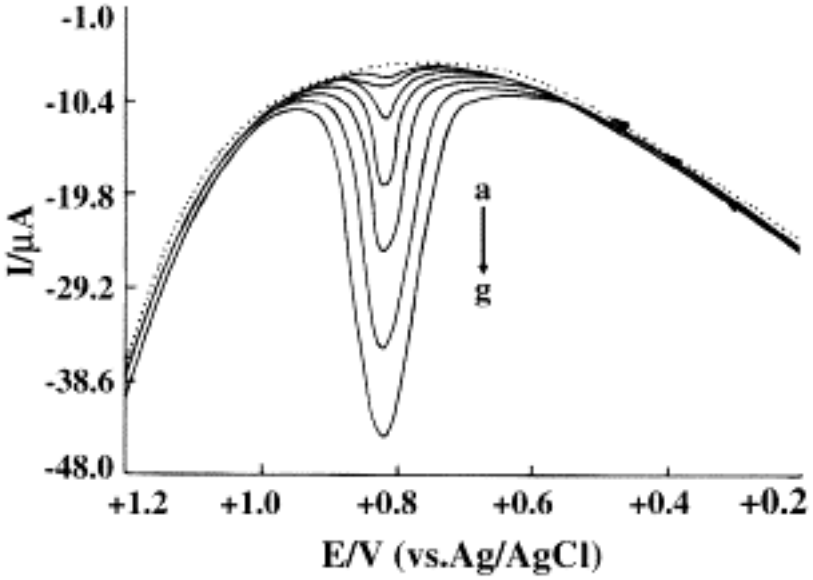

Fig. 2.5 Square wave voltammograms recorded for (i) phosphate buffer solutions (background) at the EPPGS (…...) and (ii) increasing concentrations of NF at the EPPGS electrode (—) [Curves are recorded at (a) 0.5, (b) 1, (c) 5, (d) 10, (e) 20, (f) 30 and (g) 40 μM concentration in phosphate buffer solutions of pH 7.2].

The quantitative analysis of the drug is based on the dependence of the peak current on the concentration of NF. Typical square wave voltammograms depicting the systematic increase in the peak current values with increasing concentration of NF in the range 0.5-50 μM at EPPGS is presented in **Fig. 2.5**. The linear calibration plot at EPPGS along with error bars is presented **Fig. 2.6**. In the case of BPPGS, the observed concentration range is 5-200 μM. The peak current is found to increase linearly with increasing concentration of NF at both the sensors and the linear regression equation (5) and (6) is expressed as:

$$i_p / \mu A = 0.9064\,[NF] + 1.433 \quad \text{at EPPGS} \quad (5)$$

$$i_p / \mu A = 0.0733\,[NF] + 4.619 \quad \text{at BPPGS} \quad (6)$$

where i_p is peak current in μA and [NF] is the concentration of NF in μM. The correlation coefficients for the expressions were 0.9967 and 0.9943 for EPPGS and BPPGS respectively. The current values are obtained by subtracting the background current and are reported as an average of at least three replicate determinations. The detection limit of the proposed method has been calculated by using the formula 3σ/b, where σ is the standard deviation of the blank and b is the slope of the calibration curve and has been found as 28.3×10^{-8} M and 237×10^{-8} M for EPPGS and

BPPGS respectively. The sensitivity is estimated to be 0.9064 μA μM^{-1} and 0.0733 μA μM^{-1} for EPPGS and BPPGS respectively. The repeatability was examined by performing ten replicate measurements for 0.5 μM NF under the same operational conditions. The mean value of the current was observed as 0.495 with R.S.D. of 0.8 %, which indicates repeatability and high precision of proposed procedure.

2.3.5 Specificity

The specificity of the optimized procedure for the assay of NF has been investigated by observing any interference encountered from endogenous substances present in complex matrices such as biological fluids (e.g. urine and plasma). The effect of the interferents (viz. uric acid, ascorbic acid, xanthine, and hypoxanthine) was examined by carrying out the determination of 20 μM NF in the presence of different concentrations of the interferents. The tolerance limit was defined as the concentrations of foreign substances, which gave an error less than ± 5.0% in the detection of the drug. It was observed that up to 10-fold excess of each of the interferents there was no significant change in the peak current response. This indicates that the method can be safely applied for the determination of NF in biological fluids.

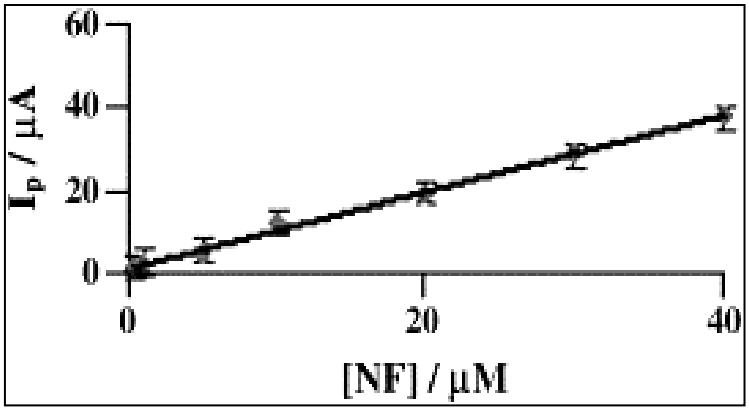

Fig. 2.6 Calibration plot with error bars observed for NF using EPPGS showing relation I_p(NF) = b[NF] + 1.433, where slope b = dI_p(NF)/d[NF] = 0.9064(+/−0.0240) μA/μM.

2.3.6 Pharmaceutical formulations

The tablets were powdered and dissolved in distilled water. The medicinal samples were further diluted so that the concentration of NF was in the working range. Pursuing the proposed method the concentration of NF in the various pharmaceutical preparations was ascertained. Results summarized in **Table 2.1** show that the content for all examined tablets falls within the tagged amount suggesting good agreement with the proposed voltammetric method.

Table 2.1 Determination of NF in pharmaceutical preparations using edge plane pyrolytic graphite sensor.

Sample	Stated content	Detected content*	Error (%)
Norflox-TZ	400 mg	395.32 mg	- 1.17
Norflox-400	400 mg	392.48 mg	- 1.88
Powerflox	400 mg	389.81 mg	- 2.55

***The RSD. value for determination was less than 2.7 % for n=3.**

2.3.7 Real sample analysis

2.3.7.1 Determination of NF in human urine

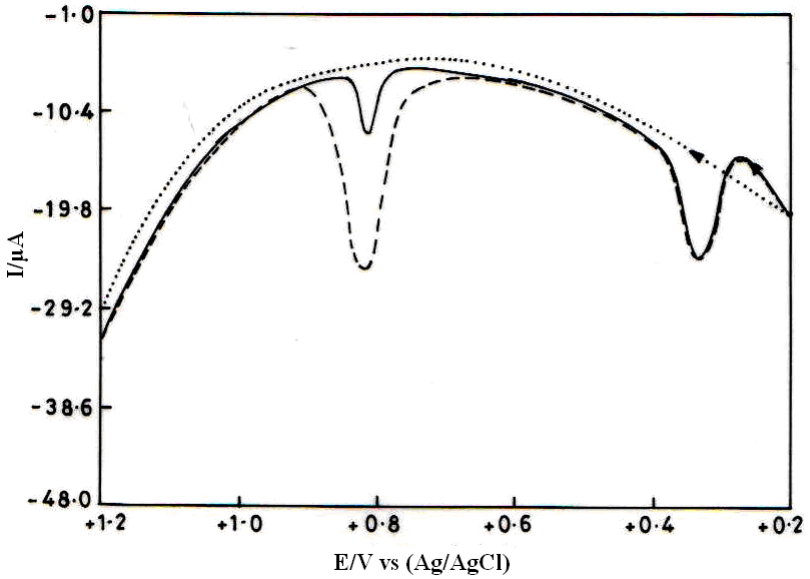

Fig. 2.7 A comparison of voltammograms observed for urine sample of patient being treated with NF (—) and after spiking with NF (- - - -) at pH 7.2 at EPPGS. Control urine is represented as (…...).

The applicability of the proposed method was examined on human urine samples obtained from patients undergoing treatment with NF. Urine sample of healthy volunteer was used as control. The urine samples of patients undergoing treatment with NF in the hospital of Indian Institute of Technology Roorkee were collected after 4 h of oral administration of 400 mg tablet of NF. The samples were used for analysis after 10 times dilution with phosphate buffer solution (pH 7.2) to minimize matrix complexity. A typical SWV of the urine sample of the patient being treated with NF at EPPGS is depicted in **Fig. 2.7**. A well-defined oxidation peak of NF at EPPGS

was observed at ~821 mV. The other voltammetric peak at ~310 mV is due to the presence of uric acid, which does not interfere in the determination of NF. The oxidation peak for ascorbic acid appears around 100 mV. The urine sample of the patient was then spiked with a known concentration of NF. The voltammograms in **Fig. 2.7** clearly depict that the peak current increases significantly for the peak at E_p ~821 mV thereby confirming that it corresponds to the oxidation of NF. The concentration of NF was determined using the regression equation and the results obtained for different urine samples, before and after spiking, are tabulated in **Table 2.2**.

Table 2.2 A comparison of observed concentration of NF in human urine after 4 h of NF administration at EPPGS.

Spiked (μM)	Observed[a] (μM)	Actual concentration (μM)*	Recovery (%)
Sample 1			
0.0	5.10	5.10	–
15.0	20.15	5.25	100.25
30.0	34.42	4.42	98.06
Sample 2			
0.0	5.32	5.32	–
15.0	20.48	5.48	100.79
30.0	36.02	6.02	101.98
Sample 3			
0.0	5.48	5.48	–
15.0	20.35	5.35	99.36
30.0	36.25	5.42	102.17

*** The R.S.D. value for the determination of NF was less than ± 3.2 % for n=3.**

2.3.8 Oxidation mechanism

Since NF oxidation occurred by the transfer of the same number of electrons and protons, therefore, two electrons and two protons transfer was involved in the electrode reaction. The electrochemical reaction process for NF at EPPGS can therefore be summarized as in **Scheme 2.1** and reported in literature [33]. Though, the detection limit reported for NF at carbon nanotube modified glassy carbon electrode [33] is about ten times lower than observed in the present studies, however, the main advantage is that no complicated modification of the electrode surface is required. In addition the purity of carbon nanotubes used significantly affects the peak current and

hence detection limit is affected [34, 35]. The use of EPPGS has been found satisfactory for the determination of NF and the detection limit is found to be 28.3×10^{-8} M. The half-life of NF is ~4 h and is excreted through urine. A comparison of response of various electrodes towards determination of NF in recent years is presented in **Table 2.3** and it can be seen that EPPGS can be easily used for the determination of NF.

Table 2.3 A comparison of voltammetric response of EPPGS with previously reported electrodes for the determination of NF.

Electrode ref. no.	Conc. range (μM)	Detection limit (μM)	Real samples
GCE [20]	15-150	3.5	No
MWCNT/GCE[12]	0.1-100	0.05	Urine
HMDE [21]	6-54	0.02	No
EPPGS present work	5-50	0.28	Urine

2.4. CONCLUSIONS

The electroanalytical determination of NF using an edge plane pyrolytic graphite sensor has been carried out. The results obtained suggest that EPPGS has a high density of states conferring good electrical conductivity and electron transfer kinetics; possibly allied to 'active sites' for adsorption [36]. This simple, sensitive, selective and quick analytical protocol reported suggests that NF can be detected at EPPGS via direct voltammetry in biological matrices. The peculiar catalytic activity of an EPPGS relies on the crystal orientation on its surface and edge plane defects [37]. The high percentage of the edge orientation results the high catalytic activity. The edge orientation on the surface of an EPPGS serves as an ''active site'' for the oxidation of NF. Highly ordered pyrolytic graphite (HOPG) is used to fabricate the edge and basal plane pyrolytic graphite. Edge plane pyrolytic graphite sensor is constructed from HOPG where the graphite layers are perpendicular to the disc surface and are separated with an interlayer spacing of ~3.35 Å. Surface defects occur in the form of steps exposing the edges of the graphite layers. Conversely a basal plane pyrolytic graphite electrode is fabricated such that the layers of graphite lie parallel to the surface [37]. The difference between the edge and basal orientations may account for the fact that functional groups are easier to adsorb on the edge plane.

Thus, it can be concluded on the basis of these investigations that NF is also oxidized in biosystems leading to the formation of products, which could serve as an important tool for the

biochemists to deeply understand the medicinal applications of the products formed under oxidative conditions in the human physiology. Thus, the present method has been satisfactorily employed for the determination of NF in pharmaceuticals and human urine samples obtained from patients being treated with the drug using SWV. The developed protocol is simple, rapid, sensitive and reproducible for the determination of NF at EPPGS.

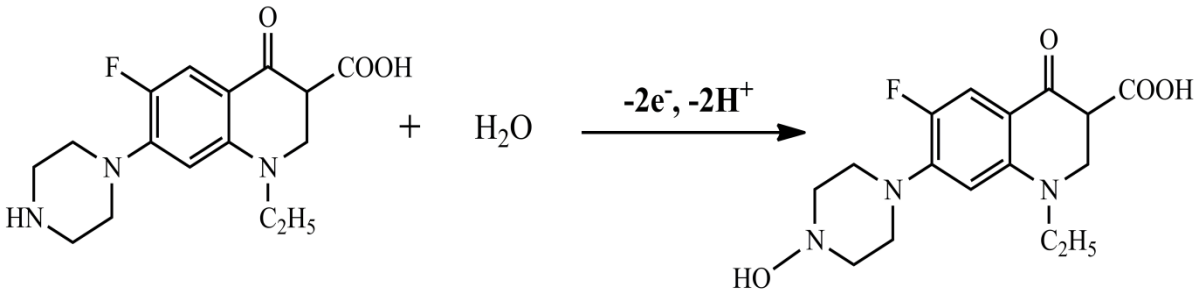

Scheme 2.1 A tentative mechanism suggested for the electro-oxidation of NF at pH 7.2.

(B) DETERMINATION OF SULFAMETHOXAZOLE

Sulfamethoxazole (SMZ) [N1-(5-methylisoxazol-3-yl) sulfanilamide] (**II**), a sulfonamide drug with anti-bacterial properties, is used for the treatment of human infections. Sulfonamide drugs are pervasively used in veterinary care and their use without a proper withdrawal period can cause accumulation of sulfonamides in eggs, milk, meat and honey as well as in fish [38-40]. Sulfonamide drugs were used as a first chemotherapeutic agent and employed for systematic prevention and cure of bacterial infection in human beings. Activity of the sulfonamide drugs has been associated with their competition with p-aminobenzoic acid (PABA) in the synthesis of folic acid for the growth of bacteria. Therefore, sulfa drugs act by inhibiting the bacterial growth rather than directly affecting the bacteria [41]. Recently, it is reported that modern classes of sulfonamides and related sulfonyl derivatives are served as an effective inhibitor for growing tumor cells, or for the medication of different types of cancer [42-44]. SMZ has been extensively used for the treatment of bacterial infections including urinary tract, pneumocystis carinii pneumonia, chronic bronchitis, meningococcal meningitis, acute otitis media, Whipple's disease and toxoplasmosis as well as in the treatment of opportunistic infection in transplantation and for AIDS related infection. Nevertheless, SMZ has also been reported to exhibit different types of side effects, like hypersensitivity reaction, gastro-intestinal distribution (mainly nausea and vomiting) and various hematological disorders such as thrombocytopenia, sulfhemoglobinemia, megaloblastosis, eosinophilia and agranulocytosis [45-49]. Hence, the determination of SMZ in

various biological samples and pharmaceutical formulations has been considered of great significance for human health and quality control.

Literature survey reveals that various techniques have been used for the determination of SMZ, such as spectrophotometry [50], ratio spectra derivative spectrophotometry [51], flow injection spectrophotometry [52], gas chromatography-mass spectrometry [53], capillary electrophoresis [54], liquid chromatography [55], high performance liquid chromatography (HPLC) using an on-line clean-up column [56], high performance thin layer chromatography [57], liquid Chromatography-mass spectrometry (LC-MS) [58] and visible and UV spectrophotometry [59]. Most of these methods were time consuming, expensive and required tedious extraction and separation steps. Recently, electrochemical methods have also attracted attention towards the determination of biomolecules and drugs due to their high sensitivity and selectivity, low cost and possibility of analysis without requirement of sample pretreatment. Hence, electrochemical methods have also been explored in the recent years for the determination of SMZ using [5,10,15,20- tetrakis(3-methoxy-4-hydroxy phenyl)porphyrinato] Cu (II) modified carbon paste sensor (TMHPP Cu (II)) [60], boron-doped diamond electrode [47, 61], multi-wall carbon nanotubes-nafion modified glassy carbon electrode (MWCNTs-Nafion/GCE) [62], CeO_2-chitosan-nanocomposite modified glassy carbon electrode (nano-CeO_2/CHIT/GC electrode) [63], multi-walled carbon nanotubes modified with antimony nanoparticles (MWCNT-SbNPs nanocomposite) [64] etc. In all these studies analysis of SMZ in biological samples has been carried out by spiking and recovery is reported and hence, the studies are of little significance. In addition, all these studies were carried out to determine SMZ concentration in food products, water and milk samples and pharmaceutical tablets. To the best of our knowledge, no effort has been made for the determination of SMZ in human urine samples using voltammetry. Hence, the aim of this study is to fabricate an electrochemical sensor for the simple and rapid determination of SMZ in human urine samples as well as in pharmaceutical formulations with high selectivity and sensitivity.

In last few years, application of conducting polymers in electrochemical sensors and biosensors has increased due to their reproducibility, electrochemical reversibility, low cost and good stability. Conducting polymers like polyaniline, polypyrrole, polythiophenes, polyazulenes and poly-1,5-diaminonapthalene (p-DAN), have been used to prepare electrochemical sensors for the monitoring of compounds of biological interest. These polymeric materials have played important role in improving the sensitivity and selectivity of the sensor, and to decrease fouling effects [65-69]. p-DAN is found to have versatile applications in the construction of chemically

modified sensors due to its electroactive nature in both acidic and aqueous solutions and also bears free NH2 groups as shown by FT-IR analysis [70]. The application of p-DAN conducting polymer has been studied at different surfaces, such as platinum and glassy carbon, pyrolytic graphite electrode with gold nanoparticles and glassy carbon electrode with multi-walled carbon nanotube in the selective monitoring of compounds [71, 72]. p-DAN has been considered as a promising candidate to form polymer drug conjugate for drug delivery purposes and it is successfully applied for the determination of various drugs as earlier reported by our group [73-75]. Here, we used only p-DAN film to fabricate the electrode due to some of great advantage such as easy synthesis, low cost in comparison to other conducting polymers, good adhesive property and dense structure [76-78].

In the present study, the electropolymerization of 1,5-DAN (**III**) in the acidic medium at glassy carbon electrode (GCE) has been carried out. The modification has been confirmed by various techniques including field emission scanning electron microscopy (FE-SEM), electrochemical impedance spectroscopy (EIS) and cyclic voltammetry (CV). The p-DAN/GCE sensor has been used for the determination of SMZ in biological samples. The experimental parameters, which affect the response of the modified GCE were optimized in terms of pH, frequency, scan rate and applied potential.

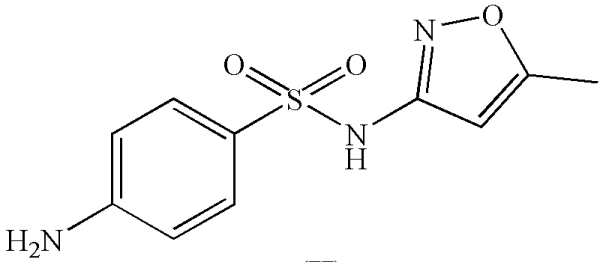

(II)

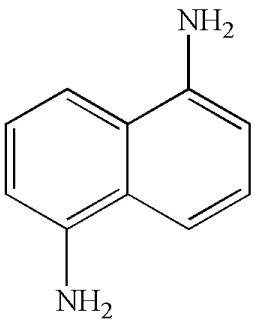

(III)

2.5 MATERIAL AND METHODS

2.5.1 Chemicals

Sulfamethoxazole, sulfuric acid, potassium chloride, potassium ferricyanide and 1,5-DAN were purchased from Sigma Aldrich, USA and used without further purification. The studies were accomplished in the pH range of 2.4-11 using 1.0 M phosphate buffer solution [27]. Sulfamethoxazole containing tablets were purchased from the local market of Roorkee. Human urine samples of patient treated with SMZ were collected from the hospital of Indian Institute of Technology, Roorkee after the permission of ethical clearance committee. All other solvents and reagents used in the experimental work were of analytical grade. Double distilled water was used throughout the experiments.

2.5.2 Apparatus

All the electrochemical work was performed by computerized bio-analytical system (BAS, West Lafayette, USA) CV-50 voltammetric analyzer. The electrochemical cell setup was equipped with p-DAN/GCE as a working electrode, Ag/AgCl (Saturated 1 M KCl) as a reference and platinum wire as a counter electrode, respectively.

Field emission scanning electron microscopic (FE-SEM) images were recorded by using Zeiss ultra plus 55. Galvanostat VersaSTAT-3 (PAR, USA) was used for the electrochemical impedance spectroscopic (EIS) studies. The pH of the phosphate buffer was measured using a Thermo Fischer, scientific Singapore digital pH meter (Eutech pH 700).

2.5.3 Fabrication of p-DAN film at the surface of GCE

GCE was polished to mirror like surface with alumina slurry and ZnO on polishing cloth, and thoroughly washed with double distilled water. The p-DAN/GCE was prepared by electropolymerization of 1 mM 1,5-DAN in 0.5 M H_2SO_4 using cyclic voltammetry, in which the potential range between −0.2 to +0.9 Vs^{-1} (vs. Ag/AgCl) was applied at the surface of the GCE for 7 cycles (scan rate: 0.1 Vs^{-1}) as reported in the literature [79]. After electropolymerization, a potential of −100 mV was applied for 100 s to facilitate the removal of adsorbed analyte to get a clean modified surface and, then it was cleaned well with double distilled water. The surface morphology of the bare GCE and p-DAN/GCE was studied by recording FE-SEM. A comparison of the FE-SEM images observed for bare GCE and p-DAN/GCE is presented in **Fig. 2.8** which clearly indicates that p-DAN has been deposited at the surface of GCE.

2.5.4 Experimental procedure

The stock solution of sulfamethoxazole (1 mM) was prepared by dissolving required amount in minimum amount of methanol (1 mL) and volume was made up to 25 mL in a volumetric flask. For voltammetric experiments, the desired volume of sulfamethoxazole was added to 2 mL of phosphate buffer of pH 7.2 (1.0 M) and the total volume was made to 4.0 mL with double distilled water. The optimum instrumental conditions for square wave voltammetry were: initial (E): 0.200 V, final (E): 1.400V, square wave amplitude (E_{sw}): 25 mV, square wave frequency (f): 15 Hz, potential step (E): 4 mV. Optimized cyclic voltammeric (CV) parameters used were: initial (E): 0.200 V, switching potential (E): 1.400 V final (E): 0.200 V, scan rate (v): 50 mVs^{-1} and full scale (+/-): 10 µA. CV studies were performed after bubbling high-purity nitrogen through the solutions for 12-15 min. All the potentials reported are versus Ag/AgCl (3 M NaCl) at an ambient temperature of 25±2 °C. The surface of p-DAN/GCE was cleaned after each run by using time based technique by applying a constant potential (-100 mV) for 100 s in buffer solution of pH 7.2.

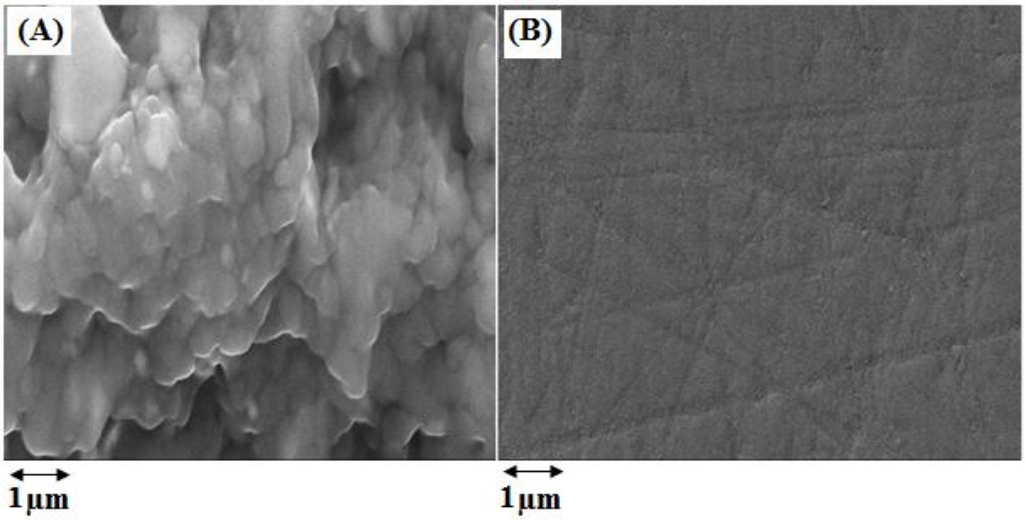

Fig. 2.8 Typical FE-SEM images of (A) p-DAN/GCE (B) bare GCE.

2.6 RESULTS AND DISCUSSIONS

2.6.1 Electrochemical characterization of p-DAN/GCE film

The electrochemical properties of bare and p-DAN coated GCE surfaces, were characterized by recording impedance spectra in 1:1 solution of 5 mM $K_3[Fe(CN)_6]$ and 0.1 M KCl solution in the frequency range of 0.1-100 KHz. **Fig. 2.9** shows the impedance spectra of bare GCE and p-DAN/GCE. A Randle's equivalent circuit was utilized for the impedance data as

represented in inset of Fig. 2.9, where R_{ct} is parallel combination of resistance to charge transfer and C_{dl} is interfacial capacitance. The values for R_{ct} were obtained by fitting the experimental data to the Randle's equivalent circuit. The value of R_{ct} for p-DAN/GCE (850 Ω) was lower than that for the bare GCE (1100 Ω). These values confirmed the conductive nature of the p-DAN film. These results also revealed that the p-DAN film successfully adhered to the surface of electrode.

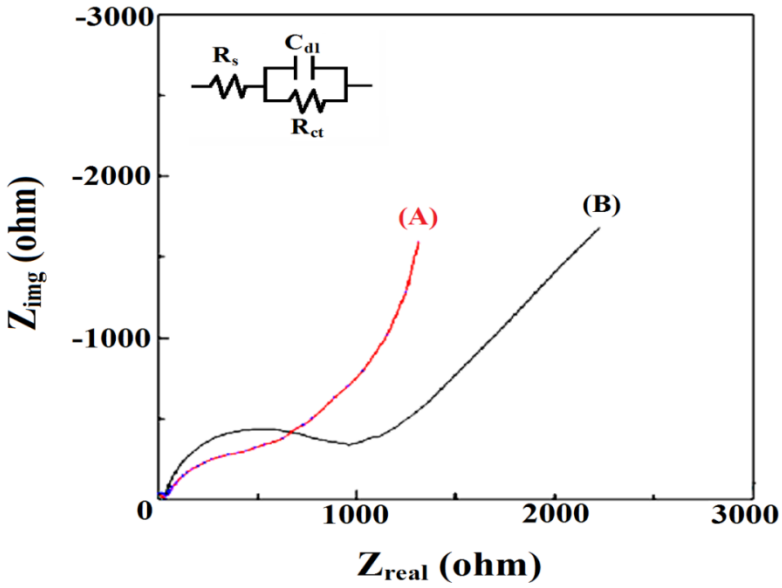

Fig. 2.9 Electrochemical impedance spectra at (A) p-DAN/GCE (B) bare GCE. The inset shows Randle's equivalent circuit.

2.6.2 Cyclic voltammetry

The cyclic voltammograms for 40 µM SMZ were recorded using bare GCE and p-DAN/GCE in the phosphate buffer solution (1 M) at pH 7.2 as represented in **Fig. 2.10**. A well-defined oxidation peak at ~980 mV was observed for the oxidation of SMZ at bare GCE, which shifted to less positive potential by ~50 mV, with a marked enhancement in peak current, at p-DAN/GCE. These results clearly indicated that p-DAN film efficiently enhanced the kinetics of the electrochemical oxidation of SMZ. In the reverse scan, no peak was observed, which clearly suggested that the oxidation of SMZ is irreversible in nature at p-DAN/GCE. To ascertain the nature of the electrode reaction, sweep rate studies were performed in the range 10-300 mVs^{-1}. The peak current of SMZ was found to increase with increasing sweep rates at p-DAN/GCE. The plots of $i_p/v^{1/2}$ versus log v for SMZ was linear and clearly indicated that the electrode process of SMZ is adsorption controlled at p-DAN/GCE [28, 80].

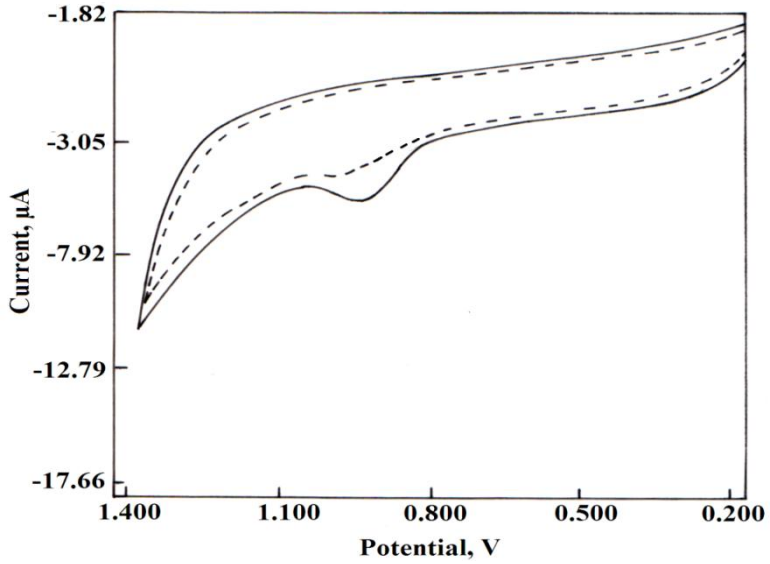

Fig. 2.10 Observed cyclic voltammogram for 40 µM SMZ at scan rate of 50 mVs^{-1} at p-DAN/GCE (—) and bare GCE (- - - -) at pH 7.2.

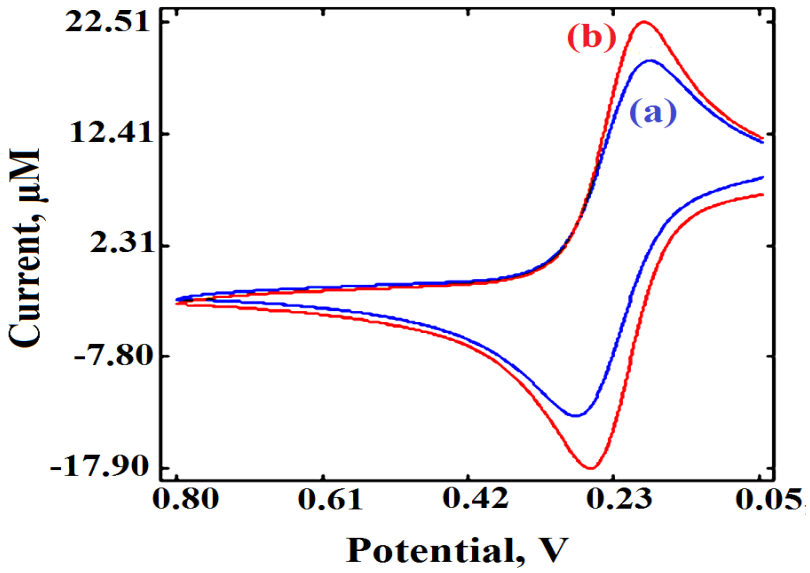

Fig. 2.11 Comparative cyclic voltammograms of 1 mM $K_3[Fe(CN)_6]$ in 0.1 M KCl using (a) bare GCE and (b) p-DAN/GCE at scan rate of 100 mVs^{-1}.

Electrochemical response of bare GCE and p-DAN/GCE was also examined by recording the cyclic voltammograms in the solution of 1 mM $K_3[Fe(CN)_6]$ and 0.1 M KCl to determine the effective surface area of the sensors. The enhancement in peak current and negative shift in peak potential was found at p-DAN/GCE (**Fig. 2.11**) in comparison to bare GCE. The surface area was calculated from the slopes of i_p versus $v^{1/2}$ plots using Randles-Sevcik equation and found as 0.039

and 0.124 cm^2 for bare GCE and p-DAN/GCE, respectively. Thus, the effective surface area of modified sensor was nearly three times larger than bare GCE.

2.6.3 Square wave voltammetry

Initially, square wave voltammograms were recorded for the 40 µM SMZ at bare GCE and p-DAN/GCE in phosphate buffer solution of pH 7.2 under optimal SWV parameters. A broad peak is obtained at the bare GCE having peak potential ~910 mV (curve a), whereas, at p-DAN/GCE the peak potential is shifted to ~850 mV (curve b), with significant enhancement in the peak current (**Fig. 2.12**). The shift in peak potential to less positive potential and enhancement in peak current indicate that the p-DAN film exhibits efficient electrocatalysis towards oxidation of SMZ. Hence, p-DAN/GCE sensor has been employed for further detailed studies of SMZ determination using SWV.

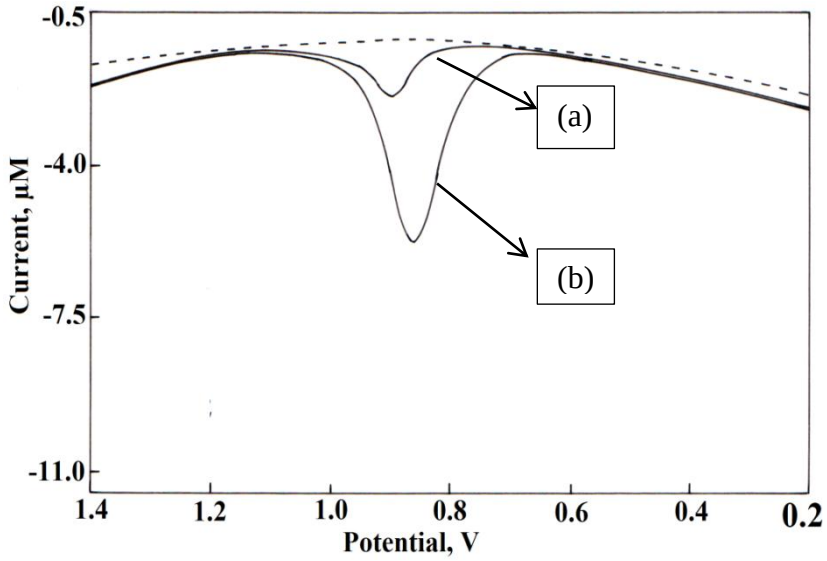

Fig. 2.12 Comparison of square wave voltammograms of 40 µM SMZ at pH 7.2 (i) curve a represents bare GCE, (ii) curve b represents p-DAN/GCE and (iii) (- - -) shows (background) phosphate buffer solution at p-DAN/GCE.

2.6.4 Effect of pH and sqare wave frequency

The electrochemical behavior of SMZ at different square wave frequencies and pH values was studied using p-DAN/GCE. The electrochemical oxidation of SMZ was studied in the phosphate buffer solutions ranging between 2.4-11.0. The pH of the solution strongly influenced the oxidation peak potential (E_p) of SMZ and the E_p shifted towards less positive potential values

with increase in pH of solution. The linear relationship between E_p and pH can be presented by the equation:

$$E_p / mV = 1272 - 58.10\ pH$$

having a correlation coefficient 0.982. The slope value of dE_p/dpH of (58.10 mV/pH) indicates that the number of protons and electrons involved in the oxidation is equal.

The influence of square wave frequency (*f*) on the oxidation peak current (i_p) was examined at pH 7.2 using p-DAN/GCE. It was observed that the peak current for the electrooxidation of 40 µM SMZ was increased linearly with increase in square wave frequency in the range 5-200 Hz. It is suggested that adsorption of SMZ occurred at the surface of p-DAN/GCE, which also confirmed the inference obtained from cyclic voltammetry. The variation of i_p with *f* can be expressed by the equation:

$$i_p / \mu A = 0.190\ f\ (Hz) + 0.681$$

having a correlation coefficient of 0.989.

2.6.5 Concentration study

To analyze the effect of SMZ concentration on the oxidation peak current, square wave voltammograms were recorded in the concentration range 0.05 µM to 150 µM using p-DAN/GCE at pH 7.2 under optimized parameters of square wave voltammetry. Systematic increase in the peak current was observed with increase in concentration of SMZ as represented in **Fig. 2.13**. It was observed that when the concentration of SMZ increased, the peak current linearly increased at p-DAN/GCE sensor. The observed linear calibration curve between peak current (i_p) and concentration of SMZ at p-DAN/GCE sensor is illustrated in **Fig. 2.14**. Linear dependence of SMZ (after subtracting background current) can be represented by the equation:

$$i_p / \mu A = 0.085\ C\ [\mu M] + 1.050$$

having correlation coefficient 0.995. The limit of detection for SMZ is calculated by using the relation $3\sigma/b$, where σ is the standard deviation of blank and b is slope of the calibration curve and found to be 0.05 nM at p-DAN/GCE sensor. The limit of detection for SMZ at bare GCE is found to be 0.1 µM, Thus, it can be seen that electropolymeriztion by p-DAN significantly lowered the detection limit as compared to the bare GCE. For any analytical technique, it is necessary to validate the method using validation characteristics such as linearity, range, accuracy, precision,

limit of detection and quantification. The typical validation parameters of present method are shown in **Table 2.4**.

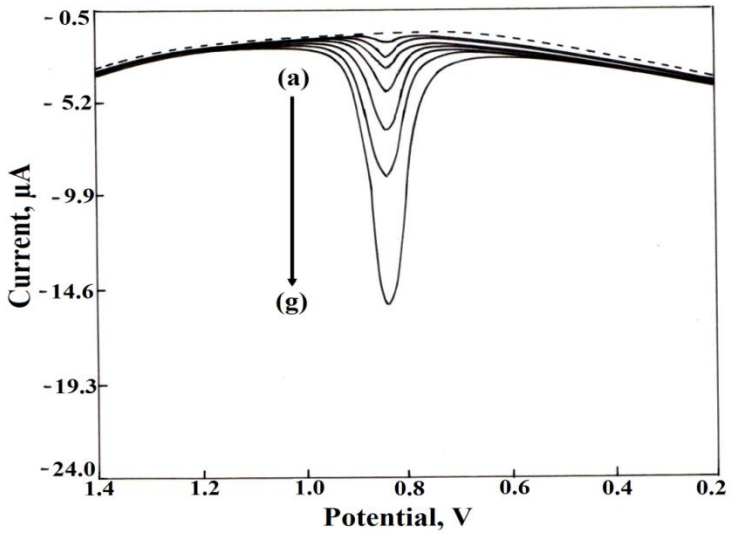

Fig. 2.13 Observed square wave voltammograms for (i) blank phosphate buffer solution (background) (…..) and (ii) increasing concentration of SMZ at (a) = 0.5; (b) = 5; (c) = 10; (d) = 20; (e) = 40; (f) = 80 and (g) 150 µM using p-DAN/GCE in phosphate buffer solution of pH 7.2.

Table 2.4 Validation characteristics for the determination of SMZ using P-DAN/GCE sensor.

Validation Parameters	Values
Concentration range (µM)	0.5-150
Correlation coefficient (R^2)	0.995
Detection limit (nM)	0.05
Limit of quantification (nM)	0.16
Sensitivity (µA/mM)	0.085
Standard error of slope (α, 0.05)	±0.0054
Standard error of intercept (α, 0.05)	±0.3407

In order to prove the accuracy and precision of the proposed method, analysis of varying concentration (low, medium and high concentrations) was done for three days (n = 3/day for within day and n = 5/day for between days). The results of precision are expressed as relative standard deviation and the accuracies were expressed as the Bais %. The results of precision and accuracy parameters are described in **Table 2.5**. The RSD obtained was in the range of 0.18-3.03 % and the

Bais % was in the range of 0.34-1.92 % for varying concentrations, which indicates good accuracy and precision of the method [81-84].

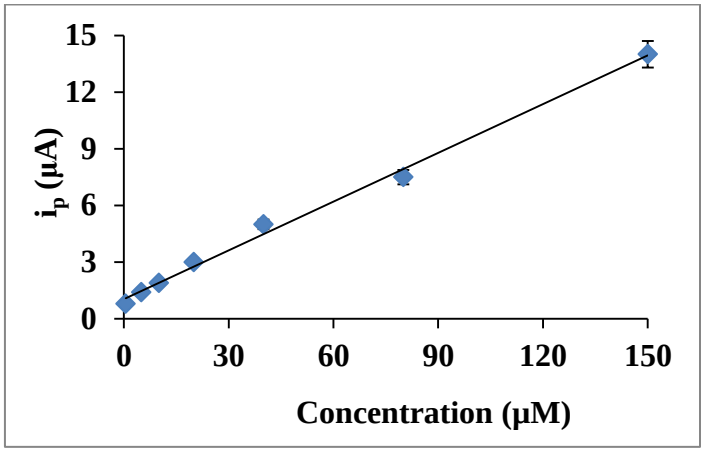

Fig. 2.14 Calibration plot observed for SMZ using p-DAN/GCE at pH 7.2.

Table 2.5 Precision and accuracy, within day and between days for the determination of different concentrations of SMZ at p-DAN/GCE sensor

SMZ (µM)	Within day (n = 3)		Between days (n = 5)	
	RSD (%)	Bais (%)	RSD (%)	Bais (%)
0.5	3.03	-1.00	2.07	0.72
50	1.53	-0.34	2.59	-1.92
150	0.67	-0.47	0.18	-0.25

2.6.6 Effect of interferents

The effect of common interfering molecules, such as ascorbic acid, uric acid, xanthine present in urine and trimethoprim (commonly given in combination with SMZ) has been analyzed on the determination of SMZ. These molecules can alter the electrochemical sensitivity of p-DAN/GCE sensor for SMZ determination by influencing its peak potential and peak current response. Interference study was carried out by measuring the voltammetric peak current response for fixed concentration of SMZ (5 µM) and varying the amount of interfering molecules up to 100 fold excess at pH 7.2. In voltammograms, peak potential of SMZ was obtained at +850 mV and other additional peaks were obtained at +100, +340, +720 and +1140 mV corresponding to the oxidation of ascorbic acid, uric acid, xanthine and trimethoprim respectively as shown in **Fig 2.15**. It was found that there is no change in the peak current as well as in the peak potential for SMZ oxidation up to 100 fold excess of the interfering molecules. These results clearly indicate the

specificity of p-DAN/GCE sensor towards the electrochemical oxidation of SMZ. Hence, p-DAN/GCE can be utilized for the determination of SMZ in biological samples and medicines.

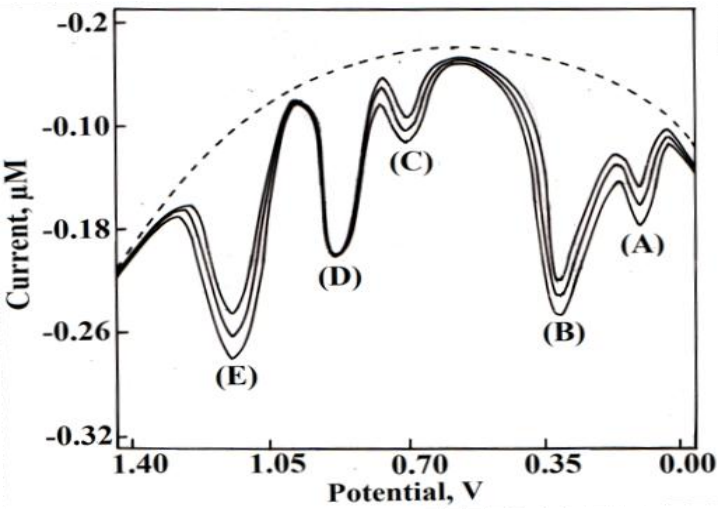

Fig. 2.15 Square wave voltammograms showing interferences of (A) ascorbic acid, (B) uric acid, (C) xanthine and (E) trimethoprim at fixed concentration of SMZ (D) (5 µM).

2.6.7 Analytical applicability

2.6.7.1 Determination of SMZ content in pharmaceutical formulations

Table 2.6 Determination of SMZ in tablets using p-DAN/GCE.

Sample	Reported amount (mg/Tablet)	Observed amount[a] (mg/Tablet)	RSD (%)	Bias (%)
Septran tablet	400.0	395.10	0.92	-1.20
Co-trimoxazole tablet	800.0	780.54	1.51	-2.43

[a] The R.S.D. for the determination was for n = 3.

In order to assess the utility of p-DAN/GCE sensor in pharmaceutical industries, different commercially available pharmaceutical samples containing SMZ, like Co-trimoxazole tablet double strength (Cadila, industrial Growth centre, Samba, State of J & K) and Septran (GlaxoSmithKline, D-5, M.I.D.C. Area, Paithan, Maharashtra) were acquired from the local market of Roorkee. The tablets were powdered and then dissolved in minimum amount of methanol and volume was made up to 25 mL with double distilled water. The samples were subsequently diluted with phosphate buffer solution upto the working range of SMZ. Applying the

identical conditions, which were used in the concentration study, the concentration of SMZ in the various pharmaceutical samples was ascertained by recording square wave voltammograms at p-DAN/GCE sensor. The obtained results are summarized in **Table 2.6**. It can be seen that the labeled values of SMZ on tablets were in good agreement with the results obtained using p-DAN/GCE sensor and hence suggested the good accuracy of the proposed sensor.

To check the validity of purposed method, results were compared with reported HPLC method using student *t*-test and *F*-test [40]. At the 95 % confidence level, calculated *t*-value and *F*-value were less than the tabulated values, indicating that there are no significant differences between the data obtained using the two methods. The results are shown in **Table 2.7**. Hence, these results show the excellent performance of the electroanalytical method using the p-DAN/GCE sensor when compared to the HPLC method.

Table 2.7 Validation of data by comparing with reported HPLC method.

Labeled amount (mg)	Found amount (mg) [a]		*t*-test [b]	*F*-test [c]
	Proposed method	Published method		
400	395.1±3.65	409±9 2.33	2.33	6.08

[a] Mean ± SD, n=3.

[b] Tabulated *t*-value at P (0.05) is 2.78.

[c] Tabulated *F*-value at P (0.05) is 19.00.

2.6.7.2 Determination of SMZ in human urine

In order to evaluate the applicability of the proposed sensor in human urine samples, determination of SMZ was carried out in urine of patients undergoing treatment with SMZ. The urine samples of patients were obtained from the hospital of Indian Institute of Technology Roorkee. The samples were collected after 6 h of oral administration of 800 mg Co-trimoxazole tablet. Prior to the analysis, the samples were diluted three times with phosphate buffer solution (pH 7.2) to minimize matrix complexity and square wave voltammograms were recorded. A well-defined anodic peak (E_p ~850 mV vs. Ag/AgCl) at p-DAN/GCE sensor was obtained corresponding to the oxidation of SMZ. The other voltammetric peaks at ~340 mV and ~1140 mV in the voltammogram are due to the oxidation of uric acid and trimethoprim respectively, which do not affect the determination of SMZ in urine samples. Ascorbic acid, which remains present in the urine samples, did not interfere in the determination of SMZ, as it oxidized at ~100 mV. The SMZ oxidation peak at ~850 mV is further confirmed by the spiking of urine samples with the known

amount of SMZ. It was observed that the oxidation peak current of SMZ increased on spiking with SMZ, confirming thereby that it corresponded to the oxidation of SMZ, while peak currents due to uric acid and trimethoprim remained unchanged. The results of SMZ obtained in different urine samples are tabulated in **Table 2.8**. The SMZ concentration in urine samples of patients was calculated by preparing standard addition plot as demonstrated in **Fig. 2.16** and was found to be 3.2 µM.

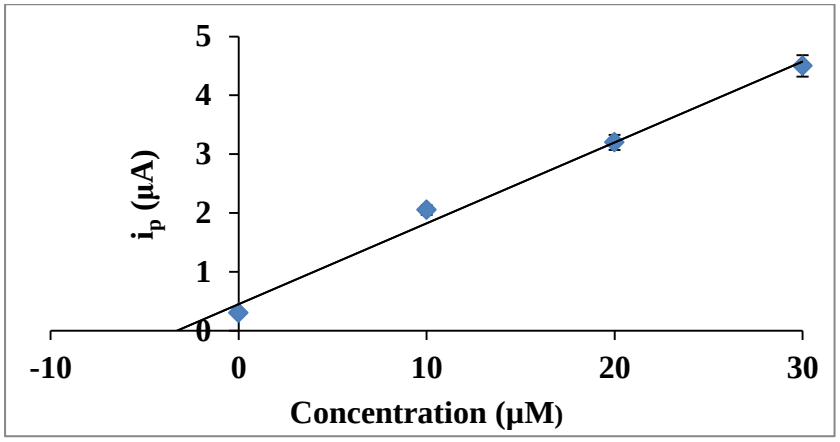

Fig. 2.16 The observed linear calibration curve between peak current and spiked SMZ concentration at p-DAN/GCE in urine sample.

Table 2.8 Recovery analysis of SMZ in urine sample of patient at p-DAN GCE.

Spiked (µM)	Observed (µM)	Actual [a] (µM)	Recovery (%)	RSD [b] (%)	Bias (%)
0	3.20	3.20	—	—	—
10	13.23	3.23	100.93	2.43	0.93
20	23.05	3.05	95.31	3.46	-4.69
40	43.15	3.15	98.43	1.54	-1.56

[a] The actual amount is observed – spiked amount.

[b] RSD value for the determination was for n = 3.

2.6.8 Stability and reproducibility

To determine the reproducibility of p-DAN/GCE sensor, successive square wave voltammetric measurements of 20 µM SMZ were recorded at pH 7.2 daily for 15 days. The modified electrode was used daily and stored in air. Marginal decrease of current sensitivity with a relative standard deviation of about 3.52 % was observed, which represented the excellent stability of the p-DAN/GCE. The results of ten repetitive measurements during intraday studies showed a

relative standard deviation (R.S.D.) of 1.96 % in current response of SMZ, which confirmed the excellent reproducibility of the developed sensor. Hence, the p-DAN/GCE exhibits efficient stability and reproducibility for the determination of SMZ.

2.7 CONCLUSIONS

In the present work, we described a method for the nanomolar concentration determination of SMZ in human urine samples as well as in pharmaceutical preparations employing a p-DAN/GCE sensor. A well-defined peak for the oxidation of SMZ appeared at ~850 mV at p-DAN coated GCE surface. Further, p-DAN film increased the electrocatalytic activity due to its high specific surface area in comparison to the bare GCE surface. The performance of p-DAN/GCE sensor towards SMZ determination is evaluated by a comparison of the detection limit and calibration range reported in the last few years as shown in **Table 2.9**.

Table 2.9 A comparison of various electrodes used for the determination of SMZ.

S. No.	Electrode used	Detection limit [M]	Sample	Reference
1	Boron-doped diamond electrode	1.15×10^{-6}	Tablet	[47]
2	MWCNT paste electrode	3.94×10^{-7}	Tablet	[46]
3	MWCNT-SbNPs nanocomposite	24×10^{-9}	Water	[64]
4	Nano CeO_2/CHIT/GC electrode	12×10^{-10}	Food	[63]
5	p-DAN/GCE sensor	5×10^{-11}	Human urine and tablet	This work

It can be concluded that the detection limit at p-DAN/GCE is superior than papers reported in recent years. The developed sensor also demonstrated the efficient ability to quantify SMZ concentration in various pharmaceutical formulations with reliable accuracy. The modified sensor has also been employed for the successful analysis of SMZ in urine samples of patients undergoing treatment with SMZ and good selectivity and sensitivity is observed.

2.9 REFERENCES

[1] A. R. Martin, J. N. Delgado, W. A. Remers; "Textbook of Organic Medicinal and Pharmaceutical Chemistry". Lippincott, Philadelphia (1991).

[2] J. L. Vılchez, O. Ballesteros, J. Taoufiki, G. Sanchez-Palencia, A. Navalon; "Determination of antibacterial norfloxacin in human urine and serum samples by solid-phase spectrofluorimetry". *Anal. Chim. Acta*, **444** (2001) 279.

[3] N. Rahman, Y. Ahmad, S. N. H. Azmi; "Kinetic spectrophotometric method for the determination of norfloxacin in pharmaceutical formulations". *Eur. J. Pharm. Biopharm*., **57** (2004) 359.

[4] O. Ballesteros, I. Toro, V. Sanz-Nebot, A. Navalon, J. L. Vılchez, J. Barbosa; "Determination of fluoroquinolones in human urine by liquid chromatography coupled to pneumatically assisted electrospray ionization mass spectrometry". *J. Chromatogr. B*, **798** (2003) 137.

[5] M. Hennenberg, J. Trebicka, D. Buecher, T. Sauerbruch, J. Heller; "Effect of the antibiotic norfloxacin on hyperdynamic circulation, vascular contractility, and extrahepatic vascular pkg activity in cirrhotic rats". *J. Hepatol*., **46** (2007) S82.

[6] V. R. More, U. S. Mote, G. B. Kolekar; "Spectroscopic studies on the interaction between norfloxacin and p-aminobenzoic acid: Analytical application on determination of norfloxacin". *Spectrochim. Acta Part A*, **74** (2009) 771.

[7] M. G. Brown, D. L. Balkwill; "Antibiotic resistance in bacteria isolated from the deep terrestrial subsurface". *Microb. Ecol*., **57** (2009) 484.

[8] M. J. Suto, J. M. Domagala, G. E. Roland, G. B. Mailloux, M. A. Cohen; "Fluroquinolones: Relationship between structural variations, mammalian cell cytotoxicity, and antimicrobial activity". *J. Med. Chem*., **35** (1992) 4745.

[9] F. V. Bambeke, J. M. Michot, J. V. Eldere, P. M. Tulkens; "Quinolones in 2005: An update". *Clin. Microbiol. Infect*., **11** (2005) 256.

[10] Y. N. Ni, Y. Wang, S. Kokot; "Multicomponent kinetic spectrophotometric determination of pefloxacin and norfloxacin in pharmaceutical preparations and human plasma samples with the aid of chemometrics". *Spectrochim. Acta A*, **70** (2008) 1049.

[11] C. L. Tong, G. H. Xiang; "Sensitive determination of norfloxacin by the fluorescence probe of terbium (III)-sodium dodecylbenzene sulfonate and its luminescence mechanism". *J. Fluoresc*., **16** (2006) 831.

[12] K. J. Huang, X. Liu, W. Z. Xie, H. X. Yuan; "Electrochemical behavior and voltammetric determination of norfloxacin at glassy carbon electrode modified with multi walled carbon nanotubes/nafion". *Colloids Surf. B: Biointerf*., **64** (2008) 269.

[13] H. J. Mascher, C. Kikuta; "Determination of norfloxacin in human plasma and urine by high performance liquid chromatography and fluorescence detection". *J. Chromatogr. A*, **812** (1998) 381.

[14] V. F. Samanidou, C. E. Demetriou, I. N. Papadoyannis; "Direct determination of four fluoroquinolones, enoxacin, norfloxacin, ofloxacin, and ciprofloxacin, in pharmaceuticals and blood serum by HPLC". *Anal. Bioanal. Chem*., **375** (2003) 623.

[15] R. N. Rao, V. Nagaraju; "Separation and determination of synthetic impurities of norfloxacin by reversed-phase high performance liquid chromatography". *J. Pharm. Biomed*., **34** (2004) 1049.

[16] J. Lim, B. Park, H. Yun; "Sensitive liquid chromatographic-mass spectrometric assay for norfloxacin in poultry tissue". *J. Chromatogr. B*, **772** (2002) 185.

[17] A. Espinosa-Mansilla, A. M. de la Pena, D. Gonzalez-Gomez, F. Salinas; "HPLC determination of enoxacin, ciprofloxacin, norfloxacin and ofloxacin with photoinduced fluorimetric (PIF) detection and multiemission scanning: application to urine and serum". *J. Chromatogr. B*, **822** (2005) 185.

[18] C. Kowalski, Z. Rolinski, T. Slawik, B. K. Glod; "Determination of norfloxacin in chicken tissues by HPLC with fluorescence detection". *J. Liq. Chromatogr. Relat. Technol*., **28** (2005) 121.

[19] G. H. Wan, H. Cui, Y. L. Pan, P. Zheng, L. J. Liu; "Determination of quinolones residues in prawn using high-performance liquid chromatography with Ce(IV)-Ru(bpy)$_3^{2+}$-HNO_3 chemiluminescence detection". *J. Chromatogr. B*, **843** (2006) 1.

[20] M. M. Ghoneim, A. Radi, A. M. Beltagi; "Determination of norfloxacin by square-wave adsorptive voltammetry on a glassy carbon electrode". *J. Pharm. Biomed. Anal*., **25** (2001) 205.

[21] Y. N. Ni, Y. R. Wang, S. Kokot; "Simultaneous determination of three fluoroquinolones by linear sweep stripping voltammetry with the aid of chemometrics". *Talanta*, **69** (2006) 216.

[22] R. L. McCreery; "Carbon electrodes: structural effects on electron transfer kinetics". in: A. J. Bard (Ed.), Electroanalytical Chemistry, Dekker, New York (1990).

[23] R. R. Moore, C. E. Banks, R. G. Compton; "Electrocatalytic detection of thiols using an edge plane pyrolytic graphite electrode". *Analyst*, **129** (2004) 755.

[24] R. N. Goyal, S. Chatterjee, A. R. S. Rana; "A single-wall carbon nanotubes modified edge plane pyrolytic graphite sensor for determination of methylprednisolone in biological fluids". *Talanta*, **80** (2009) 586.

[25] C. E. Banks, R. G. Compton; "Edge plane pyrolytic graphite electrodes in electroanalysis: An overview". *Anal. Sci*., **21** (2005) 1263.

[26] D. S. Shishmarev, N. V. Rees, R. G. Compton; "Enhanced performance of edge-plane pyrolytic graphite (EPPG) electrodes over glassy carbon (GC) electrodes in the presence of surfactants: Application to the stripping voltammetry of copper". *Electroanalysis*, **22** (2010) 31.

[27] G. D. Christian, W. C. Purdy; "The residual current in orthophosphate medium". *J. Electroanal. Chem*., **3** (1962) 363.

[28] R. S. Nicholson, I. Shain; "Theory of stationary electrode polarography: Single scan and cyclic methods applied to reversible, irreversible, and kinetic systems". *Anal Chem*., **36** (1964) 706.

[29] E. R. Brown, R. F. Large, A. Weissberger, B. W. Rossiter; "Physical methods of chemistry". Wiley-Interscience, Rochester, New York (1964).

[30] A. Radi, M. A. EL Ries, G. E. Bekhiet; "Electrochemical oxidation of the hypoglycaemic drug gliclazide". *Anal. Lett*., **32** (1999) 1603.

[31] S. Komorsky-Lovric, S. Gagic, R. Penovski; "Voltammetric determination of benzoylecgonine". *Anal. Chim. Acta*, **389** (1999) 219.

[32] M. R. C. Massaroppi, S. A. S. Machado, L. A. Avaca; "Electroanalytical determination of the herbicide picloram in natural waters by square wave voltammetry". *J. Braz. Chem. Soc*., **14** (2003) 113.

[33] C. E. Banks, R. G. Compton; "New electrodes for old: From carbon nanotubes to edge plane pyrolytic graphite". *Analyst*, **131** (2006) 15.

[34] R. N. Goyal, S. Chatterjee, A. R. S. Rana; "The effect of modifying an edge plane pyrolytic graphite electrode with single wall carbon nanotubes on its use for sensing diclofenac". *Carbon*, **48** (2010) 4136.

[35] C. E. Banks, A. Crossley, C. Salter, S. J. Wilkin, R. G. Compton; "Carbon nanotubes contain metal impurities which are responsible for the electrocatalysis seen at some nanotube modified electrodes". *Angew Chem Int Ed*., **45** (2006) 2533.

[36] K. J. Huang, X. Liu, W. Z. Xie, H. X. Yuan; "Electrochemical behavior and voltammetric determination of norfloxacin at glassy carbon electrode modified with multi walled carbon nanotubes/nafion". *Colloids Surf. B*, **64** (2008) 274.

[37] C. E. Banks, R. R. Moore, T. J. Davies, R. G. Compton; "Investigation of modified basal plane pyrolytic graphite electrodes: Definitive evidence for the electrocatalytic properties of the ends of carbon nanotubes". *Chem. Commun*., **16** (2004) 1804.

[38] J. Drews; "Drug discovery: A historical perspective". *Science*, **287** (2000) 1960.

[39] A. Posyniak, T. Sniegocki, J. Zmudzki; "Solid phase extraction and liquid chromatography analysis of sulfonamide residues in honey". *Bull. Vet. Inst. Pulawy*, **46** (2002) 111.

[40] N. Zheng, Y. Z. Li, M. J. Wen; "Development of a solid-phase extraction method for the determination of polychlorinated biphenyls in water". *J. Chromatogr. A*, **1033** (2004) 179.

[41] A. Achari, D. O. Somers, J. N. Champness, P. K. Bryant, J. Rosemond, D. K. Stammers; "Crystal structure of the anti-bacterial sulfonamide drug target dihydropteroate synthase". *Nat. Struct. Biol.*, **4** (1997) 490.

[42] A. Casini, A. Scozzafava, A. Mastrolorenzo, C. T. Supuran; "Sulfonamides and sulfonylated derivatives as anticancer agents". *Curr. Cancer Drug Targets*, **2** (2002) 55.

[43] J. P. Liou, K. S. Hsu, C. C. Kuo, C. Y. Chang, J. Y. Chang; "A novel oral indoline-sulfonamide agent, N-[1-(4-methoxybenzenesulfonyl)-2,3-dihydro-1H-indol-7-yl]-isonicotinamide (J30), exhibits potent activity against human cancer cells *in vitro* and *in vivo* through the disruption of microtubule". *J. Pharmacol. Exp. Ther.*, **323** (2007) 398.

[44] Y. Ozawa, K. Kusano, T. Owa, A. Yokoi, M. Asada, K. Yoshimatsu; "Therapeutic potential and molecular mechanism of a novel sulfonamide anticancer drug, indisulam (E7070) in combination with CPT-11 for cancer treatment". *Cancer. Chemother. Pharmacol.*, **69** (2012) 1353.

[45] G. E. Feurle, T. Marth; "An evaluation of antimicrobial treatment for Whipple's Disease". *Dig. Dis. Sci.*, **39** (1994) 1642.

[46] M. Arvand, R. Ansari, L. Heydari; "Electrocatalytic oxidation and differential pulse voltammetric determination of sulfamethoxazole using carbon nanotube paste electrode". *Mat. Sci Eng. C*, **31** (2011) 1819.

[47] C. D. Souza, O. C. Braga, I. C. Vieira, A. Spinelli; "Electroanalytical determination of sulfadiazine and sulfamethoxazole in pharmaceuticals using a boron-doped diamond electrode". *Sens. Act. B*, **135** (2008) 66.

[48] G. P. Wormser, G. T. Keusch; "Trimethoprim-sulfamethoxazole in the United States". *Ann. Intern. Med.*, **91** (1979) 420.

[49] M. A. Kielhofner; "Trimethoprim- sulfamethoxazole: pharmacokinetics, clinical uses, and adverse reactions". *Tex. Heart Inst. J.*, **17** (1990) 86.

[50] P. Nagaraja, S. D. Naik, A. K. Shrestha, A. Shivakumar; "A sensitive spectrophotometric method for the determination of sulfonamides in pharmaceutical preparations". *Acta Pharm.*, **57** (2007) 333.

[51] R. Hajian, R. Haghighi, N. Shams; "Combination of ratio derivative spectrophotometry with simultaneous standard additions method for determination of sulfamethoxazole and trimethoprim". *Asian. J. Chem.*, **22** (2010) 6569.

[52] P. D. Tzanavaras, D. G. Themelis; "Review of recent applications of flow injection spectrophotometry to pharmaceutical analysis". *Anal. Chim. Acta*, **588** (2007) 1.

[53] Y. Zhang, K. C. Agarwal, M. Beylot, M. V. Soloviev, F. David, M. Reider, K. Y. Tserng, H. Brunengraber; "Assay of the acetyl-CoA probe acetyl-sulfamethoxazole and of sulfamethoxazole by gas chromatography-mass spectrometry". *Anal. Biochem.*, **212** (1993) 481.

[54] D. Teshima, K. Otsubo, K. Makino, Y. Itoh, R. Oishi; "Simultaneous determination of sulfamethoxazole and trimethoprim in human plasma by capillary zone electrophoresis". *Biomed. Chromatogr.*, **18** (2004) 51.

[55] H. J. Nelis, F. Leger, P. Sorgeloos, A. P. D. Leenheer; "Accumulation of trimethoprim, sulfamethoxazole and N-acetylsulfamethoxazole in fish and shrimp fed medicated artemia franciscana.". *Antimicrob. Agents Chemother.*, **35** (1991) 2486.

[56] A. V. Pereira, Q. B. Cass; "High-performance liquid chromatography method for the simultaneous determination of sulfamethoxazole and trimethoprim in bovine milk using an on-line clean-up column". *J. Chromatogr. B*, **826** (2005) 139-146.

[57] D. H. Shewiyo, E. Kaale, P. G. Risha, B. Dejaegher, J. D. Beer, J. S. Verbekec, Y. V. Heyden; "Accuracy profiles assessing the validity for routine use of high-performance thin-layer chromatographic assays for drug formulations". *J. Chromatogr. A*, **1293** (2013) 159.

[58] H. N. Mistri, A. G. Jangid, A. Pudage, A. Shah, P. S. Shrivastav; "Simultaneous determination of sulfamethoxazole and trimethoprim in microgram quantities from low plasma volume by liquid chromatography–tandem mass spectrometry". *Microchem. J.*, **94** (2010) 130.

[59] Md. Azeez, B. K. Kumar, Manoranjan, G. Venkteshwarlu, B. Manindar, Y. Naresh; "Simultaneous determination of sulfamethaxazole and trimethoprim by using UV-visible spectrophotometer". *Int. J. Pharm. Sci. Rev. Res.*, **23** (2013) 224.

[60] R. Joseph, K. G. Kumar; "Differential pulse voltammetric determination and catalytic oxidation of sulfamethoxazole using [5,10,15,20-tetrakis(3-methoxy-4-hydroxy phenyl)porphyrinato] Cu(III) modified carbon paste sensor". *Drug Test. Anal.*, **2** (2010) 278.

[61] L. S. Andrade, R. C. R. Filho, Q. B. Cass, O. F. Filho; "Simultaneous differential pulse voltammetric determination of sulfamethoxazole and trimethoprim on a boron-doped diamond electrode". *Electroanalysis*, **21** (2009) 1475.

[62] S. Issac, K. G. Kumar; "Voltammetric determination of sulfamethoxazole at a multiwalled carbon nanotube modified glassy carbon sensor and its application studies". *Drug Test. Anal.*, **1** (2009) 350.

[63] M. Cai, L. Zhu, Y. Ding, J. Wang, J. Li, X. Du; "Determination of sulfamethoxazole in foods based on CeO_2/chitosan nanocomposite-modified electrodes". *Mat. Sci Eng. C*, **32** (2012) 2623.

[64] I. Cesarinoa, V. Cesarino, M. R. V. Lanza; "Carbon nanotubes modified with antimony nanoparticles in a paraffin composite electrode: simultaneous determination of sulfamethoxazole and trimethoprim". *Sens. Actuators, B*, **188** (2013) 1293.

[65] Md. A. Rahman, P. Kumar, D. S. Park, Y. B. Shim; "Electrochemical sensors based on organic conjugated polymers". *Sensors*, **8** (2008) 118.

[66] B. Guo, L. Glavasa, A. C. Albertssona; "Biodegradable and electrically conducting polymers for biomedical applications". *Prog. Polym. Sci.*, **38** (2013) 1263.

[67] H. Yoon; "Current trends in sensors based on conducting polymer nanomaterials". *Nanomaterials*, **3** (2013) 524.

[68] M. Gerard, A. Chaubey, B. D. Malhotra; "Application of conducting polymers to biosensors". *Biosens. Bioelectron.*, **17** (2002) 345.

[69] L. Chun, B. Hua, S. Gaoquan; "Conducting polymer nanomaterials: Electrosynthesis and applications". *Chem. Soc. Rev.*, **38** (2009) 2379.

[70] M. C. Pham, Md. Oulahyne, M. Mostefai, Md. M. Chehimi; "Multiple internal reflection FT-IR spectroscopy (MIRFTIRS) study of the electrochemical synthesis and redox process of poly-1,5-diaminonaphthalene". *Synth. Met.*, **93** (1998) 89.

[71] S. K. Yadav, B. Agrawal, R. N. Goyal; "AuNPs-poly-DAN modified pyrolytic graphite sensor for the determination of cefpodoxime proxetil in biological fluids". *Talanta*, **108** (2013) 30.

[72] C. S. Jin, Y. B. Shim, S. M. Park; "Electropolymerization and spectroelectrochemical characterization of poly-1,5diaminonaphthalene". *Synth. Met.*, **69** (1995) 561.

[73] S. K. Yadav, P. K. Choubey, B. Agrawal, R. N. Goyal; "Carbon nanotube embedded poly-1,5-diaminonapthalene modified pyrolytic graphite sensor for the determination of sulfacetamide in pharmaceutical formulations". *Talanta*, **118** (2014) 96.

[74] S. K. Yadav, B. Agrawal, P. Chandra, R. N. Goyal; "*In vitro* chloramphenicol detection in a *Haemophilus influenza* model using an aptamer-polymer based electrochemical biosensor". *Biosens. Bioelectron.*, **55** (2014) 337.

[75] R. N. Goyal, A. R. S. Rana, H. Chasta; "Simultaneous monitoring of aspirin, paracetamol and caffeine in human urine at poly-1,5-diaminonapthalene modified pyrolytic graphite sensor". *J. Electrochem. Soc.*, **160** (2013) G3014.

[76] Y. B. Shim, J. H. Park; "Humidity sensor using chemically synthesized poly-1,5-diaminonaphthalene doped with carbon". *J. Electrochem. Soc.*, **147** (2000) 381.

[77] Md. A. Rahman, M. S. Won, N. H. Kwon, J. H. Yoon, D. S. Park, Y. B. Shim; "Water sensor for a non-aqueous solvent with poly-1,5-diaminonapthalene nanofibers". *Anal. Chem.*, **80** (2008) 5307.

[78] M. A. Azzem, U. S. Yousef, G. Pierre; "A cyclic voltammetric and coulometric study of a modified electrode prepared by electrooxidative polymerization of 1,5-diaminonaphthalene in aqueous acidic medium". *Eur. Polym. J.*, **34** (1998) 819.

[79] A. A. Abdelwahab, H. M. Lee, Y. B. Shim; "Selective determination of dopamine with a cibacron blue/poly-1,5-diaminonaphthalene composite film". *Anal. Chim. Acta*, **650** (2009) 247.

[80] R. N. Goyal, A. Sangal; "Electrochemical investigations of adenosine at solid electrodes". *J. Electroanal. Chem.*, **521** (2002) 72.

[81] ICH. Guideline Q2A, Text on validation of analytical procedures. International conference on harmonization of technical requirements for registration of pharmaceuticals for human use, 1994.

[82] G. Shabir; "Validation of high-performance liquid chromatography methods for pharmaceutical analysis: understanding the differences and similarities between validation requirements of the US food and drug administration, the US pharmacopeia and the international conference on harmonization". *J Chromatogr A*, **987** (2003) 57.

[83] J. M. Green; "Peer reviewed: A practical guide to analytical method validation". *Anal. Chemi.*, **68** (1996) 305A.

[84] V. P. Shah, K. K. Midha, S. Dighe, I. J. McGilveray, J. P. Skelly, A. Yacobi, T. Layloff, C. T. Viswanathan, C. E. Cook, R. D. McDowall, K. A. Pittman, S. Spector; "Analytical methods validation: Bioavailability, bioequivalence, and pharmacokinetic studies". *J. Pharm. Sci.*, **81 (**1992) 309.

****

Chapter 3

ELECTROCHEMICAL AND PEROXIDASE-CATALYZED OXIDATION OF EPINEPHRINE

3.1 INTRODUCTION

Catecholamines are of particular interest because they have a significant role in biological and pharmacological processes. They are engrossed in certain types of chemical neurotransmission processes that occur in the synaptic gaps of the primary central nervous system [1, 2]. The hormone epinephrine (EPI, adrenaline) (**I**) is commonly used as the drug of choice as a vasoconstrictor, cardiac stimulator and bronchodilator. It subsists in protonated form at physiological pH. It is synthesized in the human system from L-tyrosine and exuded by the medulla of the adrenal gland along with norepinephrine. Ratiocination of concentration of the monoamine neurotransmitters such as EPI is crucial for the canvassing of neurotransmission, for diagnosis of neurological disorders, such as Parkinson's, and for developing medicines to cure the diseases [3]. Various approaches for their analysis include methods such as fluorescence [4], chemiluminescence [5], polarography/voltammetry [6], optic fiber biosensor coupled to chromatographic separation [7], capillary electrophoresis [8] and chromatography coupled with several types of detection methods [9, 10]. Some of these methods have been applied to analyze biological and pharmaceutical samples as shown and compared in a recent review [11]. The HPLC and fluorescence detection, however, has a disadvantage of requiring derivatization. Electroanalytical methods can bypass such additional procedures of derivatization because the monoamines themselves are electro-active at a certain potential [11]. Thus, electroanalytical methods have gained wide popularity in recent years [12, 13] for the analysis of the neurotransmitters and their metabolites *in vivo* or *in vitro*. Because of their simplicity, speed and sensitivity, numerous electroanalytical techniques have been reported for the determination of EPI and other catecholamines [14-18].

Peroxidases are abundant in both animal and plant systems [19]. EPI and related catecholamines are also significant constituents of plants and animals. EPI acts on target tissues through circulation in high concentrations during stress to furnish a rapid metabolic adjustment to emergencies. After functioning, EPI is quickly metabolized to sustain the normal physiological condition. Besides monoamine oxidase, cellular and extracellular soluble peroxidases (salivary peroxidase, lacrimal peroxidase, etc.) also play a vital role in EPI metabolism. Horseradish peroxidase can catalyze EPI oxidation at a very high rate in the presence of H_2O_2 [20, 21]. Many attempts have been made to study the enzymic oxidation of EPI. The oxidation of EPI by lactoperoxidase has been reported by Lovstad [22] and coloured aminochrome has been suggested as the product. Several other enzymes have also been explored for the oxidation of EPI [23-25].

Dryhurst et. al. have studied the oxidation chemistry of dopamine as well as of EPI in presence of cysteine [26, 27]. It has been found that the oxidation of dopamine leads to the formation of toxic 2,3'-linked indole-indoline dimer, whereas, in the case of EPI formation of cysteinyl conjugates is reported. The peroxide-catalyzed oxidation of purines has attracted considerable attention in past [28-32] and it has been reported that electrochemical and peroxide-catalyzed oxidation of simple purines follow the same pathway. Although the physiological functions and mechanism of action of EPI have been extensively analyzed, all of the details of its catabolism are still not clear even today.

In view of the importance of EPI in the human physiology, an attempt has been made to compare the electrochemical and peroxidase catalyzed oxidation of EPI in this chapter. The main objective of the present work was to compare the kinetics of UV-absorbing intermediate generated during electrochemical and enzymic oxidation of EPI and characterize the products formed during both the oxidations. A tentative mechanism for the oxidation of EPI is also presented.

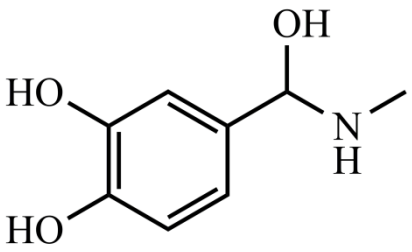

(I)

3.2 EXPERIMENTAL

3.2.1 Materials

The EPI was incurred from Sigma Aldrich, Germany. Phosphate buffers of appropriate pH and ionic strength were prepared from analytical grade chemicals (NaH_2PO_4 and Na_2HPO_4 from Merck) according to the reported method [33]. Methanol (HPLC grade) was obtained from Merck. Enzymatic oxidation of EPI was carried out using horseradish peroxidase type VIII (R_z ~3.0) obtained from Sigma Chemical Co., USA. H_2O_2 was purchased from Qualigens Fine Chemicals, Galaxo India ltd., Mumbai.

3.2.2 Instrumentation

The pyrolytic graphite electrode used for the voltammetric studies was fabricated by using the method reported in the literature [34] so that the edge plane of the pyrolytic graphite (2×2

mm^2) was exposed to the solution. The surface of the pyrolytic graphite electrode was renewed after recording each voltammogram, by rubbing it with an emery paper. The surface was washed with a jet of distilled water and gently dried by touching onto tissue paper. The surface renewal was necessary to remove the adsorbed material on the electrode surface. As the effective surface area available changed each time due to rubbing, the peak current values showed a variation of ± 10 %. Hence, an average of at least three voltammetric runs was taken for the determination of the peak current values. Cyclic sweep voltammetric studies were carried out by using BAS CV-50W Voltammetric analyzer. All potentials are referred to Ag/AgCl (3 M NaCl) at an ambient temperature, 25±2 °C. Controlled potential electrolysis was carried out in a single compartment cell equipped with three electrode system using pyrolytic graphite plate (1×4 cm^2) as working electrode, cylindrical platinum gauze as auxillary electrode and Ag/AgCl as reference electrode. The spectral changes associated with the electro-oxidation and the kinetic studies of the decomposition of the UV-absorbing intermediates generated during oxidation were monitored using Perkin-Elmer-Lambda 35 UV–vis spectrophotometer. The ^1H NMR and DEPT 135 spectra were recorded in D_2O using Avance 500 digital NMR spectrometer from Brucker (500 MHz). Chemical shifts (δ) are reported in ppm of the applied field and coupling constants (J) are expressed in Hertz (Hz).

3.2.3 Procedure

A stock solution (1 mM) of EPI was prepared in double distilled water. Working solutions of EPI were prepared by adding required volumes of the respective stock solution to the phosphate buffer solution and then the voltammograms were recorded. The solutions were deoxygenated by bubbling nitrogen gas for 8-10 min before recording the cyclic voltammograms. UV-vis spectral changes associated with the electro-oxidation of EPI were monitored in 200-400 nm region by applying a potential ~50 mV more positive than the peak potential. Nearly 2-3 ml of the electrolyzed solution was withdrawn from the working compartment of the electrolytic cell at different time intervals. In the second set of experiments, when the absorbance at λ_{max} reduced to about 50 %, electrolysis was turned off by open circuit relaxation and spectral changes were monitored at different time intervals to detect the generation of the UV-vis absorbing intermediate.

The products of the electro-oxidation of EPI were characterized at pH 7.2. For identification of the oxidation products, about 10 mg of the compound was exhaustively electrolyzed at a potential ~50 mV more positive than oxidation peak potential. The progress of the

electrolysis was monitored by recording UV-spectra at different time intervals. When the absorbance at λ_{max} reached to minimal, the exhaustively electrolyzed solution was removed from the cell, filtered using Whatman filter paper 42, lyophilized and extracted using methanol. The dried material was then analyzed by ^{1}H and DEPT 135 NMR.

3.2.4 Enzymatic oxidation

Stock solutions of horseradish peroxidase type VIII (2 μM), H_2O_2 (600 μM) and EPI (0.1 mM) were prepared fresh each day in an appropriate buffer. Usually, 0.7 mL each of the EPI and peroxidase solutions was mixed in a 1.0 cm quartz spectrophotometer cell. The enzymatic reaction was initiated by the addition of 0.7 mL of the H_2O_2 stock solution. The course of the oxidation was monitored by repetitively recording the UV-spectrum of the solution. When about 95 % of the EPI had been oxidized the reaction was terminated by addition of 0.7 mL of buffer solution containing 0.7 mg catalase (2000 units mg^{-1}, Sigma). The solution was thoroughly stirred. The reference cell for spectrophotometric studies contained all buffer, reagents and enzymes except EPI. The kinetics of decay of the UV-absorbing intermediate was usually followed at a single preselected wavelength with absorbance readings generally being taken every 5.0 s.

3.2.5 Characterization of enzymatic oxidation product

The major oxidation product formed upon peroxidase-catalysed oxidation of EPI was identified following the enzymatic oxidation of the latter species. The stock solutions of EPI (1 mM), peroxidase (2 μM) and H_2O_2 (1 mM) were prepared in an appropriate buffer. Then, 4.0 mL of the EPI solution was placed in a beaker and to it, 4.0 mL of the peroxidase solution was added. The resulting solution was stirred and the oxidation reaction initiated by addition of 4.0 mL of H_2O_2 solution. In order to identify the final product, the oxidation reaction was allowed to proceed for 20-25 min. The oxidized solution was removed from the cell, filtered using Whatman filter paper 42 and lyophilized. The dried product obtained was extracted with methanol and analyzed by ^{1}H and DEPT 135 NMR.

3.3 RESULTS AND DISCUSSIONS

3.3.1 Voltammetric studies

Cyclic voltammetric studies of 10 μM EPI at pH 7.2 exhibited a well-defined oxidation peak ~157 mV at a sweep rate of 100 mVs^{-1}, when the sweep was initiated in the positive direction. In the reverse sweep, EPI exhibits a reversible couple with peak potentials of −243

(II_c)/−214 (II_a) mV. While at pH 4.9 same concentration of EPI exhibited an oxidation peak I_a ~320 mV and in the reverse sweep, a reversible couple with peak potentials of −160 (II_c)/−135 (II_a) mV was observed. **Fig. 3.1A** shows a typical cyclic voltammogram observed for 10 µM EPI at sweep rate 100 mVs^{-1} in phosphate buffer at pH 4.9 at a pyrolytic graphite electrode. To check whether the reversible couple II_c/II_a are related to peak I_a, cyclic voltammograms were also recorded by initiating the initial sweep in negative direction. It was observed that no reduction peak is observed in this case as shown by **curve B** in **Fig. 3.1**. Thus, it is concluded that it is necessary to record peak I_a to see the redox couple II_c/II_a.

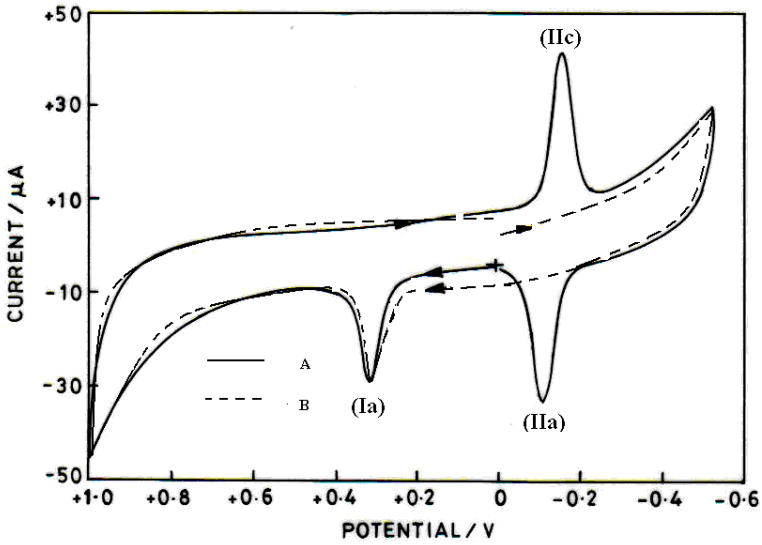

Fig. 3.1 Typical cyclic voltammograms observed for 10 µM EPI at sweep rate 100 mVs^{-1} in phosphate buffers at pH 4.9 at pyrolytic graphite electrode. Curve A (—) with initial sweep in the positive direction. Curve B (-----) with initial sweep in the negative direction.

The effect of pH on the ease of oxidation of EPI was studied at a sweep rate of 100 mVs^{-1} in the pH range 2.4-11.0. It was found that the peak potential of oxidation peak shifted to less positive potential with increase in pH. The plot of E_p vs. pH was linear with slope (dE_p/dpH) 57.6 mV/pH. Thus, it was concluded that oxidation of EPI involves equal number of electrons and protons. The peak potential of peaks (II_a) and (II_c) were also dependent on pH and shifted to less positive potentials with increase in pH. The ΔE_p value for the redox couple in the entire pH range was close to 30 mV. The ratio of peak currents of II_a/II_c was close to 0.9 in the entire pH range. Thus, it was concluded that the redox couple II_a/II_c is reversible in nature. The oxidation of EPI occurs in an overall $4e^-$, $4H^+$ process to give adrenochrome as shown in **Scheme 3.1**. To ascertain

the nature of electrode reaction, sweep rate studies were performed in the range 10-1000 mVs^{-1}. The peak current of EPI was found to increase with increasing sweep rates and the plot of $i_p/v^{1/2}$ vs. log *v* clearly indicated the adsorption of the reactant and thus it is concluded that the electrode process is adsorption controlled [35] and [36]. Cyclic voltammograms was recorded at different concentrations of EPI. It was found that the oxidation peak I_a increased with increase in concentration. The plot of i_p vs. concentration of EPI was linear up to 25 µM after which a deviation was observed. The peak current for the redox couple initially increased with increase in concentration of EPI and then became practically constant.

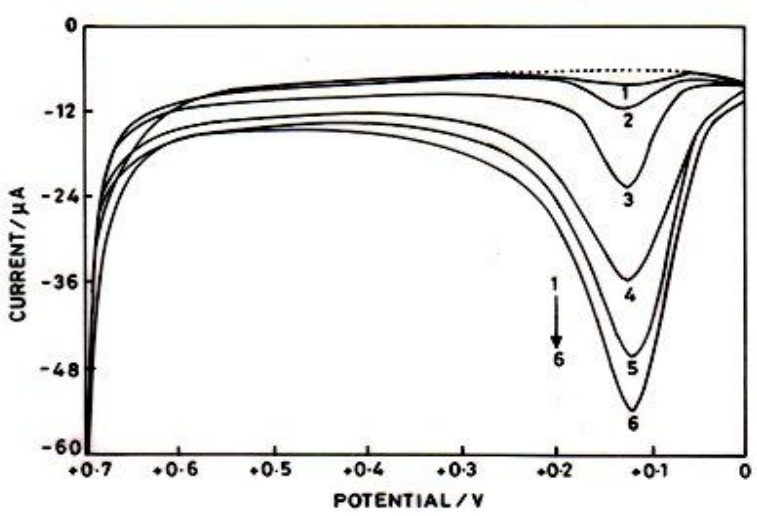

Fig. 3.2A Square wave voltammograms recorded at pyrolytic graphite electrode for (a) phosphate buffer solution (background) (…...) and (b) increasing concentration of EPI (—) [Curves were recorded at (a) 0.25, (b) 1, (c) 5, (d) 10, (e) 15 and (g) 20 µM concentration of EPI in phosphate buffer solution of pH 7.2].

As SWV is considered to be a more sensitive technique in comparison to cyclic voltammetry, hence it is used for the further determination of EPI. With increasing concentration of EPI, the peak current (i_p) for peak I_a was found to increase in the range 0.25-20 µM at pH 7.2. The graph between (i_p) and concentration obtained was found to be linear. The dependence of (i_p) on concentration can be expressed by the relation:

$$i_p\ (10^{-6}A) = 2.325\ C\ (\mu M) + 2.956$$

where C is the concentration (µM), having correlation coefficient 0.994. Typical square wave voltammograms depicting the systematic increase in the peak current values with an increase in the

concentration in the range 0.25-20 μM using pyrolytic graphite electrode are presented in **Fig. 3.2A**. The linear calibration plot along with error bars is presented in the **Fig. 3.2B**. The limit of detection and sensitivity of EPI are estimated to be 17×10^{-8} M and 2.325 μA μM^{-1} respectively.

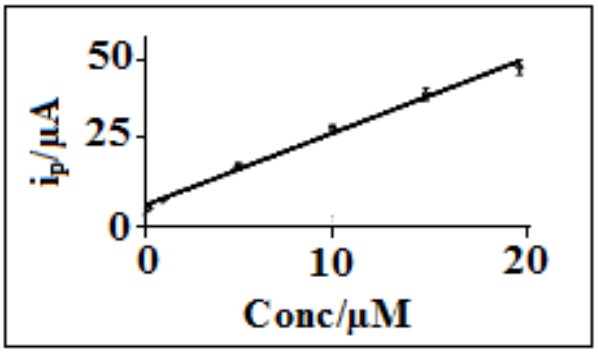

Fig. 3.2B Calibration plot observed for epinephrine using EPPGE at pH 7.2.

The effect of square wave frequency on the peak potential of EPI was studied in the frequency range 5 to 200 Hz. The peak potential of EPI was found to shift towards more positive potentials with increase in square wave frequency. The plot of E_p versus log *f* was linear. The dependence of E_p on log *f* can be represented by the relation having correlation coefficient 0.994:

$$E_p \text{ (mV)} = 96.13 \log f + 16.294$$

The effect of square wave frequency (*f*) on the peak current (i_p) of analyte was also studied in the square wave frequency range 5 to 200 Hz. The oxidation peak current (i_p) of EPI was found to increase with increase in square wave frequency (*f*). The dependence of peak current on square wave frequency was linear and can be expressed by the relation:

$$i_p \ (10^{-6}\text{A}) = 2.841 f + 8.315$$

having correlation coefficient 0.996. All these observations are in agreement with the properties of adsorption controlled electrochemical process [37-39] which also supported the results obtained from cyclic voltammetry.

The effect of pH on the oxidation of EPI was also studied in the pH range 2.4-11.0 using SWV. It was found that the peak potential shifted towards less positive potentials with increase in pH. The dependence of E_p on pH obeys the relation:

$$E_p = [566.08 - 57.332 \text{ pH}] \text{ mV versus Ag/AgCl}$$

having correlation coefficient 0.992 for the analyte. The slope of E_p versus pH plot for EPI is close to 60 mV/pH and hence, suggests that equal number of protons and electrons are involved in the electrode reaction.

3.3.2 Spectral studies

The UV-vis spectral changes of 0.1 mM EPI were recorded at pH 4.9 and 7.2. At both the pH, EPI exhibited well-defined absorption bands at λ_{max} 285 and 310 nm (**Fig. 3.3**). On the application of a potential 50 mV more positive than peak I_a, the absorbance at 285 nm systematically decreases and an increase in absorbance is observed in the regions 240-260 nm and 300-360 nm (curves 1-10, **Fig. 3.3**). Curve 10 represents the spectrum of 0.1 mM EPI after 1 h of electrolysis and absorption maximum at 285 nm turned to a shoulder. During electrolysis the colorless solution of EPI was changed to dark brown color.

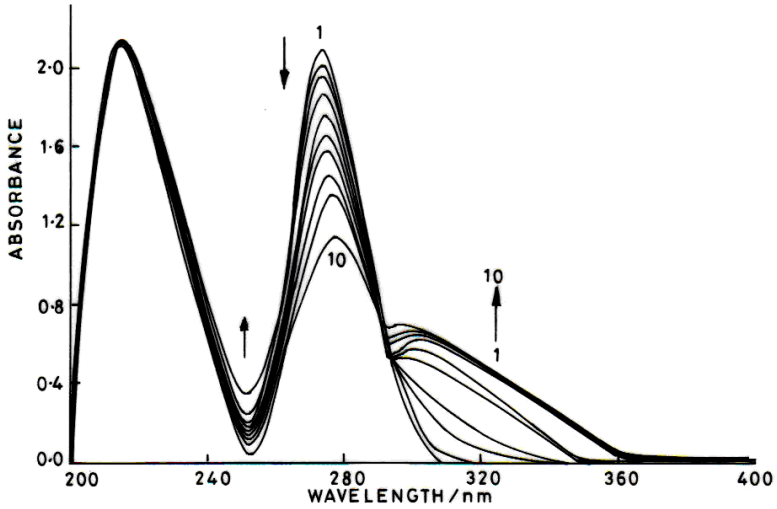

Fig.3.3 UV spectrum of 0.1 mM EPI observed in phosphate buffer of pH 7.2. Curves were recorded at: (1) 0 min, (2) 5 min, (3) 10 min, (4) 20 min, (5) 30 min, (6) 50 min, (7) 70 min (8) 100 min (9) 130 min and (10) 170 min of electrolysis after application of 0.175 V vs SCE.

The progress of electrolysis of EPI was also monitored by recording the cyclic voltammograms at different times. At pH 7.2, when a potential ~50 mV more positive than peak I_a was applied, the peak current of peak I_a systematically decreased. Peaks II_a and II_c also followed a systematic decrease. The exhaustively electrolysed solution of EPI showed only small bumps corresponding to redox couple. The kinetics of the decay of the UV-absorbing intermediate generated was studied at different pH values in the pH range 4.9 to 7.2. For this purpose, electro-oxidation was carried out and when the absorbance at λ_{max} = 285 nm reached to ~50 % of its value

(normally after 25-30 min of electrolysis), the applied potential was switched to zero and the decay of the absorbance at selected wavelengths was monitored as a function of time. At all the pH values studied, the nature of plots of the absorbance vs. time is exponential. The plots of log ($A - A_\infty$) vs. time are linear, indicating that the decay follows first-order kinetics (**Fig. 3.4**). The values of the rate constants calculated at different pH values are practically independent of pH and are presented in **Table 3.1**.

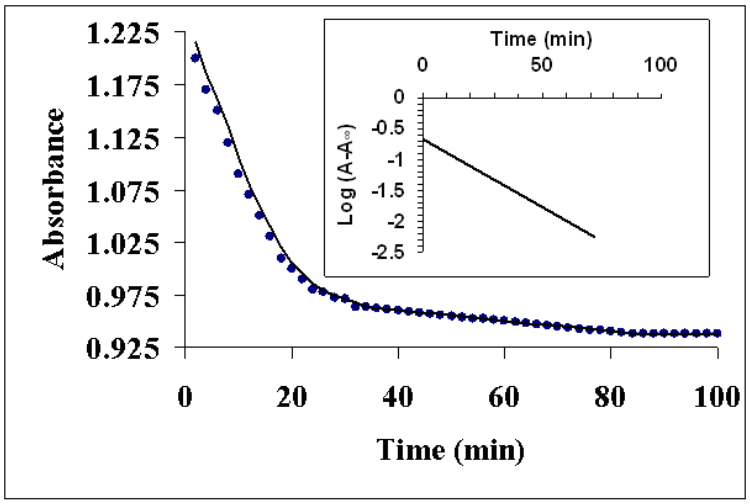

Fig. 3.4 Plot of the absorbance vs. time and log ($A-A_\infty$) vs. time (inset) measured at 310 nm for the first-order decay of the UV-absorbing intermediates generated during electro-oxidation of EPI at pH 7.2.

3.3.3 Enzymatic oxidation

The progress of peroxidase-catalysed oxidation of EPI was studied in phosphate buffers of pH 4.9, 6.0 and pH 7.2. At pH < 4.9 and > 7.5, the decay of the intermediate was very slow. To detect whether the species responsible for reversible couple in cyclic voltammetry is also generated during the enzymatic oxidation of EPI, cyclic voltammograms were recorded by initiating the sweep in the negative direction. The initial negative sweep was necessary otherwise it would be difficult to decide whether species responsible for II_c/II_a are formed due to electrochemical or enzymic oxidation. A cyclic voltammogram of 0.1 mM solution of EPI at pH 7.2 with initial negative sweep direction is shown by **curve A** in **Fig. 3.5** and no peaks corresponding to the reversible couple are observed. However, the reversible couple was obtained in the second sweep indicating thereby, that redox couple II_c/II_a was observed only after scanning peak I_a. The redox couple II_c/II_a is observed due to the $2e^-$, $2H^+$ reduction of leucoadrenochrome (III) to adrenochrome (IV) as shown in **Scheme 3.1**. **Fig. 3.5** (**curve B**) depicts a cyclic voltammogram of

0.1 mM solution of EPI at pH 7.2 with initial sweep in the positive direction. The voltammogram recorded after adding peroxidase (2 μM) is basically similar to **curve A**. Thus, in both the curves, reversible couple was observed only after recording peak I_a. However, if enzymatic oxidation is initiated by adding H_2O_2 (0.6 mM), reversible couple starts to appear in the first negative sweep.

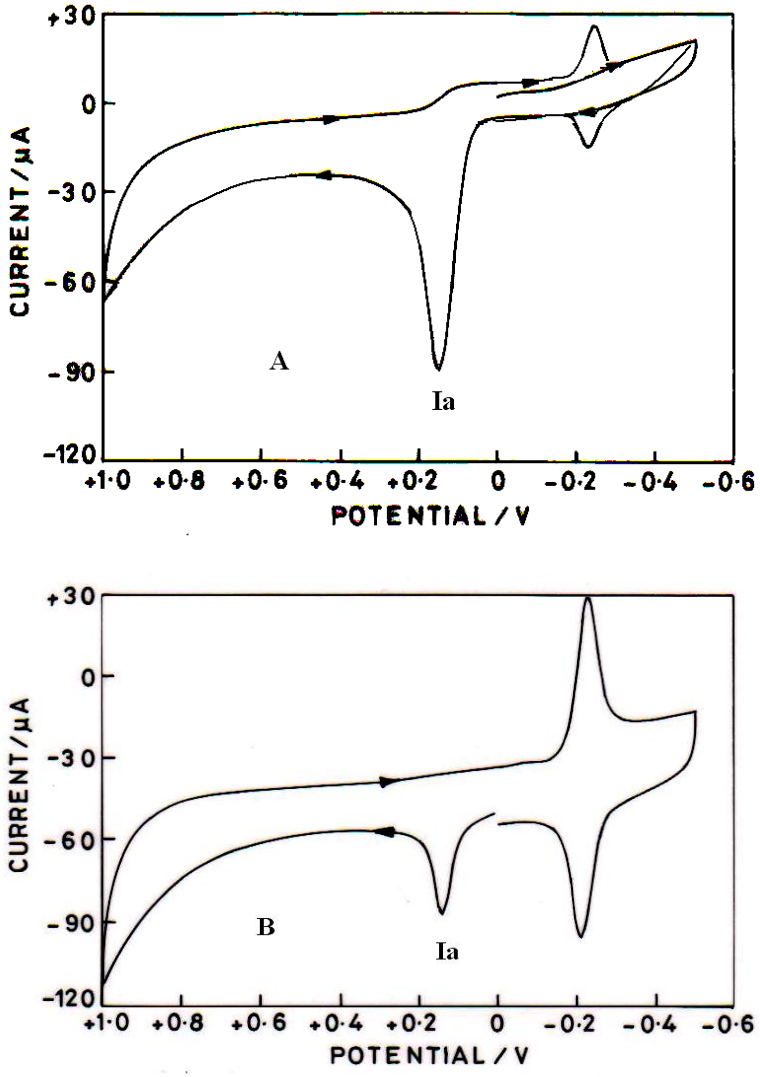

Fig. 3.5 Cyclic voltammngrams observed during the electrochemical and enzymatic oxidation of EPI at pH 7.2 (sweep rate-100 mVs^{-1}). Curve A represents a cyclic voltammogram of 0.1 mM solution of EPI with initial sweep in the negative direction. Curve B depicts a cyclic voltammogram of 0.1 mM solution of EPI with initial sweep in the positive direction.

Fig. 3.6 represents a set of cyclic voltammograms recorded after different times of the addition of H_2O_2 and a well-defined reversible couple (II_c/II_a) was observed with initial negative sweep in cyclic voltammetry. The peak current of the reversible couple initially increased and then

decreased with progress of enzymic oxidation and then became constant (**Fig 3.6, curve 6**). The peak I_a was systematically decreased with progress of enzymic oxidation and almost disappeared after 10 min of addition of H_2O_2. It is interesting to note that the E_p values of the redox couple II_c/II_a during enzymatic oxidation and electrochemical oxidation are the same. Thus, it is inferred that the enzymatic oxidation of EPI produces a species similar to that obtained in electrochemical oxidation. The spectral changes during enzymatic oxidation were also monitored to detect the UV-visible intermediate.

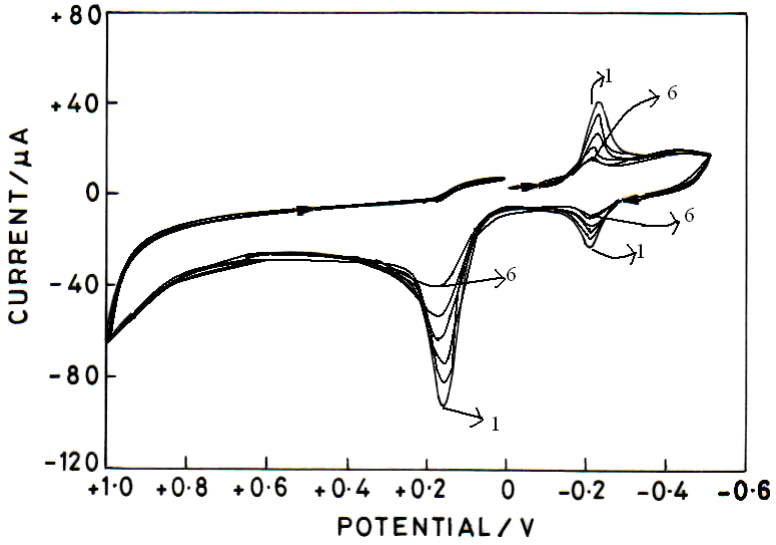

Fig. 3.6 Cyclic voltammograms recorded after the addition of H_2O_2 (0.6 mM) to EPI solution + peroxidase (2 μM). Curves were recorded at 0 (1); 2 (2); 4 (3); 6 (4); 8 (5) and 10 (6) min of initiation of enzymic oxidation.

Fig. 3.7 represents the UV spectrum of EPI containing peroxidase soon after the addition of H_2O_2. Curves 1-10 were recorded at different time intervals after initiation of enzymic oxidation. A systematic decrease in absorbance at λ_{max} = 285 nm and an increase in absorbance in the regions 300-320 nm (**curves 1-10**, **Fig. 3.7**) are observed. The kinetics of decomposition of the UV-absorbing intermediate generated during enzymatic oxidation was studied at different pH values by adding catalase (1 mg/mL) to terminate the oxidation. The changes in absorbance at selected wavelengths were monitored at different times. The absorbance vs. time plot exhibits an exponential decay, and the rate constants calculated from the linear plots of log $(A - A_\infty)$ vs. time are presented in **Table 3.1**. Clearly, the rate constants of enzymic oxidation are similar to those observed during electrochemical oxidation. The identical spectral changes and rate constants

suggest that the same intermediate species is generated during enzymic and electrochemical oxidation to give the same product. Hence, it is concluded that the electrochemical and enzymatic oxidations of EPI proceed by identical mechanisms.

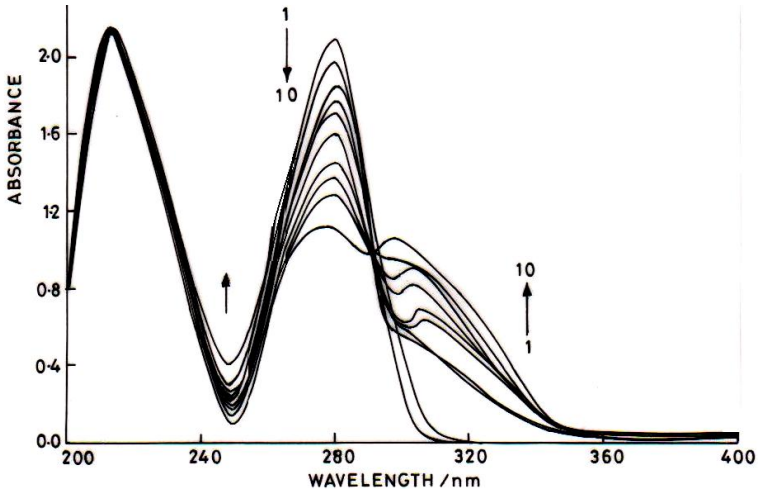

Fig. 3.7 Spectral changes observed during the enzymatic oxidation of EPI at pH 7.2. Curves were recorded at an interval of 4 min after the initiation of oxidation by the addition of H_2O_2.

Table 3.1 Observed k values for the decomposition of the UV–vis absorbing intermediate generated during electro-oxidation and enzymic oxidation of EPI.

pH	λ_{max} / nM	Rate/ k × 10^{-3} s^{-1} [a]	
		Electrochemical	Enzymatic
4.9	310	0.6328	0.6297
6.0	310	0.6462	0.6401
7.2	310	0.6410	0.6521

[a] **Average of at least three replicate determinations.**

3.3.4 Product characterization

For product identification, 15-20 mg of the compound **(I)** was exhaustively electrolyzed at pH 7.2 by applying a potential of ~ 50 mV more positive than the oxidation peak potential. The progress of the electrolysis was monitored by recording cyclic voltammograms and UV spectra at different time intervals. With progress of electrolysis colourless solution of EPI changed to dark brown and the oxidation peak in voltammetry disappeared at the end of electrolysis.

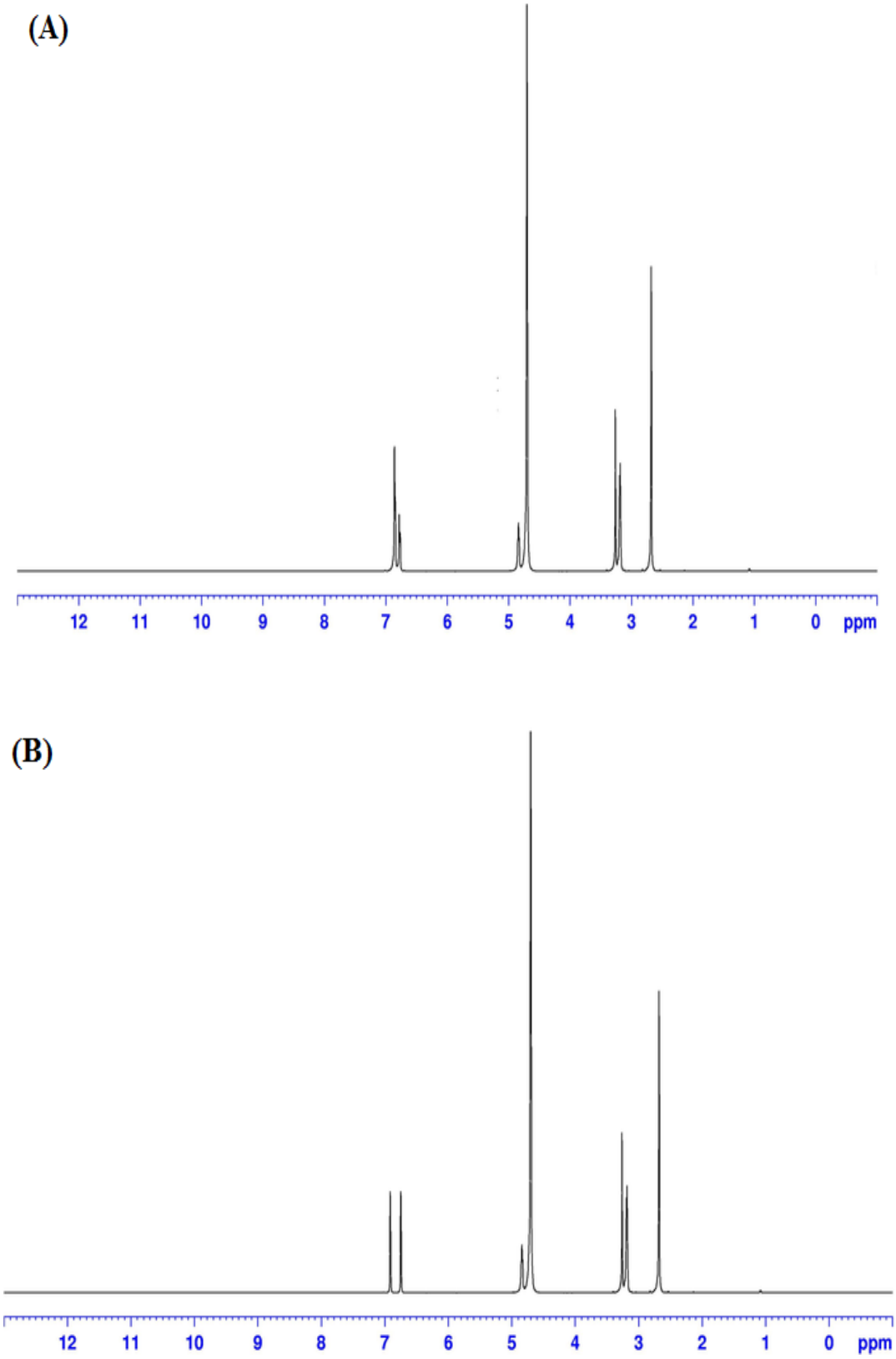

Fig. 3.8 ^{1}H NMR spectrum observed for the EPI (A) and its oxidation product (B) in D_2O solvent.

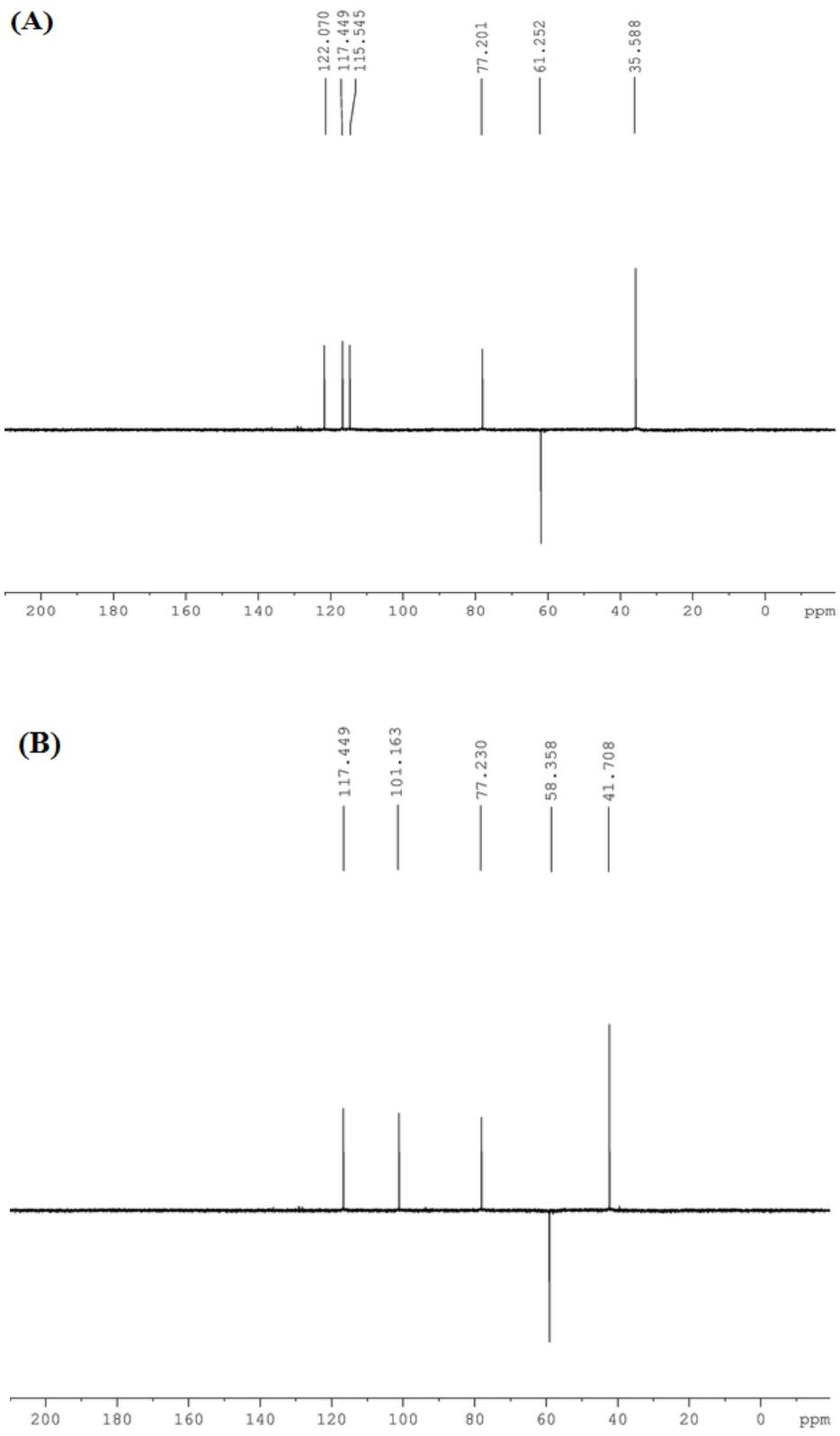

Fig. 3.9 DEPT 135 spectrum observed for the EPI (A) and its oxidation product (B) in D_2O solvent.

The ^{1}H NMR of the product in D_2O exhibited signals at ^{1}H δ_H (500 MHz; D_2O) 6.865 (1H, s), 6.784 (1H, s), 4.843 (1H, t), 3.261 (2H, d) and 2.685 (3H, s). The presence of two protons as singlets with high δ_H values indicate that the cyclization of EPI to epinephrinechrome has occurred (**Fig 3.8**). To reconfirm the characterization, DEPT 135 studies were also done. DEPT 135 of the product in D_2O exhibited signals at ^{13}C δ_H (500 MHz; D_2O) 117.45 (C-H aromatic), 101.16 (C-H aromatic), 77.23 (C-H aliphatic), 58.36 (CH_2 aliphatic), 41.71 (CH_3 aliphatic). Due to the presence of two aromatic C-H in the product, it is concluded that EPI has been cyclized into epinephrinechrome (**IV**) (**Fig. 3.9**). The final product formed in enzymatic oxidation of EPI exhibited similar NMR and DEPT signals and was same as formed during electrochemical oxidation.

The initial oxidation of EPI thus occurs in a $2e^{-}$, $2H^{+}$ reaction at hydroxyl groups to give corresponding o-quinone (**II**). The quinone (**II**) cyclizes to species (**III**) and the reversible couple observed is attributed to the formation of adrenochrome/ leucoadrenochrome couple (**IV/III**) in a $2e^{-}$, $2H^{+}$ process. The first order rate constant observed for the decay indicate the rate of cyclization. A tentative mechanism suggested for the electro-oxidation of EPI at pH 7.2 is shown in **Scheme 3.1**.

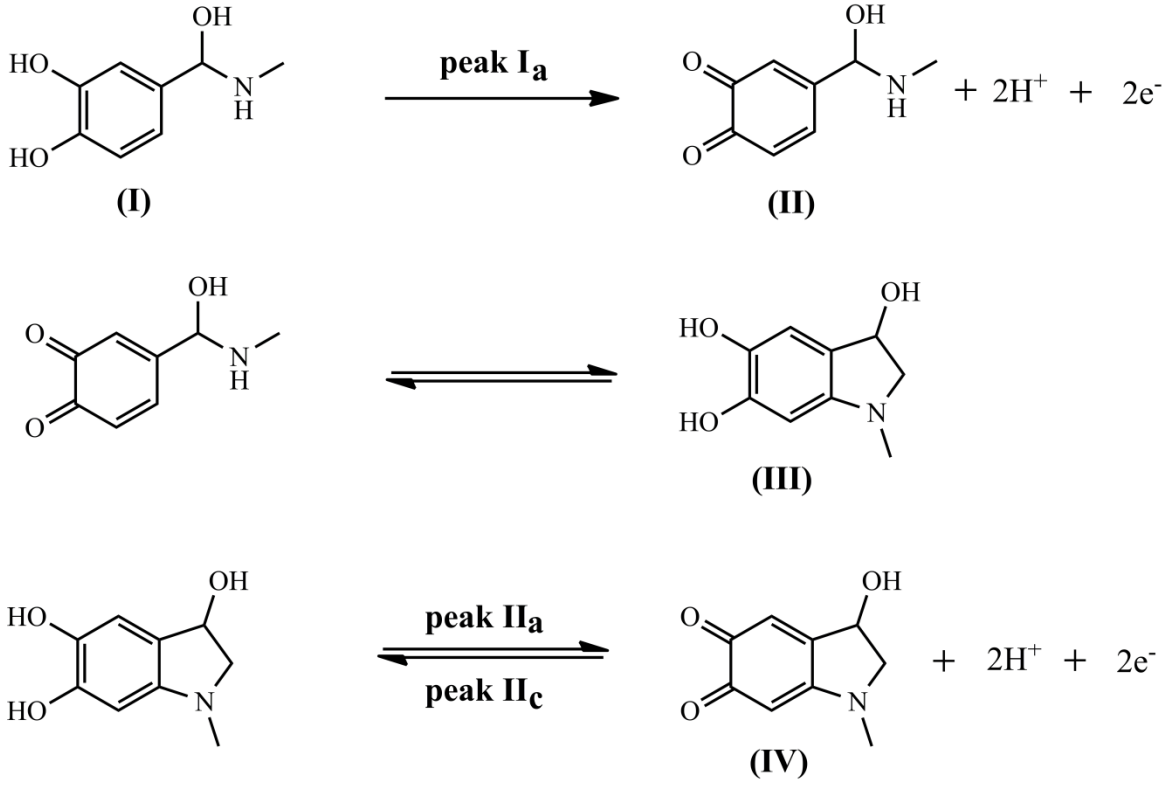

Scheme 3.1 A tentative pathway suggested for the oxidation of EPI at pH 7.2.

3.4 CONCLUSION

Table 3.2 A comparison of various electrodes used for the determination of epinephrine.

S. No.	Electrode used	Detection limit (mol/L)	Analytical range (mol/L)	Reference
1	Glassy carbon electrode modified with valine	7.6×10^{-7}	1.0×10^{-5}-1.4×10^{-4}	[33]
2	CTAB modified carbon paste electrode	7.2×10^{-6}	0.01-0.27×10^{-3}	[34]
3	White rot fungi cells based microbial biosensor	1.04	5-100	[35]
4	Glassy carbon electrode modified by electrodeposited films of caffeic acid	6×10^{-7}	2×10^{-6}-3×10^{-4}	[36]
5	p-Tetra-butyl calix [6] arene-L-Histidine chemically modified electrode	0.74×10^{-7}	1.0×10^{-6}-1.3×10^{-4}	[37]
6	Over oxidized poly pyrrole/ MWCNT modified glassy carbon	40×10^{-9}	1-8 and 10-100×10^{-9}	[17]
7	Ni macrocyclic complex modified glassy carbon	1×10^{-7}	8×10^{-7}-2×10^{-4}	[38]
8	MWCNT modified basal plane pyrolytic graphite	2×10^{-8}	1×10^{-8}-1×10^{-6}	[39]
9	Edge plane pyrolytic graphite	17×10^{-8}	25×10^{-8}-20×10^{-6}	Present method

It is believed that it would be difficult to identify and isolate the intermediates and products by direct investigations of enzyme-mediated oxidation of EPI. However, a combination of electrochemical and spectral studies may lead to a full understanding of the enzymatic oxidation of catecholamines. A comparison of the electrochemical behaviour of EPI indicates that the cyclic voltammetric and spectral behaviour are essentially same in both the cases. The investigation clearly reveals that the electrochemical oxidation of EPI proceeds via a $4e^-$, $4H^+$ mechanism. The

formation of UV- absorbing intermediate at longer wavelength (290-360 nm) supports the view that species (II) is more conjugated than the starting molecule (I). The major product of oxidation has been characterized as epiadrenochrome (IV) by ^{1}H and DEPT 135 NMR.

The use of pyrolytic graphite electrode has been found to be satisfactory for the determination of EPI and the detection limit is found to be 17×10^{-8} M. A comparison of detection limit at other electrodes reported in recent literature is presented in **Table 3.2** and indicates that the electrode is satisfactory for the determination of EPI and is better than several electrodes reported in last few years. In addition, the edge plane pyrolytic graphite electrode does not require any pre-treatment and can be easily used as received. Thus, it can be concluded on the basis of these investigations that EPI is also oxidized in biosystems leading to the formation of products, which could serve as an important tool for the biochemists to deeply understand the medicinal applications of the products formed under oxidative conditions in the human physiology. Overall, mechanistic pathway of EPI can serve as a reasonable model to enlighten the complex biological reactions occurring at the enzyme-solution interface in the biosystem.

3.5 REFERENCES

[1] Z. Yang, G. Hu, X. Chen, J. Zhao, G. Zhao; "The nano-Au self-assembled glassy carbon electrode for selective determination of epinephrine in the presence of ascorbic acid". *Colloids Surf. B,* **54** (2007) 230.

[2] J. A. Ni, H. X. Ju, H. Y. Chen, D. Leech; "Amperometric determination of epinephrine with an osmium complex and nafion double-layer membrane modified electrode". *Anal. Chim. Acta*, **378** (1999) 151.

[3] D. A. Haas; "Management of medical emergencies in the dental office: Conditions in each country, the extent of treatment by the dentist". *Anesth. Prog.*, **53** (2006) 20.

[4] M. A. Fotopoulou, P. C. Ioannou; "Post-column terbium complexation and sensitized fluorescence detection for the determination of norepinephrine, epinephrine and dopamine using high-performance liquid chromatography". *Anal. Chim. Acta*, **462** (2002) 179.

[5] J. Du, L. Shen, J. Lu; "Flow injection chemiluminescence determination of epinephrine using epinephrine-imprinted polymer as recognition material". *Anal. Chim. Acta*, **489** (2003) 183.

[6] O. D. Leite, K. O. Lupetti, O. F. Filho, I. C. Vieira, A. M. Barbosa; "Synergic effect studies of the bi-enzymatic system laccaseperoxidase in a voltammetric biosensor for catecholamines". *Talanta*, **59** (2003) 889.

[7] L. I. B. Silva, F. D. P. Ferreira, A. C. Freitas, T. A. P. R. Santos, A. C. Duarte; "Optical fiber biosensor coupled to chromatographic separation for screening of dopamine, norepinephrine and epinephrine in human urine and plasma". *Talanta*, **80** (2009) 853.

[8] M. Chicharro, A. Sanchez, A. Zapadiel, M. D. Rubianes, G. Rivas; "Capillary electrophoresis of neurotransmitters with amperometric detection at melanin-type polymer-modified carbon electrodes". *Anal. Chim. Acta*, **523** (2004) 185.

[9] V. Carrera, E. Sabater, E. Vilanova, M. A. Sogorb; "A simple and rapid HPLC-MS method for the simultaneous determination of epinephrine, norepinephrine, dopamine and 5-hydroxytryptamine: Application to the secretion of bovine chromaffin cell cultures". *J. Chromatogr. B,* **847** (2007) 88.

[10] C. Sabbioni, M. A. Saracino, R. Mandrioli, S. Pinzauti, S. Furlanetto, G. Gerra, M. A. Raggi; "Simultaneous liquid chromatographic analysis of catecholamines and 4-hydroxy-3-methoxyphenylethylene glycol in human plasma: Comparison of amperometric and coulometric detection". *J. Chromatogr. A*, **1032** (2004) 65.

[11] Y. X. Sun, S. F. Wang, X. H. Zang, Y. F. Huang; "Simultaneous determination of epinephrine and ascorbic acid at the electrochemical sensor of triazole SAM modified gold electrode". *Sens. Actuators B,* **113** (2006) 156.

[12] Y. Wang, Z. Z. Chen; "A novel poly(taurine) modified glassy carbon electrode for the simultaneous determination of epinephrine and dopamine". *Colloids Surf. B,* **74** (2009) 322.

[13] K. O. Lupetti, I. I. Vieira, O. Fatibello; "Electroregenerable anion-exchange resin with triiodide carbon paste electrode for the voltammetric determination of adrenaline". *Analyst,* **127** (2002) 525.

[14] G. Erdogdu, A. E. Karagozler; "Investigation and comparison of the electrochemical behavior of some organic and biological molecules at various conducting polymer electrodes". *Talanta,* **44** (1997) 2011.

[15] S. H. Kim, J. W. Lee, I. H. Yeo; "Spectroelectrochemical and electrochemical behavior of epinephrine at a gold electrode". *Elecrochim Acta,* **45** (2000) 2889.

[16] A. Salimi, C. E. banks, R. G. Compton; "Spectroelectrochemical and electrochemical behavior of epinephrine at a gold electrode". *Analyst,* **129** (2004) 225.

[17] S. Shahrokhian, R. S. Saberi; "Electrochemical preparation of over-oxidized polypyrrole/multi-walled carbon nanotube composite on glassy carbon electrode and its application in epinephrine determination". *Electrochim Acta,* **57** (2011) 132.

[18] R. N. Goyal, S. Bishnoi; "A novel multi-walled carbon nanotube modified sensor for the selective determination of epinephrine in smokers". *Electrochim Acta,* **56** (2011) 2717.

[19] B. C. Saunders, A. G. Holmes-Siedle, B. P. Stark, (Ed.); "In peroxidase". Butterworths, London (1964).

[20] B. Kalyanaraman, R. C. Sealy; "Electron spin resonance-spin stabilization in enzymatic systems: Detection of semiquinones produced during peroxidatic oxidation of catechols and catecholamines". *Biochem. Biophys. Res. Commun*., **106** (1982) 1119.

[21] D. Metodiewa, K. Reszka, H. B. Dunford; "Evidence for a peroxidatic oxidation of norepinephrine, a catecholamine, by lactoperoxidase". *Biochem. Biophys. Res. Commun.,* **160** (1989) 1183.

[22] R. A. Lovstad; "Effect of urate on the lactoperoxidase catalyzed oxidation of adrenaline". *Biometals,* **17** (2004) 631.

[23] S. Adak, U. Bandyopadhyay, D. Bandyopadhyay, R. K. Banerjee; "Mechanism of horseradish peroxidase catalyzed epinephrine oxidation: Obligatory role of endogenous O_2 and H_2O_2". *Biochemistry*, **37** (1998) 16922.

[24] T. Nagatsu; "Progress in monoamine oxidase (MAO) research in relation to genetic engineering". *Neurotoxicology*, 25 (2004) 11.

[25] A. Sadler, V. V. Subrahmanyam, D. Ross; "Oxidation of catechol by horseradish peroxidase and human leukocyte peroxidase: Reactions of *o*-benzoquinone and *o*-benzosemiquinone". *Toxicol. Appl. Pharmacol.*, **93** (1988) 62.

[26] F. Zhang, G. Dryhurst; "Oxidation chemistry of dopamine: Possible insights into the age-dependent loss of dopaminergic nigrostriatal neurons". *Bioorg. Chem.*, **21** (1993) 392.

[27] X. M. Shen, G. Dryhurst; "Further insights into the oxidation chemistry of norepinephrine and epinephrine in the presence of cysteine". *Bioorg. Chem.*, 25 (1997) 130.

[28] R. N. Goyal, G. Dryhurst; "Redox chemistry of guanine and 8-oxyguanine and a comparison of the peroxidase-catalyzed and electrochemical oxidation of 8-oxyguanine". *J. Electroanal. Chem.*, **135** (1982) 75.

[29] A. B. Toth, R. N. Goyal, M. Z. Wrona, T. Lacava, N. T. Nguyan, G. Dryhurst "Electrochemical and enzymic oxidation of biological purines". *Bioelectrochem. Bioenerg.*, **8** (1981) 413.

[30] R. N. Goyal, A. B. Toth, G. Dryhurst; "Electrochemical and peroxidase-catalyzed redox chemistry of 9-methyl uric acid". *J. Electroanal. Chem.*, **133** (1982) 287.

[31] R. N. Goyal, M. S. Verma; "Comparison of electrochemical and enzymic oxidation of 3-methyluric acid". *J. Chem. Soc. Perkin Trans. 2*, (1993) 1241.

[32] R. N. Goyal, V. Bansal; "Comparison of electrochemical and enzymatic oxidation of 3,9-dimethyluric acid". *Indian J. Chem.*, **34 B** (1995) 190.

[33] G. D. Christian, W. C. Purdy; "The residual current in orthophosphate medium". *J. Electroanal. Chem.*, **3** (1962) 363.

[34] R. N. Goyal, S. K. Srivastava, R. Agarwal; "Electrochemical behaviour and aggregation number of pyridinol azo dyes". *Bull. Soc. Chim. Fr.*, **4** (1985) 656.

[35] R. S. Nicholson, I. Shain; "Theory of stationary electrode polarography single scan and cyclic methods applied to reversible, irreversible, and kinetic systems". *Anal. Chem.*, **36** (1964) 706.

[36] E. R. Brown, R. F. Large, A. Weissberger, B. W. Rossiter; "Physical Methods Chemistry". Wiley-Interscience, Rochester (1964).

[37] M. R. C. Massaroppi, S. A. S. Machado, L. A. Avaca; "Electroanalytical determination of the herbicide picloram in natural waters by square wave voltammetry". *J. Braz. Chem. Soc.*, **14** (2003) 113.

[38] A. Radi, M. A. E. L. Ries, G. E. Bekhiet; "Electrochemical oxidation of the hypoglycaemic drug gliclazide". *Anal. Lett.,* **32** (1999) 1603.

[39] S. Komorsky-Lovric, S. Gagic, R. Penovski; "Voltammetric determination of benzoylecgonine". *Anal. Chim. Acta,* **389** (1999) 219.

[40] X. Li, M. Chen, X. Ma, X. Lin; "Maintaining component-based system based on reflection mechanism". *Int. J. Chem.,* **2** (2010) 206.

[41] Corona-Avendano, G. Alarcon-Angeles, M. T. Ramirez-Silva, M. Romero-Romo, A. Cuan, M. Palomar-Pardave; "Simultaneous electrochemical determination of adrenaline and ascorbic acid: influence of [CTAB]". *J. Electrochem. Soc.,* **156** (2009) 375.

[42] E. Akyilmaz, M. Turemis, I. Yasa; "Voltammetric determination of epinephrine by White rot fungi (Phanerochaete chrysosporium ME446) cells based microbial biosensor". *Biosens. Bioelectron.,* **26** (2011) 2590.

[43] W. Ren, H. Q. Luo, N. B. Li; "Electrochemical behavior of epinephrine at a glassy carbon electrode modified by electrodeposited films of caffeic acid". *Sensors,* **6** (2006) 80.

[44] H. Liu, G. Zhao, L. Wen, B. Ye; "Simultaneous voltammetric determination of epinephrine and serotonin at a p-tetra-butyl calix [6] arene-L-histidine chemically modified electrode". *J. Anal. Chem.,* **61** (2006) 1104.

[45] H. H. Cho, S. G. Kweon, S. H. Lea, Z. U. Bae; "Thymidylate synthase (TYMS) and dihydropyrimidine dehydrogenase (DPYD) polymorphisms in the Korean population for prediction of 5-fluorouracil associated toxicity". *J. Korean Electrochem. Soc.,* **10** (2007) 190.

[46] S. Shahrokhian, M. Khafazi; "Application of pyrolytic graphite modified with nano-diamond/graphite film for simultaneous voltammetric determination of epinephrine and uric acid in the presence of ascorbic acid". *Electrochim. Acta,* **55** (2010) 9090.

****

Chapter 4

DETERMINATION OF ADENINE AND ADENOSINE MONOPHOSPHATE

4.1 INTRODUCTION

Purines are six-membered rings attached to five membered rings whose derivatives play an essential role in various biological processes. Adenine (6-aminopurine) (**I**), an organic base of the purine family is one of the most primal organic molecules for life as we know it today. Adenine is one of the five main nucleobases and is cardinal to the coding of genetic information within biological systems. It is believed to be the first nucleoside base to have been synthesized [1] and is considered as an essential component in biological molecules and polymers such as nucleic acids and coenzymes [2]. Adenine combines with the sugar ribose to form adenosine, which in turn can be bonded with one to three phosphoric acid units, yielding the three nucleotides adenosine monophosphate, adenosine diphosphate and adenosine triphosphate. These adenine derivatives perform important functions in oxidative phosphorylation and trans-membrane signaling processes, and as secondary substrate or modulator for other enzymatic processes [3]. The phosphate derivative of adenosine (9′-β-D-ribosidoadenine) is called as adenosine monophosphate, which is also known as adenylic acid. The most common isomer of adenosine monophosphate is adenosine-5′-monophosphate (5′-AMP) (**II**) or 'muscle adenylic acid' in which the phosphate group is attached to the fifth carbon of the ribose moiety. 5′-AMP is regarded as the parent compound of adenosine di- and tri-phosphate.

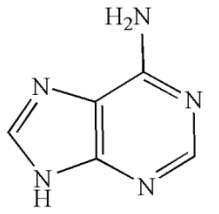

(I)

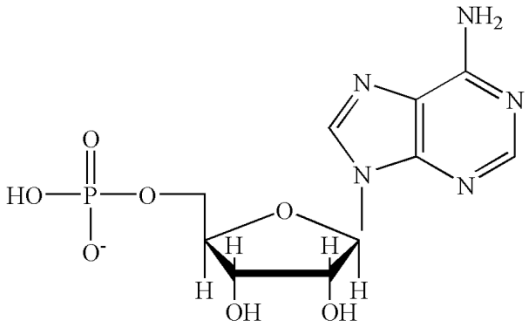

(II)

Nucleic acid plays a crucial role in the storage of genetic information and protein biosynthesis. Determining adenine concentration in nucleic acids is important to the measurement of nucleic acid concentration itself. Indeed, the presence of adenine in physiological fluids, tissues, and cells is related to the catabolism of nucleic acids, enzymatic degradation of tissues, dietary habits, and various salvage pathways [4, 5]. Therefore, the quantitative determination of adenine is a challenging and important task owing to the fact that it can be an indicator of important information on certain disease [6] and genetic diagnosis [7]. Myocardial 5′-AMP catabolism in perfused guinea pig, rat and mouse has been reported by Headrick *et al.* [8]. 5′-AMP is also a

component of several important coenzymes and in addition plays a crucial role in the incorporation of amino acids into proteins. Haug *et al.* [9] have accounted changes in the concentration of adenosine nucleotides in the blood of the pulmonary artery before and after the administration of theophylline ethylenediamine. The effects of 5′-AMP on oxidative phosphorylation in the liver have also been analyzed by Rudichenko and Dumanskii [10]. Nucleotides of adenine are found in the skeletal muscle and an estimation of their contents in normal human skeletal muscle is also reported in the literature [11, 12].

Simultaneous determination of adenine and 5′-AMP has great significance to bioscience and clinical diagnosis since both these compounds occur simultaneously in body fluids. Intracellular levels of adenine and 5′-AMP are important, because their altered concentration stimulate metabolic disorders in human system. The purine salvage enzyme, adenine phosphoribosyl-transferase (APRT) is the key enzyme that metamorphoses adenine into adenosine monophosphate [13, 14]. In patients with APRT deficiency, xanthine oxidase rapidly oxidizes accumulated adenine first into 8-hydroxyadenine and then into 2,8-dihydroxyadenine, which is then egested by the kidneys through tubular secretion and can lead to the formation of stones in urinary tract. The simultaneous determination of 5′-AMP and adenine is the subject of considerable interest, especially in human body fluids. Many chromatographic and electrochemical methods have been developed for detection and quantification of both compounds individually or with other compounds [15-22]. However, to the best of our knowledge, no attempt has been made for the simultaneous determination of these two compounds in biological fluids by voltammetry. The present study deals with the simultaneous determination of adenine and 5′-AMP employing SWV at SWNT modified EPPGE. The usefulness of carbon nanotubes (CNT) is due to their extraordinary mechanical and unique electrochemical properties, which have garnered much attention in the past few years. The CNT based electrodes are generally prepared by casting SWNT suspension on conventional electrode surface [23-25]. In the present study, SWNT modified EPPGE has been used for the simultaneous determination of adenine and 5′-AMP using SWV procedure.

4.2 EXPERIMENTAL

4.2.1 Apparatus and procedure

The square wave voltammetric experiments were carried out using a three electrode single compartment cell furnished with SWNT modified pyrolytic graphite electrode as the working

electrode, platinum wire as the counter electrode and an Ag/AgCl (3 M NaCl) as reference electrode (BAS Model MF-2052 RB-5B) respectively. The pyrolytic graphite electrode practiced as the working electrode for the electrooxidation studies was prepared in the laboratory by the reported method [26]. Experiments were executed using a BAS CV-50W voltammetric analyzer (Bioanalytical Systems, West Lafayette, USA). All the potentials quoted are versus Ag/AgCl electrode at an ambient temperature of 25±2 °C. The pH measurements were performed using a Century India Ltd. Digital pH-meter (Model CP-901) after due standardization with 0.05 M potassium hydrogen phthalate (pH 4.0 at 25 °C) and 0.01M borax (pH 9.2 at 25 °C). Optimized square wave voltammetry parameters used were: initial E: 700 mV, final E: 1300 mV, square wave amplitude (E_{sw}): 25 mV, potential step (E): 4 mV, square wave frequency (f): 15 Hz. Cyclic voltammograms were recorded in the sweep range of 10-1000 mVs^{-1} with initial sweep to positive potentials. The solutions were deoxygenated by bubbling high-purity nitrogen for 12-15 min before recording the cyclic voltammograms. Working solutions of adenine and 5′-AMP were prepared by adding required volumes of the respective stock solution (1 μM) to the phosphate buffer solution and then the voltammograms were recorded. A smaller sample amount (<0.5 ml) was required for the studies. Human blood and urine samples from healthy volunteers were obtained from the Indian Institute of Technology Hospital, Roorkee. The blood sample with EDTA as anticoagulant was centrifuged and the supernatant was taken for analysis.

4.2.2 Reagents

Adenine and 5′-AMP were incurred from Koch Light, U.K. and Sisco Research Laboratory, Mumbai respectively. They were utilized without further purification. SWNT of purity >98 % was purchased from Bucky, USA. All solvents and chemicals were of analytical grade. The studies were accomplished in the pH range of 2.4-11.0 using 1.0 M phosphate buffer solution prepared by mixing the stock solutions of Na_2HPO_4 and NaH_2PO_4, according to the method of Christian and Purdy [27]. All solutions were prepared in double distilled water.

4.2.3 Preparation of SWNT modified electrode

A 0.5 $mgmL^{-1}$ suspension was prepared by dispersing 0.5 mg SWNT in 1.0 mL N,N-dimethylformamide (DMF) by ultrasonic agitation. Prior to modification, the bare EPPGE was first deliberately scratched on an emery paper followed by washing with double distilled water. It was then touched gently with tissue paper. Eventually, the EPPGE surface was coated with a known volume (40 μL, optimized) of this suspension and permitted to dry at room temperature. This

amount has been found as the optimum amount on the basis of peak current studies. The working electrode surface with a well-coated layer of SWNT was then ready for use. The modified electrode surface was cleaned after each run by applying a potential of −200 mV for 60 s to remove the adsorbed analyte.

4.3 RESULTS AND DISCUSSION

4.3.1 Cyclic voltammetry

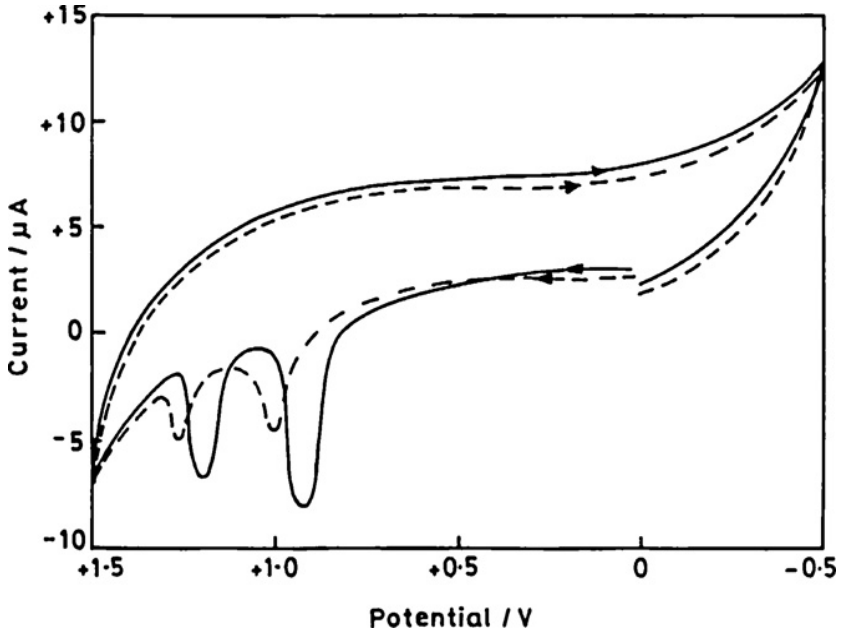

Fig. 4.1 Cyclic voltammogram obtained for 60 nM adenine and 5′-AMP at pH 7.2 at bare EPPGE (- - - - -) and SWNT modified EPPGE (—) at 20 mVs^{-1}.

The cyclic voltammograms were recorded for a mixture of 60 nM adenine and 5′-AMP at the bare and SWNT modified EPPGE in 1 M phosphate buffer solution at pH 7.2 as illustrated in **Fig. 4.1**. Well-defined oxidation peaks at ~920 and ~1210 mV were obtained for adenine and 5′-AMP respectively at SWNT modified EPPGE, which shifted to more positive potentials with a marked decrease in peak current at the bare EPPGE. These results clearly reveal that SWNT acts as a very efficient promoter to enhance the kinetics of the electrochemical oxidation of both adenine and 5′-AMP. The absence of cathodic peaks in the reverse scan clearly indicated that the oxidation of both adenine and 5′-AMP at this particular voltammetric sensor is irreversible in nature. To ascertain the nature of electrode reaction, sweep rate studies were performed in the range of 10-1000 mVs^{-1}. The peak current was found to increase with increasing sweep rates and the plot of $i_p/v^{1/2}$ versus log v clearly indicated that the electrode process is adsorption controlled

[28, 29]. As SWV is considered to be a more sensitive technique in comparison to cyclic voltammetry, hence it is used for the further determination of adenine and 5′-AMP.

4.3.2 Square wave voltammetry

Fig. 4.2 compares typical square wave voltammograms of 60 nM adenine and 5′-AMP in phosphate buffer solution at pH 7.2 recorded at two different working electrodes i.e., SWNT modified EPPGE and bare EPPGE. At bare EPPGE small peaks were observed at high potentials. Under identical conditions, well-defined oxidation peaks are observed at SWNT modified EPPGE, where the peak potential shifted negatively and the peak current increased remarkably. The significant enhancement in current response followed by a decrease in peak potential indicates that SWNT modified EPPGE acts as a promoter to enhance the electrochemical reaction and considerably accelerates the rate of electron transfer. It also indicates that the observed voltammetric response at the SWNT modified EPPGE is due to the presence of significant amount of metal impurities within the nanotubes [30, 31].

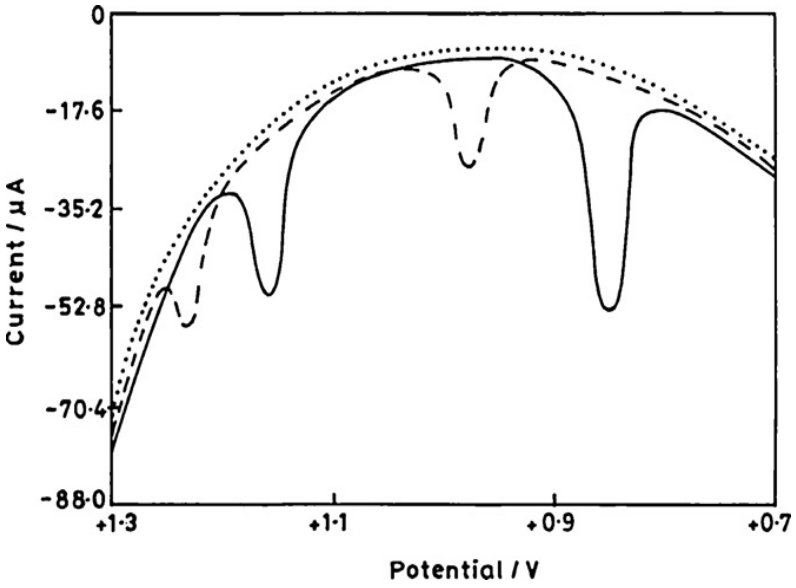

Fig. 4.2 Comparison of square-wave voltammograms of 60 nM adenine and 5′-AMP (pH 7.2) at SWNT modified EPPGE (—), bare EPPGE (- - -) and background phosphate buffer solution at pH 7.2 at SWNT modified EPPGE (. . . .).

4.3.2.1 Electrochemical investigation of adenine

The calibration curve for adenine was measured by using SWV mode and the plot of i_p versus concentration (**Fig. 4.3a**) was linear in the range of 5-100 nM at pH 7.2. The dependence of peak current (after subtracting background current) can be represented by the equation:

$i_p\,(10^{-5}\ A) = 0.0677\ C\ (nM) + 0.2517$

where C is the concentration of adenine having a sensitivity of 677 $nAnM^{-1}$ and a correlation coefficient of 0.9979. This indicated that adenine can be safely estimated in the given concentration range. The detection limit of adenine was found to be 37×10^{-10} M. The effect of pH was studied on the peak potential (E_p) of oxidation peak of 20 nM adenine in the range of 2.4-11.0 (**Fig. 4.3b**) at a square wave frequency of 15 Hz. The peak potential was found to be dependent on pH and shifted to less positive potentials with increasing pH. The linear dependence of the peak potential of oxidation peak of adenine on pH can be represented by the relation:

E_p (pH 2.4-11.0) = (1245.2–59.12 pH) mV versus Ag/AgCl

having correlation coefficient 0.991. The effect of SWV frequency on peak current and peak potential of adenine was studied in the range of 5-200 Hz. The peak current increases with an increase in SWV frequency (**Fig. 4.3c**) which suggests the adsorption nature of electrode process [32, 33]. The peak potential shifted to more positive values with increasing frequency and the plot of E_p versus log *f* was linear with a correlation coefficient of 0.992 (**Fig. 4.3d**) and this behavior suggested the nature of electrode reaction as irreversible in which electron transfer was coupled with a follow up chemical reaction [34]. The variation of E_p with log *f* can be expressed by the equation:

E_p (mV) = 305.48 log *f* + 518.68

4.3.2.2 Voltammetric determination of 5′-AMP

The voltammetric behavior of 5′-AMP was similarly studied at SWNT modified EPPGE. The peak current (i_p) of the oxidation peak (after correction of background current) increased with the increase in concentration of 5′-AMP at pH 7.2 as depicted in **Fig. 4.3a**. The plot was linear in the range of 10-100 nM with a correlation coefficient of 0.9986. The linear regression equation is:

$i_p\,(10^{-5}\ A) = 0.0476\ C\ (nM) + 0.081$

where C is the concentration of 5′-AMP having a sensitivity of 476 $nAnM^{-1}$. The detection limit of 5′-AMP at pH 7.2 is calculated by using the formula $3\sigma/b$, where σ is the standard deviation of the blank and b is the slope of the calibration curve and was found to be 76×10^{-10} M. The peak potential of 5′-AMP at modified electrode was dependent on pH and shifted to less positive potential with increase in pH (**Fig. 4.3b**). The dependence of E_p on pH can be expressed by the relation:

E_p (pH 2.4-11.0) = (1595.3 – 58.34 pH) mV versus Ag/AgCl

with a correlation coefficient of 0.9873. The E_p of 5′-AMP was also dependent on the square wave frequency (*f*) and shifted towards more positive potential with increasing frequency (**Fig. 3d**). The nature of the plot of E_p versus log *f* is linear having a correlation coefficient of 0.9912 and is expressed by the relation:

E_p (mV) = 226.16 log *f* + 880.7

which suggests the nature of electrode reaction as irreversible in which electron transfer is coupled with a follow up chemical reaction [34]. It was found that the peak current increased linearly with an increase in the square wave frequency (**Fig. 4.3c**). The linear nature of these plots suggested that adsorption played a significant role in the electrode process [32, 33].

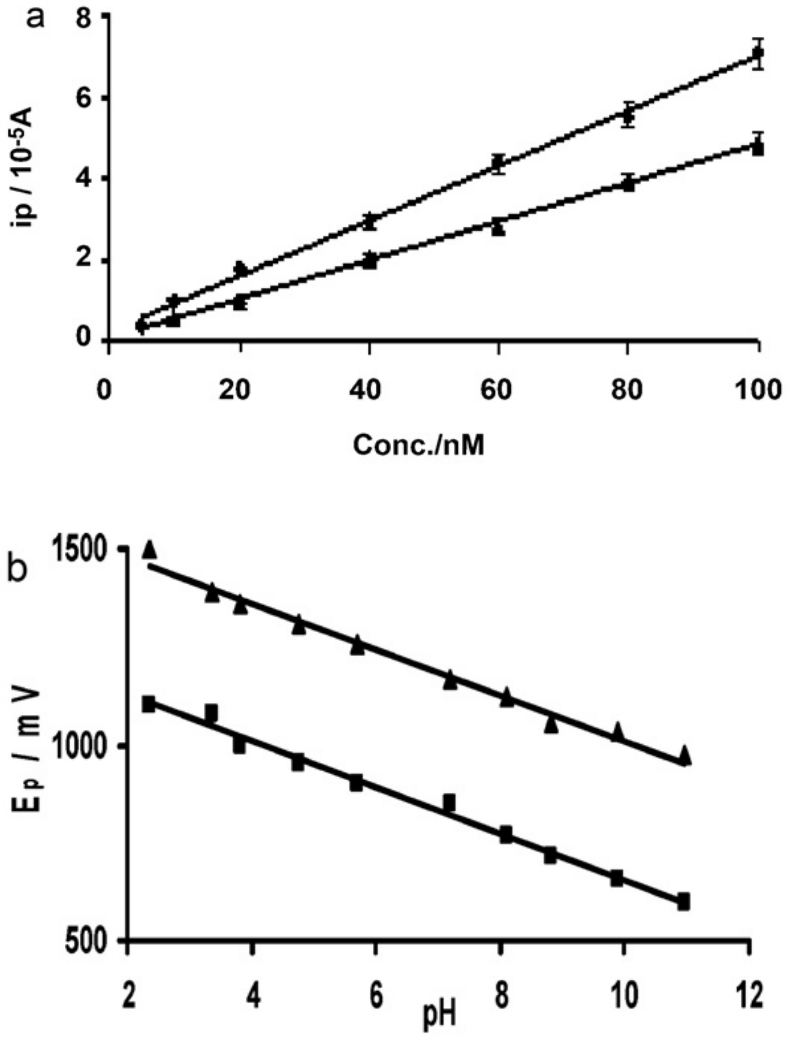

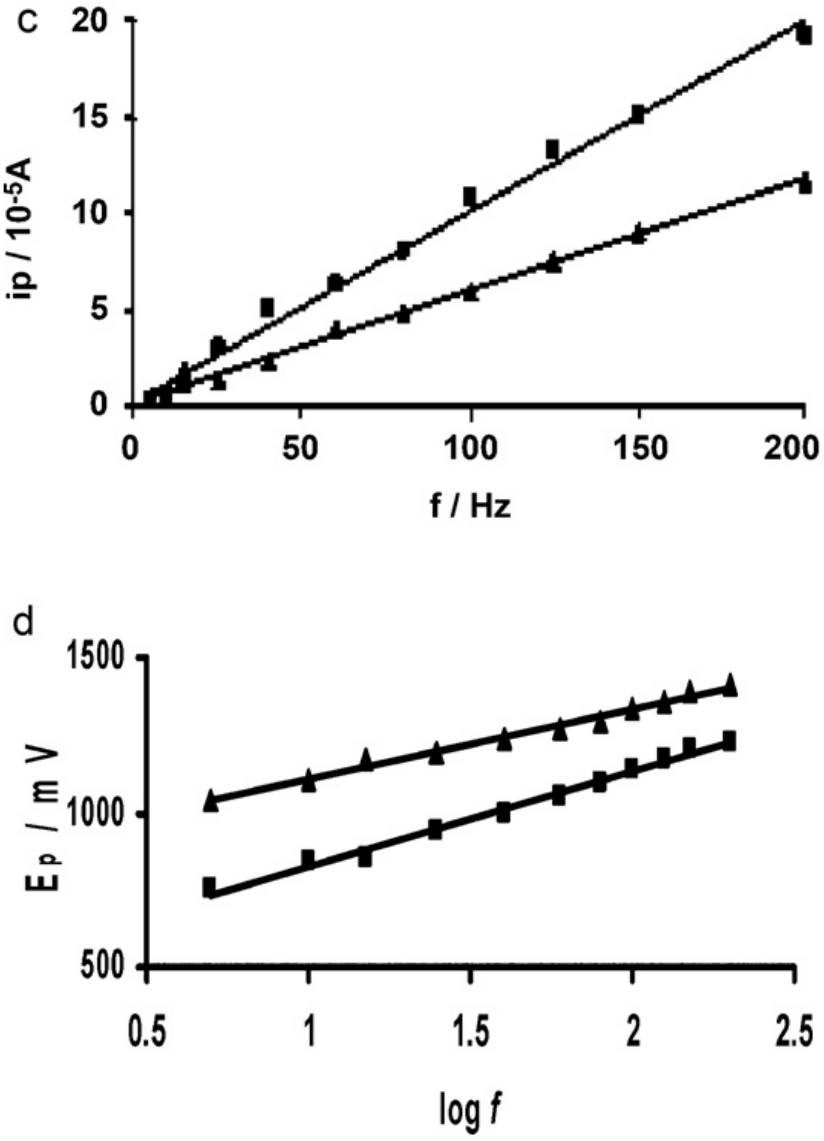

Fig. 4.3 (a) Dependence of observed peak current (i_p) against concentration of adenine (■) and 5′-AMP (▲) at SWNT modified EPPGE at pH 7.2. (b) Observed dependence of peak potential (E_p) on pH for 20 nM adenine (■) and 5′-AMP (▲) at SWNT modified EPPGE. (c) Linear dependence of peak current (i_p) on square wave frequency for 20 nM adenine (■) and 5′-AMP (▲) at pH 7.2 at SWNT modified EPPGE. (d) E_p versus log *f* plot observed for 20 nM adenine (■) and 5′-AMP (▲) at SWNT modified edge plane pyrolytic graphite electrode at pH 7.2.

4.3.3 Simultaneous determination of adenine and 5′-AMP

The main aim of present study is to investigate the electrochemical responses when 5′-AMP and adenine co-exist using the SWNT modified EPPGE. **Fig. 4.4a** shows square wave voltammograms for different concentrations of 5′-AMP keeping the concentration of adenine constant (20 nM). It clearly depicts that 5′-AMP signal increases with increase in its concentration without affecting the adenine signal. Similarly, **Fig. 4.4b** shows square wave voltammograms obtained by varying the concentration of adenine keeping the concentration of 5′-AMP constant (20 nM). It was found that the voltammetric peak of 5′-AMP was unaltered and the peak current remained almost constant. The voltammetric signal of adenine increased with increase in its concentration. Individual voltammetric curves of adenine and 5′-AMP are identical to the voltammetric curves observed in the mixture of both the compounds. It was found that neither adenine nor 5′-AMP interfere with the oxidation signals of each other and thus, the proposed method can be successfully used for the simultaneous quantitative determination of adenine and 5′-AMP.

4.3.4 Stability and reproducibility of the modified electrode

The long-term stability of the SWNT modified EPPGE was evaluated by measuring the voltammetric current response of fixed concentration of adenine (60 nM) and 5′-AMP (60 nM) after the modified electrode was stored for approximately 1 week. Only a minimal decrease of current sensitivity with a relative standard deviation (R.S.D.) of about 3.82 % for adenine and 4.45 % for 5′-AMP was observed which can be attributed to the excellent stability of the modified electrode. The reproducibility of the modified electrode has also been investigated. The intra-day precision of the method was evaluated by repeating six experiments in the same solution containing 60 nM of adenine and 60 nM of 5′-AMP using the same SWNT modified EPPGE. The R.S.D. was found to be 0.74 % and 1.26 % for adenine and 5′-AMP, respectively, and hence indicated excellent reproducibility of the modified electrode. Further, inter-day precision was investigated by measuring the current response of the modified electrode for 6 consecutive days for the same concentration of adenine (60 nM) and 5′-AMP (60 nM) and the respective relative standard deviations were found to be 1.37 % and 2.43 %. Thus, it demonstrated the good reproducibility of the method at the SWNT modified EPPGE.

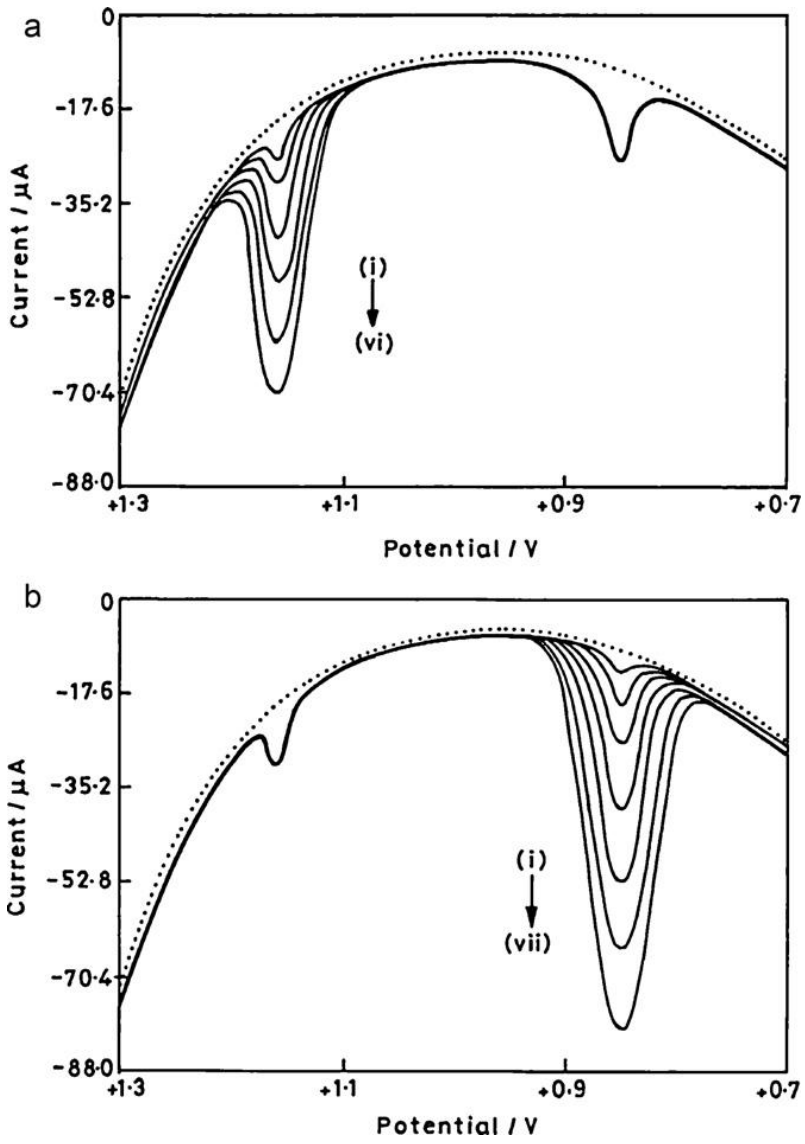

Fig.4.4 Square wave voltammograms of a mixture of adenine and 5′-AMP at SWNT modified EPPGE at pH 7.2. (a) Concentration of 5′AMP was changed (i) 10, (ii) 20, (iii) 40, (iv) 60, (v) 80, and (vi) 100 nM keeping the concentration of adenine constant (20 nM). (b) Concentration of adenine was changed (i) 5, (ii) 10, (iii) 20, (iv) 40, (v) 60, (vi) 80, and (vii) 100 nM keeping the concentration of 5′AMP constant (20 nM).

4.3.5 Effect of the amount of SWNT

The effect of different quantity of SWNT on the peak current response of adenine and 5′-AMP was studied. Different volumes of the suspension prepared by dispersing SWNT in N,N-dimethylformamide were casted on the electrode surface. It was observed that up to 40 μL there was an increase in the peak current response of both the compounds. At SWNT volume more than

40 μL, the peak current response of both the analytes became almost constant. Therefore, it can be stated that the optimum amount of SWNT required to catalyze the oxidation of these compounds is 40 μL and is used in these studies.

4.3.6 Effect of interferents

Ascorbic acid, uric acid, xanthine and hypoxanthine are common biological metabolites present in living systems, which can interfere in the electrochemical studies of adenine and 5′-AMP by influencing their peak potential and peak current response. The effect of these metabolites on the voltammetric peak response of 60 nM adenine and 60 nM 5′-AMP was studied. The tolerance limit was defined as the concentrations of foreign substances, which gave an error less than ±5.0 % in the detection of the compound. It was observed that up to 10-fold excess of each of the interferents there was no remarkable change in the peak current response. This indicates that the method can be safely applied to the determination of adenine and 5′-AMP in biological fluids.

4.3.7 Real sample analysis

4.3.7.1 Human blood plasma

Table 4.1 Recovery data of adenine and 5′-AMP added to human blood plasma.

Added	Found (nM)		Recovery (%)	
(nM)	Adenine	5′-AMP	Adenine	5′-AMP
Sample 1				
30.0	30.14	30.29	100.47	100.97
50.0	50.72	50.48	101.44	100.96
70.0	69.89	69.72	99.84	99.60
Sample 2				
30.0	29.76	29.68	99.20	98.93
50.0	50.39	50.13	100.78	100.26
70.0	70.87	71.07	101.24	101.53
Sample 3				
30.0	31.15	30.57	103.83	101.90
50.0	50.26	51.57	100.52	103.14
70.0	69.79	68.76	99.7	98.23

The R.S.D. value for determination was less than 2.1% for n=3.

The utilization of the SWNT modified EPPGE for the determination of adenine and 5′-AMP in a real sample was tested by measuring their concentration in three human blood plasma samples. Purines present in the blood can pass through the cell membrane and enter the blood stream and thus can be measured in plasma. Literature survey reveals that adenine and 5′-AMP concentration in normal human blood plasma is very low. Hence, it was decided to detect the concentration of adenine and 5′-AMP in human blood plasma by standard addition method. The voltammograms in **Fig. 4.5** depicts the peak at E_p ~850 and ~1165 mV thereby confirming that it corresponds to the oxidation of adenine and 5′-AMP respectively. The concentration of adenine and 5′-AMP in the plasma was calculated after spiking the samples with a measured amount of their standard solutions. The results obtained are presented in **Table 4.1**. The recoveries were found to be 99.20-103.83 % for adenine and 98.23-103.14 % for 5′-AMP.

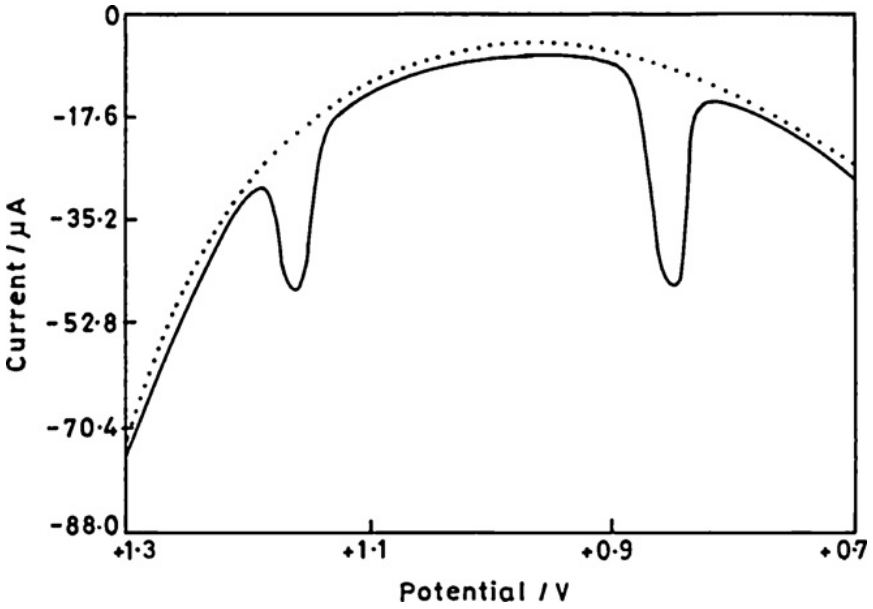

Fig. 4.5 Voltammograms observed for (a) normal human blood plasma (. . . . . .) and (b) blood plasma sample 1 spiked with adenine and 5′-AMP (—).

4.3.7.2 Human urine

The practical analytical application of the method was further established by the selective measurement of adenine and 5′-AMP in human urine without any preliminary treatment. Two human urine samples obtained from laboratory personnel were used for determination. Then, the samples were spiked with certain amounts of adenine and 5′-AMP subsequently followed by recording their square wave voltammograms. The results are summarized in **Table 4.2**. The

recovery rates ranged from 98.43 % to 103.04 % for adenine and 97.90 % to 103.93 % for 5′-AMP, respectively.

Table 4.2 Recovery data of adenine and 5′-AMP added to human urine samples.

Added (nM)	Found (nM)		Recovery (%)	
	Adenine	5′-AMP	Adenine	5′-AMP
Sample 1				
30.0	29.53	29.37	98.43	97.90
50.0	51.17	51.84	102.34	103.68
70.0	70.74	70.38	101.06	100.54
Sample 2				
30.0	30.84	31.18	102.80	103.93
50.0	51.52	51.21	103.04	102.42
70.0	69.83	69.17	99.76	98.81

The R.S.D. value for determination was less than 3.5% for n=3.

4.4 CONCLUSIONS

This work describes an extremely sensitive electroanalytical procedure for the simultaneous determination of adenine and 5′-AMP based on SWV utilizing SWNT modified EPPGE. The modified electrode not only shifted the peak potentials of the oxidation of adenine and 5′-AMP towards lower positive values but also increased the peak currents significantly in comparison to bare EPPGE. The electrocatalytic activity of SWNT has been assigned to the metallic impurities present within it in the recent times [30, 31]. The determination of adenine in presence of guanine or 2′-deoxyadenosine has also been carried out at C_{60} modified glassy carbon [35, 36]. The determination of purine free bases in acid hydrolyzed DNA has been reported at mechanically roughened pyrolytic graphite electrode [37]. In all these cases the peak potential of adenine was observed at 100-150 mV more positive potential than observed in the present studies. In addition, the peak observed is well-defined with much higher peak current (at least three times) at SWNT modified EPPGE. The detection limit reported earlier for adenine was in the range of 10-50 nM, whereas, in the proposed sensor the detection limit for adenine was found to be 3.7 nM. Thus, a comparison indicates that the detection limit for adenine is about two times lower, however, the peak with larger currents is observed at less positive potentials in the present case. 5′-AMP was also found to be oxidizable at pyrolytic graphite at ~1.4 V at pH 7.2 and the peak was close to

background discharge [38], however at modified EPPGE, the E_p shifted to less positive potentials by ~200 mV. As the adenine nucleotide 5′-AMP is much more difficult to oxidize in comparison to adenine, hence, no attempt has been made so far for the simultaneous determination of these two compounds. The SWNT modified EPPGE catalyzes the oxidation of these two purine derivatives and make their determination possible.

The method is a promising alternative to the commonly reported chromatographic methods on account of its rapidity, good recovery, reliability and low detection limit. In contrast to other reported approaches, the present method requires less sample amount, financial input and permits the combined analysis of nucleotides and nucleobases. Thus, in the present study an electroanalytical approach for the simultaneous determination of adenine and 5′-AMP using SWNT modified EPPGE is reported.

4.5 REFERENCES

[1] W. Schwartz, C. G. Bakker; "Was adenine the first purine?". *Science,* **245** (1989) 1102.

[2] R. C. Elderfield; "Heterocyclic compounds". Wiley, New York (1968).

[3] T. M. Devlin; "Textbook of biochemistry with clinical correlations". Wiley, New York (1992).

[4] H. S. Wang, H. X. Ju, H. Y. Chen; "Simultaneous determination of guanine and adenine in DNA using an electrochemically pretreated glassy carbon electrode". *Anal. Chim. Acta,* **461** (2002) 243.

[5] R. S. Sheng, F. Ni, T. M. Cotton; "Determination of purine bases by reversed-phase high-performance liquid chromatography using real-time surface-enhanced Raman spectroscopy". *Anal. Chem.,* **63** (1991) 437.

[6] E. B. Liu, B. C. Xue; "Flow injection determination of adenine at trace level based on luminol-$K_2Cr_2O_7$ chemiluminescence in a micellar medium". *J. Pharm. Biomed. Anal.,* **41** (2006) 649.

[7] C. E. Amri, M. H. Baron, M. C. Maurel; "Adenine and RNA in mineral samples Surface-Enhanced Raman Spectroscopy (SERS) for picomole detections". *Spectrochim. Acta A,* **59** (2003) 2645.

[8] J. P. Headrick, J. Peart, B. Hack, B. Garnham, G. P. Matherne; "5′-Adenosine monophosphate and adenosine metabolism, and adenosine responses in mouse, rat and guinea pig heart". *Comp. Biochem. Physiol., Part A Mol. Integr. Physiol.,* **130** (2001) 615.

[9] H. Haug, W. O. Strik, W. Meyer, K. Deibert, P. Polzien; "On the concentration changes of glucose, lactic acid, pyruvic acid and adenosine tri-, di- and monophosphoric acids (ATP, ADP, AMP) in the blood of the pulmonary artery before and after administration of theophylline ethylendiamine". *Arzneimittelforschung,* **17** (1967) 1411.

[10] V. F. Rudichenko, I. D. Dumanskii; "Effect of adenosine monophosphoric acid on oxidative phosphorylation in the liver under the prolonged action of microwaves". *Gig. Tr. Prof. Zabol.,* **10** (1976) 51.

[11] A. Lujf, J. Schwarzmeier, K. Moser; "Adenine nucleotide content (ATP, ADP, AMP) of normal human skeletal muscle". *Klin. Wochenschr.,* **49** (1971) 499.

[12] Z. I. Nechiporenko, M. D. Kurskii, I. M. Shlykova, L. A. Prishchepa, I. V. Voloshchenko; "Method for obtaining muscle adenosine monophosphoric acid". *Ukr. Biokhim. Zh.,* **53** (1981) 92.

[13] J. S. Cameron, F. Moro, H. A. Simmonds; "Gout, uric acid and purine metabolism in paediatric nephrology". *Pediatr. Nephrol.*, **7** (1993) 105.

[14] V. Edvardsson, R. Palsson, I. Olafsson, G. Hjaltadottir, T. Laxdal; "Clinical features and genotype of adenine phosphoribosyltransferase deficiency in Iceland". *Am. J. Kidney Dis.*, **38** (2001) 473.

[15] M. Arnadottir, T. Laxdal, S. Hardarson, P. Asmundsson; "Acute renal failure in a middle-aged woman with 2,8-dihydroxyadeninuria". *Nephrol. Dial. Transplant.*, **12** (1997) 1985.

[16] S. Cechova, B. J. Venton; "Transient adenosine efflux in the rat caudate-putamen". *J. Neurochem.*, **105** (2008) 1253.

[17] T. A. Ivandini, K. Honda, T. N. Rao, A. Fujishima, Y. Einaga; "Simultaneous detection of purine and pyrimidine at highly boron-doped diamond electrodes by using liquid chromatography". *Talanta*, **71** (2007) 648.

[18] H. Liu, G. Wang, D. Chen, W. Zhang, C. Li, B. Fang; "Fabrication of polythionine/NPAu/MWNTs modified electrode for simultaneous determination of adenine and guanine in DNA". *Sens. Actuators B*, **128** (2008) 414.

[19] B. D. Kabulov, A. K. Sharipov, M. K. Ishankulova, Y. V. Muminov; "HPLC analysis of uracil, adenosine, and phosphaden". *Khim. Farm Zh.*, **26** (1992) 86.

[20] P. Ronner, E. Friel, K. Czerniawski, S. Fraenkle; "Luminometric assays of ATP, phosphocreatine, and creatine for estimation of free ADP and free AMP". *Anal. Biochem.*, **275** (1999) 208.

[21] H. Lin, D. K. Xu, H. Y. Chen; "Simultaneous determination of purine bases, ribonucleosides and ribonucleotides by capillary electrophoresis-electrochemistry with a copper electrode". *J. Chromatogr. A*, **760** (1997) 227.

[22] H. C. Dai, Q. K. Zhuang, N. Q. Li, H. X. Luo, X. X. Gao; "Electrochemical study of the effect of ADP and AMP on the kinetics of glutamate dehydrogenase". *Bioelectrochemistry*, **51** (2000) 35.

[23] J. Wang, M. Musameh, Y. Lin; "Solubilization of carbon nanotubes by nafion toward the preparation of amperometric biosensors". *J. Am. Chem. Soc.*, **125** (2003) 2408.

[24] C. H. Wang, C. Y. Li, C. F. Wang; "Application of a single-wall carbon nano-tube film electrode to the determination of trace amounts of folic acid". *Microchim. Acta*, **152** (2006) 233.

[25] J. Wang, M. Li, Z. Shi, N. Li, Z. Gu; "Direct electrochemistry of cytochrome *c* at a glassy carbon electrode modified with single-wall carbon nanotubes". *Anal. Chem.,* **74** (2002) 1993.

[26] R. N. Goyal, S. Bishnoi; "Voltammetric determination of amlodipine besylate in human urine and pharmaceuticals". *Bioelectrochemistry,* **79** (2010) 234.

[27] G. D. Christian, W. C. Purdy; "Residual current in orthophosphate medium". *J. Electroanal. Chem.,* **3** (1962) 363.

[28] R. H. Wopshall, I. Shain; "Effects of adsorption of electroactive species in stationary electrode polarography". *Anal. Chem.,* **39** (1967) 1514.

[29] R. N. Goyal, A. Sangal; "Electrochemical investigations of adenosine at solid electrodes". *J. Electroanal. Chem.,* **521** (2002) 72.

[30] R. N. Goyal, S. Chatterjee, A. R. S. Rana; "The effect of modifying an edge-plane pyrolytic graphite electrode with single-wall carbon nanotubes on its use for sensing diclofenac". *Carbon,* **48** (2010) 4136.

[31] R. N. Goyal, S. P. Singh; "Simultaneous voltammetric determination of dopamine and adenosine using a single walled carbon nanotube-modified glassy carbon electrode". *Carbon,* **46** (2008) 1556.

[32] M. R. C. Massaroppi, S. A. S. Machado, L. A. Avaca; "Electroanalytical determination of the herbicide picloram in natural waters by square wave voltammetry". *J. Braz. Chem. Soc.,* **14** (2003) 113.

[33] S. K. Lovric, S. Gagic, R. Penovski; "Voltammetric determination of benzoylecgonine". *Anal. Chim. Acta,* **389** (1999) 219.

[34] A. Radi, M. A. E. L. Ries, G. E. Bekhiet; "Electrochemical oxidation of the hypoglycaemic drug gliclazide". *Anal. Lett.,* **32** (1999) 1603.

[35] R. N. Goyal, S. P. Singh; "Voltammetric quantification of adenine and guanine at C_{60} modified glassy carbon electrodes". *J. Nanosci. Nanotechnol.,* **6** (2006) 3699.

[36] R. N. Goyal, S. Chatterjee, S. Bishnoi; "Voltammetric determination of 2′-deoxyadenosine and adenine in urine of patients with hepatocellular carcinoma using fullerene-C_{60}- modified glassy carbon electrode". *Electroanalysis,* **21** (2009) 1369.

[37] S. Hason, L. Fojt, P. Sebest, M. Fojta; "Improved electrochemical detection of purine nucleobases at mechanically roughened edge-plane pyrolytic graphite electrode". *Electroanalysis,* **21** (2009) 666.

[38] R. N. Goyal, A. Sangal; "Electrochemical oxidation of adenosine monophosphate at pyrolytic graphite electrode". *J. Electroanal. Chem.*, **557** (2003) 147.

****

Chapter 5

DETERMINATION OF TRYPTOPHAN

5.1 INTRODUCTION

Tryptophan (2-amino-3-(1H-indol-3-yl)-propionic acid), Trp (**I**) is an important and essential amino acid for humans and herbivores, and is also a potent precursor of several metabolites such as serotonin, melatonin and niacin [1]. It is an indispensable ingredient of various types of proteins, therefore, must be added in human nutrition for establishing and maintaining positive balance of nitrogen. The intake of Trp is necessary as food products and pharmaceutical preparations, since, it is not synthesized in our body [2]. It has been reported that improper metabolism of Trp produces a toxic product in brain which is the possible reason of hallucination, delusions and schizophrenia [3]. Literature survey reveals that Trp is the major constituent of drugs which are used for the treatment of various types of brain related disorders such as depression, schizophrenia and hypertension [3, 4]. The distribution of Trp content in human hair has been found to influence the hair pigmentation [5]. Recent reports have indicated that the concentration of Trp present in biological fluids is very low and its altered level causes metabolic disorders, therefore, the rapid and consistent determination of Trp in human body fluids and vegetable food products is of great significance in biochemical research and clinical purposes [6].

Several techniques have been used for the determination of Trp including high performance liquid chromatography [7-10], ion exchange chromatography [11], liquid chromatography with fluorescence detection [12, 13], thin layer chromatography with fluorescence detection [14], capillary electrophoresis [15, 16], fluorometry [17], chemiluminescence [18-20] and spectrometric techniques [21]. Most of these techniques require heavy and expensive instrumentation along with complicated, tedious and time consuming derivatization, sample preparation and extraction steps. In the last decade electroanalytical techniques have attracted considerable attention for the determination of biomolecules and drugs due to their simplicity, low cost, high sensitivity and rapidness. Several types of modified electrodes have also been used for the determination of Trp including haemin-modified glassy carbon electrode [22], glassy carbon electrode modified with butyrylcholine [2], nafion modified electrode [23], carbon paste electrode incorporating 1-[4-(ferrocenyl ethynyl) phenyl]-1-ethanone (4FEPE) [24] and many more [25-33]. In recent years multi walled carbon nanotubes have attracted generous interest as electrode surface modifier due to their fascinating electronic, chemical and mechanical properties [34]. Further, the fuctionalization of CNTs improved their solubility in biological fluids as well as selectivity of binding to bio-targets of interest [35]. Nanostructure network of nanoparticals have unusual charge/mass transport mechanisms which improved the charge and mass transfer [36]. Gold nanoparticles have been

found to enhance the electrode conductivity by facilitating electron transfer thus, improve the electrochemical sensitivity and selectivity [37].

In this chapter, effect of surface modification of ITO by the use of multi walled carbon nanotubes (MWNT) and gold nanoparticles attached carboxylated multi walled carbon nanotubes (AuNP-MWNT) has been studied for the electrochemical oxidation of Trp. A detailed comparison for oxidation of tryptophan has been made for the electrochemical response at bare ITO, MWNT/ITO and AuNP-MWNT/ITO. It is expected that such imperative and fascinating comparison concerning the electro-catalytic activity of the combination of functionalized nanotubes with gold nanoparticles towards the oxidation of tryptophan will provide information about the catalytic activity of MWNT and gold nanoparticles. Good sensitivity, selectivity, reproducibility and stability of AuNP-MWNT/ITO make it attractive for further developments in the field of electrochemical sensors for monitoring similar type of biomolecules in human body fluids as well as in pharmaceutical formulations.

5.2 EXPERIMENTAL

5.2.1 Reagents

Tryptophan was obtained from Loba Chemie, India. Indium tin oxide electrodes spurted glass sheets of size 10 mm×20 mm×1.1 mm and resistivity 30 Ω cm^{-2} were obtained from Geomatec, Japan. MWNT (purity > 98 %, outer diameter 10-15 nm and inner diameter 2-6 nm) and $HAuCl_4$ were purchased from Aldrich (USA). Ascorbic acid was purchased from Wako pure chemicals industries Ltd., Japan. All solutions were prepared in double distilled water. The urine samples of healthy volunteers were collected from laboratory personnel's and plasma samples were obtained from the hospital of Indian Institute of Technology Roorkee, Roorkee after getting clearance from the ethics committee of the institute.

5.2.2 Instrumentation

BAS (Bioanalytical systems, West Lafayette, USA) CV-50W voltammetric analyzer was used for the voltammetric measurements. The voltammetric experiments were performed using three electrodes single compartment cell equipped with an ITO or MWNT/ITO or AuNP-MWNT/ITO electrode as working, platinum wire as counter and Ag/AgCl (3 M NaCl) as reference electrode. Phosphate buffers solutions of pH range 2.4-10.0 (μ = 1.0 M) were prepared according to the reported method [38]. The pH of the buffer solutions was measured using Eutech Instruments pH 510, pH meter after standardization with 0.05 M potassium hydrogen

phthalate (pH 4.0 at 25 °C) and 0.01 M borax (pH 9.2 at 25 °C). The optimized square wave voltammetric (SWV) parameters used were: square wave amplitude (E_{sw}): 25 mV; potential step (E): 4 mV; square wave frequency (*f*): 15 Hz. Cyclic voltammograms were recorded after bubbling high-purity nitrogen for 12-15 min. All potentials reported are with respect to Ag/AgCl (3 M NaCl) at an ambient temperature of 25±2 °C. The surface morphology of the bare and modified ITOs was characterized by recording FE-SEM using Quanta 200-F (FEI Company) FE-SEM instrument.

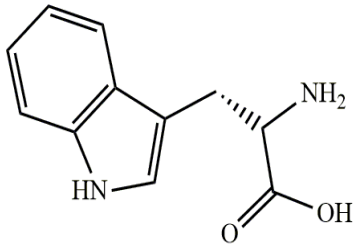

(I)

5.2.3 Procedure

The gold nanoparticles (AuNP) solution was prepared by reducing Au^{3+} ions to Au^0 with ascorbic acid [39, 40]. For this purpose 50 mL of 2.2 mM aqueous ascorbic acid was added to 50 mL of 1.34 mM aqueous $HAuCl_4$ under stirring. The change in solution colour from yellow to deep red indicated the formation of gold nanoparticles which was again confirmed by recording FE-SEM images. In order to make MWNT water soluble, carboxylation was carried out according to the reported method [41].

In order to modify the bare surface of ITO, 100 µL of 1 mg/mL carboxylated MWNT (aq.) was dropped on the clean surface of ITO electrode (10 mm×10 mm×1.1 mm) and dried at 60 °C. In the second case, 100 µL solution of the AuNP prepared was dropped on the MWNT layered ITO, followed by drying at 60 °C. The electrodes were prepared by connecting with a thin strip of copper adhesive tape, and then casing with a scotch tape that is made to have a 2 mm-diameter hole on one side. The electrodes were then ready to use for voltammetric experiments. Typical FE-SEM images of the bare and modified ITO electrodes are given in **Fig. 5.1**. The deposition of MWNT on ITO surface can be clearly seen as shown in **Fig. 5.1 (a)**. Whereas in **Fig. 5.1 (b)** white crumb parts observed are gold nanoparticles and, on the backdrop, consistently formed MWNT layer are clearly observed on the surface of ITO. The bare ITO {**Fig. 5.1 (c)**} simply shows a smooth surface.

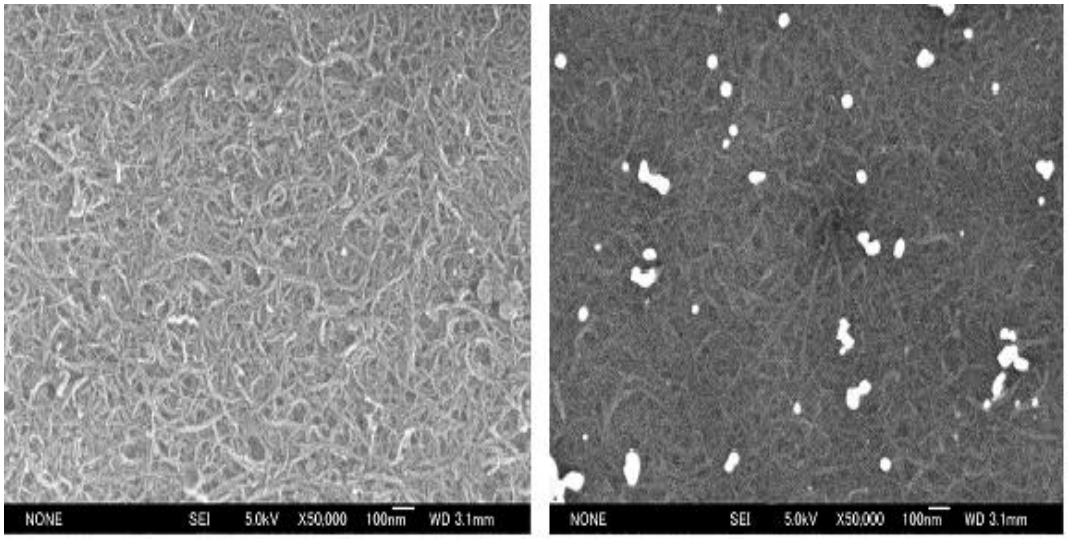

(a) **(b)**

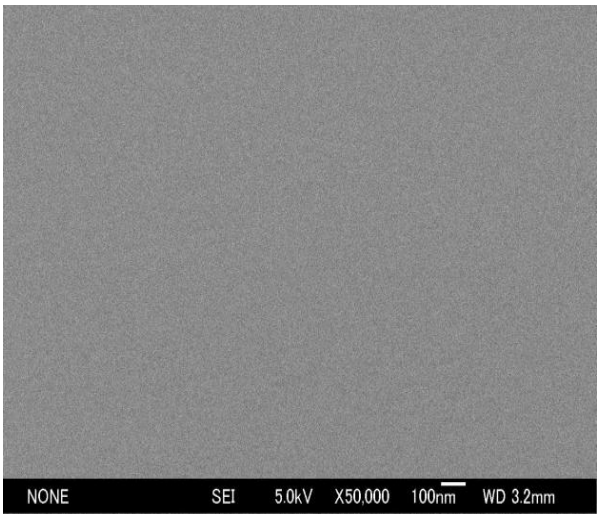

(c)

Fig. 5.1 Typical FE-SEM images observed for (a) MWNT/ITO, (b) AuNP-MWNT/ITO and (c) bare ITO surfaces.

5.3 RESULTS AND DISCUSSION

5.3.1 Effect of modification on surface area

The surface area of MWNT/ITO and AuNP-MWNT/ITO was calculated to determine the efficacy of surface modification. For this purpose, cyclic voltammograms were recorded for 1 mM $K_3Fe(CN)_6$ using 0.1 M KCl as the supporting electrolyte at different scan rates. A well-defined redox couple was observed at both the electrodes due to the presence of Fe^{+3}/Fe^{+2}. The peak

potentials of the redox couples were 265/190 and 237/183 mV at sweep rate of 50 mVs^{-1} using MWNT/ITO and AuNP-MWNT/ITO electrodes, respectively. Thus, the peak separation of anodic and cathodic peaks at AuNP-MWNT/ITO indicates the increased reversibility of the system over MWNT/ITO electrode. There was an enhancement in the peak current values at AuNP-MWNT/ITO electrode in comparison to MWNT/ITO electrode. The surface areas of modified electrodes were found as 0.069 cm^2 and 0.142 cm^2, for MWNT/ITO and AuNP-MWNT/ITO respectively. As the effective surface area of bare ITO electrode was 0.0314 cm^2 the effective surface area of the MWNT/ITO and AuNP-MWNT/ITO increased after surface modification. The effective surface area of AuNP-MWNT/ITO electrode is almost 2 times larger than that of MWNT/ITO and 4 times larger than bare ITO electrode, thereby, indicating that carboxylated MWNTs are helpful towards binding AuNPs on the MWNT layer at ITO surface.

5.3.2 Comparison of modified ITOs

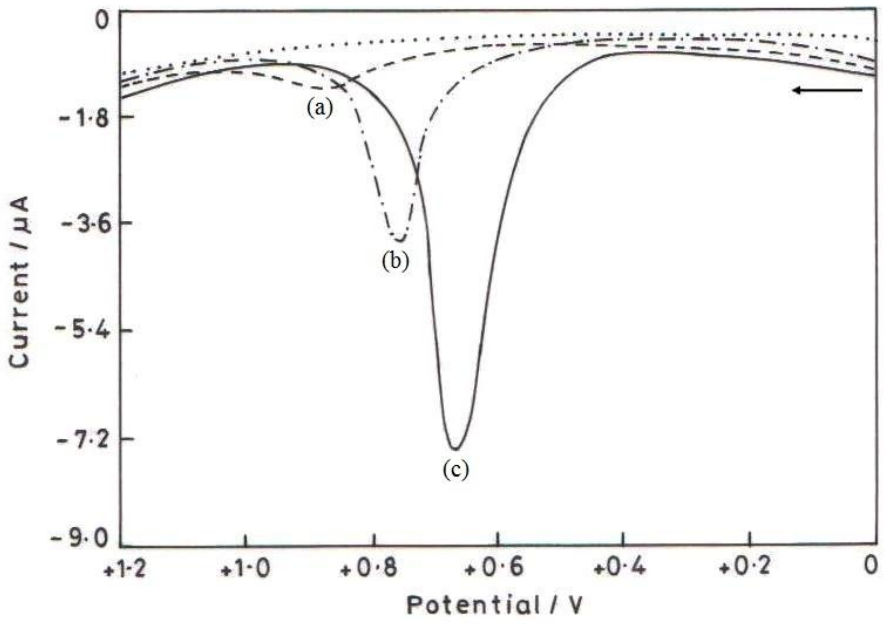

Fig. 5.2 A comparison of square wave voltammograms of 55 µM Trp using (a) bare ITO (- - -), (b) MWNT/ITO (−·−·−·), (c) AuNP-MWNT/ITO (—) at pH 7.2. The background is shown by (….).

The electrochemical behavior of tryptophan was studied by square wave voltammetry using bare ITO, MWNT/ITO and AuNP-MWNT/ITO in order to elucidate the effect of surface modification for Trp determination. **Fig. 5.2** depicts the electrochemical response of 55 µM tryptophan under optimal parameters in phosphate buffer of pH 7.2 using above mentioned three

electrodes. A broad bump is observed at bare ITO having peak potential ~870 mV (**curve a**). At MWNT/ITO tryptophan the E_p shifted to ~760 mV (**curve b**), whereas, at AuNP-MWNT/ITO the E_p further shifted to ~669 mV (**curve c**) with enhancement in the peak current. A comparative study clearly indicates that a substantial decrease (~190 mV and ~100 mV) in peak potential of Trp oxidation is observed as compared to bare surface of ITO using AuNP-MWNT and MWNT coatings on ITO, respectively. A significant enhancement in the peak current is also observed for modified electrodes as compared to bare ITO electrode. The shift in peak potential to less positive potential and enhancement in peak current indicate that the composite film containing the combination of carbon nanotubes with gold nanoparticles exhibits efficient electrocatalysis towards Trp oxidation. Hence, AuNP-MWNT/ITO electrode has been used for further detailed studies for tryptophan determination.

5.3.3 Cyclic voltammetry

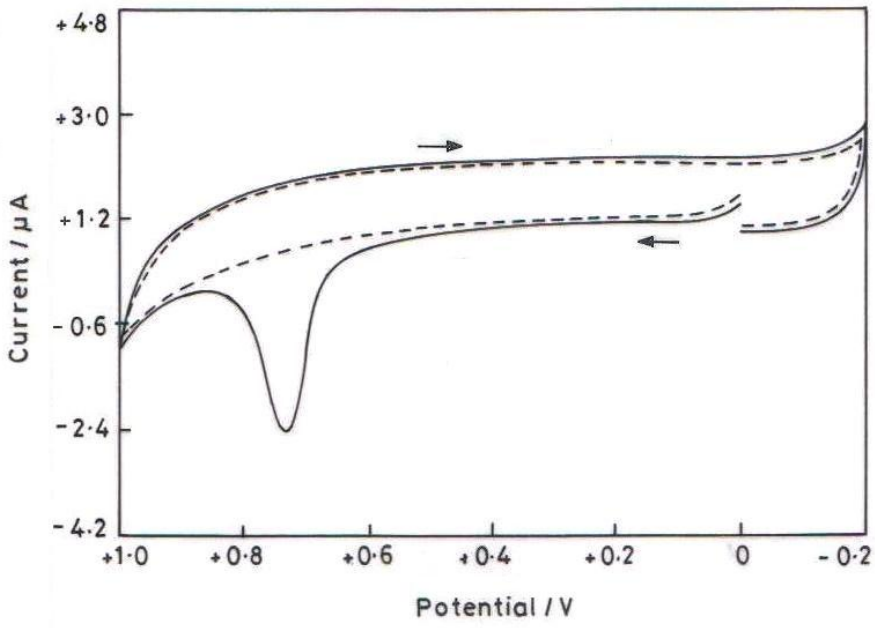

Fig. 5.3 Cyclic voltammograms obtained for blank phosphate buffers solutions (- - - -) and 55 µM tryptophan at pH 7.2 using AuNP-MWNT/ITO (—) at 20 mVs^{-1}.

Cyclic voltammograms were recorded for blank phosphate buffer solution (pH 7.2) for 55 µM Trp at AuNP-MWNT/ITO electrode as presented in **Fig. 5.3**. A well-defined single oxidation peak at ~729 mV was obtained using AuNP-MWNT/ITO. The absence of peaks in the reverse scan clearly indicated that the oxidation of tryptophan at this electrochemical sensor is irreversible in

nature. To ascertain the nature of the electrode reaction, sweep rate studies were performed in the range 10-1000 mVs^{-1}. The peak current was found to increase with increasing sweep rates and the plot of $i_p/v^{1/2}$ versus log *v* clearly indicated that the electrode process is adsorption controlled [42, 43]. As Trp is found to be oxidised at less positive potentials (~669 mV) with increased peak current using square wave voltammetric technique in comparison to cyclic voltammetry (~729 mV), hence, square wave voltammetry was used for the determination of tryptophan in real samples.

5.3.4 Electrochemical behavior of tryptophan

The influence of pH on the voltammetric oxidation of 90 µM tryptophan was determined by using square wave voltammetry at AuNP-MWNT/ITO in the pH range of 2.4-10.0. It was observed that peak potential (E_p) of Trp shifted towards less positive potentials with increase in the value of pH as illustrated in **Fig. 5.4 (a)**. The plot obtained between peak potential and pH was linear and the dependence of E_p on pH can be represented by the relation:

$$E_p = [1044 - 53.37\ pH]\ mV \text{ versus } Ag/AgCl$$

having correlation coefficient of 0.997. The value of the slope of E_p versus pH curve was close to 59 mV/pH and indicated that equal number of electrons and protons ($2e^-$ and $2H^+$) were involved in the oxidation of Trp. A similar oxidation reaction of Trp has been reported in the literature [2].

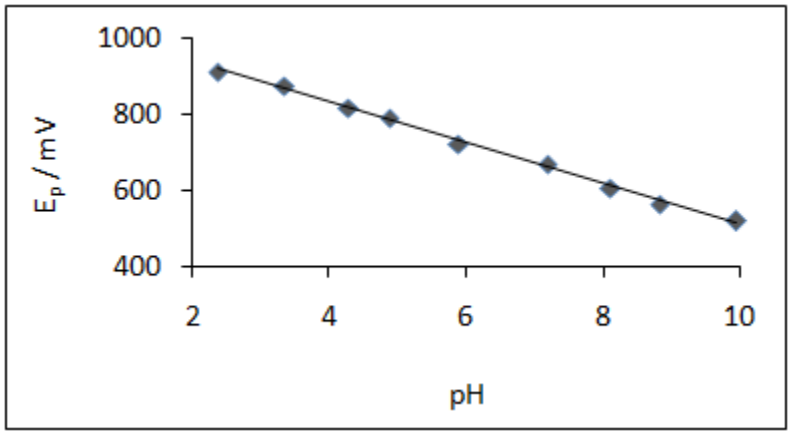

(a)

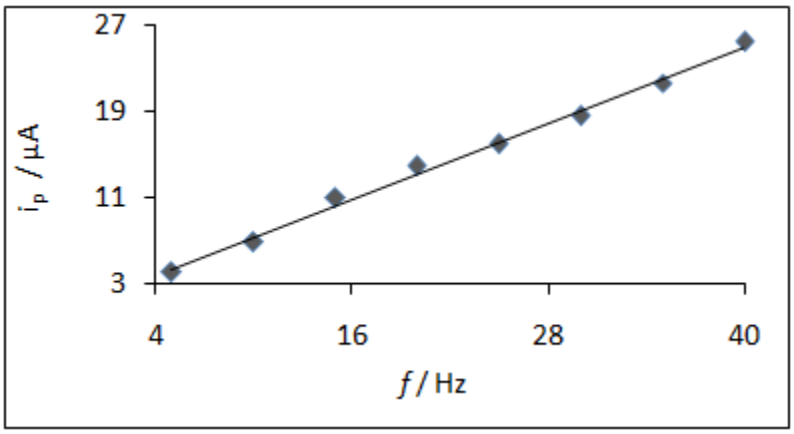

(b)

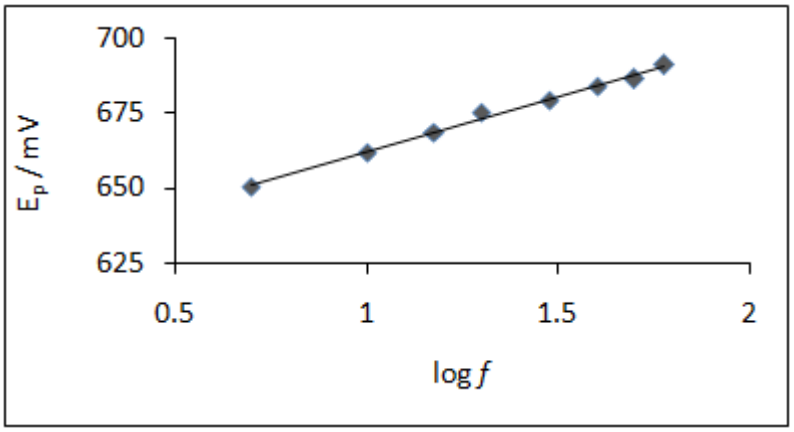

(c)

Fig. 5.4 (a) Dependence of observed peak potential (E_p) on pH, (b) Plot of i_p versus frequency (f) and (c) dependence of E_p on logarithm of square wave frequency (log f) for 90 µM Trp using AuNP-MWNT/ITO.

The influence of square wave frequency (f) on peak current and peak potential of tryptophan was examined at pH 7.2 using AuNP-MWNT/ITO. A linear relationship was observed between the oxidation peak current and square wave frequency having correlation coefficient of 0.994 as shown in **Fig. 5.4 (b)**, which indicated adsorption of tryptophan at the electrode surface [44, 45]. The dependence of peak current on square wave frequency using AuNP-MWNT film modified ITO can be expressed by the relation:

$$i_p / \mu A = 0.591\, f\ (\text{Hz}) + 1.407$$

having correlation coefficient 0.994. It was found that the peak potential also shifted linearly towards more positive potentials with increase in frequency. The E_p versus log *f* plot was found to be linear {**Fig. 5.4 (c)**} and the variation of E_p can be expressed by the equation:

$$E_p\ /\text{mV} = 36.68 \log f + 625.4$$

having correlation coefficient 0.993. These results are in agreement with the adsorption controlled irreversible electrochemical process [46] and also support the observations obtained from cyclic voltammetric studies.

5.3.5 Detection limit and sensitivity

To monitor the effect of surface modification of ITO, the variation of oxidation peak current with Trp concentration was studied using bare ITO, MWNT/ITO and AuNP-MWNT/ITO electrodes in order to compare vital analytical parameters including sensitivity and detection limit. Square wave voltammograms representing the systematic increase in oxidation peak current with increase in concentration in the range 0.5-90 μM using AuNP-MWNT/ITO at pH 7.2 are illustrated in **Fig . 5.5**. It was found that when the concentration (C) increases the oxidation peak current (i_p) linearly increases at all the three electrodes. The linear calibration curves at all the three electrodes are depicted in **Fig. 5.6**. Linear dependence of peak current (after subtracting background current) on concentration can be expressed by the equations:

$i_p\ /\mu\text{A} = 0.119\ C\ (\mu\text{M}) + 0.268$ at AuNP-MWNT/ITO

$i_p\ /\mu\text{A} = 0.058\ C\ (\mu\text{M}) + 0.089$ at MWNT/ITO

$i_p\ /\mu\text{A} = 0.005\ C\ (\mu\text{M}) + 0.003$ at bare ITO

having correlation coefficients 0.998, 0.998 and 0.997, respectively. The detection limit was calculated by using the relation 3σ/b, where σ is standard deviation of blank and b is the slope of calibration curve and found to be 0.025 μM, 0.054 μM and 0.30 μM for AuNP-MWNT/ITO, MWNT/ITO and bare ITO, respectively. Thus, it can be seen that surface modification of ITO by MWNT and AuNP-MWNT lowered the detection limit by ~6 times and ~12 times as compared to bare ITO. The observed sensitivities at AuNP-MWNT/ITO, MWNT/ITO and bare ITO are 0.12 μA μM^{-1}, 0.06 μA μM^{-1} and 0.005 μA μM^{-1}, respectively. Therefore, it can be concluded that addition of AuNP to MWNT/ITO further enhance the oxidation of tryptophan in terms of imperative analytical parameters such as detection limit, sensitivity, peak potential and current. The robustness of the method was examined by the consistency of peak height and peak shape with

the deliberately small changes in the experimental parameter such as square wave frequency, square wave amplitude and pH. It is a measure of its capacity to retain unaffected by small, but deliberate variations in method parameters and provides an indication of its reliability during normal usage. These parameters were deliberately changed one at a time and the effect of these changes on the assay studies was carried out. It was found that such a variation did not cause change in peak current and peak shape and hence, the proposed procedure was considered robust. Owing to comparatively better electroanalytical performance at AuNP-MWNT/ITO it is decided to use this electrode for electroanalysis of tryptophan in biological samples.

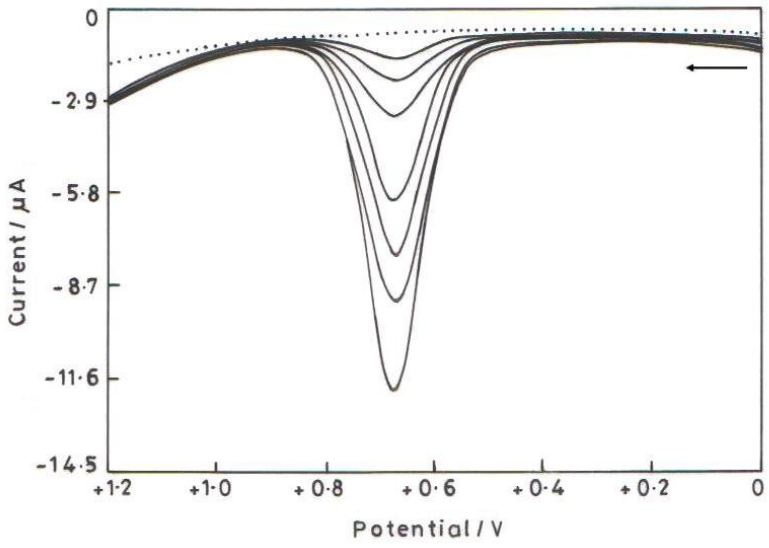

Fig. 5.5 Observed square wave voltammograms for (i) blank phosphate buffer solution (background) (…..) and (ii) increasing concentration of Trp [curves were recorded at (a) = 5; (b) = 10; (c) = 20; (d) = 40; (e) = 55; (f) = 70 and (g) 90 µM concentration] using AuNP-MWNT/ITO in phosphate buffers solutions of pH 7.2.

5.3.6 Real sample analysis using AuNP-MWNT/ITO

In order to establish the analytical utility of the proposed sensor, attempts have been made to determine tryptophan in urine and blood plasma samples by using standard addition method. Blood plasma samples were ultra-centrifuged at a speed of 1000 rpm for 5 min. and supernatant blood plasma was used for the determination of tryptophan. Urine and blood samples were diluted 2 and 4 times, respectively with phosphate buffer solution of pH 7.2 prior to analysis. Three human plasma and urine samples obtained from healthy volunteers were spiked with known amounts of standard Trp ranging from 10 to 50 µM, followed by recording their square wave voltammograms.

In all the cases well-defined peak was observed with E_p ~669 mV corresponding to the oxidation of tryptophan. The concentration of Trp was calculated using calibration plot for AuNP-MWNT/ITO and the results observed are listed in **Table 5.1**. The recoveries varied in the range from 97.6 % to 101.6 % in the case of urine and from 96.6 % to 103.3 % in the case of plasma. The recovery data lie in the acceptable range and hence, the proposed sensor can be utilized successfully for the determination of Trp in human body fluids with adequate accuracy.

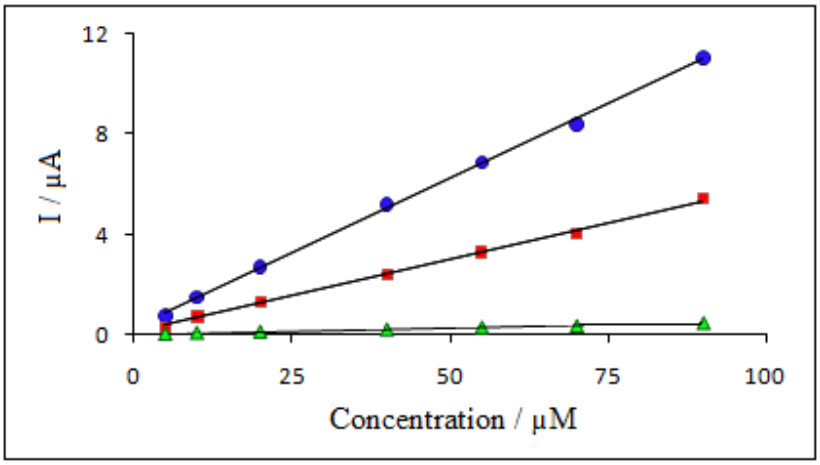

Fig. 5.6 Calibration plots observed for Trp using bare ITO (▲), MWNT/ITO (■) and AuNP-MWNT/ITO (●) at pH 7.2.

5.3.7 Stability and reproducibility of electrode

The stability of AuNP-MWNT/ITO electrode was evaluated by measuring the voltammetric current response of constant tryptophan concentration (20 µM) over a period of 8 days. The electrode was used day by day and stored in air at room temperature. It was observed that during first 5 days the current response had almost remain unchanged and in the next 3 days the current sensitivity decreased about 2.62 % of its initial value. These results suggest that the modified electrode possesses adequate stability for Trp determination. To characterize the reproducibility of AuNP-MWNT/ITO electrode, successive voltammetric measurements of 20 µM Trp were carried out at pH 7.2. The results of eight repetitive measurements showed relative standard deviation (R.S.D.) of 1.96 % and 2.19 % for intra-day and inter-day precision, respectively, which confirmed the excellent reproducibility of the method using AuNP-MWNT/ITO electrode.

Table 5.1 Recovery results obtained for tryptophan in human urine and plasma samples at AuNP-MWNT/ITO.

Spiked	Urine*		Plasma*	
(μM)	Detected (μM)	Recovery (%)	Detected (μM)	Recovery (%)
Sample 1				
10.0	10.16	101.60	9.86	98.60
30.0	29.85	99.50	30.26	100.87
50.0	49.50	99.00	50.00	100.00
Sample 2				
10.0	10.00	100.00	9.76	97.60
30.0	30.09	100.30	30.16	100.53
50.0	49.92	99.84	51.09	102.18
Sample 3				
10.0	9.76	97.60	9.66	96.60
30.0	30.34	101.13	30.96	103.20
50.0	50.60	101.20	51.64	103.28

*** The R.S.D value was < 2.3 % for urine and < 1.9 % for plasma for n = 3.**

5.3.8 Selectivity of the method

Tryptophan often exists together with high concentration of electroactive biomolecules like uric acid and ascorbic acid in natural environments that can interfere with each other. Hence, in order to examine the selectivity of AuNP-MWNT/ITO, influence of major interferents such as uric acid, ascorbic acid and dopamine was evaluated. For this purpose square wave voltammograms of a solution having mixture of standard ascorbic acid, dopamine, uric acid and Trp were recorded at pH 7.2 using AuNP-MWNT/ITO. It was found that well-separated peaks at ~50, ~150, ~300 and ~669 mV were observed corresponding to the oxidation of ascorbic acid, dopamine, uric acid and Trp, respectively. In order to further confirm the selectivity of modified sensor concentration of each interfering substance increased from 5 to 1000 fold by keeping the tryptophan concentration constant. The experimental results show that no substantial changes in peak current response of Trp were observed for entire concentration range. Therefore, it is concluded that AuNP-MWNT/ITO can be securely used for the determination of tryptophan in biological samples even in complex media.

5.4 CONCLUSIONS

Table 5.2 A comparison of voltammetric response of AuNP-MWNT/ITO with previously reported electrodes for the determination of tryptophan.

S. No.	Electrode	Linear range (μM)	Detection limit (μM)	Ref. No.
1	GCE/Nafion/TiO_2	5-140	0.70	25
2	GNP/CILE	5-900	4.0	26
3	PGA/CNTPE	0.05-100	0.01	27
4	Macrocyclic/CPE	1.96-1000	0.098	28
5	CILE	8-1000	4.80	29
6	CNF-CPE	0.10-119	0.10	30
7	Au-NPs/GCE	0.09-50	0.08	31
8	AuNP/CNT/GCE	0.03-2.5	0.010	32
9	4-ABA/GCE	1-100	0.20	33
10	AuNP-MWNT/ITO	0.5-90.0	0.025	Proposed method

CPE- Carbon paste electrode, CILE- carbon ionic liquid electrode.

It has been unfold that AuNP-MWNT/ITO shows an appealing voltammetric performance in comparison to bare ITO and MWNT/ITO electrodes due to its high current sensitivity and low detection limit towards tryptophan. The oxidation peak current of Trp was found to increase significantly alongwith a substantial shift in peak potential towards less positive potential by using AuNP-MWNT/ITO in comparison to bare ITO and MWNT/ITO electrodes. The origin of electrocatalytic properties of nanotubes has been assigned to the embedded metal impurities in CNT samples and edge-plane-like defects which are present at the open ends of nanotubes [47, 48]. Further, gold nanoparticles seems to increase the electrocatalytic activity of MWNT modified electrode due to their superhydrophobicity, high specific surface area and surface enhanced Raman scattering [49]. Carboxylated MWNTs are helpful towards binding AuNPs on the MWNT layer at ITO surface. Thus, the electrocatalytic activity was found to be extensively increased by using the noble combination of gold nanoparticles with carbon nanotubes. To further evaluate the performance of the AuNP-MWNT/ITO sensor towards Trp determination. A comparison of detection limit and calibration range reported in the last few years for Trp is presented in **Table 5.2**. It can be seen that the detection limit of the proposed sensor is better than several papers

reported in last few years and is comparable with others. The proposed sensor has also been utilized for the electrochemical determination of Trp in human blood plasma and urine samples with reproducible results.

5.5 REFERENCES

[1] J. B. Raoof, R. Ojani, M. Baghayeri; "Simultaneous electrochemical determination of glutathione and tryptophan on a nano-TiO_2/ferrocene carboxylic acid modified carbon paste electrode". *Sens. Actuators B,* **143** (2009) 261.

[2] G. P. Jin, X. Q. Lin; "The electrochemical behavior and amperometric determination of tyrosine and tryptophan at a glassy carbon electrode modified with butyrylcholine". *Electrochem. Comm.*, **6** (2004) 454.

[3] S. Shahrokhian, L. Fotouhi; "Carbon paste electrode incorporating multi-walled carbon nanotube/cobalt salophen for sensitive voltammetric determination of tryptophan". *Sens. Actuators B,* **123** (2007) 942.

[4] S. Meyers; "Use of neurotransmitter precursors for treatment of depression". *Altern. Med. Rev.*, **5** (2000) 64.

[5] A. Bertazzo, M. Biasiolo, C. V. L. Costa, E. C. D. Stefani, G. Allegri; "Tryptophan in human hair: Correlation with pigmentation". *IL Farmaco,* **55** (2000) 521.

[6] G. F. Oxenkrug; "Metabolic syndrome, age-associated neuroendocrine disorders, and dysregulation of tryptophan-Kynurenine metabolism". *Ann. N. Y. Acad. Sci.*, **1199** (2010) 1.

[7] J. You, Y. Shan, L. Zhen, L. Zhang, Y. Zhang; "Determination of peptides and amino acids from wool and beer with sensitive fluorescent reagent 2-(9-carbazole)-ethyl chloroformate by reverse phase high-performance liquid chromotography and liquid chromotography mass spectrometry". *Anal. Biochem.*, **313** (2003) 17.

[8] Y. Dale, V. Mackey, R. Mushi, A. Nyanda, M. Maleque, J. Ike; "Simultaneous measurement of phenylalanine and tyrosine in phenylketonuric plasma and dried blood by high-performance liquid chromatography". *J. Chromatogr. B,* **788** (2003) 1.

[9] Q. Zhen, B. Xu, L. Ma, G. Tian, X. Tang, M. Ding; "Simultaneous determination of tryptophan, kynurenine and 5-hydroxytryptamine by HPLC: Application in uremic patients undergoing hemodialysis". *Clin. Biochem.*, **44** (2011) 226.

[10] X. Zhang, Y. He, M. Ding; "Simultaneous determination of tryptophan and kynurenine in plasma samples of children patients with Kawasaki disease by high-performance liquid chromatography with programmed wavelength ultraviolet detection". *J. Chromatogr. B,* **877** (2009) 1678.

[11] G. Ravindran, W. L. Bryden; "Tryptophan determination in proteins and feedstuffs by ion exchange chromatography". *Food Chem.*, **89** (2005) 309.

[12] C. Delgado-Andrade, J. A. Rufian-Henares, S. Jimenez-Perez, F. J. Morales; "Tryptophan determination in proteins and feedstuffs by ion exchange chromatography". *Food Chem.*, **98** (2006) 580.

[13] F. Mattivi, U. Vrhovsek, G. Versini; "Determination of indole-3-acetic acid, tryptophan and other indoles in must and wine by high-performance liquid chromatography with fluorescence detection". *J. Chromatogr. A*, **855** (1999) 227.

[14] N. Kato, T. Kojima, S. Yoshiyagawa, H. Ohta, A. Toriba, H. Nishimura, K. Hayakawa; "Rapid and sensitive determination of tryptophan, serotonin and psychoactive tryptamines by thin-layer chromatography/fluorescence detection". *J. Chromatogr. A*, **1145** (2007) 229.

[15] A. V. C. Simionato, E. P. Moraes, E. Carrilho, M. F. M. Tavares, E. Kenndler; "Determination of amino acids by capillary electrophoresis-electrospray ionization-mass spectrometry: An evaluation of different protein hydrolysis procedures". *Electrophoresis*, **29** (2008) 2051.

[16] W. J. M. Underberg, J. C. M. Waterval; "Derivatization trends in capillary eletrophoresis: An update". *Electrophoresis*, **23** (2002) 3922.

[17] E. Sikorska, A. Gliszczynska-Swigło, M. Insinska-Rak, I. Khmelinskii, D. De Keukeleire, M. Sikorski; "Simultaneous analysis of riboflavin and aromatic amino acids in beer using fluorescence and multivariate calibration methods". *Anal. Chim. Acta*, **613** (2008) 207.

[18] Y. D. Liang, J. F. Song; "Flow-injection chemiluminescence determination of tryptophan through its peroxidation and epoxidation by peroxynitrous acid". *J. Pharm. Biomed. Anal.*, **38** (2005) 100.

[19] J. W. Costin, P. S. Francis, S. W. Lewism; "Selective determination of amino acids using flow injection analysis coupled with chemiluminescence detection". *Anal. Chim. Acta*, **480** (2003) 67.

[20] S. Hanaoka, J. M. Lin, M. Yamada; "Chemiluminescence behavior of the decomposition of hydrogen peroxide catalyzed by copper(II)-amino acid complexes and its application to the determination of tryptophan and phenylalanine". *Anal. Chim. Acta*, **409** (2000) 65.

[21] D. Tsikas, M. Raida, J. Sandmann, S. Rossa, W. G. Forssmann, J. C. Frolich; "Electrospray ionization mass spectrometry of low-molecular-mass S-nitroso compounds and their thiols". *J. Chromatogr. B*, **742** (2000) 99.

[22] C. G. Nan, Z. Z. Feng, W. X. Li, D. J. Ping, C. H. Qin; "Electrochemical behavior of tryptophan and its derivatives at a glassy carbon electrode modified with hemin". *Anal. Chim. Acta*, **452** (2002) 245.

[23] K. A. Frith, J. L. Limson; "pH tuning of Nafion® for selective detection of tryptophan". *Electrochim. Acta*, **54** (2009) 3600.

[24] J. B. Raoof, R. Ojani, H. Karimi-Maleh; "Carbon paste electrode incorporating 1-[4-(ferrocenyl ethynyl) phenyl]-1-ethanone for electrocatalytic and voltammetric determination of tryptophan". *Electroanalysis*, **20** (2008) 1259.

[25] Y. Fan, J. H. Liu, H. T. Lu, Q. Zhang; "Electrochemistry and voltammetric determination of L-tryptophan and L-tyrosine using a glassy carbon electrode modified with a nafion/TiO_2-graphene composite film". *Microchim. Acta*, **173** (2011) 241.

[26] A. Safavi, S. Momeni; "Electrocatalytic oxidation of tryptophan at gold nanoparticle-modified carbon ionic liquid electrode". *Electroanalysis*, **22** (2010) 2848.

[27] X. Liu, L. Luo, Y. Ding, D. Ye; "Poly-glutamic acid modified carbon nanotube-doped carbon paste electrode for sensitive detection of L-tryptophan". *Bioelectrochemistry*, **82** (2011) 38.

[28] A. Srivastava, R. Gaichore; "Macrocyclic compounds based chemically modified electrodes for voltammetric determination of L-tryptophan using electrocatalytic oxidation". *Anal. Lett.*, **43** (2010) 1933.

[29] Q. Jiang, W. Sun, K. Jiao; "Electrochemical behavior and determination of L-tryptophan on carbon ionic liquid electrode". *J. Anal. Chem.*, **65** (2010) 648.

[30] X. Tang, Y. Liu, H. Hou, T. You; "Electrochemical determination of L-tryptophan, L-tyrosine and L-cysteine using electrospun carbon nanofibers modified electrode". *Talanta*, **80** (2010) 2182.

[31] C. Li, Y. Ya, G. Zhan; "Electrochemical investigation of tryptophan at gold nanoparticles modified electrode in the presence of sodium dodecylbenzene sulfonate". *Colloid. Surface. B*, **76** (2010) 340.

[32] Y. Guo, S. Guo, Y. Fanga, S. Dong; "Gold nanoparticle/carbon nanotube hybrids as an enhanced material for sensitive amperometric determination of tryptophan". *Electrochim. Acta*, **55** (2010) 3927.

[33] K. J. Huang, C. X. Xu, W. Z. Xie, W. Wang; "Electrochemical behavior and voltammetric determination of tryptophan based on 4-aminobenzoic acid polymer film modified glassy carbon electrode". *Colloids Surf. B*, **74** (2009) 167.

[34] R. N. Goyal, A. R. S. Rana, Md. A. Aziz, M. Oyama; "Effect of gold nanoparticle attached multi-walled carbon nanotube-layered indium tin oxide in monitoring the effect of paracetamol on the release of epinephrine ". *Anal. Chim. Acta*, **693** (2011) 35.

[35] J. B. Raoof, R. Ojani, F. Chekin; "Fabrication of functionalized carbon nanotube modified glassy carbon electrode and its application for selective oxidation and voltammetric determination of cysteamine". *J. Electroanal. Chem.,* **633** (2009) 187.

[36] F. N. Crespilho, V. Zucolotto, C. M. A. Brett, O. N. Oliveira Jr., F. C. Nart; "Enhanced charge transport and incorporation of redox mediators in layer-by-layer films containing PAMAM-encapsulated gold nanoparticles". *J. Phys. Chem. B*, **110** (2006) 17478.

[37] R. N. Goyal, V. K. Gupta, M. Oyama, N. Bachheti; "Differential pulse voltammetric determination of atenolol in pharmaceutical formulations and urine using nanogold modified indium tin oxide electrode". *Electrochem. Commun.,* **8** (2006) 65.

[38] G. D. Christian, W. C. Purdy; "The residual current in orthophosphate medium". *J. Electroanal. Chem.,* **3** (1962) 363.

[39] J. Wagner, J. M. Kohler; "Continuous synthesis of gold nanoparticles in a microreactor". *Nano Lett.,* **5** (2005) 685.

[40] D. Andreescu, T. K. Sau, D. V. Goia; "Stabilizer-free nanosized gold sols". *J. Colloid Interface Sci.*, **298** (2006) 742.

[41] M. A. Aziz, H. Yang; "Surfactant and polymer-free electrochemical micropatterning of carboxylated multi-walled carbon nanotubes on indium tin oxide electrodes". *Chem. Commun.,* **7** (2008) 826.

[42] R. H. Wopshall, I. Shain; "Effects of adsorption of electroactive species in stationary electrode polarography". *Anal. Chem.,* **39** (1967) 1514.

[43] R. N. Goyal, A. Sangal; "Electrochemical investigations of adenosine at solid electrodes". *J. Electroanal. Chem.,* **521** (2002) 72.

[44] S. Komorsky-Lovric, S. Gagic, R. Penovski; "Voltammetric determination of benzoylecgonine". *Anal. Chim. Acta,* **389** (1999) 219.

[45] M. R. C. Massaroppi, S. A. S. Machado, L. A. Avaca; "Electroanalytical determination of the herbicide picloram in natural waters by square wave voltammetry". *J. Braz. Chem. Soc.,* **14** (2003) 113.

[46] A. Radi, M. A. EL Ries, G. E. Bekhiet; "Electrochemical oxidation of the hypoglycaemic drug gliclazide". *Anal. Lett.,* **32** (1999) 1603.

[47] X. Liu, V. Gurel, D. Morris, D. W. Murray, A. Zhitkovich, A. B. Kane, R. H. Hurt; "Bioavailability of nickel in single-wall carbon nanotubes". *Adv. Mater.*, **19** (2007) 2790.

[48] C. E. Banks, R. R. Moore, T. J. Davies, R. G. Compton; "Investigation of modified basal plane pyrolytic graphite electrodes: Definitive evidence for the electrocatalytic properties of the ends of carbon nanotubes". *Chem. Commun.*, (2004) 1804.

[49] H. Zang, J. J. Xu, H. Y. Chen; "Shape-controlled gold nanoarchitectures: Synthesis, superhydrophobicity, and electrocatalytic properties". *J. Chem. Phys.*, **112** (2008) 13886.

****

Chapter 6

DETERMINATION OF ASPIRIN, PARACETAMOL, AND CAFFEINE

6.1 INTRODUCTION

Multidrug pharmaceutical preparations for the remedy of pains of weaker genesis have attracted considerable attention in the last few years [1]. A common combination of paracetamol (PAR) **(I)**, aspirin (ASA) **(II)** and caffeine (CF) **(III)** is in market for several years for pain as an over-the-counter medicine. This combination of analgesics has been found to exhibit a positive benefit to risk ratio and has been considered safe for self-medication for the relief from different kinds of pain [2, 3]. The clinical studies on combination analgesics have revealed that they show a broader spectrum of analgesic action because of different modes of action of individual components [1]. The synergistic effects of ASA, PAR and CF have been studied on the inhibition of PGE_2 synthesis in microglial cells to explain the effect [4]. The combination of ASA, PAR and CF has also been recommended by US Headache Consortium and German Migraine and Headache Society for the treatment of migraine under self-medication [5, 6]. A comparison of combination of ASA, PAR and CF with sumatriptan, a leading prescription for migraine, in a clinical study has indicated the combination as more effective [7]. However, the overdoses of these compounds have been found to induce variety of effects. ASA overdose causes acute liver failure, sepsis, and hypotension [8], PAR poisoning is common in pediatrics [9] and CF overdose has been found to cause arrhythmia, tachycardia, coma and even death [10]. Owing to common use, misuse and important effects of these drugs in human system variety of analytical methods have been used for the determination of these compounds individually as well as simultaneously. The most common methods include spectrophotometric methods, chromatographic methods and solid phase molecular fluorescence analysis [11-14]. These methods are adequate in terms of their accuracy, but are usually very expensive; more complex and a long time is required for derivatization, extraction and purification of the species prior to their determination. Electrochemical techniques have also been implemented for the individual estimation of PAR [15-19], ASA [20-22] and CF [23-27] at variety of electrodes. However, only a single attempt has been made for their simultaneous determination using less sensitive electrode [28]. Thus, the development of a fast, sensitive and reliable method for the simultaneous monitoring of the trace quantities of these compounds in human body fluids and pharmaceutical preparations is still highly needed. The aim of this study was to develop a voltammetric sensor for simple and rapid analysis of PAR, ASA and CF in human urine samples.

In this chapter, simultaneous determination of ASA, PAR and CF has been carried out using square wave voltammetry (SWV) that offers the advantage of great sensitivity. The technique has been proved to be highly sensitive for the analysis of organic molecules including

drugs owing to its simplicity, low cost and relatively short analysis time as compared to the other routine analytical techniques including chromatography. The determination has been carried out using poly-1,5-diaminonapthalene (p-DAN) modified pyrolytic graphite sensor (MPGS). Conductive polymers have acquired much attention due to their potential applications to battery electrodes, electrochromic devices, electroluminescent devices, and biological sensors [29]. Of these, aromatic compounds possessing two amine groups have been studied for polymer film-coated electrodes [30-33]. Among them, p-DAN has shown incredible interest due to its fascinating properties. Recently, p-DAN and p-DAN-nanofibers have been used for electrode fabrication and successfully showed a great potential for sensor applications [34-35]. Therefore, the aim of the present work is simultaneous determination of all the three compounds in human urine and pharmaceutical samples using MPGS. As edge plane has been found to be a better substrate for modification in comparison to basal plane and other conventional electrodes like glassy carbon due to its strong adsorption property and wide potential window [36-38], hence the p-DAN was deposited at the edge plane surface of pyrolytic graphite. The electron transfer rate constants for a large variety of redox couples at edge surface have been found to be nearly thousand times faster than other conventional electrodes [39]. A comparison of the bare and p-DAN modified graphite sensor indicated that MPGS is more sensitive towards the determination of these compounds.

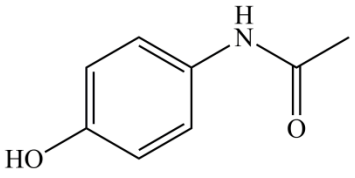

(I)

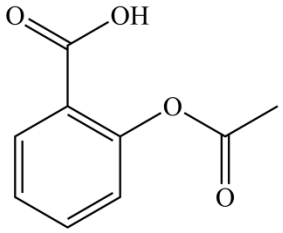

(II)

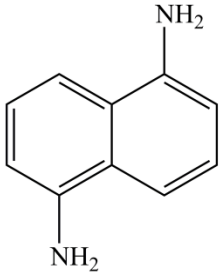

(III)

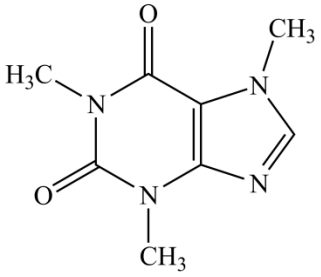

(IV)

6.2 EXPERIMENTAL

6.2.1 Reagents and apparatus

ASA was obtained from Sigma-Aldrich, USA and CF was purchased from the Adams Chemical Company, USA. PAR was received as a gift from Sri Krishna Pharmaceuticals Ltd., Hyderabad. The plane pyrolytic graphite pieces (2x2x6 mm^3) were obtained from Pfizer Inc., New York, USA and electrode was prepared according to the reported procedure [40]. 1,5-diaminonapthalene (1,5-DAN) **(IV)** was purchased from Sigma-Aldrich. Perchloric acid ($HClO_4$) was acquired from Rankem chemicals. Ajubi (Technopharm Pvt. Ltd., Haridwar, Uttrakhand), Anacin (Wyeth Consumer Healthcare Division, Bandra, Mumbai), Cozy-Plus (Ind-Swift limited, Solan, H.P.), Ecosprin-75 (USV limited, Govand, Mumbai) were obtained from the local market of Roorkee. Phosphate buffers in the pH range 2.4-11.0, (μ = 1.0 M) were prepared according to the method of Christian and Purdy [41]. The voltammetric experiments were carried out using BAS CV-50W voltammetric analyzer (Bioanalytical Systems, West Lafayette, USA) equipped with single compartment glass cell having three electrodes. An Ag/AgCl (3 M NaCl) was used as reference electrode (BAS Model MF-2052 RB-5B), Pt wire as counter electrode and bare or MPGS as working electrodes. The pH of the buffer solutions was measured by using Century India Ltd., digital pH meter (Model CP-901).

6.2.2 Procedure

Stock solutions of ASA, PAR and CF (1 mM) were prepared by dissolving the required amount in double distilled water. The required volume of the stock solution was added, using micro pipette, to electrolytic cell containing 2 mL of phosphate buffer and the total volume was made 4 mL with double distilled water. Voltammograms were then recorded using voltammetric analyzer under optimized parameters. The optimized parameters used throughout the experiment using SWV were: initial (E): 200 mV, final (E): 1800 mV, step (E): 4 mV, square wave amplitude (E_{sw}): 25 mV, square wave frequency (*f*): 15 Hz. Cyclic voltammograms were recorded in the sweep range 10-1000 mVs^{-1} with initial sweep to positive potentials. Cyclic voltammograms were recorded after deaeration of solutions by bubbling of high-purity nitrogen for 12-15 min. All the potentials reported are with respect to Ag/AgCl electrode at an ambient temperature of 25±2 °C.

6.2.3 Fabrication of p-DAN on edge surface of pyrolytic graphite

Prior to modification the surface of pyrolytic graphite was rubbed on an emery paper (P-400) then washed thoroughly with double distilled water and dried. p-DAN film was grown on the surface (area = 3 mm^2) in 1 M $HClO_4$ containing 10 mM 1,5-DAN. Electropolymerization was carried out potentiodynamically (by cyclic scanning of the potential between −0.1 and + 1.0 V vs. Ag/AgCl reference electrode) at scan rate of 100 mVs^{-1} for 20 scans as reported in literature [42, 43]. After the stable polymer film was prepared on the electrode, it was rinsed with distilled water carefully in order to remove soluble products as well as monomer of 1,5-DAN before it was subjected to further experiments.

Electrochemical response of polymer film was examined by comparing the surface area of bare and MPGS. For this purpose cyclic voltammograms of 1 mM $K_3[Fe(CN)_6]$ were recorded at different scan rates using 0.1 M KCl as supporting electrolyte. The surface area was calculated from the slopes of i_p versus $v^{1/2}$ plots using Randles-Sevcik equation and found as 0.069 and 0.318 cm^2 for bare and MPGS, respectively.

6.2.4 Analysis of real samples

Urine sample of healthy volunteer received from the laboratory personnel was used as control. The human urine samples of patients undergoing treatment with Ajubi (480 mg tablet three times a day) containing PAR (300 mg), ASA (150 mg) and CF (30 mg) were collected after 4h of oral administration of the first tablet each day from the hospital of Indian Institute of Technology, Roorkee. The samples were collected after 1, 2 and 3 days of treatment. In order to minimize the matrix complexity urine samples were diluted ten times with phosphate buffer of pH 7.2 prior to recording voltammograms.

6.3 RESULTS AND DISCUSSION

6.3.1 Cyclic voltammetry

Initially, electrochemical response of a solution having 5 nM of each ASA, PAR and CF was recorded at a sweep rate of 50 mV/s using bare and MPGS by cyclic voltammetry. At bare electrode, three anodic peaks were obtained at ~530, 1318 and 1450 mV corresponding to the oxidation of ASA, PAR and CF respectively. In the reverse sweep a peak at ~476 mV which formed a quasi reversible couple with peak at 520 mV was also observed. At MPGS, three anodic peaks were obtained at ~520, 1310 and 1440 mV (**Fig. 6.1**) corresponding to the oxidation of PAR, ASA and CF respectively. In the reverse sweep a peak at 470 mV which formed a quasi reversible

couple with peak at 520 mV. However, the peak currents at MPGS were nearly two times larger in comparison to bare sensor for all the three compounds. To ascertain the nature of electrode reaction, sweep rate studies were performed in the range 10-300 mVs^{-1}. The peak current of ASA, PAR and CF was found to increase with increasing sweep rates at bare as well as at MPGS. The plots of $i_p/v^{1/2}$ versus log *v* for all the three compounds were linear (**Fig. 6.2**) and clearly indicated that the electrode process of these compounds involves adsorption complications at these electrodes [44, 45].

As SWV is more sensitive technique with well-established advantages such as discrimination against background current, low detection limit, hence, further study for the analysis of ASA, PAR and CF was carried out by using this technique.

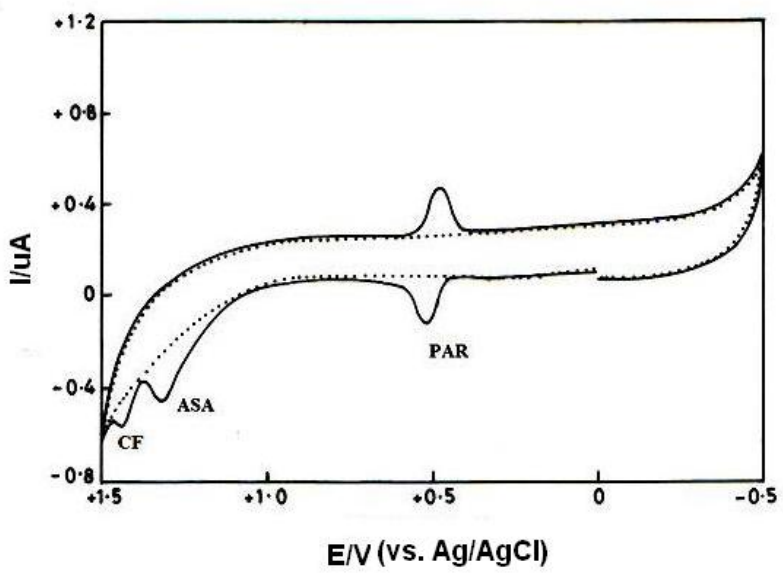

Fig. 6.1 Cyclic voltammogram of homogeneous solution of equal concentration (5 nM) of each PAR, ASA and CF in phosphate buffer of pH 7.2 using MPGS (—) at scan rate of 50 mV/s and dotted CV (. . .) is the response of MPGS in phosphate buffer.

6.3.2 Square wave voltammetry

Initially, square wave voltammograms were recorded for a ternary mixture of ASA, PAR and CF at bare pyrolytic graphite and MPGS in phosphate buffer solution of pH 7.2 using the optimized parameters of SWV as shown in **Fig. 6.3** At both the sensors, three well-defined peaks were observed corresponding to the oxidation of ASA, PAR and CF. The shape of peaks at unmodified sensor was rather broad and peak potentials were slightly more positive as compared to MPGS. However, the three well-separated peaks with shift of peak potential towards less positive

potential with a significant enhancement in peak current at MPGS clearly revealed that the proposed voltammetric sensor acts as a very efficient promoter to enhance the kinetics of the electrochemical process as compared to unmodified surface. Hence, MPGS has been utilized for further detailed studies.

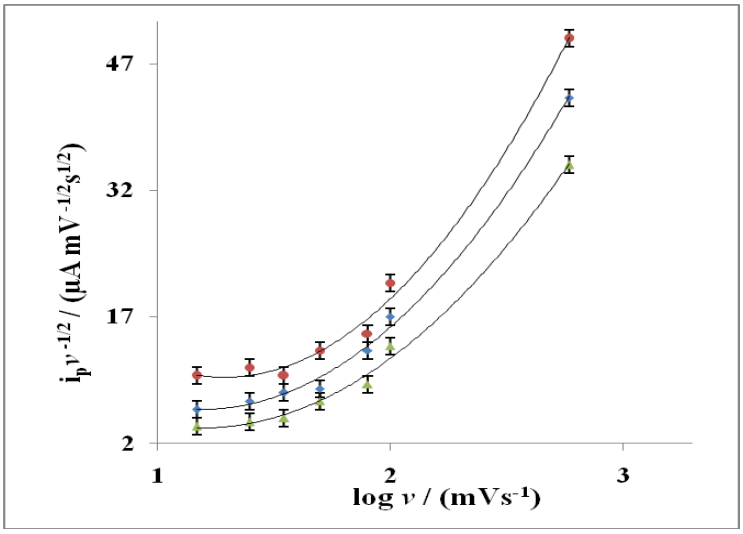

Fig. 6.2 Observed dependence of ip/√*v* on log *v* for 0.5 μM PAR (■), ASA (●) and CF (▲) at pH 7.2 using MPGS.

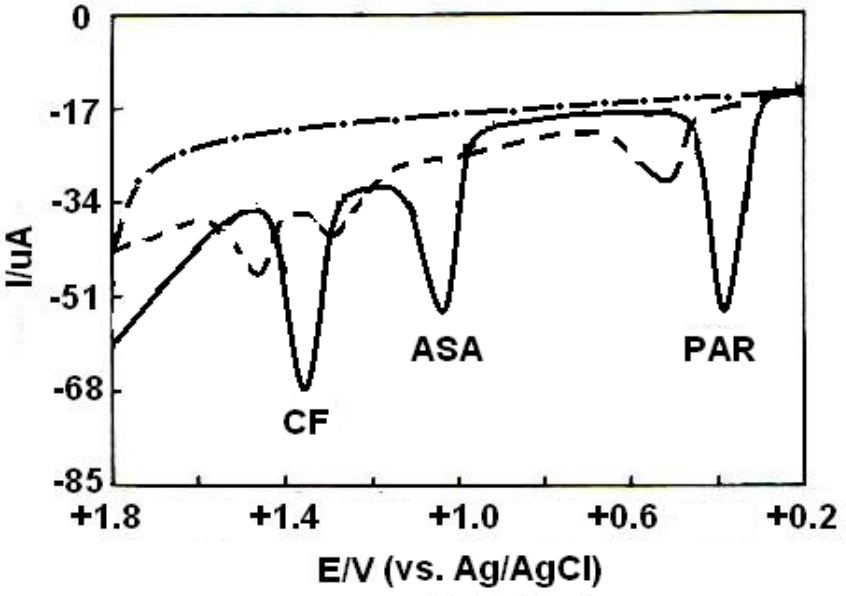

Fig. 6.3 Square wave voltammograms of homogeneous solution of equal concentration of each PAR, ASA and CF (120 nM) using (a) bare (----) and (b) MPGS (—) at pH 7.2, and (−·−·−·) line is the response of MPGS in phosphate buffer of pH 7.2.

6.3.3 Electrochemical behavior of ASA, PAR and CF

6.3.3.1 Effect of pH

The effect of pH on oxidation potential of ASA, PAR and CF was evaluated in the pH range of 4.3-10.9 at MPGS. It was observed that peak potential of all the three compounds shifted to less positive potential with increase in pH. The E_p versus pH plots is linear and dependence of anodic peak potential of all three analytes on the pH of supporting electrolyte can be presented by the equations:

E_p/mV = [1287 – 28.97 pH] versus Ag/AgCl for ASA

E_p/mV = [871 – 59.73 pH] versus Ag/AgCl for PAR

E_p/mV = [1773 – 59.21 pH] versus Ag/AgCl for CF

for ASA, PAR and CF respectively having correlation coefficients 0.990, 0.994 and 0.998. The value of dE_p/dpH ~30 mV/pH for ASA indicates that number of protons involved in oxidation are one half of the electrons, whereas, the value close to 60 mV/pH in PAR and CF suggests that equal number of protons and electrons are involved in the electrode reactions as reported earlier [46]. A comparison of slope and intercept of E_p vs. pH curves for ASA, PAR and CF at bare sensor indicated that the values of slope were practically similar to MPGS; however, the intercepts were 1290, 867 and 1808 respectively.

6.3.3.2 Effect of square wave frequency

The variation of square wave frequency (*f*) with peak current (I_p) of ASA, PAR and CF was studied in the frequency range of 5-100 Hz at pH 7.2. The peak current (I_p) of 5 nM ASA, PAR and CF shows a linear increase with square wave frequency suggesting thereby, that electrode reaction for all three compounds is adsorption controlled [45, 47] which also supported the inferences obtained from cyclic voltammetry studies. Linear relations between I_p and *f* for all three compounds can be expressed by the following equations:

$I_p/\mu A = 0.335\, f + 0.110$ for ASA

$I_p/\mu A = 0.348\, f + 0.077$ for PAR

$I_p/\mu A = 0.281\, f + 1.679$ for CF

with correlation coefficient of 0.995, 0.990 and 0.989 for ASA, PAR and CF, respectively.

6.3.3.3 Effect of concentration

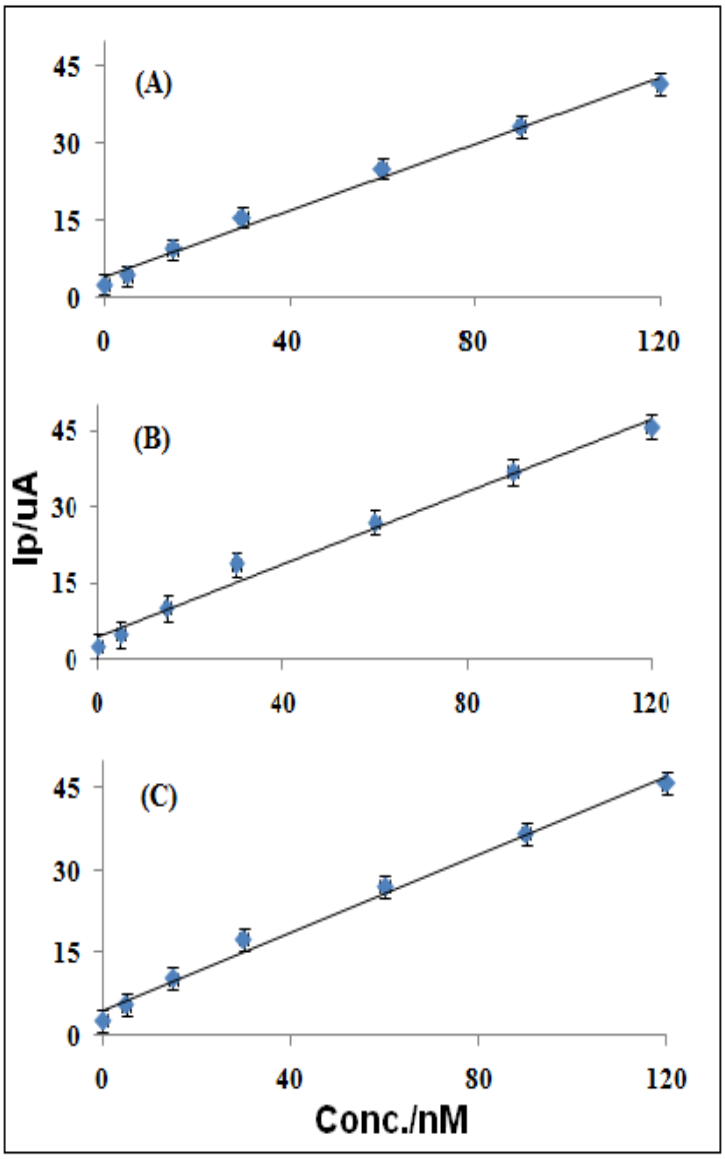

Fig. 6.4 Calibration plots observed for (A) ASA, (B) PAR and (C) CF using MPGS at pH 7.2.

Square wave voltammogram were recorded for various concentrations of ASA, PAR and CF in phosphate buffer solutions of pH 7.2 when present together at MPGS. The concentration of only one component was varied at a time keeping the other two fixed. It was observed that with increase in the concentration of these compounds, oxidation peak current increased. The peak current versus concentration plots showed a good linearity for ASA, PAR and CF in the concentration range 0.1-120 nM as depicted in **Fig. 6.4**. Current values were obtained by subtracting the background current of buffer solution and average of three replicate measurements

was used to plot calibration curves. Linear regression equations for calibration plots can be represented as:

$I_p/\mu A = 0.323\ C\ [nM] + 4.007$ for ASA

$I_p/\mu A = 0.357\ C\ [nM] + 4.540$ for PAR

$I_p/\mu A = 0.354\ C\ [nM] + 4.601$ for CF

with a correlation coefficients of 0.991, 0.986 and 0.992 for ASA, PAR and CF respectively. The limits of detection were calculated by using the formula $3\sigma/b$, where σ is the standard deviation of blank solution and b is the slope of calibration curves and were found to be, 0.93×10^{-10}, 0.57×10^{-10} and 0.64×10^{-10} M for ASA, PAR and CF, respectively. The sensitivities of ASA, PAR and CF determination were calculated as 0.323, 0.357 and 0.354 $\mu A\ nM^{-1}$ respectively.

6.3.3.4 Simultaneous determination of ASA, PAR and CF

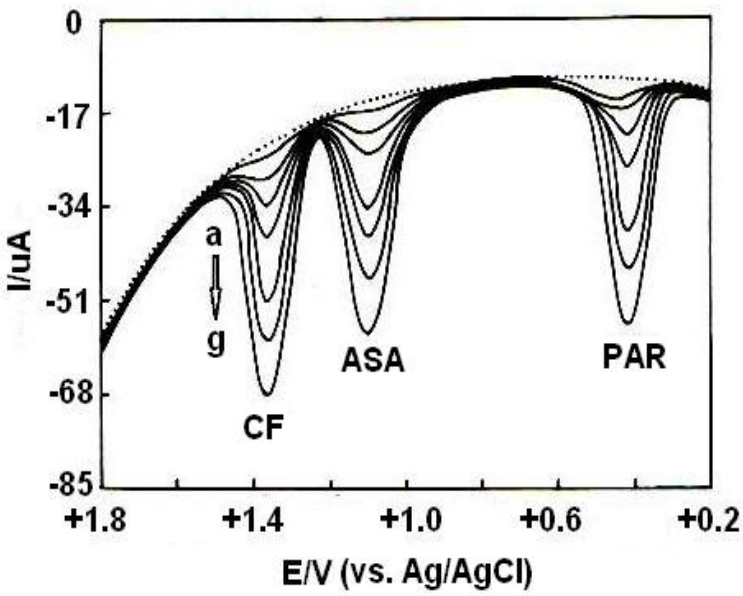

Fig. 6.6 Square wave voltammograms obtained at MPGS for a mixture of PAR, ASA and CF at equal concentrations: a = 0.1, b = 5, c = 15, d = 30, e = 60, f = 90, g = 120 nM.

Square wave voltammograms are recorded at MPGS to evaluate the electrochemical response of different concentration of ASA, PAR and CF when present in the same solution. For this, in the first set of experiments, the concentrations of two compounds were increased simultaneously while keeping the concentration of the third one constant (**Fig. 6.5A-6.5C**). It was observed that the oxidation peak current for the two compounds systematically increased, whereas,

the oxidation current of the third compound remained constant. The plot of concentration versus peak current was linear and follows the same relation as observed for variation of single compound (**Fig. 6.4**). For the second case, the concentration of all the three compounds was varied simultaneously (**Fig. 6.6**) and square wave voltammograms were recorded. Three separate peaks for ASA, PAR and CF oxidation were observed without interfering each other. It was found that when concentrations of all three compounds increased simultaneously the peak current of the three components increased. The increase in peak current followed the same linear relation as observed during individual variation of ASA, PAR and CF. Thus, it can be concluded that the proposed MPG sensor can be successfully applied for the simultaneous determination of ASA, PAR and CF in real samples.

6.3.3.5 Reproducibility and stability of MPGS

The reproducibility of the modified sensor has been evaluated by repetitive determinations of ternary mixture of ASA, PAR and CF (30 nM each) at pH 7.2. The results of six replicate measurements showed a relative standard deviation (R.S.D.) of 2.12 % indicating that the results are reproducible. Further, inter-day precision was examined by measuring the current response of the modified sensor for six consecutive days for the same 30 nM concentration of ASA, PAR and CF and the R.S.D. was found to be 3.12 %. To confirm the reproducibility of the results further, four different modified sensors with approximately same exposed surface area were independently constructed. They showed an acceptable reproducibility with a R.S.D. of 1.47 % for 30 nM of ASA, PAR and CF.

To characterize the stability of the MPGS, the voltammetric current response of fixed concentration of 30 nM of ASA, PAR and CF was measured after the modified sensor was stored over a period of 10 days. The sensor was used daily and stored in air. Only a minimal decrease of current sensitivity with a R.S.D. of about 3.52 % was observed which can be attributed to the excellent stability of the modified sensor. Thus, the MPGS exhibit good stability and reproducibility for the simultaneous determination of ASA, PAR and CF.

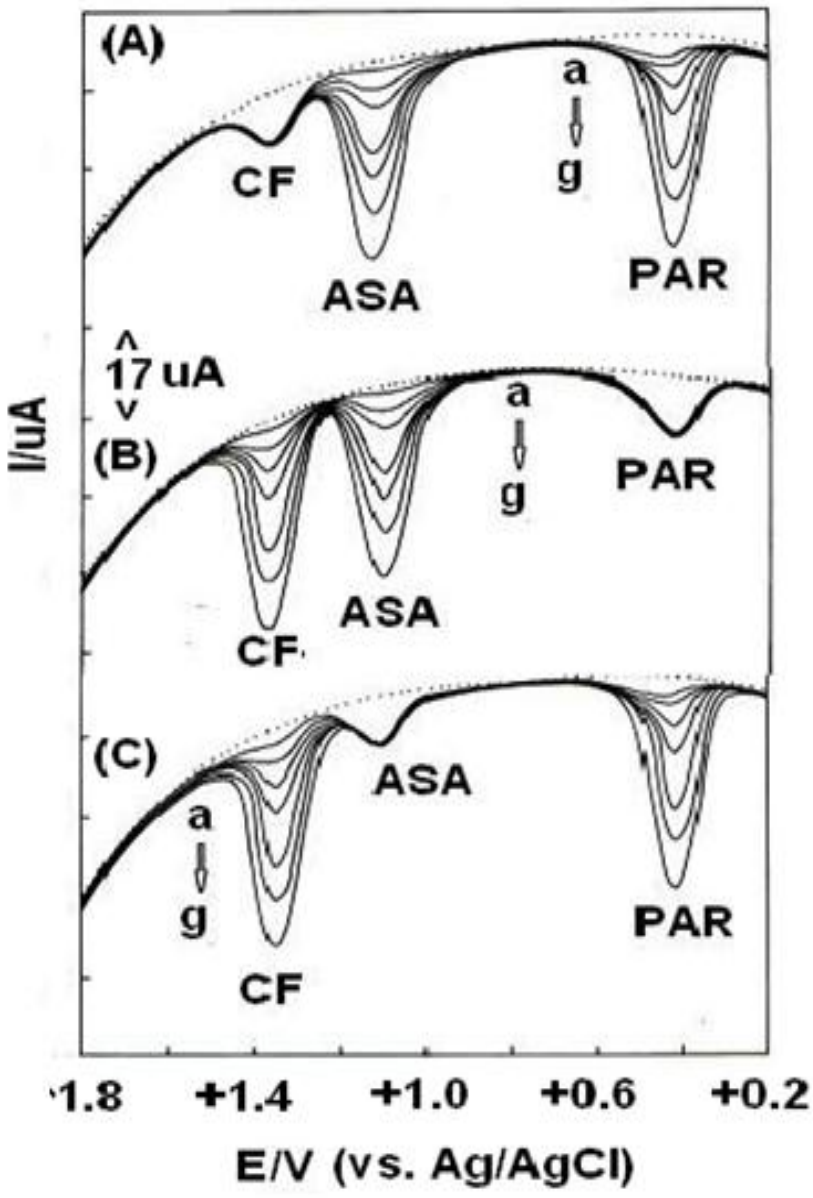

Fig. 6.5 Square wave voltammograms observed for different concentrations of (A) ASA and PAR at a fixed concentration of CF = 15 nM (B) CF and ASA at a constant concentration of PAR= 15 nM (C) CF & PAR at a constant concentration of ASA = 15 nM. The phosphate buffer (background) is shown by (. . .) and concentrations of two compounds were: a = 0.1, b = 5, c = 15, d = 30, e = 60, f = 90, g = 120 nM.

6.3.3.6 Effect of interferents

Ascorbic acid, uric acid, dopamine and xanthine are common biological metabolites present in living systems which can intervene in the electrochemical studies of PAR, ASA and CF

by influencing their peak potential and peak current response. The effect of these metabolites on the voltammetric peak response of 30 nM each of ASA, PAR and CF was studied at MPGS. It was observed that dopamine and ascorbic acid oxidized below +0.2 V vs. Ag/AgCl and did not affect the peak current of PAR even at 5 mM concentration. Uric acid (+0.28 V vs. Ag/AgCl) and xanthine (+0.82 V vs. Ag/AgCl) did not interfere in the determination up to 1 mM concentration. As concentration of ascorbic acid and uric acid in human urine is ~1 mM, whereas, dopamine and xanthine is in µM range, hence, these compounds do not interfere in the determination. The tolerance limit was defined as the concentrations of foreign substances, which gave an error less than ±5.0 % in the detection of the drugs. It was observed that each of the interferents do not affect the peak current response of ASA, PAR and CF by more than ±3.5 %. Thus, the method can be safely applied to the determination of ASA, PAR and CF in biological fluids.

6.3.4 Analytical applicability

6.3.4.1 Analysis of pharmaceutical preparations

Table 6.1 Determination of PAR, ASA and CF in pharmaceutical tablets using MPGS.

	Stated content (mg)			Detected content* (mg)			Error (%)**		
Sample	PAR	ASA	CF	PAR	ASA	CF	PAR	ASA	CF
Ajubi	150	300	30	148.45	294.84	29.24	-1.03	-1.72	-2.53
Anacin	500	—	30	492.32	—	29.51	-1.54	—	-1.63
Cozy-Plus	500	—	30	489.57	—	29.63	-2.09	—	-1.23
Ecosprin-75	—	75	—	—	73.94	—	—	-1.41	—

*** the RSD value for determination was less than 2.6 % for n=3.**

**** Error (%) =[detected content – stated content]/stated content×100**

In order to assess the pertinence of the proposed method, different commercial samples in combination or in pure form containing ASA, PAR and CF were analyzed. The tablets were powdered and dissolved in 50 ml distilled water. The medicinal samples were further diluted so that the concentration of ASA, PAR and CF reached in the working range. Pursuing the proposed method the concentration of ASA, PAR and CF in the various pharmaceutical preparations were ascertained by recording voltammograms and the peak current measurement. Results summarized in **Table 6.1** show that the content for all the examined tablets falls within the labelled value suggesting the good agreement with the proposed voltammetric method.

6.3.4.2 Analysis in human urine samples

Table 6.2 Simultaneous determination of PAR, ASA and CF in urine samples of patients treated with tablet Ajubi using MPGS after one day of treatment.

Added	Paracetamol (μM)			Aspirin (μM)			Caffeine (μM)		
(μM)	Found [a]	Actual	Recovery (%)	Found [a]	Actual	Recovery (%)	Found [a]	Actual	Recovery (%)
Sample 1									
0.00	1.10	1.10	—	0.31	0.31	—	0.57	0.57	—
0.30	1.45	1.15	103.57	0.63	0.33	103.27	0.86	0.53	98.85
0.60	1.71	1.11	100.58	0.92	0.32	101.09	1.15	0.55	98.29
Sample 2									
0.00	1.07	1.07	—	0.36	0.36	—	0.63	0.63	—
0.30	1.35	1.05	98.52	0.67	0.37	101.51	0.92	0.62	98.92
0.60	1.64	1.04	98.20	0.94	0.34	97.92	1.26	0.66	102.43
Sample 3									
0.00	1.12	1.12	—	0.33	0.33	—	0.60	0.60	—
0.30	1.40	1.10	98.59	0.65	0.35	103.17	0.92	0.62	102.22
0.60	1.75	1.15	101.74	0.91	0.31	97.85	1.23	0.63	102.25

[a] **The R.S.D. value for the determination was less than ± 3.8 % for n=3.**

The concentration of ASA, PAR and CF in urine sample of patients undergoing treatment with the combination drug therapy was determined due to two reasons. First is that CF is on the World Anti-Doping Agency's prohibited list [47] and its use by athletes necessitates a therapeutic use exemption, while the second is the overdose of multidrug formulation consisting of PAR and ASA with CF may lead to cause various adverse effects such as vomiting, diarrhea, abdominal pain etc. Hence, it is considered worthwhile to analyze the three compounds at MPGS in the urine of patients undergoing therapy. For this purpose urine samples were diluted ten times with phosphate buffer solution before recording square wave voltammograms in order to reduce matrix complexity. The diluted urine sample of normal person (control) in the potential range scanned exhibited only single peak at 280 mV (**Fig. 6.7**) which is found to be due to the oxidation of uric acid, a common metabolite present in urine. Three well-defined anodic peaks (E_p ~420 , 1100 and

1360 mV vs. Ag/AgCl) were noticed corresponding to the oxidation of PAR, ASA and CF respectively in patients urine (sample 1) along with a peak at 280 mV as shown in **Fig. 6.7**. The concentration of ASA, PAR and CF was determined in urine samples using calibration plots. The results of analysis for urine samples collected after 1 day is presented in **Table 6.2**. To further confirm the concentration of all the three compounds in different urine samples, standard addition method was used. For this purpose diluted urine samples were spiked with known concentrations of ASA, PAR and CF followed by recording square wave voltammograms under identical conditions. The results obtained for urine samples of three different patients are tabulated in **Table 6.2**. The actual concentration of ASA, PAR and CF in urine sample of patient undergoing treatment with the drug was evaluated and found to be in the range 0.33±0.03, 1.09±0.03 and 0.60±0.03 µM respectively with relative standard deviation (RSD) ±4.0 % for n = 5.

The urine samples collected after 2 and 3 days of the treatment were also analyzed for PAR, ASA and CF in similar manner and the results obtained are presented as histograms in **Fig. 6.8**. It is observed that the amount of PAR, ASA and CF excreted in urine did not change significantly. Thus, the unmetabolized drugs are excreted and are not accumulated in the body.

Oxidation reactions for PAR, ASA and CF are well known and the oxidation products found were N-acetyl-p-quinone imine for PAR, which involve two proton and two electron transfer reaction [48], and 3,6-dioxocyclohexa-1,4-dienecarboxylate or 5,6-dioxocyclohexa-1,3-dienecarboxylate for ASA, which involved two electron and one proton transfer reaction [49]. The oxidation of CF, however, involves four electrons and four protons reaction to give 4,5-diol analogue which rapidly fragmented to give final products [20, 50].

6.3.4.3 Comparison with bare pyrolytic graphite surface

A comparison of detection limit of PAR, ASA and CF at MPGS was made with bare pyrolytic graphite surface. It was observed that well-defined peaks were also observed in the entire pH range at bare surface. However, the peak currents at MPGS were significantly larger as compared to the bare surface. The detection limits observed at the bare surface were 0.035, 0.026 and 0.031 µM for PAR, ASA and CF, which were much higher than observed at MPGS. Thus, it is concluded that MPGS is significantly better as compared to the bare pyrolytic graphite surface.

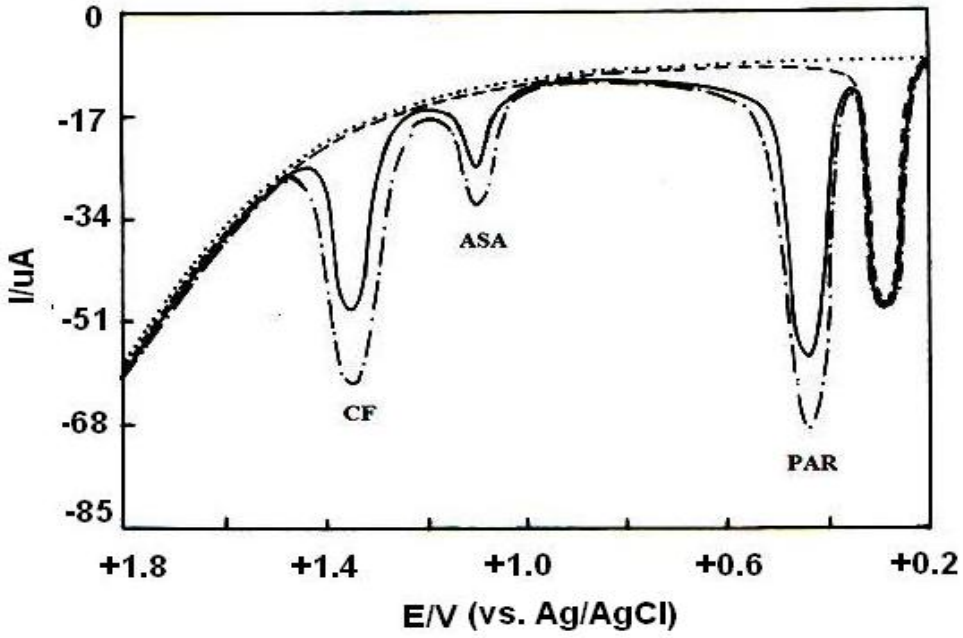

Fig. 6.7 A comparison of voltammograms observed for urine sample of patient (Sample 1) being treated with tablet Ajubi containing PAR, ASA and CF (—) and after spiking with 30 nM each of PAR, ASA and CF (–·–·–·–·–·) at pH 7.2 at MPGS. Control urine is represented as (- - - -) and the background is represented as (……).

6.4 CONCLUSIONS

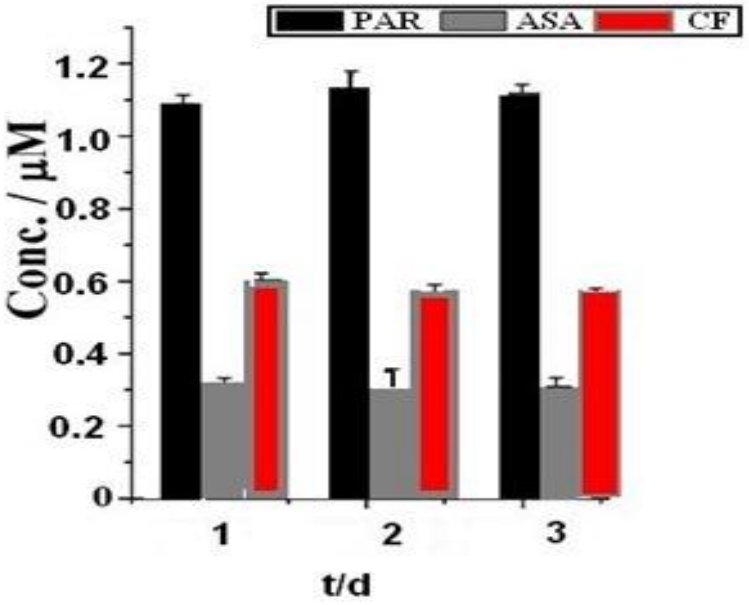

Fig. 6.8 Comparative analysis of PAR, ASA and CF excreted in human urine after different days of the treatment.

The proposed method describes an extremely sensitive electroanalytical procedure for the simultaneous monitoring of ASA, PAR and CF in pharmaceuticals products and human urine samples employing MPGS with excellent sensitivity and selectivity. These compounds oxidized at poly-1,5-diaminonapthalene layer and well-separated peaks are observed. The analysis of these drugs in urine samples clearly indicates that the amount of ASA, PAR and CF excreted is practically similar during the treatment. Long term stability and excellent reproducibility of the proposed sensor offers a good possibility for extending the method for analysis of ASA, PAR and CF in routine and research laboratories. The main advantage of the present method is that poly-1,5-diaminonapthalene layer contribute to its efficiency leading to the lowering of oxidation peak potential and marked enhancement in the peak current. The positive charge on the amino groups of 1,5-diaminonapthalene in p-DAN may also attract carboxylic and ─OH groups in ASA and PAR to cause increase in peak current as reported earlier in case of p-DAN and poly-1,10-diaminonapthalene [30, 33] for biomolecules. In addition, the edge plane contributes considerably faster electrode kinetics for electrochemical reaction and is also the likely reason for the improved detection limit. Thus, oxidation of ASA, PAR and CF occurs at bare as well as modified sensor and the only difference is in the I_p and E_p of these compounds. The increased current at MPGS leads to the better detection limit for these compounds. The developed protocol also showed good ability to quantify ASA, PAR and CF contents in various pharmaceutical tablets with reliable accuracy and also the proposed sensor has also been utilized successfully for the analysis of urine samples of patients undergoing treatment with multidrug formulation of ASA, PAR and CF. The detection limit observed for the three components is lower than reported earlier [28]. The unmetabolized drugs excreted in urine samples with no special pretreatment of samples have been determined. Hence, the proposed sensor can also be recommended for detecting doping cases of CF at the site of competitive games due to its rapid response and accuracy.

6.5 REFERENCES

[1] B. Aicher, O. Kraupp; "Effectiveness of fixed analgesic combinations exemplified by thomapyrin". *Wein. Klin. Wochenschr.*, **108** (1996) 219.

[2] E. V. Hersh, P. A. Moore, G. L. Ross; "Over the counter analgesics and antipyretics: A critical assessment". *Clin. Ther.,* **22** (2000) 500.

[3] B. L. Fiebich, E. C. Jalil, M. Mantovani, M. Heinzmann, R. V. Akundi, M. Hull, R. Knorle, P. Schnierle, G. Finkenzeller, B. Aicher; "Modulation of catecholamine release from rat striatal slices by the fixed combination of aspirin, paracetamol and caffeine". *Pharmacol. Res.*, **53** (2006) 391.

[4] B. L. Fiebich, K. Lieb, M. Hull, B. Aicher, J. R. Van, M. Pairet, G. Engelhardt; "Effects of caffeine and paracetamol alone or in combination with acetylsalicylic acid on prostaglandin E_2 synthesis in rat microglial cells". *Neuropharmacology*, **39** (2000) 2205.

[5] H. C. Diener, V. Pfaffernath, L. Pageler, H. Peil, B. Aicher; "The fixed combination of acetylsalicylic acid, paracetamol and caffeine is more effective than single substances and dual combination for the treatment of headache: A multicentre, randomized, double-blind, single-dose, placebo-controlled parallel group study". *Cephalalgia*, **25** (2005) 776.

[6] S. D. Silberstein; "Practice parameter: Evidence-based guidelines for migraine headache (an evidence-based review)". *Neurology*, **55** (2000) 754.

[7] J. Goldstein, S. D. Silberstein, J. R. Saper, A. H. Alkind, T. R. Smith, R. M. Gallagher, J. P. Battikha, H. Hoffman, J. Baggish; "Acetaminophen, aspirin, and caffeine versus sumatriptan succinate in the early treatment of migraine: Results from the ASSET trial". *Headache,* **45** (2005) 973.

[8] H. Kato, K. Yoshimoto, H. Ikegaya; "Two cases of oral aspirin overdose". *J. Forensic legal Med.*, **17** (2010) 280.

[9] L. James, J. E. Sullivan, D. Roberts; "The propre use of acetaminophen". *Paediatr. Child Health*, **16** (2011) 544.

[10] S. Kerrigan, T. Lindsey; "Concentration of drugs in blood of suspected impaired drivers". *Forensic Sci. Int.*, **153** (2005) 67.

[11] E. R. Sartori, R. A. Medeiros, R. C. Rocha-Filho, O. Fatibello-Filho; "Square-wave voltammetric determination of acetylsalicylic acid in pharmaceutical formulations using a boron-doped diamond electrode without the need of previous alkaline hydrolysis step". *J. Braz. Chem. Soc.*, **20** (2009) 360.

[12] S. Majdi, A. Jabbari, H. Heli; "A study of the electrocatalytic oxidation of aspirin on a nickel hydroxide modified nickel electrode". *J. Solid State Electrochem.*, **11** (2007) 601.

[13] M. M. Sena, R. J. Poppi; "Integrated high capacity solid phase extraction-MS/MS system for pharmaceutical profiling in drug discovery". *J. Pharm. Biomed. Anal*., **34** (2004) 27.

[14] J. C. L. Alves, R. J. Poppi; "Simultaneous determination of acetylsalicylic acid, paracetamol and caffeine using solid-phase molecular fluorescence and parallel factor analysis". *Anal. Chim. Acta*, **642** (2009) 212.

[15] M. E. Bosch, A. J. R. Sanches, F. S. Rojas, C. B. Ojeda; "Determination of paracetamol: historical evolution". *J. Pharm. Biomed. Anal*., **42** (2006) 291.

[16] C. Wang, C. Li, F. Wang, C. Wang; "Covalent modification of glassy carbon electrode with l-cysteine for the determination of acetaminophen". *Microchim. Acta*, **155** (2006) 365.

[17] R. M. de Carvalho, R. S. Freire, S. Rath, L. T. Kubota; "Effects of EDTA on signal stability during electrochemical detection of acetaminophen". *J. Pharm. Biomed. Anal*., **34** (2004) 871.

[18] Q. Chu, L. Jiang, X. Tian, J. Ye; "Rapid determination of acetaminophen and p-aminophenol in pharmaceutical formulations using miniaturized capillary electrophoresis with amperometric detection". *Anal. Chim. Acta*, **606** (2008) 246.

[19] R. N. Goyal, S. P. Singh; "Voltammetric determination of paracetamol at C_{60}-modified glassy carbon electrode". *Electrochim. Acta*, **51** (2006) 3008.

[20] N. Spataru, B. V. Sarada, D. A. Tryk, A. Fujishima; "Anodic voltammetry of xanthine, theophylline, theobromine and caffeine at conductive diamond electrodes and its analytical application". *Electroanalysis*, **14** (2002) 721.

[21] J. Sawynok; "Pharmacological rationale for the clinical use of caffeine". *Drugs*, **49** (1995) 37.

[22] R. N. Goyal, S. Bishnoi, B. Agrawal; "Electrochemical sensor for the simultaneous determination of caffeine and aspirin in human urine samples". *J. Electroanal. Chem*., **655** (2011) 97.

[23] S. R. Snider, B. Waldeck; "Increased synthesis of adrenomedullary catecholamines induced by caffeine and theophylline". *Arch. Pharmacol*., **281** (1974) 257.

[24] B. Brunetti, E. Desimoni, P. Casati; "Determination of caffeine at a nafion-covered glassy carbon electrode". *Electroanalysis*, **19** (2007) 385.

[25] R. T. Kachoosangi, G. G. Wildgoose, R. G. Compton; "Sensitive adsorptive stripping voltammetric determination of paracetamol at multiwalled carbon nanotube modified basal plane pyrolytic graphite electrode". *Anal. Chim. Acta*, **618** (2008) 54.

[26] N. F. Atta, M. F. El-Kady, A. Galal; "Palladium nanoclusters-coated polyfuran as a novel sensor for catecholamine neurotransmitters and paracetamol". *Sens. Actuators B*, **141** (2009) 566.

[27] X. Kang, J. Wang, H. Wu, J. Liu, I. A. Aksay, Y. Lin; "A graphene-based electrochemical sensor for sensitive detection of paracetamol". *Talanta*, **81** (2010) 754.

[28] B. J. Sanghavi, A. K. Srivastava; "Simultaneous voltammetric determination of acetaminophen, aspirin and caffeine using an in situ surfactant-modified multiwalled carbon nanotube paste electrode". *Electrochim. Acta*, **55** (2010) 8638.

[29] S. M. Park, in: H. S. Nalwa (Ed.); "Handbook of organic conductive molecules and polymers". Wiley, Chichester (1997).

[30] A. Volkov, G. Tourillon, P. Lacaze, J. E. Dubois; "Electrochemical polymerization of aromatic amines: IR, XPS and PMT study of thin film formation on a Pt electrode". *J. Electroanal. Chem.*, **115** (1980) 279.

[31] H. S. White, H. D. Abruna, A. J. Bard; "Semiconductor electrodes: XLI. improvement of performance n-Wse_2 of formula electrodes by electrochemical polymerization of *o*-phenylenediamine at surface imperfections". *J. Electrochem. Soc.*, **129** (1982) 265.

[32] C. S. Jin, Y. B. Shim, S. M. Park; "Electropolymerization and spectroelectrochemical characterization of poly-1,5-diaminonaphthalene". *Synth. Met.*, **69** (1995) 561.

[33] J. W. Lee, D. S. Park, Y. B. Shim, S. M. Park; "Electrochemical characterization of poly-1,8-diaminonaphthalene: a functionalized polymer". *J. Electrochem. Soc.*, **139** (1992) 3507.

[34] M. S. Won, J. H. Yoon, Y. B. Shim; "Determination of selenium with a poly-1,8-diaminonaphthalene-modified electrode". *Electroanalysis*, **17** (2005) 1952.

[35] Md. A. Rahman, M. S. Won, N. H. Kwon, J. H. Yoon, D. S. Park, Y. B. Shim; "Water sensor for a nonaqueous solvent with poly-1,5-diaminonapthalene nanofibers". *Anal. Chem.*, **80** (2008) 5307.

[36] W. J. Lin, C. S. Liao, J. H. Jhang, Y. C. Tsai; "Graphene modified basal and edge plane pyrolytic graphite electrodes for electrocatalytic oxidation of hydrogen peroxide and β-nicotinamide adenine dinucleotide". *Electrochem. Commun.*, **11** (2009) 2153.

[37] K. Ding, Q. Wang; "Comparison of admittance plots for glass carbon (gc) and edge plane pyrolytie graphite (eppg) electrodes in three typical kinds of electrolytes port". *Electrochim. Acta*, **25** (2007) 401.

[38] R. R. Moore, C. E. Banks, R. G. Compton; "Electrocatalytic detection of thiols using an edge plane pyrolytic graphite electrode". *Analyst*, **129** (2004) 755.

[39] R. T. Kachoosangi, C. E. Banks, R. G. Compton; "Simultaneous determination of uric acid and ascorbic acid using edge plane pyrolytic graphite electrodes". *Electroanalysis*, **18** (2006) 741.

[40] R. N. Goyal, V. K. Gupta, S. Chatterjee; "Fullerene-C_{60}-modified edge plane pyrolytic graphite electrode for the determination of dexamethasone in pharmaceutical formulations and human biological fluids". *Biosens. Bioelectro*., **24** (2009) 1649.

[41] G. D. Christian, W. C. Purdy; "The residual current in orthophosphate medium". *J. Electroanal. Chem*., **3** (1962) 363.

[42] A. A. Abdelwahab, H. M. Lee, Y. B. Shim; "Selective determination of dopamine with a cibacron blue/poly-1,5-diaminonaphthalene composite film". *Anal Chim Acta*, **650** (2009) 247.

[43] S. K. Yadav, B. Agrawal, R. N.Goyal; "AuNPs-poly-DAN modified pyrolytic graphite sensor for the determination of cefpodoxime proxetil in biological fluids". *Talanta*, **108** (2013) 30.

[44] R. S. Nicholson, I. Shain; "Theory of stationary electrode polarography: Single scan and cyclic methods applied to reversible, irreversible, and kinetic systems". *Anal. Chem*., **36** (1964) 706.

[45] E. R. Brown, R. F. Large, A. Weissberger, B. W. Rossiter; "Physical methods of chemistry". Wiley-Interscience, Rochester, New York (1964).

[46] P. Wang, X. Wang, G. Zhu; "Sol–gel-derived carbon ceramic composite electrodes bulk-modified with 1:12-silicomolybdic acid". *New J. Chem*., **24** (2000) 481.

[47] S. Lamina, D. I. Musa; "Ergogenic effect of varied doses of coffee-caffeine on maximal aerobic power of young African subjects". *Afr. Health Sci.*, **9** (2009) 270.

[48] D. J. Miner, J. R. Rice, R. M. Riggin, P. T. Kissinger; "Ergogenic effect of varied doses of coffee-caffeine on maximal aerobic power of young African subjects". *Anal. Chem*., **53** (1981) 2258.

[49] M. Houshmand, A. Jabbari, H. Heli, M. Hajjizadeh, A. A. Moosavi-Movahedi; "Electrocatalytic oxidation of aspirin and acetaminophen on a cobalt hydroxide nanoparticles modified glassy carbon electrode". *J. Solid State Electrochem.*, **12** (2008) 1117.

[50] R. N. Goyal, A. K. Jain, N. Jain; "Comparison of the Electrochemical and enzymic oxidation of 1,3,7-trimethyluric acid at solid electrodes". *Bull. Chem. Soc. Japan*, **69** (1996) 1987.

****